Glaucoma risk stratification using novel genetic and clinical risk factors

By

Ayub Qassim, MBBS

Thesis

Submitted to Flinders University

for the Degree of

Doctor of Philosophy

College of Medicine and Public Health

Principal supervisor: Professor Jamie Craig

11/02/2021

Table of contents

Abstract

Primary open-angle glaucoma (POAG) is one of the most heritable common human diseases. POAG remains the leading cause of irreversible blindness worldwide, despite the ongoing advances in the medical and surgical treatment options of glaucoma. This is largely due to its asymptomatic and progressive natural history as treatment cannot restore an already lost vision. Nonetheless, treatment — via reduction of intraocular pressure (IOP) — is highly effective in slowing down disease progression, and in most cases, halting vision loss. There is no established cost-effective screening strategy for glaucoma in Australia, and there is currently no way of knowing which glaucoma suspect will progress to a blinding disease. Thus, the current national guidelines recommend routine follow-up of all 'at-risk' individuals, which adds a significant burden to health care resources since the majority of glaucoma suspects will not need any intervention.

This thesis addressed this gap in knowledge by investigating novel risk factors of glaucoma development and progression. Leveraging 'big data' from population studies and genetic consortia, several novel genetic risk variants were identified to be associated with POAG and glaucoma-related phenotypes, improving our understanding of the biological pathways involved in POAG pathogenesis. The aggregate effects of these genetic risk variants were demonstrated (using polygenic risk scores) to be highly predictive of the risk of glaucoma development, progression, treatment intensity, and diurnal IOP variations. Since IOP remains the only modifiable risk factor for glaucoma, the IOP-lowering benefits of cataract surgery and selective laser trabeculoplasty were ascertained, with a focus on predictive factors for individuals who would most likely benefit from these interventions. A novel approach to monitor IOP change post-intervention was piloted using a cloud-connected and patient-administered home tonometer. Finally, a novel glaucoma progression risk prediction was developed using corneal biomechanical properties — namely, corneal stiffness parameter, in synergy with central corneal thickness.

The outcomes of this thesis have markedly enhanced our capacity in glaucoma risk stratification via genetic and clinical biomarkers of disease progression. The insights gained from this research will lead to translational implications for policy development and rational deployment of an evidence-based glaucoma suspect monitoring both in Australia and internationally. This can be facilitated by further research implementing a risk-stratified monitoring and treatment strategy such that these decisions are personalised for each patient, substantially reducing the cost of follow-up and reducing unnecessary treatment, and that fewer patients will irreversibly lose vision.

Declaration

I certify that this thesis:

1. does not incorporate without acknowledgment any material previously submitted for a degree or diploma in any university; and
2. to the best of my knowledge and belief, does not contain any material previously published or written by another person except where due reference is made in the text.

Signed,

Ayub Qassim

15/02/2021

Acknowledgement

This research would not have been possible without the extraordinary support from my supervisors, colleagues, and family. I was very fortunate to launch my research career and share my journey with such brilliant minds and astute scholars. I thank Professor Jamie Craig for providing me with the incredible opportunity to study under his guidance and supervision, as well as supporting and mentoring me consistently throughout the last three years. Associate Professor Owen Siggs and Dr Mark Hassall have been an enormous source of knowledge and support and without their guidance I would not have been equipped with the tools of reproducible, scalable and rigorous research. I also want to thank Dr Emmanuelle Souzeau for her supervision, attention to detail, and uplifting encouragement throughout my studies. My supervision was further complemented by the support of Associate Professor John Landers and Dr Jimmy Breen, for whom I am very thankful. I have been seriously privileged to work under the guidance of such world-leading researchers and inspirational and compassionate humans.

I would like to thank the generous contributions and guidance of many clinicians and scientists who helped me achieve my research outcomes. The knowledge and skill set of Professor Stuart MacGregor, Associate Professor Puya Gharahkhani and Mr Xikun Han have been enormously valuable in all of the genetic research that we have conducted. I would like to thank all of the researchers and contributors involved in the PROGRESSA program, namely Professors Robert Casson, Stuart Graham, and Alex Hewitt, Associate Professors Paul Healey and Ashish Agar, and Dr Anna Galanopoulos. I would like to specifically thank Professor Robert Casson, Professor Stuart Graham, and Associate Professors Paul Healey for their active and sincere contributions in improving my research skills, manuscript presentation and data analysis. I have learnt so much from collaborating with these esteemed clinicians and scientists, and could have never imagined progressing thus far without their direction.

The team at the Flinders University Department of Ophthalmology and Flinders Medical Centre Eye Clinic is full of amazing people with whom I shared the majority of my PhD journey. I would like to thank Dr Mona Awadalla, Dr Sean Mullany, Mr Lachlan Knight, Ms Deb Sullivan, Ms Thi Nguyen, Mr Henry Marshall, Dr Georgie Howlitt, Dr Tiger Zhou, Dr Ebony Liu, Mrs Bronwyn Sheldrick, Mrs Caroline Austin, Mrs Karen Hall, Mrs Lefta Leonardos, Ms Jacqui Pearce, Ms Angela Chappell, and Ms Carly Emerson for their administrative, technical and clinical support along the way. This work presented in this thesis would not have been possible by the timeless contributions of these kind people.

I have enjoyed the company and wisdom of so many inspiring individuals, and have learnt so much along the way. This thesis has been a journey of friendship, reflection, and self improvement, just as much as it has been a journey of scientific discovery and research. Dr Sean Mullany, Mr Lachlan Knight, Ms Thi Nguyen, Dr Mona Awadalla, Mr Henry Marshall, Ms Deb Sullivan, Ms Lauren Pattimore, and more recently, Dr Georgie Howlitt and Dr Ella Berry, have been the friendliest, funniest, and warmest companions that I could have ever asked for to share my journey with.

This acknowledgement will not be complete without the explicit mention of the great and ongoing support I have received from my family and partner. I am touched by their everlasting encouragement and heart-warming assistance.

Finally, I would like to thank the amazing people at the Avant Foundation for awarding me with a full time-scholarship in my third year, and Flinders University and Professor Jamie Craig for their scholarships in my earlier study years. I am grateful that you have allowed me to continue to follow my passion in research without worrying about my financial future.

With these acknowledgements in mind, I am proud of what I have achieved in this thesis, and hope to have made an impact in the clinical and scientific communities in advancing our understanding of glaucoma. I owe so much of what I have achieved to the amazing people mentioned above, and I am humbled to sign my name to the frontpage of this thesis.

Thesis outcomes

Manuscripts published during the Doctoral candidature

1. **Qassim A**, Souzeau E, Hollitt G, et al. Risk stratification and clinical utility of polygenic risk scores in Ophthalmology. *TVST*. *In press*.
2. Mullany S, Xiao L, Souzeau E, **Qassim A**, Siggs OM, Hassall M, Craig JE. Glaucoma and Dementia: Cognitive Impairment is Associated with Normal-Tension Glaucoma. *BMJ Ophthalmology*. *In press*.
3. **Qassim A**, Mullany S, Awadalla MS, Hassall MM, Nguyen T, Marshall H, et al. A polygenic risk score predicts intraocular pressure readings outside office hours and early morning spikes as measured by home tonometry. *Ophthalmology Glaucoma. In press.*
4. **Qassim A**, Mullany S, Abedi F, Marshall H, Hassall MM, Kolovos A, et al. Corneal stiffness parameters are predictive of structural and functional progression in glaucoma suspects. *Ophthalmology. In press.*
5. Gharahkhani P, Jorgenson E, Hysi P, Khawaja AP, Pendergrass S, Han X, **Qassim, A,** et al. A large cross-ancestry meta-analysis of genome-wide association studies identifies 69 novel risk loci for primary open-angle glaucoma and includes a genetic link with Alzheimer's disease. *Nature Comms. In press.*
6. Marshall H, Mullany S, **Qassim A,** Hassall M, Siggs O, Ridge B, et al. Cardiovascular Disease predicts structural and functional progression in early glaucoma. *Ophthalmology. In press.*
7. **Qassim A**, Souzeau E, Siggs OM, Hassall MM, Han X, Griffiths HL, et al. An Intraocular Pressure Polygenic Risk Score Stratifies Multiple Primary Open-Angle Glaucoma Parameters Including Treatment Intensity. *Ophthalmology*. 2020 Jul 1;127(7):901–7.
8. Siggs OM, Awadalla MS, Souzeau E, Staffieri SE, Kearns LS, Laurie K, **Qassim, A,** et al. The genetic and clinical landscape of nanophthalmos and posterior microphthalmos in an Australian cohort. *Clinical Genetics.* 2020;97(5):764–9.
9. **Qassim A**, Walland MJ, Landers J, Awadalla M, Nguyen T, Loh J, et al. Effect of phacoemulsification cataract surgery on intraocular pressure in early glaucoma: A prospective multi-site study. *Clin Experiment Ophthalmol*. 2020 May;48(4):442–9.
10. Craig JE,* Han X,* **Qassim A,*** Hassall M, Bailey JNC, Kinzy TG, et al. Multitrait analysis of glaucoma identifies new risk loci and enables polygenic prediction of disease susceptibility and progression. *Nat Genet.* 2020 Jan 20;52(2):160–166.

11. Han X,* **Qassim A,*** An J, Marshall H, Zhou T, Ong J-S, et al. Genome-wide association analysis of 95 549 individuals identifies novel loci and genes influencing optic disc morphology. *Human Molecular Genetics*. 2019 Nov 1;28(21):3680–90.
12. Marshall HN, Andrew NH, Hassall M, **Qassim A**, Souzeau E, Ridge B, et al. Macular Ganglion Cell–Inner Plexiform Layer Loss Precedes Peripapillary Retinal Nerve Fiber Layer Loss in Glaucoma with Lower Intraocular Pressure. *Ophthalmology*. 2019 Aug 1;126(8):1119–30.
13. Awadalla MS,* **Qassim A**,* Hassall M, Nguyen TT, Landers J, Craig JE. Using Icare HOME tonometry for follow-up of patients with open-angle glaucoma before and after selective laser trabeculoplasty. *Clin Exp Ophthalmol.* 2020 Apr;48(3):328-33
14. Siggs OM, Souzeau E, Breen J, **Qassim A**, Zhou T, Dubowsky A, et al. Autosomal dominant nanophthalmos and high hyperopia associated with a C-terminal frameshift variant in MYRF. *Mol Vis*. 2019;25:527–34.
15. Awadalla MS, Fitzgerald J, Andrew NH, Zhou T, Marshall H, Qassim A, et al. Prevalence and type of artefact with spectral domain optical coherence tomography macular ganglion cell imaging in glaucoma surveillance. PLoS ONE. 2018;13(12):e0206684.

Manuscripts under review

1. Siggs OM, **Qassim A,** Han X, Souzeau E, Kuruvilla S, Marshall HN, Mullany S, et al. Polygenic and monogenic contributions to age at diagnosis and progression of open-angle glaucoma.
2. Han, X, Steven K, **Qassim A**, Marshall HN, Bean C, Tremeer M, An J, Siggs OM, et al. Automated AI labelling of optic nerve head enables new insights into cross-ancestry glaucoma risk and genetic discovery in over 280,000 images from the UK Biobank and Canadian Longitudinal Study on Aging.
3. Knight LSW, Ruddle JB, …, **Qassim A**, et al. Childhood and Early-Onset Glaucoma Classification and Genetic Profile in an Australasian Disease Registry.

Non-peer reviewed articles

1. **Qassim A**, Mullany S, Knight LSW, Siggs OM, Craig JE. Reply to correspondence (editorial invitation) Re: Corneal stiffness parameters are predictive of structural and functional progression in glaucoma suspects. *Ophthalmology. In press.*
2. **Qassim A**, Siggs OM. Predicting the genetic risk of glaucoma. Biochemist (London), 2020;42(5):26–30. Available online, doi: 10.1042/BIO20200063

Conference presentations

1. **Qassim, A,** et al. A polygenic risk score predicts intraocular pressure fluctuation and readings outside office hours as measured by home tonometry. ARVO 2020, held online.
2. **Qassim, A,** *et al.* A polygenic risk score predicts intraocular pressure fluctuation and readings outside office hours as measured by home tonometry. ANZGS 2020, Adelaide, Australia.
3. **Qassim, A,** *et al.* The effect of phacoemulsification cataract surgery on intraocular pressure in early glaucoma: a prospective multi-site study. ANZGS 2020, Adelaide, Australia.
4. **Qassim, A,** *et al.* Clinical phenotypes of glaucoma patients stratified by an intraocular pressure polygenic risk score. CMPH Emerging Leader Showcase 2019, Adelaide, Australia.
5. **Qassim, A,** *et al.* Clinical phenotypes of glaucoma patients stratified by an intraocular pressure polygenic risk score. Australian PRS Symposium 2019, Sydney, Australia.
6. **Qassim, A,** *et al.* Clinical phenotypes of glaucoma patients stratified by an intraocular pressure polygenic risk score. RANZCO 2019 annual meeting, Sydney, Australia.
7. **Qassim, A,** *et al.* The effect of phacoemulsification cataract surgery on intraocular pressure in early glaucoma: a prospective multi-site study. RANZCO 2019 annual meeting, Sydney, Australia.
8. **Qassim, A,** *et al.* Glaucoma polygenic risk score predicts treatment intensity and RNFL loss in glaucoma suspects. ARVO 2019 annual meeting, Vancouver, Canada.
9. **Qassim, A,** *et al.*, Clinic Utility Of Polygenic Risk Score In Early Glaucoma: Application In A National Prospective Early Manifest Glaucoma Cohort. RANZCO congress 2018, Adelaide, Australia.

Collaborations or joint conference presentations

1. Mullany, S, ..., **Qassim, A**, et al. Normal tension glaucoma is associated with cognitive impairment, ANZGS 2020, Adelaide, Australia
2. Craig, JE, **Qassim, A,** *et* al. A glaucoma polygenic risk score strongly associated with disease prediction and treatment intensity, ARVO 2019 annual meeting, Vancouver, Canada.
3. Awadalla, MS, Hassall, M, **Qassim, A,** *et al.* The correlation between Glaucoma polygenic risk score and IOP measured by Icare HOME tonometry within and outside of office hours, ARVO 2019 annual meeting, Vancouver, Canada.
4. Hassall, M, **Qassim, A,** *et al.*. A Polygenic Risk Score That Predicts Familial Genetic Risk In Glaucoma. RANZCO congress 2018, Adelaide, Australia.

Talks

1. Glaucoma, the silent thief of sight, 3 Minute Thesis finals, 2019, Adelaide, Australia
2. The impact of common IOP genetic variants on POAG phenotype, Flinders Health Research Week, 2019, Adelaide, Australia

Awards

1. ANZGS: Best presentation award, 2020
2. AVANT Doctor in Training Scholarship, 2020
3. Flinders University RHD Scholarship, 2019
4. 3MT Heat 2 Winner,
5. 3MT Finalist, 2019
6. CMPH travel grant award, 2019
7. CMPH HDR Student Publication Award, 2019
8. RANZCO: ORIA Best Paper, 2019
9. Flinders University Research Student Conference Travel Grant, 2019

List of abbreviations

AMD	Age-Related Macular Degeneration
ANZRAG	The Australian & New Zealand Registry of Advanced Glaucoma
AUC	Area Under the Curve
BMES	Blue Mountain Eye Study
CCT	Central Corneal Thickness
CH	Corneal Hysteresis
CI	Confidence Interval
DD	Disc Diameter
EMGT	Early Manifest Glaucoma Trial
FDT	Frequency Doubling Technology
GAT	Goldmann Applanation Tonometry
GCIPL	Ganglion Cell Inner Plexiform Layer Complex
GHT	Glaucoma Hemifield Test
GPA	Guided Progression Analysis
GWAS	Genome-Wide Association Study
HRT	Heidelberg Retina Tomograph
HVF	Humphrey Visual Field
IGGC	International Glaucoma Genetics Consortium

IOP	Intraocular Pressure
LD	Linkage Disequilibrium
MD	Mean Deviation
MIGS	Minimally Invasive Glaucoma Surgery
MTAG	Multi-Trait Analysis of Gwas
NHMRC	National Health And Medical Research Council
OCT	Optical Coherence Tomography
OHTS	Ocular Hypertension Treatment Study
OR	Odds Ratio
OSA	Obstructive Sleep Apnoea
POAG	Primary Open-Angle Glaucoma
PoPLR	Permutation Analyses of Pointwise Linear Regression
PROGRESSA	Progression Risk of Glaucoma: RElevant SNPs With Significant Association
PRS	Polygenic Risk Score
PSD	Pattern Standard Deviation
RNFL	Retinal Nerve Fibre Layer
SD	Standard Deviation
SE	Standard Error
SLT	Selective Laser Trabeculoplasty
SNP	Single Nucleotide Polymorphism

UKBB	UK Biobank
UKGTS	UK Glaucoma Treatment Study
VCDR	Vertical Cup-to-Disc Ratio

Chapter 1: Introduction

Glaucoma refers to a group of ocular disorders with multifactorial aetiology united by a clinically characteristic degeneration of the optic nerve with associated visual field loss (Casson et al. 2012). Thus the term glaucoma includes several distinct optic neuropathies with overlapping causes, risk factors, treatment options, and prognosis (Jost B. Jonas et al. 2017). Collectively, glaucoma is the leading cause of irreversible blindness globally, and second to macular degeneration in Australia (Taylor et al. 2005; Y.-C. Tham et al. 2014). The prevalence of glaucoma is expected to continue to increase, primarily due to the aging population, with an estimated 350,000 Australians to be affected with glaucoma by 2040, a 75% increase (Y.-C. Tham et al. 2014). This poses a significant burden on individuals and the health care system at the current standard of care where patients with suspected or established glaucoma are closely monitored, and sometimes prescribed lifelong treatment that may not always be required.

Glaucoma is clinically defined by a visible thinning of the neuroretinal rim of the optic nerve head and an enlargement of the optic cup, which correspond to the neurodegenerated retinal ganglion cells (Figure 1.1) (Casson et al. 2012; Robert N. Weinreb, Aung, and Medeiros 2014). These structural clinical signs translate to a functional vision loss in the corresponding structure-function region, where the disease is termed perimetric glaucoma. In the early stages of the disease, the appearance of the optic nerve head that is suspicious for glaucoma is not always accompanied by any visual field defects using routine Standard Automated Perimetry; such individuals, or eyes, are termed glaucoma suspects (Casson et al. 2012). The clinical utility of newer imaging technologies, such as optical coherence tomography (OCT) and confocal scanning laser ophthalmoscopy, has allowed the detection of structural defects that provide evidence of glaucoma prior to the onset of visual field defects (Lisboa et al. 2012). These eyes are sometimes termed as preperimetric glaucoma, although there are no standardised diagnostic criteria to differentiate this group from the aforementioned glaucoma suspects. Thus the clinical diagnosis of glaucoma can be thought of as a continuous spectrum of progressive retinal ganglion cell death and the subsequent vision loss (Figure 1.2) (R. N. Weinreb et al. 2004).

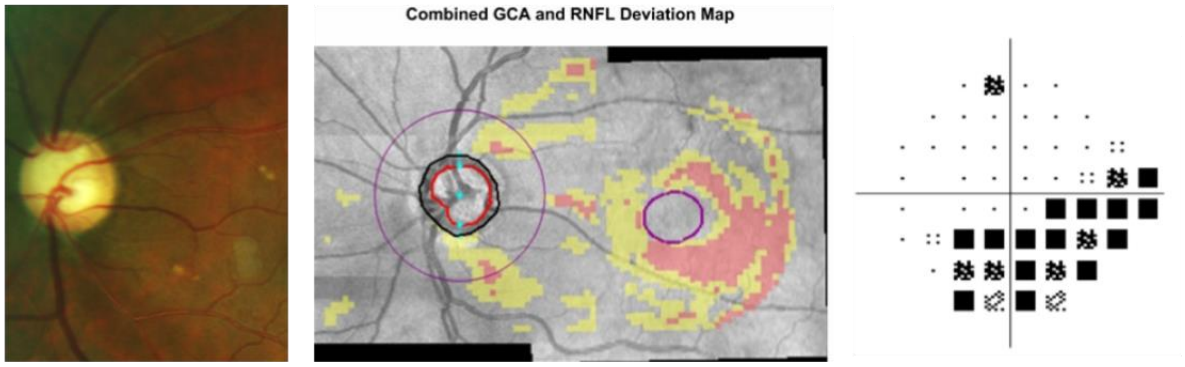

Figure 1.1. The constellation of clinical features that define glaucoma. The image on the left is a colour fundus photograph of a left eye's optic nerve head, showing characteristic thinning of the neuroretinal rim (asymmetrically in the early stages of glaucoma; in this case, it is thinnest superiorly), and enlargement of the optic cup (the relatively pale inner yellow part of the optic disc). The image in the centre is an en face red-free photograph of the retina, with colour-coded overlays of optical coherence tomography thickness assessment of a left eye's optic disc and macula, showing characteristic thinning of the retina nerve fibre layer bundles and the macular ganglion cell inner plexiform layers. The image on the right is a visual field pattern standard deviation map of the central 24 degrees of a left eye, showing an inferior arcuate pattern of visual field loss and an early superior nasal step, corresponding to the superior and inferior retinal nerve fibre bundles respectively.
RNFL: retinal nerve fibre layer; GCA: ganglion cell analysis.

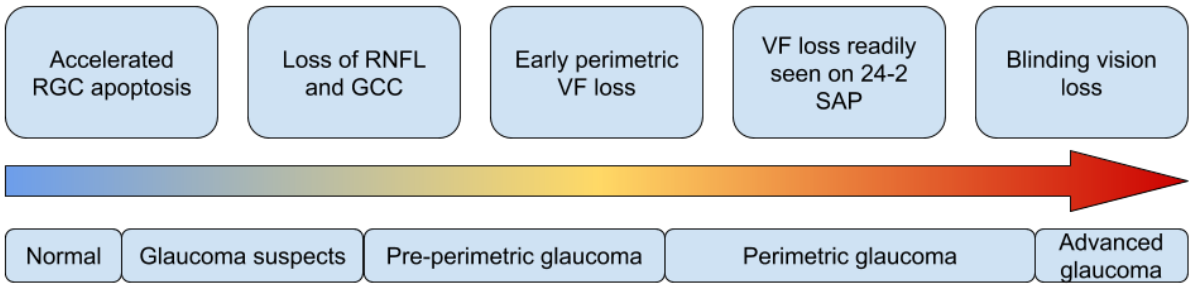

Figure 1.2. The clinical spectrum of glaucoma disease progression. In the preclinical stage, accelerated retinal ganglion cell (RGC) death takes place prior to a measurable loss in the retinal nerve fibre layer (RNFL) or ganglion cell complex (GCC) is detected. Measurement of the RNFL and GCC thickness is often done using optical coherence tomography. Early perimetric visual field (VF) loss may be detected using frequency doubling technology, short-wavelength perimetry, or in some cases a focused VF testing on the central 10 degrees of vision (Hood et al. 2019). The onset of perimetric glaucoma is often defined by reproducible VF loss seen on Standard Automated Perimetry (SAP) on the central 24 degrees of the VF. Progressive peripheral vision loss occurs until central vision is affected which ultimately leads to total blindness.
RGC: retinal ganglion cell; RNFL: retinal nerve fibre layer; GCC: ganglion cell complex; VF: visual field; SAP: standard automated perimetry.

The progressive and accelerated retinal ganglion cell apoptosis seen in glaucomatous eyes is mediated by an elevated intraocular pressure (IOP), which causes neuronal axonal injury at the optic nerve head (Casson et al. 2012; Robert N. Weinreb, Aung, and Medeiros 2014). Despite this, an elevated IOP can occur in otherwise normal eyes — termed ocular hypertension — and is not diagnostic of glaucoma in isolation (Casson et al. 2012; Paul Mitchell et al. 1996; P. A. Graham 1972). Similarly, progressive glaucomatous optic neuropathy can occur in individuals with IOP consistently within the normal limits, which is sometimes referred to as normal tension glaucoma (Collaborative Normal-Tension Glaucoma Study Group 2001). Nonetheless, the importance of IOP in glaucoma pathogenesis and the wide availability of medical and surgical options to reduce IOP makes it the most important and the only modifiable risk factor for glaucoma (Robert N. Weinreb, Aung, and Medeiros 2014).

IOP is regulated by the secretion and outflow of the aqueous humour, a clear fluid that circulates the anterior segment of the eye. In a normal population, IOP follows a slightly right-skewed distribution, with a mean of 16 mmHg and standard deviation of 2.9 (Paul Mitchell et al. 1996; Bonomi et al. 1998). The anterior segment is anatomically divided into the anterior and posterior chambers by the iris, where the pupil is the transitional space through which the aqueous circulates (Figure 1.3). Aqueous humour is actively secreted by the non-pigmented epithelial cells of the ciliary body in the posterior chamber and flows into the anterior chamber through the pupil (Goel et al. 2010). Drainage of the aqueous humour occurs at the iridocorneal angle via a pressure dependent mechanism through the trabecular meshwork into Schlemm's canal and ultimately into the episcleral vein (Figure 1.3) (Goel et al. 2010). A secondary outflow pathway, termed the uveoscleral outflow pathway, contributes to aqueous humour drainage to the surrounding ocular tissue mostly independent to the pressure, analogous to lymphatic drainage (Brubaker 2001). Whether the aqueous humour drainage at the iridocorneal angle is uninterrupted or not is the primary method of classifying the aetiology, and consequently the treatment options of glaucoma (Casson et al. 2012).

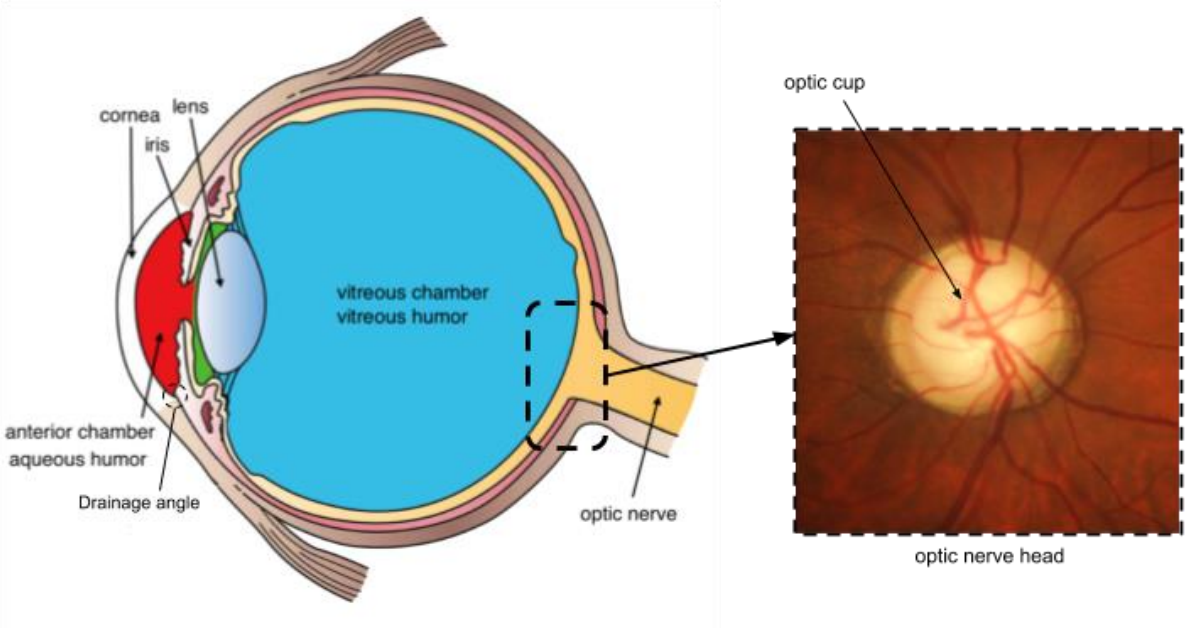

Figure 1.3. A cross-sectional view of the eye (left) and a colour fundus photograph of a glaucomatous optic nerve head (right). Aqueous humour is secreted in the posterior chamber (green coloured space anterior to the lens), and exists the eye via the iridocorneal angle (dashed circle) in the anterior chamber (red coloured space anterior to the iris). Elevated intraocular pressure causes mechanical stress and strain of the optic nerve head and surrounding tissues that leads to retinal ganglion cell death, which is seen clinically by a pathologically enlarged optic cup. he cross-sectional artwork on the left was created by Holly Fischer and reproduced for this figure under a Creative Commons Attribution 3.0 Unported license.

The morphology of the anterior chamber angle divides glaucoma broadly into two major subtypes: open-angle glaucoma and angle-closure glaucoma. Further subclassification is based on the presence or the absence of secondary causes of elevated IOP (Jost B. Jonas et al. 2017). Primary open angle glaucoma (POAG) is the commonest type of glaucoma in Australia and worldwide (Bourne et al. 2016; Y.-C. Tham et al. 2014; Taylor et al. 2005; Paul Mitchell et al. 1996), where the iridocorneal angle appears open and anatomically normal with no secondary causes of elevated IOP or aqueous humour outflow resistance. Pseudoexfoliation syndrome and pigment dispersion syndrome are the two most common secondary causes of open angle glaucoma, where exfoliation material or pigment particles may partially obstruct conventional aqueous humour outflow pathways (Robert N. Weinreb, Aung, and Medeiros 2014). In contrast, angle-closure glaucoma occurs when aqueous outflow is obstructed by the apposition of the iris to the anterior capsule of the lens (primary angle-closure glaucoma), or secondary to other causes (Casson et al. 2012). Acute angle-closure glaucoma is a clinically distinct condition where IOP has rapidly increased to very high levels resulting in pain, nausea, conjunctival hyperaemia, and blurred vision from corneal oedema (Casson et al. 2012). This acute presentation is unlike the often asymptomatic progressive

neurodegeneration that characterises chronic forms of glaucoma such as POAG. The research presented in this thesis is focused on POAG, which represents about 80% of all glaucoma in Australia (Y.-C. Tham et al. 2014).

POAG is completely asymptomatic in the early stages but causes gradual and progressive loss of peripheral vision (Figure 1.2) (Jost B. Jonas et al. 2017). This 'silent' clinical phase, accompanied by a lack of established screening programs or clinical biomarkers makes glaucoma a diagnostic challenge. For example, in The Blue Mountain Eye Study, a community population study set in New South Wales, Australia, approximately 50% of the glaucoma cases were undiagnosed at the time of the screening eye examination (Paul Mitchell et al. 1996). Unless treated, POAG causes progressive neurodegeneration and vision loss that is often unnoticed by the patients. Long-term follow up studies have estimated that glaucoma leads to blindness in at least one eye in up to 27% of the cases (Hattenhauer et al. 1998). Once POAG is diagnosed however, treatment is highly effective in slowing down disease progression in a majority of cases (Robert N. Weinreb, Aung, and Medeiros 2014; Conlon, Saheb, and Ahmed 2017).

Currently, lowering IOP is the only effective strategy for glaucoma treatment. Treatment options for POAG include topical medications, laser trabeculoplasty, or incision surgery (Conlon, Saheb, and Ahmed 2017). Evidence for the efficacy of IOP-lowering treatment in reducing the risk of glaucoma onset and progression is supported by two landmark randomised trials conducted in the late 1990s: the Ocular Hypertension Treatment Study (OHTS) and the Early Manifest Glaucoma Trial (EMGT) (Leske et al. 1999; Gordon and Kass 1999). In the OHTS study, 1,636 individuals with ocular hypertension and no evidence of perimetric glaucoma were randomised to topical IOP-lowering medications or observation (Gordon and Kass 1999). The primary finding of this trial was that a reduction of IOP by about 20% using topical drops resulted in nearly half the risk of developing glaucoma during follow-up (cumulative probability of 4.4% in the medication group and 9.5% in the observation group; hazard ratio = 0.4; 95% confidence interval [CI], 0.27–0.59) (Kass et al. 2002). Furthermore, medical treatment reduced the rate of visual field loss, measured by the rate of change in the global visual field mean deviation, from a mean of -0.23 dB/year to -0.06 dB/year (Carlos G. De Moraes et al. 2012). In the EMGT study, 255 individuals with early perimetric glaucoma were randomised to either treatment with a combined laser trabeculoplasty and topical IOP-lowering medications, or observation (Leske et al. 1999). This trial showed that the risk of glaucoma progression decreased by 10% for each 1 mmHg reduction in IOP, and that treatment effectively halved the overall risk of progression (hazard ratio = 0.5, 95% CI 0.35–0.71) (Leske et al. 2003).

The efficacy of early treatment of ocular hypertension and POAG was confirmed more than a decade later in the first randomised, triple-blinded, placebo-controlled clinical trial: The United Kingdom Glaucoma Treatment Study (UKGTS) (D. F. Garway-Heath et al. 2013). In this trial, 516 individuals with early perimetric open-angle glaucoma were randomised to either latanoprost topical drop, or placebo (D. F. Garway-Heath et al. 2013; G. Lascaratos et al. 2013). With a relative IOP reduction of 2.9 mmHg (95% CI 2.2–3.6) in the treatment arm, there was a significant benefit of treatment in slowing disease progression: 15% of the patients in the treatment group progressed on visual field testing at the trial primary end-point of 24 months, compared to 26% in the placebo group (adjusted hazard ratio = 0.44, 95% CI 0.28–0.69) (D. F. Garway-Heath et al. 2015). More recently, another randomised controlled trial, Laser in Glaucoma and Ocular Hypertension Trial (LiGHT), compared the efficacy of selective laser trabeculoplasty to topical medical therapy in the management of early POAG or ocular hypertension patients (G. Gazzard et al. 2018; Konstantakopoulou et al. 2018). The absolute IOP reduction was similar between both groups, and a similar proportion of each treatment arm achieved the trial protocol-set target IOP (A. Garg et al. 2019; Gus Gazzard et al. 2019). This finding is in agreement with previous studies showing an equivalent efficacy of selective laser trabeculoplasty to topical medications in lowering IOP (Wong et al. 2015).

While IOP-lowering treatment of POAG or ocular hypertension is highly effective, there are some key challenges to the practical implementation of early vision-saving treatment. Topical glaucoma drops, and to a lesser extent, laser trabeculoplasty, are not without risk and morbidity (Beckers et al. 2008; Shen, Huang, and Yang 2019; Wong et al. 2015). Furthermore, the aforementioned trials showed that a majority of the untreated patients with ocular hypertension or early POAG did not progress rapidly, or at all within the trial periods (Leske et al. 2003; Kass et al. 2002; D. F. Garway-Heath et al. 2015). Therefore, a more comprehensive strategy is needed to identify individuals at the highest risk of progression, and those who would likely benefit the most from early treatment. This is particularly relevant to a majority of individuals in the early glaucoma spectrum (i.e. glaucoma suspects; Figure 1.2), who do not fit the inclusion criteria of the aforementioned clinical trials; therefore, the trial results are not directly applicable to this group. An increasing number of glaucoma suspects are being diagnosed and referred for surveillance, in part due to the wide adoption of OCT and automated perimetry in optometric practice, which further adds stress to the healthcare system (Drexler et al. 2014; Newman and Andrew 2018). Denis et al. (2004) estimated the total costs of monitoring each ocular hypertensive patient to be AU$446 annually, which adds up to AU$772 once treatment is commenced. Thus, there is an urgent need for an effective risk stratification strategy to identify high-risk individuals who would benefit from screening tests, or early intervention.

Limitations of community screening of POAG

There are currently no proven and cost-effective strategies to identify POAG patients in the community (J. Burr et al. 2007). While elevated IOP and characteristic changes of the optic nerve head — such as higher vertical cup to disc ratio (VCDR) and neuroretinal rim thinning — are strongly associated with glaucoma, these phenotypes show poor discrimination of glaucoma patients in an unstratified population screening setting (J. Burr et al. 2007). Further stratification can be achieved using demographic risk factors of developing glaucoma. These include older age (e.g. above 68 years), ethnicity (sub-Saharan African ethnic origin), and a family history of glaucoma (Jost B. Jonas et al. 2017).

As discussed earlier, IOP is a strong risk factor for the development of glaucoma, and remains the target of all of the current treatment options. However, the primary challenge in using IOP as a glaucoma screening tool is the wide physiological range of IOP in normal eyes (Paul Mitchell et al. 1996). There is no single IOP cut-off that can adequately identify glaucomatous eyes (J. Burr et al. 2007). For instance, approximately a third of POAG patients have clinically measured IOPs that remain within 'normal' ranges despite apparent porgressive glaucomatous optic neuropathy (Collaborative Normal-Tension Glaucoma Study Group 2001; Casson et al. 2012). On the other hand, individuals may have IOPs that would be considered 'elevated' in reference to a statistical distribution of the population IOP measurements, but never progress or develop glaucoma (Casson et al. 2012; Kass et al. 2002).

The Baltimore Eye Survey evaluated 5,308 community dwelling adults living in Baltimore, Maryland, USA with reference to glaucoma (James M. Tielsch et al. 1991). Detailed ophthalmic examination had identified 196 participants with glaucoma. IOP measurements and expert review of fundus photographs were then reviewed retrospectively as screening tools. At the traditional statistically derived cut-off of 21 mmHg (Paul Mitchell et al. 1996; Hashemi et al. 2005; Hollows and Graham 1966; Leske et al. 1997), the sensitivity of IOP in detecting glaucoma was only 47%, with a specificity of 92% (James M. Tielsch et al. 1991). Similarly, VCDR and thinnest neuroretinal rim width had poor sensitivities. For example, a VCDR measurement of 0.7 or greater had a very poor sensitivity of 18%, while being highly specific for the diagnosis of POAG (specificity of 99%) (James M. Tielsch et al. 1991). These stratification cut-offs were not significantly improved when combined with baseline demographic risk factors of age and family history (James M. Tielsch et al. 1991). Thus, basic demographic and ocular measurements are insufficient in risk stratifying the general population for glaucoma.

Non-invasive and objective assessment of the optic nerve head has also been trialed as a screening tool. Confocal scanning laser ophthalmoscopy using Heidelberg Retina Tomograph (HRT; Heidelberg Engineering, Heidelberg, German) is a noncontact device that provides a rapid and reproducible three-dimensional image of the optic nerve head (Mikelberg et al. 1995). In a pilot study targeting 303 high risk individuals in Montreal, Canada, Harasymowycz and colleagues (2005) reported that HRT had a sensitivity of 85% in identifying glaucomatous eyes with 12 true positives and 2 false negatives, and a specificity of 88%. Larger population studies on HRT as a screening tool have failed to replicate the findings of the pilot Canadian study (Maslin, Mansouri, and Dorairaj 2015). In particular, Healey and colleagues (2010) reported on using HRT in a population-based assessment of 1,644 participants of The Blue Mountain Eye Study. The study participants were of older age (mean age 73.7 years) where glaucoma prevalence is expected to be high, yet the sensitivity and the specificity of HRT were 64% and 85% respectively, which was insufficient as a standalone screening tool (Healey et al. 2010). The use of HRT as a glaucoma screening tool was also evaluated in a population setting in The Singapore Malay Eye Study (Y. Zheng et al. 2010). Of the 3,280 Malay participants, 112 individuals with a previous diagnosis of glaucoma were evaluated with HRT using 196 healthy individuals as controls, where the sensitivity and the specificity were 71% and 86% respectively (Y. Zheng et al. 2010). A large optic disc size was associated with higher false positives in this study, which further limits the general utility of HRT in a population setting.

A systematic review on the clinical effectiveness of screening of open angle glaucoma evaluated all the studies published on IOP, fundus photography HRT and visual field threshold testing up to 2006 (J. Burr et al. 2007). None of the published tools at the time had sufficient sensitivities and specificities to be used for glaucoma screening in a general population setting (J. Burr et al. 2007). Since then, OCT has been increasingly utilised in ophthalmology, and in many ways, has replaced confocal scanning laser ophthalmoscopy including HRT. The commercialisation and development of user-friendly clinician focused OCT software has revolutionised the diagnosis and management of retinal diseases (H. A. Quigley 2019). In glaucoma, OCT provides rapid, non-contact and highly reproducible imaging of the optic nerve head and inner retinal layers (Bussel, Wollstein, and Schuman 2014). The use of OCT in glaucoma diagnosis and progression is well documented (Abe et al. 2016; Vinay Kansal et al. 2018). A meta-analysis of 150 studies on using OCT for glaucoma diagnosis reported a pooled area under the receiver operating characteristic curve of 0.897 for retinal nerve fibre layer (RNFL) thickness assessment and 0.858 for macular ganglion cell inner plexiform layer complex (GCIPL) thickness assessment (Vinay Kansal et al. 2018). OCT has now been widely

adopted by community optometrists and commonly used to detect early glaucomatous changes prior to the onset of visual field changes (Ly et al. 2019).

Despite the wide adoption of routine OCT imaging, there has not been any high-quality studies investigating the utility of OCT as a glaucoma screening tool. In a cross-sectional study, Li et al. (2010) performed OCT optic nerve head assessment using Stratus OCT (Carl Zeiss Meditec) on 333 community-based volunteers in Montreal, Canada. To increase the pre-test positive predictive value, participants were recruited only if they had a family history of glaucoma, were aged 50 years or older, or were of Caribbean, African of Hispanic origins. After exclusions related to missing data or poor quality scans and including only the right eye per participant, 210 eyes were finally available for analysis, out of which six eyes had definitive glaucoma. Definitive glaucoma was diagnosed based on the fundoscopic appearance of the optic nerve head (using disc damage likelihood scale) that was suspicious for glaucoma, with a corresponding visual field defect detected on a frequency doubling technology (FDT) perimetry. Using a combination of optic cup area and peripapillary RNFL thickness measurements resulted in a modest sensitivity of 67% and a high specificity of 96% in detecting definite glaucoma (G. Li et al. 2010).

This study had several limitations that precludes generalisation of its findings. The time-domain OCT used in the study has now been largely superseded by the spectral-domain OCT, which has a higher resolution, image quality (signal to noise ratio), acquisition speed, and improved eye tracking technologies allowing for a more reliable and accurate assessment (de Boer et al. 2003; Leung et al. 2011). These factors account for nearly a third of the original sample reported by Li et al. (2010) to be excluded from the final analysis. Additionally, current generation OCT analysis software allows for a better inner retinal layer visualisation and clinical assessment of glaucomatous structural damage, and includes additional parameters than those used by Li et al. (2010). For instance, macular ganglion cell complex imaging detects structural glaucomatous damage that may predate RNFL loss and would not be apparent on an optic disc OCT (Hood et al. 2013; K. E. Kim and Park 2018; H. Marshall et al. 2020). FDT perimetry used in the study as the outcome measure has its own diagnostic limitations. For example, the FDT visual field diagnostic criteria used by Li et al. (2010) had a sensitivity of 67% for glaucoma (Gardiner et al. 2006), which may have resulted in an underestimation of the prevalence of glaucoma in the cohort. Finally, a better pre-test risk stratification using known clinical risk factors such as IOP may have yielded a higher specificity and positive predictive values. There are currently no published studies on using newer OCT devices and analyses for open angle glaucoma screening.

The utility of FDT as a screening tool has been reported in population settings in Japan, China and the United States (Boland et al. 2016; Iwase et al. 2007; Y. X. Wang et al. 2007). FDT perimetry is quick to perform using a portable device and can detect visual field loss before it is apparent on Standard Automated Perimetry (Harry A. Quigley 1998; Cello, Nelson-Quigg, and Johnson 2000; Casson et al. 2001; Felipe A. Medeiros, Sample, and Weinreb 2004). However, FDT appears to be more sensitive in moderate to advanced glaucoma compared to early glaucoma (Cello, Nelson-Quigg, and Johnson 2000; Felipe A. Medeiros, Sample, and Weinreb 2004). In a population-based cross-sectional study from Japan, abnormal FDT had a fairly poor positive predictive value for detecting definite perimetric glaucoma (18.9%), which was worst for detecting early disease (Iwase et al. 2007). Similar results were obtained from the population-based Beijing Eye Study (Y. X. Wang et al. 2007). In the US study, 25% of the cohort were unable to complete FDT reliably necessitating further diagnostic evaluation (Boland et al. 2016). An abnormal (or unreliable) FDT had a moderate sensitivity of 55% and a specificity of 77% for detecting glaucoma (Boland et al. 2016). As noted previously, a pretest risk stratification would improve the accuracy of a screening test as it focuses on primarily screening high-risk individuals and maximises the positive predictive value. For instance, when Boland et al. (2016) analysed the performance of FDT in a subgroup of participants with a VCDR of 0.6 or greater, the sensitivity of detecting glaucoma improved to 66%. Overall, the results of these population-based studies indicate that FDT is not suitable for a population-level screening program of glaucoma, particularly in the absence of *a priori* risk stratification.

In summary, there are currently no cost-effective and reliable screening strategies to identify POAG patients in the general population. Traditional clinical features of glaucoma are neither sensitive nor specific enough for screening purposes. While the advent of OCT has revolutionised the diagnosis and monitoring of glaucoma via a rapid, objective and repeatable assessment of glaucomatous structural damage, it suffers from a modest sensitivity and a high rate of false positives when the target population is selected based on demographic risk factors only. Owing to the perceived benefit of early glaucoma diagnosis, the current NHMRC (National Health and Medical Research Council) guidelines (published in 2010) recommend targeted screening of high-risk individuals using a “more than one modality” although the optimal combination of tests has not been defined (NHMRC 2010).

A modern implementation of a cost-effective glaucoma screening program should include a combination of known demographic and clinical risk factors, in addition to an objective assessment of the optic nerve head. This information may then be reviewed digitally by a specialist for a potential glaucoma diagnosis and risk assessment, which has been shown to be an accurate and cost-effective alternative to in-person examinations, particularly in remote

communities (Thomas et al. 2014). Ultra low-cost OCT devices with adequate resolutions and contrast-to-noise ratios are being developed which would reduce the cost of implementing such screening strategies, particularly in developing economies (Song et al. 2019). Encouragingly, there is evidence that OCT imaging can be adequately performed by non-expert photographers with comparable sensitivities and specificities for screening purposes, which would further improve cost-effectiveness (M. M. Liu et al. 2018). There is clearly a need for a more targeted screening protocol with a higher pre-test glaucoma probability, and a lower cost per screening test, to identify individuals at the highest risk of developing glaucoma, and those who will benefit the most from earlier interventions.

Clinical risk factors of glaucoma progression

POAG is a progressive disease, with a wide clinical presentation spectrum ranging from early glaucoma with no vision loss (e.g. pre-perimetric glaucoma) to advanced glaucoma where there is no light perception in the affected eye (Figure 1.2) (R. N. Weinreb et al. 2004). The rate of progression is highly variable between individuals, and most individuals with ocular hypertension or suspicious optic nerve head appearances do not develop glaucoma (Kass et al. 2002). Conversely, a minority of glaucoma patients have a highly progressive disease, with a rapid decline in perimetric vision that results in blindness within a few years of disease onset unless aggressive IOP-lowering treatment is implemented (A. Heijl et al. 2013). In a longitudinal study of 583 POAG patients, the average rate of change in the visual field mean deviation was estimated to be -0.80 dB per year (standard deviation 0.82 dB/year), in a negatively skewed distribution (A. Heijl et al. 2013). In this study, 11% of the POAG patients did not have a negative rate of change of their visual field mean deviation over >5 years of follow-up (i.e., a very stable disease) (A. Heijl et al. 2013). In contrast to the majority (60%) of the cohort who did not have a statistically significant negative slope, 5.6% of the patients progressed at an extremely rapid rate worse than -2.5 dB per year (A. Heijl et al. 2013). This inter-individual variation of the rate of glaucoma progression means that identifying risk factors predictive of glaucoma progression is highly relevant to the clinical care of patients at any point in the glaucoma disease spectrum.

The lack of a gold standard for defining and quantifying glaucoma progression is a major obstacle when comparing trials examining risk factors for glaucoma progression. Traditionally, progressive cupping and neuroretinal rim thinning on stereoscopic examination of the optic nerve head was considered to be the hallmark of glaucoma progression. More recently, the widespread utility of OCT in glaucoma has allowed a quantifiable assessment of structural glaucoma progression that can be defined as a significant thinning of the peripapillary RNFL

and GCIPL. However, progression based on visual field loss as detected by Standard Automated Perimetry remains the most commonly used trial end-point as visual field loss is closely associated with visual morbidity and vision related quality of life (Parrish et al. 1997).

Glaucoma progression has been studied in several landmark trials over the last two decades (Kass et al. 2002; Leske et al. 2003, 2007; J. Caprioli and Coleman 2008; Ernest et al. 2013; D. F. Garway-Heath et al. 2015). Age is the most consistently reported risk factor for glaucoma progression (Ernest et al. 2013). In the EMGT, participants aged 68 years old or older were at 51% increased risk of progression relative to the younger age group (Leske et al. 2007). In a retrospective case-controlled study, Chan et al. (2017) reported that older age was significantly associated with a rapid visual field progression, defined by a visual field mean deviation rate exceeding -1 dB per year. Therefore, age is one of the most important risk factors in glaucoma, as older age is associated with a higher risk of developing glaucoma, glaucoma progression, and a significantly more rapid visual field loss.

The presence of a disc hemorrhage is another known strong risk factor for glaucoma progression, particularly in individuals with normal tension glaucoma (Ernest et al. 2013; Kosior-Jarecka et al. 2019). Disc haemorrhages are characteristic linear, splinter-like haemorrhages on the outer edge of the optic nerve head and adjacent to retinal nerve fibre bundle (Drance 1989). These haemorrhages are thought to represent an ischaemic injury in the form of an optic nerve head microinfarction that precedes retinal ganglion cell death, although their exact aetiology and pathogenesis remain elusive (Begg, Drance, and Sweeney 1971). In the UKGTS, the presence of disc haemorrhage at the baseline visit was predictive of visual field deterioration (hazard ratio = 1.87, with a 95% CI 1.04–3.36), which remained consistent in multivariable analysis (Founti et al. 2020). Recurrent disc haemorrhages on follow-up was also reported to be an important risk factor of glaucoma progression in the EMGT, whereby a higher percentage of follow-up visits with a clinically observed disc haemorrhage was independently associated with glaucoma progression in multivariable analyses (Leske et al. 2007). Optic disc OCT imaging has allowed a closer examination of the effects of disc haemorrahges on the peripapillary RNFL. In a study of 44 eyes with a first-detected disc haemorrhage, 73% of the eyes showed progressive RNFL thinning that was adjacent to the disc haemorrhage site (by clock-hour analysis) in the majority of the cases (Suh et al. 2012). The rate of RNFL thinning following disc hemorrhages was characterised in a prospective longitudinal study of 40 eyes from 37 participants (Akagi et al. 2017). In the optic disc quadrant where the disc haemorrhage was observed, the rate of RNFL thinning was -2.25 µm/year, which was significantly faster to the rate of RNFL thinning in other quadrants nearly three-fold (a rate of -0.69 µm/year in the other quadrants) (Akagi et al. 2017). These

studies suggest a localised peripapillary RNFL vulnerability following a disc haemorrhage which leads to the progressive visual field loss observed in the previously mentioned trials (Founti et al. 2020; Leske et al. 2007).

In addition to being a crucial risk factor in the development of glaucoma, elevated IOP has been consistently reported to be associated with glaucoma progression (Founti et al. 2020; Gordon et al. 2002, 2007; Leske et al. 2003, 2007; Carlos G. De Moraes et al. 2012; T. C. W. Chan et al. 2017). In the EMGT, a higher baseline IOP of at least 21 mmHg was associated with a 1.77-fold increase in risk of glaucoma progression compared to those with a baseline IOP below 21 mmHg (Leske et al. 2007). A higher mean follow-up IOP was also significantly associated with progression, with a 12% increased risk of progression for each 1 mmHg higher mean follow-up IOP (Leske et al. 2007). In the UKGTS, a higher IOP measured either at baseline or at the first follow-up visit was associated with visual field progression (Founti et al. 2020; Gerassimos Lascaratos et al. 2014). All three IOP measurement techniques used in the UKGTS, namely Goldmann applanation tonometry, dynamic contour tonometry, and Ocular Response Analyser (Reichert Inc, Buffalo, New York), were associated with the progression outcome (Founti et al. 2020; Gerassimos Lascaratos et al. 2014). Interestingly however, the corneal compensated IOP measured by the Ocular Response Analyser was a significantly better predictor of progression than the standard IOP measurement by Goldmann applanation tonometry (Gerassimos Lascaratos et al. 2014; Founti et al. 2020). This was independently supported by another study showing that the the corneal compensated IOP explained a greater variance in the rate of visual field progression than Goldmann applanation tonometry IOP (R^2 24.5% vs 11.1% respectively, with 95% CI of the difference 6.6–19.6) (B. N. Susanna, Ogata, Daga, et al. 2019). These results suggest that isolating the clinically measured IOP from the corneal influence improves its utility as a risk predictor for glaucoma progression.

The concept of corneal influence on IOP was best demonstrated in the OHTS study, where participants had ocular hypertension at baseline (Gordon et al. 2002). In this study, a lower central corneal thickness (CCT) was a strong predictor of future glaucoma development, whereby for each 40 µm thinner CCT, there was approximately a 2-fold increase in the risk of POAG (Gordon et al. 2002, 2007). Commonly used IOP measurement techniques including those measured by the current gold standard, Goldmann applanation tonometer, are significantly influenced by corneal biomechanics such as CCT (Kohlhaas et al. 2006). Thus, the CCT-associated risk of glaucoma is thought to be related to its confounding effects on the clinically measured IOP, and CCT is not thought to be an independent risk factor of glaucoma onset and progression (although this remains a point of debate) (Felipe A. Medeiros and Weinreb 2012). In the long-term follow-up report of the EMGT of up to 11 years follow-up, a

thinner CCT was found to be a risk factor of glaucoma progression only in those with a higher baseline IOP, with a significant interaction between IOP and CCT, emphasising that CCT-mediated risk is likely attributable to an underestimation of IOP (Leske et al. 2007). In the UKGTS, where treatment allocation was randomised, masked and placebo-controlled, baseline CCT was not found to be a significant predictor of visual field progression (Founti et al. 2020). The strength of this randomised-controlled study is that any known confounding interaction between CCT and IOP that would influence clinical decision making is omitted. Thus, while CCT is an important clinical measurement that influences glaucoma progression by confounding clinically measured IOP, it is unlikely to be an independent risk factor of glaucoma progression.

Nonetheless, corneal biomechanics as potential risk factors for glaucoma progression have attracted increasing attention. While CCT may not be an independent risk factor of glaucoma progression, the idea that the underlying corneal biomechanical properties confer an additional vulnerability to the IOP-mediate optic nerve head stress and strain remained under eager investigations. This has led to the development of the Ocular Response Analyzer, a non-contact tonometer that additionally measures corneal biomechanical properties, namely corneal hysteresis and corneal resistance factor (Luce 2005). Corneal hysteresis (CH) is a biomechanical property of the cornea related to its ability to absorb and release energy such as during applanation (Luce 2005; F. A. Medeiros and Weinreb 2006). In other words, CH represents the viscoelastic damping ability of the corneal tissue in relation to an airpuff, which may reflect the corneal extracellular matrix composition. It is hypothesised that corneal biomechanical properties, including CCT, may correspond to the biomechanical properties of the peripapillary sclera and the lamina cribrosa, the primary site of the glaucomatous optic nerve head injury (J. B. Jonas and Holbach 2005).

Soon after the introduction and availability of Ocular Response Analyzer, a lower CH was reported to be associated with glaucomatous visual field progression (Congdon et al. 2006). Similarly, POAG patients with asymmetrical visual field loss were found to have a lower CH in the worse-affected eye (Anand et al. 2010). The retrospective evidence that a lower CH was associated with a faster visual field progression (C. V. G. De Moraes et al. 2012), was validated by a prospective observational cohort study of 68 individuals with POAG followed for an average of 4 years (Felipe A. Medeiros et al. 2013). A lower baseline CH was significantly associated with a faster rate of visual field loss, whereby each 1 mmHg lower CH was associated with a 0.25% per year faster rate of Visual Field Index (Felipe A. Medeiros et al. 2013). More recently, Susanna et al. (2018) investigated the role of CH in glaucoma suspects in a prospective longitudinal study of 287 eyes from 199 glaucoma suspects. A lower baseline

CH was found to be a significant predictor of progression of the glaucoma suspects into perimetric glaucoma, with a 21% increased risk of developing glaucoma during follow-up for each 1 mmHg lower CH (95% CI 1.04–1.41) (C. N. Susanna et al. 2018). The role of CH was further supported by a prospective study showing that in seemingly well-controlled glaucomatous eyes with clinically measured IOP consistently below 18 mmHg, a lower CH and CCT remained significant predictors of further visual field progression (B. N. Susanna, Ogata, Jammal, et al. 2019). Despite the supporting evidence for the clinical application of CH, the exact material property inferred by a lower CH remains difficult to interpret as CH does not directly relate to corneal rigidity, stiffness, or elasticity (Dupps 2007).

An alternate device that measures corneal biomechanical properties is Corvis ST (Oculus, Wetzlar, Germany). This newer non-contact system uses an ultra-high-speed camera to capture the corneal deformation response to an air puff using cross-sectional image analysis (Hong et al. 2013). Corvis ST measures numerous corneal biomechanical parameters such as the time, velocity and amplitude of the cornea to first applanation, point of highest concavity and second applanation. In a cross-sectional study, eyes with POAG were found to have a smaller corneal deformation amplitude, peak distance of the corneal applanation, and the time to second applanation (Tian et al. 2016). However, a follow-up study reported that the corneal deformation amplitude to be higher in advanced glaucoma compared to mild disease, though the difference in topical glaucoma medications between the groups precluded from any inferences relating to corneal biomechanics (Jung et al. 2017). In another cross-sectional study of medically controlled glaucomatous eyes, a lower first and second applanation times, a smaller radius of deformed cornea, and a shorter whole eye movement were associated with glaucoma, relative to normal eyes (Miki et al. 2019). These results suggest that glaucomatous eyes on topical medications appear to be more deformable than healthy eyes (Miki et al. 2019). Clinical application of Corvis ST parameters has so far been limited, with the majority of studies being retrospective association studies, and have not taken into accounting the confounding effects of topical glaucoma drops, IOP, and CCT (W. Wang, Du, and Zhang 2015). Furthermore, as Corvis ST is a relatively new device, the clinical interpretation and relevance of the majority of the measured parameters is lacking (Reznicek et al. 2013; Miki et al. 2019). However, Corvis ST presents an opportunity to closely investigate corneal biomechanics in glaucoma, and further studies are needed to take advantage of its capabilities in assessing corneal biomechanics.

Several other ocular features are known risk factors of glaucoma progression (Ernest et al. 2013). Particularly, a worse baseline glaucomatous visual field, such as a higher visual field pattern standard deviation or glaucomatous visual field loss of both eyes, are predictive of

further progression (Ernest et al. 2013; Leske et al. 2007; Founti et al. 2020; T. C. W. Chan et al. 2017). The presence of pseudoexfoliation syndrome is also thought to be a risk factor of glaucoma progression which is primarily attributable to the higher IOP observed in this secondary form of open-angle glaucoma (Ernest et al. 2013). A high myopia, defined by spherical equivalent of -6 diopters or worse, is also thought to be associated with visual field progression (Y. A. Lee et al. 2008), although the evidence of refractive error on a continuous scale (e.g. spherical equivalent measurements) as a risk factor for glaucoma progression is lacking (Founti et al. 2020; Leske et al. 2007; Ernest et al. 2013; Teng et al. 2010; K. Nouri-Mahdavi et al. 2004).

The presence of comorbid cardiovascular disease is an emerging systemic risk factor of glaucoma progression. In the long-term follow-up report of the EMGT cohort, a self-reported history of cardiovascular disease was a significant predictor of visual field progression in those with a higher baseline IOP (hazard ratio = 2.8, 95% CI 1.4–5.3) (Leske et al. 2007; S. L. Graham et al. 1995). In the low baseline IOP subgroup, a lower systolic blood pressure on follow-up was associated with visual field progression, which may be related to a nocturnal blood pressure dip leading to ocular hypoperfusion (Leske et al. 2007). These findings were not apparent at the initial report of the EMGT results (Leske et al. 2003). In a retrospective study assessing risk factors of a rapid visual field progression (rates of visual field mean deviation exceeding -1 dB/year), a history of cardiovascular disease was reported more commonly in the rapid progressors than the non-rapid progressors (56% vs 32%) (T. C. W. Chan et al. 2017). These associations were not reproduced in the UKGTS, as neither cardiovascular diseases as a group, nor individual diseases were significantly different amongst those who progressed compared to those who did not (Founti et al. 2020). Interestingly, a history of smoking was found to be protective of glaucoma progression in this study (hazard ratio = 0.59; 95% CI 0.37–0.93), which if true, may be attributable to a neuroprotective effect of nicotine or other substances found in cigarettes (Founti et al. 2020; Breckenridge et al. 2016).

Obstructive sleep apnoea (OSA) is a common sleep disorder that causes repetitive upper airway closure (leading to raised intrathoracic and intraocular pressures) and nocturnal hypoxia. Systemically, OSA is an independent risk factor of cardiovascular disease and hypertension (Yaggi et al. 2005). In a population-based control-matched study of an insurance database from Taiwan, a history of OSA was associated a higher incidence of developing open-angle glaucoma within 5-year (hazard ratio adjusted to baseline demographics and comorbidities = 1.67; 95% CI 1.30–2.17) (C.-C. Lin et al. 2013). This finding was further supported by a meta-analysis showing OSA to be associated with glaucoma, with a pooled

odds ratio ranging from 1.4 to 1.7 (Shi et al. 2015). The postulated mechanism linking OSA and glaucoma is that the nocturnal hypoxia in OSA leads to additional hypoxic injury in an already vulnerable optic nerve head found in glaucoma, particularly normal tension glaucoma (Shi et al. 2015). This is supported by several studies showing that the peripapillary RNFL is thinner in individuals with a moderate to severe OSA (J. S. Wang et al. 2016; S. S. Y. Lee et al. 2019). Whether OSA is also a risk factor for glaucoma progression is unclear.

In a retrospective analysis of 32 participants enrolled in a polysomnography database (a sleep study registry) who also had a diagnosis of glaucoma, moderate to severe sleep apnoea was significantly associated with RNFL progression, defined by a statistically significant negative linear slope (Y. Y. Fan et al. 2019). RNFL progression was reported to be present in 65% of the individuals with moderate to severe OSA, compared to 27% in those with no or mild OSA, a statistically significant difference (Y. Y. Fan et al. 2019). Another retrospective study investigated the effect of OSA of visual field progression comparing 15 POAG patients with OSA to 109 POAG patients without OSA (Yamada et al. 2018). The group with OSA was found to have a faster visual field mean deviation slope compared to the group without OSA in univariate analysis (-1.61 dB/year vs -0.26 dB/year, which was statistically significant) (Yamada et al. 2018). These findings were not supported in another study of 25 POAG patients with OSA, where the OSA severity did not correlate with the visual field rate of change, or a binary outcome of glaucomatous visual field progression (Swaminathan et al. 2018). These studies were limited by a retrospective design, a small sample size, and a poor characterisation of the glaucoma phenotype. Glaucoma is a highly heterogeneous disease that remains undiagnosed in the community (Paul Mitchell et al. 1996), and a definite clinical diagnosis requires detailed examination and phenotyping. Similarly, OSA is difficult to diagnose accurately without a formal sleep study, and remains undiagnosed in a majority of affected individuals (Bearpark et al. 1995). This could explain why a self-reported history of sleep apnoea was not associated with glaucoma progression the UKGTS study (Founti et al. 2020). Therefore, a study design with a more comprehensive clinical assessment of POAG and OSA is needed to address these limitations and investigate OSA as a potential risk factor in glaucoma progression.

In summary, elevated IOP and older age are two of the most well recognised risk factors for glaucoma progression (Ernest et al. 2013). Several other ocular and systemic factors are emerging as potential risk factors for glaucoma progression (Blumberg, Skaat, and Liebmann 2015). Corneal biomechanics has long been thought be important in glaucoma (Wolfs et al. 1997; Herndon et al. 1997; Gordon et al. 2002), and newer devices such as the Ocular Response Analyzer and Corvis ST have allowed a more detailed examination of these

biomechanical factors in the context of progression risk prediction (Luce 2005; Hong et al. 2013). Systemically, cardiovascular diseases have gained increasing momentum as potential risk factors in glaucoma progression; whether these associations are attributable to the ocular manifestations of the cardiovascular diseases or to the confounding treatments such as antihypertensive medications is not yet known (Wey et al. 2019; Yoshikawa et al. 2019; H. Marshall et al. 2020; Chong et al. 2020). An effective clinical glaucoma progression risk stratification would enable a focused attention and resource allocation to individuals at the highest risk of glaucomatous vision loss, and may guide clinical practice to an earlier intervention in such individuals.

The role of genetics in primary open angle glaucoma

There is a strong genetic contribution to the risk of developing glaucoma, and particularly POAG (Janey L. Wiggs and Pasquale 2017). In a population-based familial aggregation study from the Rotterdam study, first-degree relatives of glaucoma patients were reported to have 9 times the risk of developing glaucoma compared to relatives of controls (Wolfs et al. 1998). In a population-based prevalence survey from Baltimore, a positive family history of glaucoma was a significant risk factor for a diagnosis of POAG, which was strongest when the family history was from affected siblings than other family members (J. M. Tielsch et al. 1994). In an extensive study of insurance claims in the US involving over one third of the entire US population, glaucoma was found to be one of the most heritable common human diseases, more so than cardiovascular diseases and cancers (K. Wang et al. 2017). In this study, the genetic heritability of glaucoma was estimated to be about 70%, which was ranked as the third most heritable disease out of the 149 studied diseases (K. Wang et al. 2017). This is in keeping with the fact that there are currently no known environmental factors that are clearly associated with POAG (Pasquale and Kang 2009).

Linkage studies, in combination with Sanger sequencing, have identified rare but highly penetrant variants in genes associated with POAG, such as myocilin (*MYOC*) (Stone et al. 1997), optineurin (*OPTN*) (Rezaie et al. 2002), and TANK binding kinase 1 (*TBK1*) (Fingert et al. 2011). In contrast to *MYOC* and *OPTN* where pathogenic variants are implicated, copy number variants of *TBK1* (duplication or triplication) are implicated in causing glaucoma via a gain of function mechanism (M. S. Awadalla et al. 2015; Janey L. Wiggs and Pasquale 2017; Fingert et al. 2011). Variants in these genes cause glaucoma in a familial pattern with an autosomal dominant mode of inheritance with incomplete age-related penetrance (Janey L. Wiggs and Pasquale 2017). These genetic variants are highly relevant to the patients and their families; however, only 6% of the overall POAG cases are attributable to well defined highly

penetrant genetic variants in Mendelian genes (Fingert et al. 1999; W. L. Alward et al. 2003). In contrast to POAG, variants in Mendelian genes play a much bigger role in juvenile early age of onset glaucoma where they account for nearly a third of the cases (J. L. Wiggs et al. 1998; E. Souzeau et al. 2013).

The effects of Mendelian variants on POAG phenotype have been well described. Pathogenic variants in the *MYOC* gene are most commonly associated with high IOP and more advanced disease (E. Souzeau et al. 2017). In a study of 73 individuals with *MYOC* variants enrolled in a glaucoma registry who were initially diagnosed clinically (as opposed via genetic screening), the mean age of diagnosis was 48 years-old, which was significantly younger than non-Mendelian POAG (E. Souzeau et al. 2017). These *MYOC* carriers had significantly elevated IOPs with a mean highest recorded IOP of 32 mmHg, and had moderate to advanced visual field loss on presentation with an average visual field mean deviation of -10 dB (E. Souzeau et al. 2017). In contrast, duplications and triplications involving *TBK1* and missense variants in *OPTN* cause familial normal tension glaucoma, and are typically not found in high tension glaucoma (Aung et al. 2005; M. S. Awadalla et al. 2015; Ariani et al. 2006). In a study of 11 glaucoma patients with a missense *OPTN* p.E50K variant, the mean highest recorded IOP was 16.5 mmHg, with all individuals having normal tension glaucoma (i.e., clinically measured IOP no higher than 21 mmHg at any time) (Aung et al. 2005). The age of glaucoma diagnosis was also significantly younger to other individuals with normal tension glaucoma, with a mean age of diagnosis of 41 years (Aung et al. 2005). Similar to the pathogenic *MYOC* variant carriers, the majority of the individuals with *OPTN* p.E50K had moderate to advanced glaucomatous visual field loss on presentation, with an average visual field mean deviation of -16 dB (Aung et al. 2005). The clinical phenotype of individuals with copy number variants of *TBK1* is similar to the *OPTN* p.E50K carriers, with a mean age of diagnosis of 45 years in one study, and a mean highest recorded IOP of 14 mmHg (M. S. Awadalla et al. 2015).

The vast majority of POAG cases have no known pathogenic genetic variants implicated, even when familial aggregation is present (Janey L. Wiggs and Pasquale 2017). Family-based linkage studies require large and well-characterised pedigrees to identify disease-causing variants. Massive parallel sequencing (sometimes referred to as next-generation sequencing) allows a high throughput analysis of the whole, or parts of the genome via parallel sequencing of millions of small DNA fragments (Behjati and Tarpey 2013). One example of this technique is whole exome sequencing, where hypothesis-free bioinformatic analysis can be conducted in a case-control setting to identify potential disease-associated coding variants. The primary limitation of this approach is the relatively high cost of sequencing and bioinformatic analysis — although this is increasingly becoming more affordable — compounded by the need of large

sample sizes (e.g. 100–1000s of cases and controls) to identify variants at a statistically acceptable level of significance (Atwal et al. 2014; R. Do, Kathiresan, and Abecasis 2012).

While whole exome sequencing in glaucoma genetics is still at its infancy, several studies have implicated new genetic variants to be potentially associated with glaucoma. Applications of whole exome sequencing in glaucoma has so far primarily focused on the discovery of genes involved in congenital glaucoma, usually associated with anterior segment dysgenesis or craniofacial abnormalities (Ferre-Fernández et al. 2017; Lim et al. 2013; Micheal et al. 2016; Reis et al. 2016). Early application of whole exome sequencing in POAG implicated unfolded protein response and plasma membrane homeostasis pathways to be involved in the pathogenesis of POAG (T. Zhou et al. 2017). An exome variant analysis near glaucoma-associated loci previously identified in common variant genome-wide association studies has implicated *CARD10* (Caspase Recruitment Domain Family Member 10) to be enriched in POAG cases, a gene involved in the regulation of cellular apoptosis (T. Zhou et al. 2016). Whole exome sequencing can also be used to further investigate known pathogenic variants in larger cohorts. For example, whole exome sequencing of 1,333 normal tension glaucoma cases has implicated *MYOC* p.Gln368Ter variant to be involved in normal tension glaucoma, whereas *MYOC* was traditionally thought to be associated primarily with high tension glaucoma cases (Janey L. Wiggs and Pasquale 2017; W. L. M. Alward et al. 2019).

In an exome-wide association study of 398 Han Chinese POAG individuals and 2,010 controls, potentially pathogenic rare variants in *RAMP2* (Receptor Activity Modifying Protein 2) were implicated in 0.34% of the POAG cases (Gong et al. 2019). *RAMP2* is involved in cellular receptor transportation, and in a follow-up functional investigation, ablation of one *RAMP2* allele in mice led to retinal ganglion cell death (Gong et al. 2019). In another whole exome sequencing study, *PMEL* (Premelanosome Protein) was implicated in the pathogenesis of pigment dispersion syndrome, a secondary cause of open-angle glaucoma (Lahola-Chomiak et al. 2019). *PMEL* encodes a key component of the melanosome, the organelle essential for melanin synthesis, storage and transport, which may be related to the pigment release in anterior chamber seen in this syndrome (Kobayashi et al. 1994). Functional deletion of this gene in a zebrafish model resulted in pigmentation defects and anterior segment enlargement, which was postulated by the authors to be related to pathology of pigment dispersion syndrome (Lahola-Chomiak et al. 2019). The potential role of these variants in glaucoma risk or pathogenesis require further investigation, particularly a replication in independent cohorts.

Whole genome genotyping (using DNA microarrays) is an alternative method of identifying genetic variants associated with a disease that is significantly more affordable and readily

available than whole genome or exome sequencing, although genotyping is usually limited to single nucleotide variants (X. Chen and Sullivan 2003). This can be used to perform a hypothesis-free genome-wide association study (GWAS) of common variants with glaucoma using a case-control study design. A few million single nucleotide variants are found in each person's unique genetic sequence, bearing in mind that the majority are not thought to be associated with any disease (Abecasis et al. 2010).

Only relatively common variants — with allele frequency of at least 5% — are statistically confidently discovered to be associated with a trait in GWAS, although increasing sample sizes will improve the ability to detect robust associations with rarer variants. The earliest replicated common variant that was identified to be associated with POAG in GWAS was a locus near *CAV1* and *CAV2* (Thorleifsson et al. 2010). Subsequent GWAS have identified additional POAG-associated loci near or at *TMCO1*, *CDKN2B-AS1* and *SIX6*, amongst others (J. L. Wiggs et al. 2012; K. P. Burdon et al. 2011; P. Gharahkhani et al. 2014). These common variants have small effect sizes individually, and explain a small proportion of POAG heritability, estimated to be around 5% (A. P. Khawaja and Viswanathan 2018).

Despite this, several studies reported correlation between individual variants and glaucoma progression. In a hypothesis driven study, 142 POAG patients with a minimum of 8 years of follow-up from one hospital were tested for a common variant in the *MYOC* promoter region (c.-1000C>G), which was found in 14% of the cohort (Colomb et al. 2001; Polansky, Juster, and Spaeth 2003). In a retrospective event analysis of time to progression by optic disc or visual field criteria, carriers of the *MYOC* c.100C>G variant were found to be at a higher risk of progression (hazard ratio was not reported in the original manuscript) (Polansky, Juster, and Spaeth 2003). This study design was limited by *a priori* selection of the genetic risk variant, retrospective recruitment, genotyping and analysis, and a lack of replication. Indeed, a follow-up meta-analysis failed to show the association between this variant with POAG, and raised the possibility of publication bias (T. Liu et al. 2008). While these limitations preclude generalisability and clinical application of the findings, this early study highlighted that common genetic variants could potentially influence glaucoma progression.

In a cohort with mixed ethnicities (though primarily of Asian ancestry), Li et al. (2015) identified a common variant near *TGFBR3-CDC7* to be associated with POAG. Of note, this locus was previously reported to be strongly associated with the optic disc area (Khor et al. 2011), which may limit its predictive utility for POAG given that a higher amount of optic nerve cupping may be physiological in individuals with larger optic discs (Crowston et al. 2004). A single-hospital study of 469 Chinese POAG patients from Singapore reported that a common genetic variant

in *TGFBR3-CDC7* was associated with glaucomatous visual field progression (Trikha et al. 2015). None of the other 9 loci known to be associated with POAG at the time were significantly associated with progression (Trikha et al. 2015). This result failed to replicate in another study of 440 Chinese POAG patients, where none of the known common variants were associated with glaucoma progression (Y. Chen et al. 2018). A later GWAS of POAG and optic nerve head parameters identified the *TGFBR3-CDC7* locus to be primarily associated with optic disc size and VCDR (H. Springelkamp et al. 2017). Interestingly when the optic disc size was adjusted for, the association between this locus and VCDR was negligible, suggesting that it is unlikely to be a significant POAG risk locus (H. Springelkamp et al. 2017).

A variant near *TMCO1* was one of the earliest and most strongly associated POAG susceptibility loci identified (K. P. Burdon et al. 2011). Carriers of this common risk variant — with an allele frequency of 11% to 14% in European ancestry individuals — were at 68% increased risk of developing POAG relative to non-carriers (95% CI of odds ratio 1.43–1.98) (K. P. Burdon et al. 2011). In another study, this risk variant was associated with an earlier age of POAG diagnosis where carriers were diagnosed 2–3 years younger than non-carriers (Sharma et al. 2012). The *TMCO1* locus is strongly associated with a raised IOP, which is likely the pathway by which it leads to a higher POAG risk (H. Springelkamp et al. 2017). In a subset of the non-Hispanic white OHTS participants who had undergone genotyping (752 individuals with ocular hypertension, representing 46% of the original study participants), carriers of the risk allele near *TMCO1* had a 12% higher cumulative frequency of developing glaucoma than non-carriers (odds ratio per risk allele = 1.73, 95% CI 1.28–2.34) (Scheetz et al. 2016). This association was not significant when the whole cohort was analysed together (Scheetz et al. 2016). This study also reported a lack of significant association of the aforementioned *TGFBR3-CDC7* locus with progression (Scheetz et al. 2016; Trikha et al. 2015). No other single locus was associated with progression to established glaucoma in this study (Scheetz et al. 2016). Replication of the *TMCO1* findings is needed, particularly in those with POAG rather than ocular hypertension. In the aforementioned study in Chinese POAG patients by Chen et al. (2018), none of the POAG loci, including that near *TMCO1*, were associated with visual field progression.

The relative lack of understanding of glaucoma pathogenesis has been a major obstacle to predicting glaucoma progression and severity, particularly when patients are in the early stages. The high heritability of POAG coupled with the natural history of disease progression and the effectiveness of treatment makes POAG an ideal candidate for further genetic studies to identify causative or susceptibility genetic loci, and to better understand the genetic

architecture of POAG onset and progression and identify individuals at high risk of developing glaucoma or progressing to blindness. A better understanding of the biological mechanisms underpinning POAG is desperately needed and will help optimise the timing and intensity of interventions for the individual, as well as screening and targeting therapy to high risk populations, preventing visual field loss and its associated morbidity.

The rapid development of genomics in recent years has substantially accelerated our understanding of the genetic architecture of many complex diseases. The increased affordability and throughput of genomic arrays, development of better tools to process genomic data, and the availability of increasingly large public datasets has allowed an unprecedented exploration of human genomic variation.

The clinical utility of polygenic risk scores in ophthalmology

The text in the following section is part of a larger manuscript currently published in *TVST* (in press) titled Risk stratification and clinical utility of polygenic risk scores in Ophthalmology, where I am the first author. The content has been edited to fit the structure of the thesis.

A better understanding of an individual's risk of disease, the severity of disease in those who develop it, and their response to therapy are cornerstones of personalised medicine — the notion that screening, management and interventions can be tailored specifically to an individual, or at least stratified across groups of similar individuals. This section will focus on the polygenic risk model of diseases, and its application in ophthalmology with a particularly focus on POAG,

Monogenic or Mendelian diseases are primarily driven by alterations in a single gene. These genetic variants are typically rare but have a high effect size and penetrance, meaning that they generally confer a high risk of developing the associated disease. This is exemplified by variants in the previously discussed *OPTN* and *TBK1* genes leading to familial normal tension glaucoma with highly penetrant autosomal dominant inheritance (Rezaie et al. 2002; Fingert et al. 2011).

In contrast, complex diseases have a polygenic genetic architecture which may involve hundreds or thousands of contributing genes (Timpson et al. 2018). In these common complex diseases, each genetic variant has a relatively small effect and does not lead to the disease by itself. Therefore, the discovery of these disease-associated genomic variants requires studies of large cohorts, especially for common variants with very small effect sizes. This is

commonly the result of GWAS where millions of genetic variants are studied across many thousands of individuals for association to a disease or trait. It is important to note that individual single nucleotide polymorphisms (SNP) discovered by GWAS are relatively common in the normal population, often with a minor allele frequency above 5%. That is, these variants are present in at least 5% of the normal population if heterozygous, or slightly lower proportions accounting for homozygous people; thus, the study of disease association of these variants requires a large and ideally, well phenotyped cohort. Disease association for rarer variants requires a different approach such as linkage mapping or whole exome sequencing of families with the same rare disease. Many common adult-onset diseases have polygenic as well as environmental contributions, including POAG, age-related macular degeneration (AMD), type 2 diabetes, dyslipidemia and coronary artery disease (Dron and Hegele 2019; Inouye et al. 2018; Timpson et al. 2018; Janey L. Wiggs and Pasquale 2017; Fritsche et al. 2016). For example, while there is a strong genetic contribution to AMD risk, smoking has been well established as a key modifiable environmental risk factor for the development and progression of AMD (Vingerling et al. 1996; Chakravarthy et al. 2007).

While each SNP explains only a small proportion of genetic risk and heritability, the additive effects of tens, hundreds or up to hundreds of thousands of SNPs in some studies amount to a risk equivalent to a single monogenic variant (Khera et al. 2018). Furthermore, common variants of very small effect sizes are difficult to isolate statistically from noise in GWAS, yet they still contribute to disease risk and account at least partially for the missing heritability unexplained by the currently discovered variants (J. Yang et al. 2010). As larger studies discover additional loci (Inouye et al. 2018; MacGregor et al. 2018; Fritsche et al. 2016), it is evident that SNPs with small effect sizes conjointly play a significant role in genetic risk (Boyle, Li, and Pritchard 2017). The complex interplay of these genetic networks and the effect of one locus on multiple phenotypes (termed pleiotropy), likely due to their involvement in a shared biological pathway, as well as environmental influences are important in the development of complex traits (Boyle, Li, and Pritchard 2017; Pickrell et al. 2016).

A polygenic risk score (PRS), sometimes referred to as a genetic risk score, is a quantitative probabilistic summary of an individual's genetic susceptibility to a disease or trait (Figure 1.4). In its simplest form, it is a sum of the number of risk alleles carried by an individual (Chatterjee, Shi, and García-Closas 2016). More commonly, the variants are weighted by their magnitude of effect on the disease or trait (the estimated regression coefficient of the variant) based on the summary statistics of the GWAS (Chatterjee, Shi, and García-Closas 2016). This allows the risk score to reflect the effect size of the variants in addition to their total numbers, and therefore is a more accurate risk predictor.

Disease-associated SNPs included in a PRS are discovered via GWAS, where several million SNPs are statistically compared to a disease (case-control setting) or a phenotype. To minimise false discovery from multiple testing, a stringent genome-wide P-value threshold of 5×10^{-8} is used in discovery studies, and P-value adjustment methods such as Bonferroni correction are used for validation studies. However, SNPs with borderline significance not meeting the genome-wide threshold may still be associated with disease (Boyle, Li, and Pritchard 2017; Panagiotou and Ioannidis 2012), thus a PRS may improve the estimate of the 'true' genetic risk and predictive power by including a larger number of SNPs using more lenient statistical thresholds (Chatterjee, Shi, and García-Closas 2016). To account for correlated and co-inherited SNPs (said to be in high linkage disequilibrium [LD]), SNPs which are in high LD to others are usually excluded via P-value thresholding; alternatively, LD is modelled into the PRS mathematically using methods such as LDpred or lassosum (Vilhjálmsson et al. 2015; Mak et al. 2017).

When applied in a clinical context, the raw number of an individual's PRS (e.g. 12.395) is not intuitive to interpret, and so is better presented as their percentile risk relative to the normal population or study cohort (e.g. 90th percentile). For instance, a person in the 90^{th} percentile of a weighted PRS carries disease-associated alleles whose combined effect sizes (i.e. the genetic burden) exceeds that of 90% of the normal population or study cohort. A commonly used PRS stratification method is quintiles, where the bottom 20% is considered low risk, the top 20% as high risk, and the rest as intermediate risk (Inouye et al. 2018; Khera et al. 2018; Mega et al. 2015; A. Qassim et al. 2020). Similarly, tertile or decile groups may be used. Importantly, a PRS allows disease risk stratification but is never a diagnostic tool: its clinical utility is best achieved when combined with demographic and/or clinical factors usually evaluated in routine clinical risk assessment.

Authors sometimes seek to quantify the utility of a PRS using the area under the receiver operating characteristic curve (AUC). AUC is a summary statistic that indicates the discriminatory powers of a test to differentiate a binary outcome or set of categories. Mathematically, it is calculated as the area under the curve fitted to all the test sensitivities for each corresponding specificity (often one minus specificity). It can be used to set an optimal test threshold for maximised sensitivity or specificity. Although commonly reported in the PRS literature, the AUC has been justifiably criticised due to its lack of clinical interpretation. It is a metric of test performance in the study cohort and does not inform the individual about their risk, nor does it quantify the magnitude of risk (Pepe and Janes 2008). Furthermore, from the clinical point of view, PRS is best suited as a genetic disease risk probability index as opposed

to a diagnostic test implied by the dichotomous end-point commonly used in AUC calculations. In the case of aging diseases such as POAG and AMD, a further limitation of the AUC strategy is the uncertain likelihood of younger individuals developing the disease in question later in life. Instead, the utility of the PRS can be reported by how informative it is in identifying high-risk individuals compared to low-risk or average-risk individuals. This can be done by reporting the odds ratio of developing the disease between the genetic risk groups, or additionally, by reporting the PRS association to a disease specific metric such as the age of diagnosis, or severity measure.

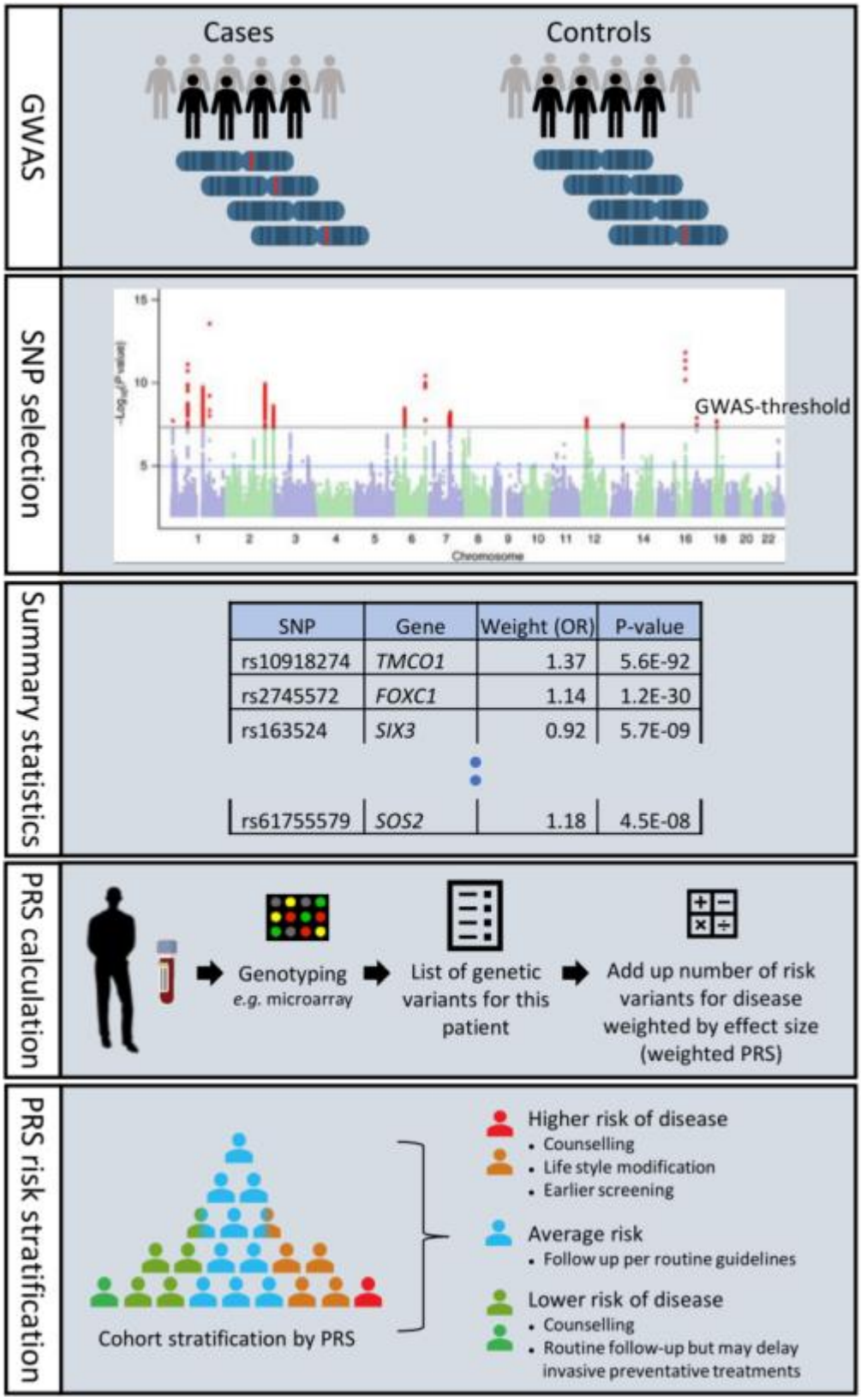

Figure 1.4. Development and clinical utility of a polygenic risk score for a sample disease.
GWAS: genome-wide association study. PRS: polygenic risk score. SNP: single-nucleotide variant; OR: odds ratio.

The clinical utility of PRS relies on its ability to effectively identify individuals who would benefit from modified screening approaches for disease detection (frequency or age threshold for screening tailored to risk group) or interventions for disease management or progression (e.g. prioritisation of therapeutic interventions, and management of risk and benefits of interventions). In non-ophthalmic diseases, the clinical utility of PRS has been mainly reported in cardiovascular diseases, cancers and psychiatric conditions (Hsu et al. 2015; Khera et al. 2018; Mavaddat et al. 2019; Mistry et al. 2018; Rutten-Jacobs et al. 2018). For instance, disease risk stratification by PRS is effectively able to identify individuals at the highest risk of developing coronary artery disease, stroke, atrial fibrillation and type 2 diabetes (Khera et al. 2018; Rutten-Jacobs et al. 2018). This allows early intervention with lifestyle modification or medications which has been shown to attenuate disease risk in high-risk individuals (Fang et al. 2019; Khera et al. 2016; Rutten-Jacobs et al. 2018). For example, statin therapy has a greater absolute risk reduction of primary coronary heart events in high-risk PRS individuals than intermediate or low-risk groups (Mega et al. 2015). Furthermore, screening programs, particularly for breast and colorectal cancers, can be effectively personalised to the individualised risk based on PRS and demographic stratification (Weigl et al. 2018; Mavaddat et al. 2019).

The clinical utility of PRS has also been demonstrated in common ophthalmic conditions. Fritsche et al. (2016) reported an AMD PRS including 52 AMD-associated SNPs, where individuals in the highest decile had a 44-fold higher risk of developing advanced AMD relative to the lowest decile. PRS was also informative of the risk of AMD progression whereby in one study, 50% of individuals at the highest quartile of the PRS had clinical AMD progression compared to 7% and 22% in the lowest quartile and intermediate group respectively (Ding et al. 2017). In the setting of myopia, PRS is predictive of severity; for instance, Mojarrad et al. (2019) reported that individuals in the highest risk decile of a myopia PRS had 6.1-fold (95% CI 3.4–10.9) higher risk of developing high myopia relative to the rest. This may be of particular clinical significance, as high myopia is associated with complications that can lead to irreversible vision impairment, most commonly due to myopic macular degeneration (V. J. Verhoeven et al. 2015).

The study of the genetic architecture of POAG has been complemented by genetic association studies of related ocular traits associated with POAG — termed *endophenotypes* — namely IOP and optic disc nerve head morphology such as the VCDR (H. Springelkamp et al. 2017). POAG and its endophenotypes are highly heritable with heritability estimates ranging from 0.5 to 0.7 for the glaucoma endophenotypes and POAG respectively (MacGregor et al. 2018; A. P. Khawaja et al. 2018).

The high heritability of POAG and its correlated endophenotypes, in addition to the effectiveness of early intervention (e.g. topical medications, laser, or incisional surgery) to prevent otherwise irreversible vision loss, has made POAG a focus of PRS stratification. The earliest studies have demonstrated significant but modest discriminatory powers for a glaucoma PRS (F. Mabuchi et al. 2017; Y. C. Tham et al. 2015; Zanon-Moreno et al. 2017). In 2015, Tham et al. (2015) developed a glaucoma PRS combining 7 IOP-associated and 18 VCDR-associated SNPs known at the time, and reported a modestly higher odds of developing POAG in the top tertile of the PRS relative to the bottom tertile in a multi-ethnic cohort from Singapore (IOP-PRS odds ratio = 2.50, 95% CI 1.54–4.02; VCDR-PRS odds ratio = 2.31, 95% CI 1.50–3.55). Mabuchi et al. (2017) conducted an unweighted PRS utilising 9 IOP-associated SNPs in a Japanese cohort and reported a modest association with higher tension POAG (odds ratio per risk allele = 1.12; 95% CI 1.01–1.24). These early studies were limited by including only a small number of SNPs in the PRS and applying it to relatively small POAG cohorts. Moreover, Mabuchi et al. did not weight the loci effect size — an approach now superseded by weighted PRS (Chatterjee, Shi, and García-Closas 2016).

Backed up by larger GWAS, recent glaucoma PRS studies have utilised an increasingly larger number of variants associated with POAG and its endophenotypes. MacGregor et al. (2018) generated a PRS using 101 IOP-associated SNPs and 2 previously reported VCDR-associated SNPs, and showed that the top PRS decile of an independent Australian case-control glaucoma cohort had a significantly higher risk of POAG relative to the bottom decile (odds ratio = 5.6, 95% CI 4.1–7.6). This magnitude of risk was previously only reported for rarer monogenic variants (X. Han et al. 2019). Gao et al. (2019) constructed an inclusive PRS using 1,691 SNPs associated with IOP using a more lenient statistical threshold ($P < 5x10^{-5}$) and reported a 6-fold higher POAG risk in the top quintile relative to the bottom quintile of an independent subset of the study cohort (odds ratio = 6.34, 95% CI 4.82–8.33). While this improved risk prediction may be attributed to a more inclusive SNP selection in the PRS, it should be noted that a limitation of this study was that the test cohort and the GWAS discovery cohort were both from the same population study (UK Biobank); a validation in an independent POAG cohort may yield lower risk predictions.

Another PRS constructed from 68 VCDR-associated SNPs applied to a Latino population showed a relatively modest risk of POAG (odds ratio = 1.75, 95% CI 1.09–2.81 for the top quintile relative to the bottom quintile) (Nannini et al. 2018). This is likely due to input SNPs being derived from GWAS of primarily European and Asian ancestries, which are unlikely to capture all risk variants relevant to the Latino population. Additionally, VCDR-associated

variants alone have a lower discriminatory power in identifying POAG and highlights the importance of utilising multiple glaucoma endophenotypes at a more inclusive statistical threshold. Another POAG PRS study that utilised 12 POAG-associated SNPs reported a younger age of POAG diagnosis to be predicted by the PRS (5 years younger on average in the top 5% of the PRS relative to the bottom 5%) (B. J. Fan et al. 2019).

There were significant gaps in knowledge in the glaucoma PRS literature prior to my thesis. Previously reported PRS were limited to a small selection of SNPs that significantly underestimated the genetic risk of glaucoma. Additionally, the variants included in the scores were limited to one endophenotype and did not utilise variant weighting or improved statistical variant selection (e.g. P-value thresholding). Importantly, the clinical implication and utility of glaucoma genetic risk stratification using PRS was not explored in detail, nor validated in other datasets. At the start of my PhD, I hypothesised that a more comprehensive glaucoma PRS may be used to personalise glaucoma monitoring and management in high-risk compared to average or low-risk individuals.

Conclusion

The natural history of POAG is a progressive retinal ganglion cell death that leads to irreversible blindness. Treatment is highly effective in slowing disease progression, or the onset of glaucoma in the setting of ocular hypertension. However, a majority of glaucoma suspects or those with early glaucoma do not lose a meaningful amount of visual field for many years, if at all. In contrast, a minority of patients present with a rapidly progressing vision loss requiring intensive follow-up and treatment. There is currently a gap in knowledge regarding the known risk factors that are associated with glaucoma progression, with a raised IOP being the most important and only modifiable risk factor. Thus, the current best practice is to routinely follow-up all glaucoma suspects with a detailed assessment at each visit to quantify disease trajectory, which causes a significant cost to the health care system.

Glaucoma is one of the most heritable common human diseases, with an additional significant genetic contribution to its endophenotypes such as IOP and optic nerve head morphology. Polygenic risk scores are a powerful tool in disease risk stratification, and prognostication in common complex diseases. The ideal clinical use scenario is in conditions with high clinical utility, such as where early intervention can alter the natural history of the disease and reduce morbidity or mortality. This makes POAG an ideal case scenario for the application of genetic risk stratification using polygenic risk scores, which could guide screening programs, follow-up intensity, and early treatment. The body of this thesis explores novel clinical and genetic

risk factors that are associated with the risk of development and progression of glaucoma, with a focus on polygenic risk scores, IOP-lowering interventions, and corneal biomechanics.

Chapter 2: Methods

Introduction

There are several interconnected studies in this thesis exploring genetic and clinical risk factors associated with glaucoma progression. Each study has a unique design, sample selection outcome measures, and analytical techniques which are reported in the corresponding chapter. Cohort descriptions and recruitment strategies, and overlapping methodologies are summarised in this chapter for reference.

All studies reported in this thesis sampled participants from a glaucoma registry (ANZRAG) or a longitudinally monitored glaucoma cohort (PROGRESSA). A large population study, the UK Biobank, was also used in genome-wide association studies and in generating the polygenic risk scores. Several studies aimed to investigate an association between clinical and genetic risk factors and glaucoma progression. The definition of glaucoma progression is not consistent in the literature and depends on the clinical context. Various definitions are detailed in this chapter with reference to the definitions used in this thesis. Finally, a consistent approach to data analysis and statistical hypothesis testing was used throughout the thesis and summarised herein.

Description of study cohorts

Throughout this thesis, data from three major studies were used. Participant characteristics, enrollment process, and follow-up protocols are detailed below for each study.

Progression Risk Of Glaucoma: RElevant SNPs of Significant Association (PROGRESSA)

PROGRESSA is a longitudinal, multi-centre Australian study following up early glaucoma cases or glaucoma suspects to establish clinical and genetic risk factors for glaucoma progression. Participant enrollment began in 2012, with an initial aim of recruiting subjects for 6-monthly follow-up over a 5 year period. Additional funding and interest has allowed the study to continue monitoring participants as long as clinically indicated. Recruitment is currently ongoing at the time of writing, with over 1,700 participants enrolled.

Participants were recruited at several public and private ophthalmology practices across three states in Australia (South Australia, New South Wales and Tasmania). The key recruitment criteria include an optic nerve head appearance suspicious or probable for glaucoma based on the disc damage likelihood scale, and an open angle on gonioscopy (Bayer et al. 2002). Briefly, the neuroretinal rim width was assessed with slit lamp biomicroscopy or stereo

photography in relation to the optic disc size. The thinnest width of the neuroretinal rim was used to grade an optic disc for risk of glaucoma in reference to the optic disc size (i.e., rim to disc ratio). Additional inclusion criteria were: age between 18 and 85 years; an ability to provide written consent; and an ability to attend 6-monthly visits for a minimum of 5 years. Exclusion criteria at recruitment included: an inability to perform reliable visual field testing; mean deviation worse than -6.0 dB; best corrected visual acuity worse than 6/18 in either eye; angle closure; or the presence of other non-glaucomatous conditions that affect the visual field. At enrollment, blood samples were taken for genotyping on HumanCoreExome arrays (Illumina, San Diego, CA, USA).

Extended clinical information was collected at enrollment, then more briefly at each visit every 6 months. Initially, a detailed medical and ophthalmic history was taken with a specific focus on cardiovascular and vasospastic diseases, as well as a detailed medication record. Self-reported family history of glaucoma was recorded and summarised into the number of family members affected with glaucoma, and the relationship of the closest relative with glaucoma. There was no strict definition of a family member in terms of relative closeness (i.e. first, second or third degree), although a family tree of affected relatives was recorded. Ophthalmic examinations included best corrected visual acuity, IOP measured by Goldmann applanation tonometry, CCT measured by pachymetry (Pachmate DGH55; DGH Technology Inc, Exton, PA), gonioscopy, and optic disc examination. A dilated fundus examination, optic disc photography, and additional pachymetry were performed once every 12 months, while gonioscopy was performed at the initial visit and as clinically indicated thereafter.

Visual field assessment was performed at each visit. Participants performed Humphrey Visual Field (HVF; Humphrey Field Analyzer; Carl Zeiss Meditec; Dublin, CA) 24-2 Swedish Interactive Thresholding Algorithm Standard (SITA-Standard) at the baseline visit and each follow-up visit. Visual field grading of reliable HVFs — defined by rates of fixation loss, false positive, and false negative events less than 33% — was performed at the baseline visit and each subsequent visit. A reliable visual field test was considered abnormal if: the results of the glaucoma hemifield test (GHT) were “Outside Normal Limits”; and/or returned a global pattern standard deviation (PSD) of $P < 5\%$ (i.e., lower than 5% of the normative dataset); and/or there was a cluster of at least 3 contiguous points in the pattern deviation probability plot in a glaucoma region, all of which were depressed at a $P < 5\%$ level with at least one point depressed at $P < 1\%$ (i.e., a visual field location PSD lower than 1% of the normative dataset) (Hodapp-Parrish-Anderson criteria) (Hodapp, Parrish, and Anderson 1993; Anders Heijl 2002). Glaucomatous visual field regions were defined as paracentral, Bjerrum, nasal step, or temporal wedge in each hemifield. A second confirmatory HVF test was required to

demonstrate a cluster in the same glaucoma region with the same criteria described above. Alternatively, the second HVF test was considered confirmatory if it showed an abnormal PSD or GHT (as defined above) and there was a cluster in the same region of at least 3 contiguous points in pattern deviation probability plot all depressed at P < 5%. This criterion was used to categorise participants at baseline into two subgroups: glaucoma suspects when the baseline HVF was normal; and early manifest glaucoma when the baseline HVF was abnormal.

Ancillary tests for glaucoma monitoring included spectral domain OCT at each visit. OCT scans were performed using a Cirrus HD-OCT (Carl Zeiss Pty Ltd, Dublin, USA), and used to measure the thickness of the peripapillary RNFL, and the macular GCIPL. Scans were manually reviewed for segmentation errors and artefacts affecting thickness analysis, and such scans were excluded from longitudinal analysis (Mona S. Awadalla et al. 2018). Additionally, scans with quality scores <6 were excluded as recommended by the manufacturer. The longitudinal rate of change in RNFL and GCIPL thickness were measured (in µm per year). OCT Guided Progression Analysis was additionally used to assess for RNFL and GCIPL progression (detailed below).

All protocols were approved and monitored by the South Australian Southern Area Clinical Human Research Ethics Committee, Central Adelaide Local Health Network Human Research Ethics Committee, the Bellberry Human Research Ethics Committee, and NSW Macquarie University Human Research Ethics Committee. All participants provided written and informed consent once all of the risks and benefits were explained to them.

The Australian & New Zealand Registry of Advanced Glaucoma (ANZRAG)

ANZRAG is a clinical and genetic registry of glaucoma cases from Australia and New Zealand that was established in 2007 to identify genetic risk variants of severe or familial glaucoma. ANZRAG comprises participants across the whole spectrum of glaucoma, ranging from glaucoma suspects to end-stage glaucoma, and includes both open and closed angle glaucoma cases. However, as the early phases of recruitment focused mainly on advanced glaucoma cases with open angles, a majority of the current participants have advanced open-angle glaucoma. Recruitment methodology and cohort description have been described previously (Emmanuelle Souzeau et al. 2012), but will be summarised here for its relevance to this thesis, and to provide an update on the methodology since the previous publication. Recruitment for ANZRAG is currently ongoing at the time of writing.

Referral to ANZRAG was initiated through the participants' treating clinicians, however self-referral with subsequent verification of the clinical details through participants'

ophthalmologists was also allowed. Referral was initiated via a paper- or web-based submission, and details verified by registry staff. Diagnosis of glaucoma was clinical, based on optic nerve head appearance, IOP, and visual field testing, and was made by the referring ophthalmologist (Casson et al. 2012). Cases were classified as advanced glaucoma if the worst affected eye had a HVF mean deviation < -15 dB, or there was a marked loss of at least two of the four central visual field points on the pattern deviation probability plot (P < 0.5%). Additionally, glaucoma-related loss of central visual acuity was considered an advanced case if field testing was unable to be performed. Non-advanced glaucoma was defined by optic nerve head changes with corresponding visual field defects consistent with glaucoma, but not fitting the aforementioned criteria (Casson et al. 2012).

Details of clinical assessments were collected at the time of recruitment by the referring clinician. The type of glaucoma diagnosis including secondary or developmental forms of glaucoma and gonioscopic angle status was recorded. Family history of glaucoma was recorded as the number of family members affected by glaucoma, and the relationship to the closest relative with glaucoma. Additionally, the age of glaucoma diagnosis, self-reported ethnicity, best corrected visual acuity, maximum recorded pre-treatment IOP, refraction, CCT, vertical cup-to-disc ratio, and previous glaucoma surgeries were recorded. Clinicians were able to update the clinical records in the registry after recruitment, although this was not required.

Blood or saliva samples were collected from the participants at enrollment for genotyping. Genotyping in ANZRAG participants was performed over several stages through the course of recruitment and was performed using Illumina Omni1M, OmniExpress or HumanCoreExome arrays (Illumina, San Diego, CA, USA). Genotyping quality control, imputation, and association analyses were conducted separately for each phase before being meta-analysed for association studies. Human research ethics approval was obtained from the relevant committees of the Southern Adelaide Clinical Human Research Ethics Committee/Flinders University, the University of Tasmania, QIMR Berghofer Institute of Medical Research and the Royal Victorian Eye and Ear Hospital. Written informed consent was obtained from all participants in accordance with the Declaration of Helsinki.

UK Biobank (UKBB)

UKBB is a large-scale cohort study that included over 500,000 participants aged between 40-69 years in 2006–2010 from across the United Kingdom. Recruitment, genotyping and detailed phenotyping is described elsewhere.(Bycroft et al. 2018; Chua et al. 2019) The ophthalmic and genetic data relevant to this thesis are summarised here.

Ophthalmic data were collected by participant administered health questionnaires and ancillary testing in 2009–2010. Visual acuity and autorefraction were performed first, followed by IOP and corneal hysteresis measurements. One IOP measurement was taken for each eye using the Ocular Response Analyzer (Reichert, Philadelphia, Pennsylvania, USA). Monoscopic colour fundus photographs of the optic disc were also acquired (Topcon 3D OCT-1000 Mark II system). Of note, only a subset of the UKBB cohort underwent ocular phenotyping over two visits. In total, 127,850 individuals had IOP measurements and 82,911 had fundus photography.

Whole-genome genotyping was performed using DNA derived from blood samples on Axiom arrays covering 805,426 single nucleotide variants (Affymetrix Santa Clara, USA). After standard quality control procedures, ~96M genotypes were imputed using Haplotype Reference Consortium and UK10K haplotype resources (Bycroft et al. 2018; T. U. Consortium and The UK10K Consortium 2015; T. H. R. Consortium and the Haplotype Reference Consortium 2016). In the association analyses, single nucleotide polymorphisms with a minor allele frequency less than 0.01 or imputation quality score less than 0.3 were removed. All participants provided informed written consent. The study was approved by the National Research Ethics Service Committee North West – Haydock, and all study procedures were performed in accordance with the World Medical Association Declaration of Helsinki ethical principles for medical research.

Among the 487,409 individuals who passed initial genotyping QC, 409,694 participants were of white British ancestry, according to self-reported ethnicity and genetic principal components (Bycroft et al. 2018). To maximize the effective sample size for genetic analyses, UKBB participants with self-reported ancestry recorded as non-white British (including a substantial number of individuals reporting their ancestry as ‘Irish’ or ‘any other white background’), but with the first two genetic principal components within the region of those classified as white British in the n=409,694 set in Bycroft et al. (2018) were retained for analysis. With these criteria, 438,870 individuals were identified for genome-wide association studies who were genetically similar to those of white-British ancestry. Additional detailed information pertaining to the genotype data and quality control procedures has been reported by Bycroft and colleagues (2018).

Glaucoma progression definitions

In this thesis, I investigated clinical and genetic risk factors associated with glaucoma progression. However, there is no consensus 'gold standard' definition for glaucoma progression, and it remains largely a clinical decision. Several landmark glaucoma trials assessing glaucoma progression as the outcome have used different criteria as the measurement outcome.

In the The Ocular Hypertension Treatment Study, progression was defined by masked 'expert' reviews of serial optic nerve head photographs, or of visual fields that were abnormal on pattern standard deviation or glaucoma hemifield test (Gordon and Kass 1999). The Early Manifest Glaucoma Trial used masked review of flicker chronoscopy of optic disc photographs, or criteria-led visual field progression (Leske et al. 1999). An eye was deemed to be progressing if any three visual field locations were significantly different ($P < 5\%$) on "Progression Analysis Probability Plot" from the baseline 2 field tests based on a test-retest probability map that was developed specifically for the study (i.e., change in a visual field location threshold sensitivity that is expected less than 5% of stable glaucoma patients) (Anders Heijl et al. 2003). In the Advanced Glaucoma Intervention Study, progression was defined by a complex study-specific scoring system that assessed the visual field sensitivity of several points relative to its location and adjacent field locations' threshold sensitivities ("Advanced Glaucoma Intervention Study" 1994). In the recent United Kingdom Glaucoma Treatment Study, progression was based on visual field criteria only. Eyes were deemed to be progressing if any three visual field locations threshold sensitivities were significantly worse than the baseline field test in two consecutive fields using the aforementioned Progression Analysis Probability Plot, followed by another set of three points in the subsequent two fields using the same criteria (D. F. Garway-Heath et al. 2015).

The heterogeneity of the progression criteria used in clinical trials limits comparability between the progression outcomes. Furthermore, there is increasing evidence that trend based analysis may be more sensitive in detecting earlier glaucoma progression (David F. Garway-Heath et al. 2018; Z. Wu et al. 2019; Kouros Nouri-Mahdavi 2005). Saeedi et al. (2019) compared six visual field progression algorithms in a large external dataset of over 13,000 eyes and reported a poor agreement between the compared algorithms (Cohen's kappa range, 0.12–0.52). The lack of uniform progression criteria is further compounded by the development and clinical adoption of newer technologies that assess glaucomatous optic nerve damage. For instance, OCT has superseded photographic optic disc assessment and confocal scanning laser ophthalmoscopy used in earlier studies, but has yet to be used as the

outcome measure in a randomised controlled trial. Despite the attempts at combining OCT and visual field data for monitoring glaucoma progression (David F. Garway-Heath et al. 2018; Felipe A. Medeiros et al. 2012), implementing such algorithms in clinical care has not yet taken place.

In this section, the methods used for the assessment of glaucoma progression are detailed. Three complementing outcome measures were assessed. Structural progression utilised data from OCT measurements of the optic disc and macula to assess for glaucomatous retinal ganglion cell damage. Functional progression utilised visual field data to assess for glaucomatous visual field loss. Finally, changes in IOP were used as an indirect assessment of the effectiveness of an IOP-lowering intervention. Lowering IOP can be thought of as a surrogate outcome of progression when investigating IOP-lowering interventions, since IOP is the only modifiable risk factor glaucoma progression and the aim of all current glaucoma treatments (Anders Heijl et al. 2002; D. F. Garway-Heath et al. 2015).

Structural progression

OCT imaging of the optic disc allows for an accurate measurement of the peripapillary RNFL thickness. For each eye, RNFL thickness can be divided into four quadrants, with superior and inferior quadrants corresponding to the superior and inferior RNFL arcuate bundles respectively (Denniss, Turpin, and McKendrick 2019; Hood and Kardon 2007). The average circumferential RNFL thickness additionally includes the temporal and nasal quadrants, although these quadrants do not correspond well with glaucomatous field loss in a 24-2 HVF (Hood and Kardon 2007; David F. Garway-Heath et al. 2000; Suda et al. 2018). Macular GCIPL is another site of glaucomatous structural damage that can be readily measured by OCT (Hood et al. 2013; K. E. Kim and Park 2018). For each eye, macular GCIPL can be divided into the superior and inferior halves, which have functional correspondence to central visual field locations that are best assessed on a 10-2 HVF (Hood et al. 2013, 2019).

Progression can be measured by either a trend- or event-based approach. Trend-based analyses measure the rate of peripapillary RNFL or macular GCIPL thickness change per year using serial OCT scans. OCT thickness data can be exported readily by the OCT Review Software (version 9.5; Carl Zeiss Pty Ltd) using research export functionality. Event-based analyses were generated by the Cirrus OCT software in the form of OCT Guided Progression Analysis (GPA). In this method, the software aligns serial OCT thickness maps and compares the thickness of each superpixel (defined as 4x4 pixels) relative to the 2 baseline scans. A significant change is flagged by the software if the change in thickness of 20 contiguous superpixels exceeds the test-retest variability in two consecutive scans (*Cirrus HD OCT 5000*

Manual 2016). There have not been any studies directly comparing the validity of trend-based thickness change to GPA, noting that the latter is limited by using proprietary software that is not readily reproducible.

Progressive thinning of the peripapillary RNFL and macular GCIPL are markers of glaucoma disease progression (Abe et al. 2016; W. J. Lee et al. 2017; C. Lin et al. 2017; Hou, Lin, and Leung 2018; Yu et al. 2016). In a prospective study of 240 eyes with primary open angle glaucoma, Yu et al. (2016) reported progressive thinning of the RNFL by GPA criteria was associated with a 4-fold higher risk of visual field progression by the Early Manifest Glaucoma Trial criteria. Interestingly, trend based progression of the RNFL in the same study carried an 8.4-fold higher risk of visual field progression, supporting the use of trend-based analysis over GPA (Yu et al. 2016). Similarly, Hou et. al. (2018) reported that progressive GCIPL thinning (using GPA) was associated with a 3.5-fold higher risk of visual field progression.

Despite the overlap between RNFL and GCIPL progression in glaucomatous eyes, these progression outcomes may reflect different patterns of glaucomatous structural damage. Using the PROGRESSA cohort, we reported that eyes that progress on GCIPL prior to RNFL progression have a lower maximum recorded IOP, and a lower baseline RNFL thickness than those progressing on RNFL first (H. N. Marshall et al. 2019). GCIPL rate of thinning remains a useful tool in monitoring glaucoma progression in advanced glaucoma where the peripapillary RNFL has already thinned to the floor of the thickness range — referred to as the RNFL 'bottom' (Lavinsky et al. 2018; Shin et al. 2017). Thus, detecting structural glaucoma progression is best achieved by joint analyses of RNFL and GCIPL thickness change over time.

In this thesis, preference has been given to trend-based OCT analysis using the rate of change in RNFL or GCIPL thickness per annum. This is because thickness data from each scan can be readily exported using the OCT software, and subsequently analysed for reproducible results. This additionally allows periodic updates of the dataset as the PROGRESSA cohort undergoes further follow-up. Furthermore, differences in quantitative outcomes may be apparent earlier and with lower sample sizes than using event-based approaches (Z. Wu et al. 2019). An example of OCT GPA reports of RNFL and GCIPL scans is shown in Figure 2.1 and Figure 2.2 respectively.

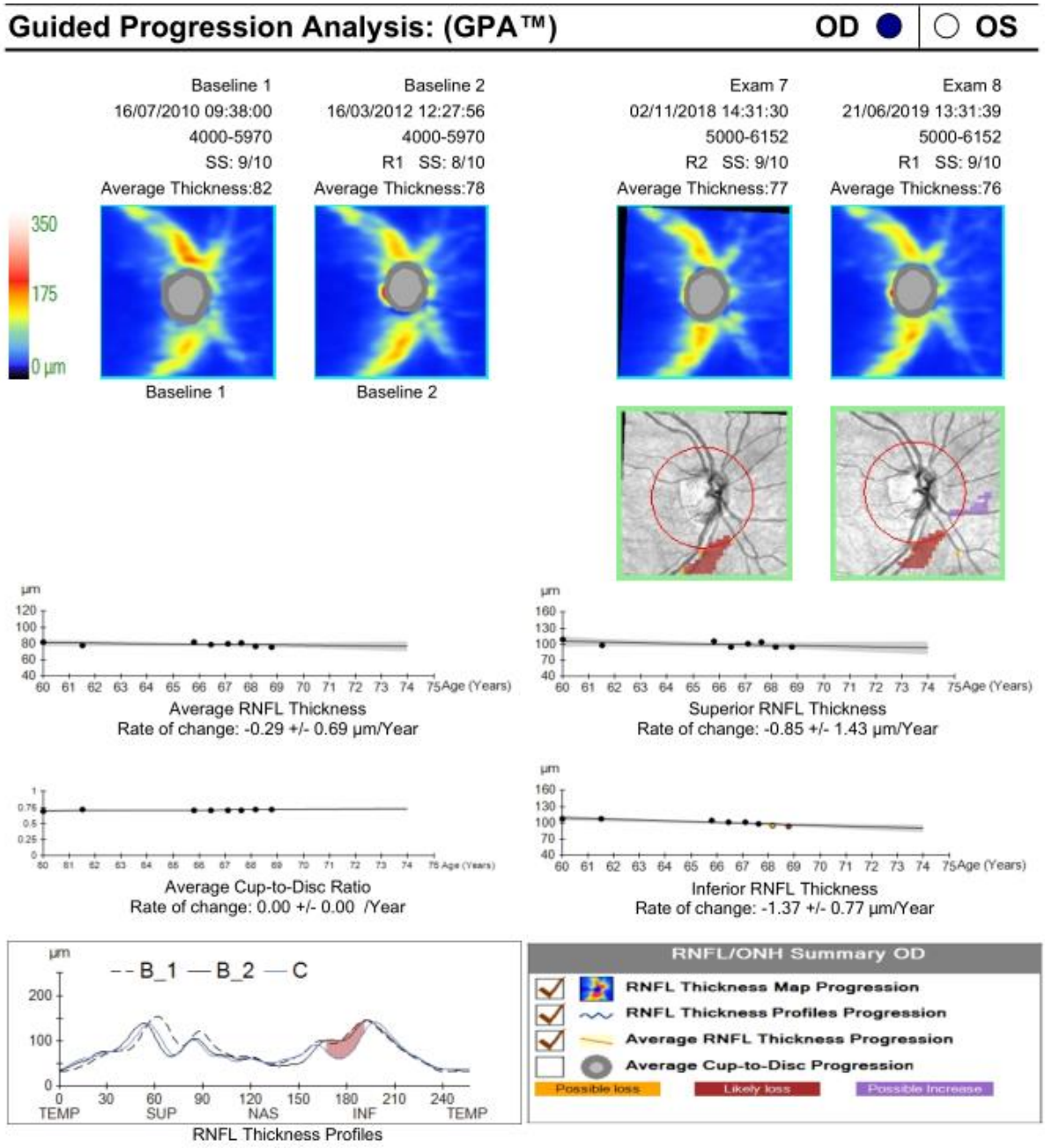

Figure 2.1. OCT RNFL Guided Progression Analysis of the right eye of a PROGRESSA participant. Thickness maps are shown at the top of the report, followed by the change in thickness probability map, where the inferior RNFL bundle is coloured red (GPA algorithm). This indicates that the inferior superpixels have decreased in thickness relative to the baseline two scans, by a margin exceeding the test-retest variability in two consecutive scans. The average and quadrant rates of the RNFL change is displayed below this. Finally, the RNFL thickness profile visualises the change of the circumferential RNFL thickness relative to the baseline (red shaded area corresponds to GPA "Likely loss" in the inferior zone).

OCT: optical coherence tomography; RNFL: retinal nerve fibre layer; GPA: guided progression analysis.

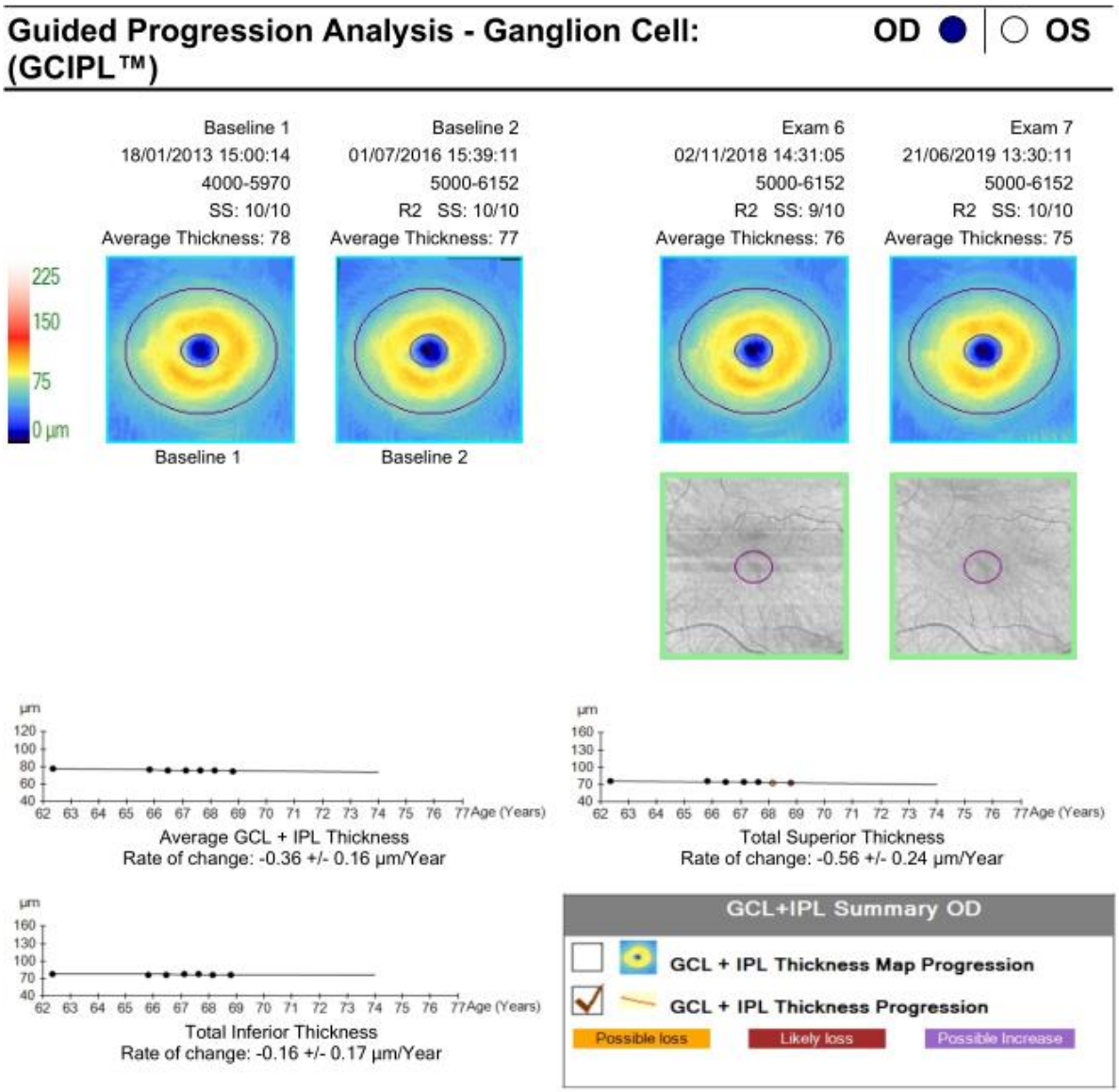

Figure 2.2. OCT GCIPL Guided Progression Analysis of the right eye of the same PROGRESSA participant shown in Figure 2.1. No significant change is seen in the thickness map progression analysis (no red or yellow coloured zones). The average and hemifield rates of the GCIPL change is shown. The GPA algorithm reports the superior thickness change as “Likely loss”, indicating that the superior hemifield GCIPL thickness for the last two scans (i.e., event-based) is significantly lower than the baseline scans, by a margin exceeding the test-retest variability, despite this not being seen in the thickness map analysis (which is a limitation of event-based approach). This not uncommon observation would suggest that using the thickness map to identify glaucoma-pattern thinning is a better indicator of progression in event-based analysis (Yu et al. 2016; W. J. Lee et al. 2017; Shin et al. 2017).

OCT: optical coherence tomography; RNFL: retinal nerve fibre layer; GPA: guided progression analysis.

Functional progression

Serial HVF data was exported using Zeiss FORUM Glaucoma Workplace software (Carl Zeiss Pty Ltd). This allows exporting reliability indices, global summary values (such as mean deviation and GHT), threshold sensitivities for each visual field location, as well as the pattern deviation probability maps in one file. A custom script written in R (R Core Team, Vienna, Austria) was used to extract and tabulate the data for further analyses. This allowed for reproducibility and scalability as new data was acquired.

Detecting early glaucomatous visual field progression can be challenging in early glaucoma and glaucoma suspects such as the PROGRESSA cohort. Reliable visual field progression outcomes require long duration of follow-up and repeat visual field examinations to assess for reproducibility (Z. Wu et al. 2019). Furthermore, significant trends of a decline in global visual field sensitivity summaries (such as the rate of change in the mean deviation or the visual field index) are often not apparent in the early states of glaucoma (Felipe A. Medeiros et al. 2012). Early glaucomatous visual field loss starts in a localised region (e.g. nasal step), due to the asymmetrical retinal ganglion cell damage by glaucoma. As clinicians initiate IOP-lowering treatments that are effective at slowing down visual field loss, detecting progressive glaucomatous field loss is more difficult in pragmatic study designs such as the PROGRESSA study (D. F. Garway-Heath et al. 2015).

Two visual field progression criteria were used in this thesis to detect focal or early glaucoma progression. The first method was an assessment of reliable HVFs for a cluster of new visual field defects in the pattern deviation map. This criteria was set in the PROGRESSA protocol for baseline field assessment (detailed previously), and was revised as a progression end-point (Figure 2.3) (Gordon and Kass 1999). An eye was deemed to have progressed if there was a new cluster of visual field defects that were reproduced in a consecutive field in the same glaucoma region as defined by Loomis et al. (2014) (but not necessarily the same visual field locations). A cluster of visual field defects was defined as 3 contiguous points abnormal in the pattern deviation probability plot at $P < 5\%$, at least one of which is $P< 1\%$. If the GHT was “Outside Normal Limits” or the global PSD was $P < 5\%$ on the two consecutive HVFs, then the individual points only needed to be abnormal on the pattern deviation probability plot at $P < 5\%$.

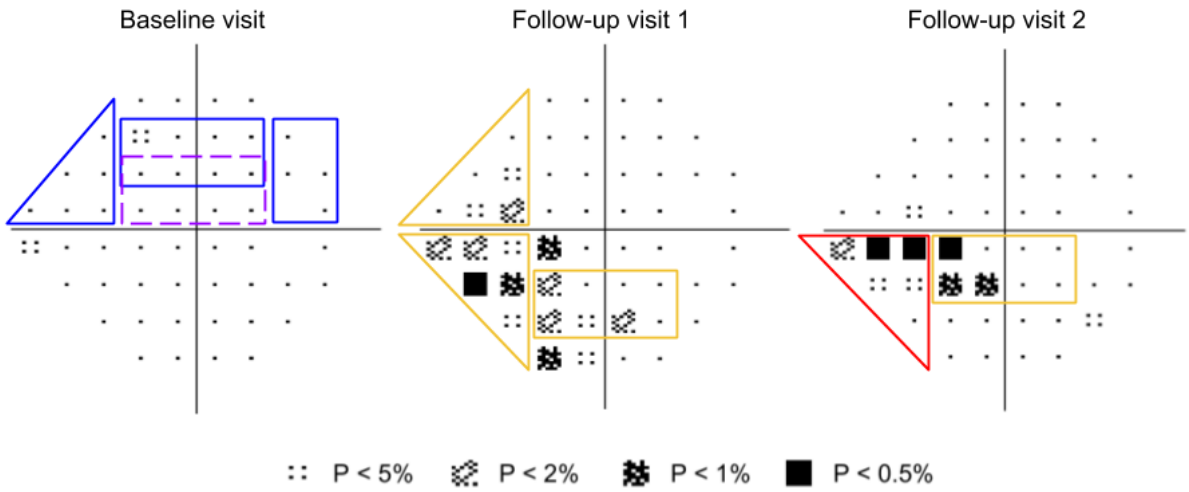

Figure 2.3. Cluster based visual field progression end-point. Four regions in the pattern deviation probability plot are identified for reviewing focal visual field loss, highlighted in the superior field of the baseline visit. These are the nasal (blue rectangle), Bjerrum (blue long rectangle), temporal (blue tall rectangle) and paracentral (dashed purple rectangle) zones (Loomis et al. 2014). Note that there is an overlap between the paracentral and the Bjerrum zones. New defects in follow-up fields are identified (yellow), and confirmed in a subsequent field (red), marking the progression end-point. An abnormal visual field location on the pattern deviation probability plot is expressed in terms of the percentage of normal subjects that could be expected to have such a sensitivity (e.g., P < 5% means that fewer than 5% of the subjects in the HVF normative dataset had a lower pattern deviation sensitivity) (Anders Heijl 2002).

Permutation analyses of pointwise linear regression (PoPLR) is another method used to assess visual field progression (O'Leary, Chauhan, and Artes 2012). PoPLR has been validated as a sensitive and accurate method to detect glaucomatous visual field progression at a relatively earlier timeframe than other methods (O'Leary, Chauhan, and Artes 2012; Saeedi et al. 2019; Rabiolo et al. 2019). In this method, pointwise linear regression (PLR) of the observed chronological order of visual fields is generated (Figure 2.4). In PLR, the rates of changes in the total deviations (i.e. age-adjusted threshold sensitivities) for each of the 52 visual field locations (54 points minus 2 blind spots on a 24-2 HVF) are calculated using linear regression. The overall statistical significance of the observed change is compared to 5,000 random permutations of the field data of the same eye (Figure 2.4). A significant progression is reported when the observed sequence of fields is statistically significantly different ($P<0.05$) from the permuted PLRs (i.e. random chance), allowing an individualised progression end-point derived from within an individuals' data (O'Leary, Chauhan, and Artes 2012). Progression analysis using PoPLR has been implemented in the freely available R package *visualFields* (version 0.6) (Marin-Franch and Swanson 2013).

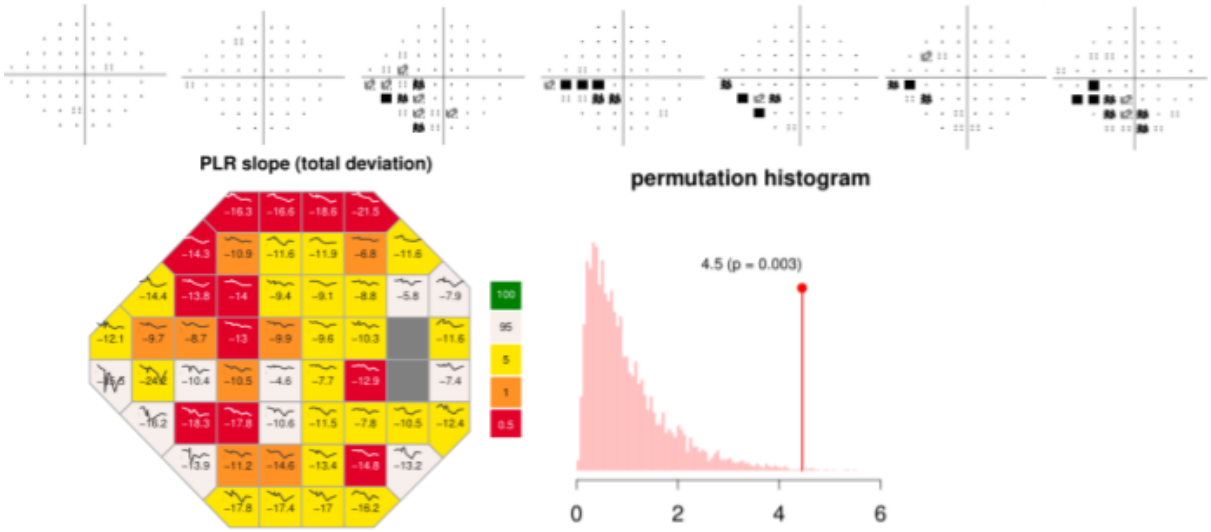

Figure 2.4. Visual field progression using permutation analyses of pointwise linear regression (PoPLR). Pointwise linear regression (bottom left) of the observed visual fields (top) is compared to 5,000 permutations of the visual field examinations (bottom right). Progression occurs when the observed visual field sequence is significantly different to the permutations (P < 0.05). The null distribution (histogram, bottom right) is derived from permutations of a patient's own field data, representing what is expected if the visual field change is random.
PLR: pointwise linear regression.

Reduction in intraocular pressure

Elevated IOP is a major risk factor for the development and progression of glaucoma (Ernest et al. 2013). Thus, the effectiveness of clinical interventions used in the treatment of glaucoma is commonly measured by the magnitude of reduction in IOP as an indirect marker of glaucoma progression (D. F. Garway-Heath et al. 2015; Gus Gazzard et al. 2019; Vold et al. 2016; Craven et al. 2012). The Early Manifest Glaucoma Trial has shown that on average, for every 1 mmHg reduction of IOP from baseline, there was a 10% reduction in risk of glaucoma progression (hazard ratio 0.90, 95% confidence interval 0.86–0.94) (Leske et al. 2003). In this thesis, reduction in IOP has been used as a study outcome when investigating the effectiveness of IOP-lowering interventions as a surrogate marker of glaucoma progression, namely cataract surgery and selective laser trabeculoplasty.

Statistical methods and analysis techniques

Exploratory analyses and data science

Analysis of large clinical datasets requires well structured and annotated datasets. A tabulated dataset where each unique observation is recorded in a separate row, and each variable is recorded in a separate column is referred to as tidy data (Wickham 2014). Observations can be recorded for each individual, or for each eye (i.e. for all eligible eyes) depending on the

study design. Distinct labels are favoured over free text for categorical variables, such that grouped or frequency analyses can be readily performed without manual data handling. This format permits reproducibility, and analyses that are scalable to updated study datasets.

PROGRESSA and ANZRAG datasets were securely stored in Flinders Medical Centre using Microsoft Access databases, and readily exportable to spreadsheet format. Reproducible data cleanup, exploratory analyses, and subsequent statistical hypothesis testing could then be performed on tidy data using scripts written in R. Additional functionalities can be added to R by installing freely available open-source packages. For instance, the *tidyverse* packages provided a simplified grammar for data wrangling to generate an analysis-ready tidy dataset, and the *nanair* package (version 0.5.2) was used to visualise missing data as an exploratory tool. Specific key packages that are used in this thesis are described for reference.

Clinical data such as OCT and HVF were exported in Portable Document Format (PDF) using Zeiss FORUM software. The R package *pdftools* (version 2.3.1) was used to extract text elements from PDFs, followed by extraction of relevant numerical and text strings via regular expression patterns using the *stringr* package (version 1.4.0). The extracted data was then tabulated into tidy format using *tidyverse* packages for further analyses. For HVF data, *visualFields* package (version 0.6) is used to analyse the extracted visual field threshold sensitivities (Marin-Franch and Swanson 2013). Statistical analysis was typically performed using base packages implemented in R. Additionally, mixed-effects regression models which were used to analyse repeated observations within a dataset (such as measurements performed for each eye for each patient), were implemented in the packages *lme4* (versions 1.1.23) for linear models, *glmTMB* (version 1.0.1) for generalised linear models, and *coxme* (version 2.2.6) for Cox hazard models (Bates et al. 2015).

Accounting for inter-eye correlation

Commonly used statistical analyses, such as ordinary least squares linear regression and generalised linear regression models, assume independence between observations. This poses a challenge in ophthalmic research where correlated measurements (such as IOP) from both eyes of each patient are relevant to the research question. Failing to account for repeated measurements and correlations within the study sample leads to overestimating the variable effect size, and increases the chances of a type 1 error (Sheu 2000). There are several methods used in this thesis to account for inter-eye correlation.

A simplified approach to ensure independent observations in statistical analyses is to include one eye for each patient in a study. This approach is particularly useful when studying

variables that are patient-specific and assumed to affect both eyes equally, such as genetic risk variants. For instance, using the worst-affected eye from early glaucoma patients would measure a clinically relevant outcome due to the asymmetry in early glaucomatous damage (Poinoosawmy et al. 1998). However, when investigating variables that are eye-specific, such as per-eye interventions or corneal biomechanics measurements, advanced statistical approaches that account for intra-sample correlation are needed (Q. Fan, Teo, and Saw 2011).

There are two statistical modeling frameworks to account for correlated observations. Generalised estimating equations are used to estimate population average effects of variables, while mixed-effects models use a hierarchical framework with clustered data (Q. Fan, Teo, and Saw 2011). Both models provide robust estimates in non-independent datasets and generally perform similarly in most circumstances (Hubbard et al. 2010). In this thesis, mixed-effects models were used as they provide a more flexible framework of clustered analyses, and provide effect size estimates of the studied variable for each eye, as opposed to the population average estimates in generalised estimating equations (Hubbard et al. 2010).

Mixed-effects regression models estimate the effect-size of the studied variables on an outcome measure (called the fixed effects), while accounting for the hierarchical nature of the variables within the dataset (called the random effects). Fixed effects variables include ocular or systemic factors that are hypothesised to predict the outcome variable. Random effects are potentially correlated clusters within the dataset, such as the individual patients (where measurements from each eye may be correlated), or clinic sites (where the measurements and treatments of a group of individuals may be correlated).

The most commonly used linear mixed-effects regression model in this thesis used a random intercept model for each patient. This means that regression for each patient's data (i.e. for each eye or visit) would have a different intercept, such that the correlated measurements are statistically accounted for. Inferences and test statistics on mixed-effect models require an approximation of the degrees of freedom using Satterthwaite's formula, which has been implemented in the R package *lmerTest* (version 3.1.2) (Kuznetsova, Brockhoff, and Christensen 2017). The R syntax for a random intercept mixed-effect model for the outcome measurement y is:

$$y \sim var + (1 \mid id)$$

where var is the variable of interest, and $(1 \mid id)$ denotes a random intercept for each participant.

Conclusion

This chapter presented some of the challenges in glaucoma research from the study design point of view. In particular, there is no consensus definition of glaucoma progression. The methods used in this thesis were summarised, encapsulating both structural and functional domains. This chapter serves as a reference point for cohort descriptions, progression end-points, and statistical techniques used throughout this thesis.

Chapter 3: Genetic discoveries in glaucoma and glaucoma endophenotypes

Published manuscripts

The contents of this chapter have been published in two peer-reviewed manuscripts in which I am a joint first author. The results of the genetic discoveries involving optic disc diameter were published in a manuscript in *Human Molecular Genetics* in 2019, volume 28, issue 21, pages 3680–3690 (Xikun Han et al. 2019). My contributions to this manuscript involved study concept and design (30%), data collection in the form of grading the fundus photos (80%), data analysis including differential and foetal gene expression and statistical analysis (30%), data interpretation including the results of the genome-wide association study (75%), drafting the manuscript (50%), and critical revision of the manuscript for important intellectual content (50%). Xikun Han contributed equally to this manuscript including study concept and design (30%), data collection in the form of organising UK Biobank fundus photos (10%), data analysis including conducting the genome-wide association analysis (60%), data interpretation (15%), drafting the manuscript (50%), and critical revision of the manuscript for important intellectual content (50%). Jiyuan An was involved in study concept and design (5%), administrative and technical support by creating a custom software to view and grade fundus photos (50%), and data analysis (5%) in the form of assisting in performing genome-wide association analysis. Henry Marshall contributed to data collection by grading a sample of fundus photos (15%). Tiger Zhou contributed to data collection by generating the RNA-Seq gene expression libraries (5%). The remaining authors collectively contributed to study concept and design, critical revision of the manuscript for important intellectual content, obtaining funding, and supervision.

Genetic discoveries for vertical cup-to-disc ratio and primary open angle glaucoma were published in a manuscript in *Nature Genetics* in 2020, volume 52, issue 2, pages 160–166 (Xikun Han et al. 2019; Craig et al. 2020). My contributions to the manuscript involved study concept and design (20%), data collection in the form of grading the fundus photos (30%), data analysis including differential gene expression and statistical analysis (20%), data interpretation including the results of the genome-wide association study (20%), drafting the manuscript (30%), and critical revision of the manuscript for important intellectual content (30%). Jamie Craig, Xikun Han, Alex Hewitt, and Stuart MacGregor contributed equally to the manuscript including study design, data collection and analysis, results interpretation, drafting the manuscript, obtaining funding and supervision. Specifically, Jamie Craig and Alex Hewitt graded the vertical cup-to-disc ratios (50% each). Additionally, this manuscript is co-authored

by 54 other authors who collectively contributed to study design, critical revision of the manuscript for important intellectual content, and supervision.

Introduction

POAG is one of the most heritable common human diseases (K. Wang et al. 2017). There is no single definitive biomarker for glaucoma, and diagnosis involves assessing clinical features, with characterisation of the optic nerve head carrying the strongest evidential weight. POAG is asymptomatic in the early stages, and currently approximately half of all cases in the community are undiagnosed even in developed countries (P. Mitchell et al. 1996). Overlap of features shared by healthy optic nerves with those in early stages glaucoma makes it a difficult disease to diagnose early, necessitating costly ongoing monitoring of patients for progressive optic nerve degeneration (Robert N. Weinreb and Khaw 2004). Glaucoma endophenotypes such as elevated IOP and enlarged VCDR are also highly heritable (Sanfilippo et al. 2010). Thus, genetic studies of these correlated traits can be leveraged to discover glaucoma associated risk variants.

A better understanding of factors that influence optic disc morphology is of high clinical relevance. Optic disc size affects the structural morphology of the optic nerve head and may influence the vulnerability of the nerve fibres (Hoffmann et al. 2007). There is a strong correlation between the optic disc size and the VCDR (clinically and genetically) and this should be taken into account in funduscopic examination (Crowston et al. 2004). Adjusting optic disc parameters such as VCDR for disc size improves their diagnostic power and clinical utility for glaucoma assessment (J. B. Jonas et al. 2000). For example, adjusting the VCDR to DD improves its sensitivity of identifying eyes with perimetric glaucoma from 67% to 76.6% (at 80% specificity) (J. B. Jonas et al. 2000) .

GWAS of POAG and its endophenotypes have led to the discovery of several common variants associated with POAG (Janey L. Wiggs and Pasquale 2017; H. Springelkamp et al. 2017; K. P. Burdon et al. 2011; Kathryn P. Burdon et al. 2012; Henriët Springelkamp et al. 2014). Common variants are often defined as those with an allele frequency — the relative frequency of a genetic variant at a particular locus in a population — greater than 5%. Despite these loci being common, their effect size and contribution to POAG risk are individually relatively small, and previously contributed to less than 5% of POAG heritability (A. P. Khawaja and Viswanathan 2018). These risk loci are involved in biological pathways such as cell division, cytokine signaling and lipid metabolism, which are thought to be important in the pathogenesis of POAG (Janey L. Wiggs and Pasquale 2017). Loci associated with glaucoma endophenotypes are additionally often reported to be POAG risk loci. For instance, the POAG risk loci *TMCO1*, *GAS7* are strongly associated with IOP, while *CDKN2B-AS1* and *SIX1* are strongly associated with VCDR (H. Springelkamp et al. 2017; MacGregor et al. 2018). Thus,

understanding the genetic architecture, and the genetic variants associated with these glaucoma endophenotypes would improve our understanding of glaucoma genetics, and may assist in discovering additional POAG risk loci.

Earlier GWAS of glaucoma and its endophenotypes have been limited in power due to smaller sample sizes. For instance, prior to the work presented in this chapter, less than 20 loci were implicated with optic disc size or VCDR (Macgregor et al. 2010; Ramdas et al. 2010; Khor et al. 2011; Gasten et al. 2012; Henriët Springelkamp et al. 2015; H. Springelkamp et al. 2017). Soon after the public release of the UKBB data, Macgregor et. al. (2018) have conducted the largest GWAS meta-analysis of IOP on 133,492 individuals and identified 101 independent IOP associated SNPs, 85 of which were novel. These included all but one of the previously reported IOP SNPs, highlighting the added power of this dataset. For POAG, prior studies have implicated 14 loci to be associated with POAG, including those near *CAV1*, *CAV2*, *TMCO1*, *CDKN2B-AS1*, and *ABCA1* (K. P. Burdon et al. 2011; Thorleifsson et al. 2010; Yuhong Chen et al. 2014; P. Gharahkhani et al. 2014; Bailey et al. 2016; H. Springelkamp et al. 2015, 2017).

Outlined in this chapter is my original contribution to knowledge in the genetic discoveries of optic disc size and VCDR using the largest GWAS of these traits to date. The results of these studies are then incorporated with published GWAS of IOP, and combined with glaucoma disease status using a recently developed multiple trait analysis of GWAS approach to identify novel risk loci for POAG (Turley et al. 2018).

Methods

The following section has been previously published in two peer-reviewed manuscripts, and has been edited to fit the structure of the thesis (Craig et al. 2020; Xikun Han et al. 2019).

Study cohort

Genome-wide association studies (GWAS) of the optic nerve head traits were performed using measurements obtained from the UKBB European ancestry participants. The cohort characteristics and genotyping details were previously detailed in Chapter 2. A glaucoma case-control GWAS was also performed using the UKBB European ancestry participants. Additional datasets with ocular phenotyping data were used either as replication or joint-analysis as follows.

The International Glaucoma Genetics Consortium (IGGC) consists of 37,930 participants enrolled in 19 studies from European and Asian ancestries. Detailed genotyping and ocular

phenotyping information for each study has been described previously (H. Springelkamp et al. 2017). Optic nerve head phenotyping included VCDR, optic cup and disc area measurements. In IGGC, the genetic data was established from various genotyping arrays between the studies, with additional imputation carried out with reference to the 1000 Genomes reference panel (H. Springelkamp et al. 2017; Siva 2008). We obtained the publicly available VCDR and optic disc area measurements from the European ancestry subset of the IGGC to match the ancestry of our discovery cohort (H. Springelkamp et al. 2017). The IGGC optic disc area measurements were used for replicating the UKBB optic disc size GWAS, followed by a joint analysis approach to increase the discovery power. Additionally, the IGGC VCDR measurements contributed to a multiple trait analysis of GWAS in the discovery study of glaucoma-associated variants.

Optic disc diameter measurements were additionally obtained from the EPIC-Norfolk Eye Study, a subset of the EPIC-Norfolk who underwent detailed ophthalmic assessment (Anthony P. Khawaja et al. 2013). The main EPIC-Norfolk study recruited and examined 25,639 participants between 1993 and 1997 (Day et al. 1999), and was part of a pan-European prospective cohort study designed to investigate the aetiology of major chronic diseases (Riboli and Kaaks 1997). For the eye study, a total of 8,623 participants were seen between 2004 and 2011. Digital photographs of the optic disc and macula were taken using a TRC-NW6S non-mydriatic retinal camera and IMAGEnet Telemedicine System (Topcon Corporation, Tokyo, Japan) with a 10-megapixel Nikon D80 camera (Nikon Corporation, Tokyo, Japan). Pupils were not dilated. Images were graded at the Moorfields Reading Centre. Measurement of the vertical diameter of the optic disc was made using adobe photoshop C55 software. 99.7% of EPIC-Norfolk are of European descent and we excluded participants of non-white European ancestries. The EPIC-Norfolk Eye Study was carried out following the principles of the Declaration of Helsinki and the Research Governance Framework for Health and Social Care. The study was approved by the Norfolk Local Research Ethics Committee (05/Q0101/191) and East Norfolk & Waveney NHS Research Governance Committee (2005EC07L). All participants gave written, informed consent.

Initial genotyping on a small subset of EPIC-Norfolk was undertaken using the Affymetrix GeneChip Human Mapping 500K Array Set and 1,096 of these participants contributed to the IGGC meta-analysis (H. Springelkamp et al. 2017). Subsequently, the rest of the EPIC-Norfolk cohort were genotyped using the Affymetrix UK Biobank Axiom Array (the same array as used in UK Biobank). SNP exclusion criteria included: call rate < 95%, abnormal cluster pattern on visual inspection, plate batch effect evident by significant variation in minor allele frequency, and/or Hardy-Weinberg equilibrium $P < 10^{-7}$. Sample exclusion criteria included: DishQC <

0.82 (poor fluorescence signal contrast), sex discordance, sample call rate < 97%, heterozygosity outliers (calculated separately for SNPs with minor allele frequency >1% and =<1%), rare allele count outlier, and implausible identity-by-descent values. We removed related individuals with pairwise relatedness corresponding to third-degree relatives or closer across all genotyped participants. Following these exclusions, there were no ethnic outliers. Data were pre-phased using SHAPEIT version 2 and imputed to the Phase 3 build of the 1000 Genomes project (October 2014) using IMPUTE (version 2.3.2). We examined the relationship between allele dosage and mean of right and left vertical disc diameter using linear regression adjusted for age, sex and the first five principal components. Analyses were carried out using SNPTEST software (version 2.5.1) (Marchini et al. 2007).

Following the GWAS of optic disc diameter and VCDR, we conducted a multi-trait GWAS of glaucoma, combining case-control GWAS with glaucoma endophenotypes (Figure 3.1). Replication of the glaucoma loci was performed on the ANZRAG and The National Eye Institute Glaucoma Human Genetics Collaboration Heritable Overall Operational Database (NEIGHBORHOOD) studies. Details of the ANZRAG cohort were previously described in Chapter 2. For this analysis, 3,071 POAG cases of European descent were compared to 6,750 controls (Emmanuelle Souzeau et al. 2012; P. Gharahkhani et al. 2014). For sub-analyses restricted to advanced POAG, there were 1,734 advanced POAG cases and 2,938 controls. Details of the participants of the NEIGHBORHOOD study have been described elsewhere (Bailey et al. 2016; Janey L. Wiggs et al. 2013; J. L. Wiggs et al. 2012). Participants were recruited from 8 distinct studies with various genotyping arrays. Additional genotype imputation was carried out with reference to the 1000 Genomes reference panel (Siva 2008), and after quality control, analysis was performed controlling for age, sex and study-specific covariates. GWAS results were generated through meta-analysing summary data from eight independent datasets (3,853 POAG cases, 33,480 controls) of European ancestry from the United States (Janey L. Wiggs et al. 2013).

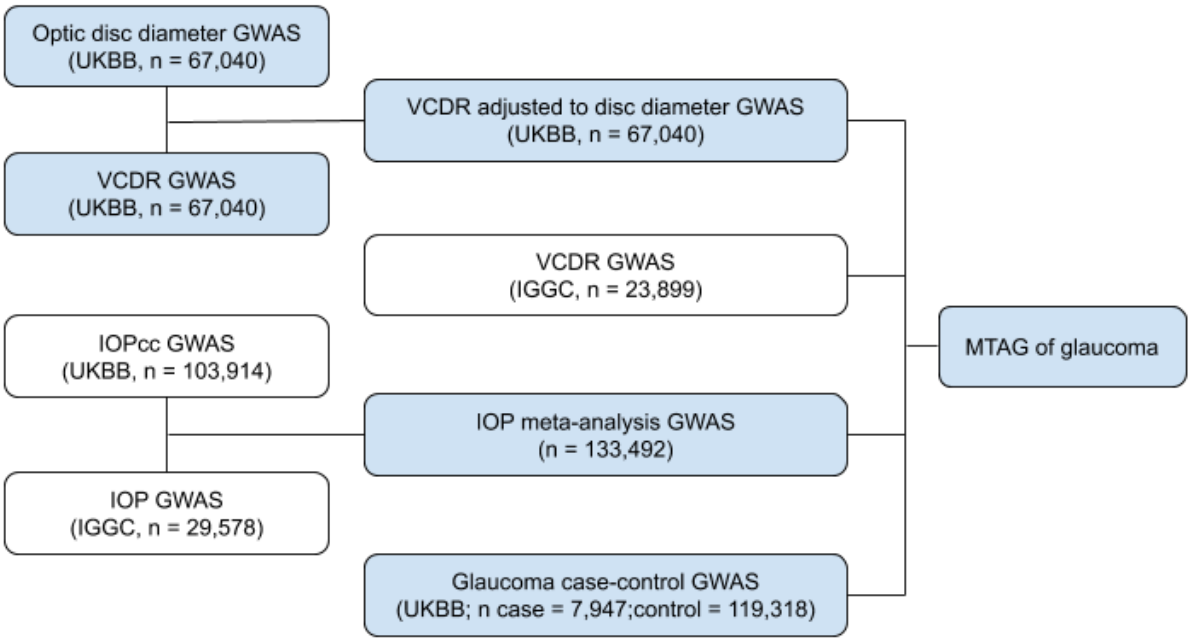

Figure 3.1. An overview of the cohorts and genome-wide association studies (GWAS) used in conducting the multiple trait analysis of GWAS (MTAG) of glaucoma. The blue shade represents new GWAS conducted for this study, while the white shade represents previously published and publicly available GWAS summary statistics.
GWAS: genome-wide association study; VCDR: vertical cup-to-disc ratio; IOP: intraocular pressure; IOPcc: corneal compensated IOP; IGGC: International Glaucoma Genetics Consortium; UKBB: UK Biobank; MTAG: multiple trait analysis of GWAS.

Optic nerve head phenotyping

Optic nerve head measurements were performed on fundus photographs of participants of the UK Biobank (UKBB) who underwent detailed ophthalmic examinations (Chapter 2). In the UKBB, 87,685 left fundus retinal eye images were available (two assessment visits), covering 84,871 participants (UKBB Field: 21015). The optic disc diameter and the VCDR were measured. The longest vertical optic disc diameter (DD) was measured at the inner edges of the scleral ring from the non-stereo fundus images by two examiners (detailed in the chapter heading). VCDR was assessed by two fellowship-trained ophthalmologists and recorded in 0.05 intervals (examiners detailed in the chapter heading). The images had a 45^{o} field of view and were cropped and enlarged to facilitate grading using a custom Java program, which loads the fundus photographs sequentially, and records the reviewer's grading in a time-efficient manner.

The second visit fundus photo measurements were used if available, otherwise, we used the first visit measurements (N=52,199, proportion 76%). If the left eye images were ungradable, we used the right eye images instead (N=6,181, proportion 9%, UKBB Field 21016). Non-

white British ancestry participants, based on principal components, were excluded as described in Chapter 2. In total, 67,040 participants' DD and VCDR were measured and included in our analysis. With data only available on one eye we were unable to assess left-right VCDR asymmetry although this is not relevant to our primary goal of identifying novel genetic associations with VCDR.

Two thousand images were randomly selected for quality control (Figure 3.2). For DD, Pearson's correlation coefficient of the DD measurements between the two examiners was 0.64 (95% CI: 0.61–0.67; Figure 3.2A). For VCDR, Pearson's correlation coefficient of the VCDR measurements between the two ophthalmologists was 0.75 (95%CI: 0.72–0.77; Figure 3.2B), which is in keeping with previous publications (Wolfs et al. 1999; Morgan et al. 2005; Harper, Reeves, and Smith 2000).

Additionally, we downloaded the publicly available disc area and VCDR GWAS summary statistics for individuals of European ancestry from IGGC. This included 22,504 participants with disc area measurements, and 23,899 participants with VCDR measurements. Furthermore, optic disc size measurements of 6,005 participants in the EPIC-Norfolk study were used. These participants were distinct to the group of EPIC-Norfolk participants included inthe IGGC sample (N = 1,096) (H. Springelkamp et al. 2017).

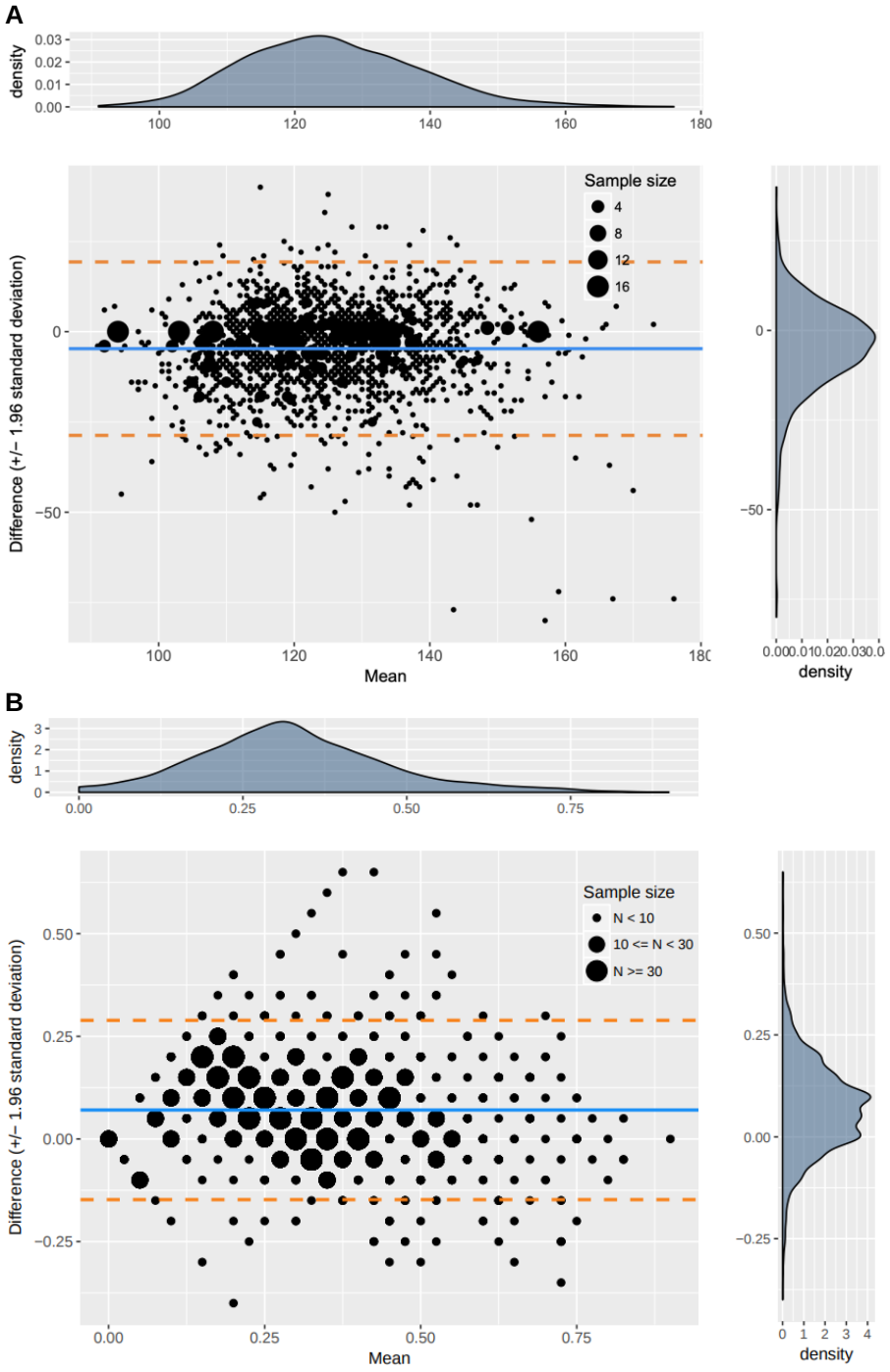

Figure 3.2. Bland-Altman plots for vertical disc diameter **(A)** and vertical cup-to-disc ratio **(B)** measurements. The x-axis represents the mean value of two measurements, the y-axis represents the difference between two measurements, the blue line is the mean value of difference, and the dashed orange lines are the 95% limits of agreement (95% confidence interval for the mean value of difference). The black dots are scaled by the number of samples. The right and top panels are the density plots for the difference of the measurements and the mean value of measurements, respectively.

Genome-wide association analyses

For DD GWAS in UKBB, we first applied a rank-based inverse-normal transformation to the vertical disc diameter measurements (Aulchenko et al. 2007). Since disc diameter and disc area are monotonically related, applying such a transformation makes the phenotype correlation between diameter and area effectively approach one, although to render them back to the same output scale, one should multiply by the standard deviation of the trait, which is approximately 0.4 mm^2 for disc area (H. Springelkamp et al. 2017). To ensure consistency with previously reported results, all our analyses are presented on the disc area scale (H. Springelkamp et al. 2017).

For association analyses of the transformed DD and VCDR in UKBB, we used a linear mixed model in BOLT-LMM software (version 2.3) to account for cryptic relatedness and population stratification (Loh et al. 2015). Analysis was performed under an additive genetic model, adjusted for the effect of sex, age, the first ten principal components, two indicator variables for the examiners who performed the measurements, and fundus retinal image assessment visits (Kai Wang, Li, and Hakonarson 2010). In addition, to adjust for the effect of optic nerve head size, as large optic discs are associated with higher VCDR, DD was added as a covariate in VCDR GWAS (B. Bengtsson 1976; Crowston et al. 2004).

A stepwise model selection procedure in the GCTA-COJO software (version 1.91.7beta) was used to identify independent lead genome-wide significant SNPs (Jian Yang et al. 2012). GCTA-COJO uses GWAS summary results and estimates linkage disequilibrium (LD) from a reference sample (randomly selected 5,000 UKBB white British ancestry individuals, considering SNPs within a two megabase window) for the conditional and joint association analysis. Although the joint analysis can uncover SNPs with $P<5\times10^{-8}$ in the joint test and $P<5\times10^{-8}$ in the standard (unconditional) test, here we only report SNPs with both unconditional P values and joint P values less than 5×10^{-8}. For genomic regions with multiple independent SNPs, we defined a 'locus' as a region at least 400 kilobases from the adjacent locus. Bivariate LD score regression was used to estimate the genetic correlation between pairs of traits (Loh et al. 2015).

To replicate the lead SNPs from UKBB DD GWAS, we conducted a sample size based meta-analysis in METAL (2011-03-25 release) for IGGC and EPIC-Norfolk datasets (Willer, Li, and Abecasis 2010). For the UKBB and IGGC meta-analysis, we performed the inverse-variance weighted fixed-effect meta-analysis in METAL (Willer, Li, and Abecasis 2010). In our sensitivity analysis, rather than performing meta-analysis using the effect size estimates and standard

errors, we also conducted the multiple trait analysis of GWAS (MTAG, software version 1.08) approach, a framework to generalize the standard inverse-variance meta-analysis method, with the approach able to joint analyse the same trait with different measures or even different traits with a high genetic correlation (detailed below) (Turley et al. 2018). For the VCDR findings, we used the IGGC dataset in a joint analysis to extend our effective sample size to discover glaucoma-associated variants instead of replication of VCDR variants.

Multitrait glaucoma GWAS

We first conducted a GWAS on glaucoma in UKBB, and combined it with GWAS of key endophenotypes for glaucoma: VCDR adjusted to DD and IOP using MTAG (Figure 3.1) (Turley et al. 2018). This method allows combining multiple genetically correlated traits to maximize power for identifying new loci and improving genetic risk prediction. Specifically, our MTAG analysis outputs glaucoma-specific effect size estimates and P-values for SNPs across the genome. Newly associated loci ($P<5\times10^{-8}$) were then validated in two independent cohorts with well-characterised POAG (an Australasian cohort of advanced glaucoma [ANZRAG] and a consortium of cohorts from the United States [NEIGHBORHOOD]).

We meta-analysed UKBB IOP GWAS results (N = 103,914) with those from the IGGC (N = 29,578**)** using the inverse variance weighted method (METAL software) (Willer, Li, and Abecasis 2010). The methods and results of the UKBB IOP GWAS have been published previously (MacGregor et al. 2018). Briefly, the average corneal-compensated IOP (IOPcc) across both eyes of 103,914 UKBB participants was included in a GWAS after excluding non-white British ancestry participants and glaucoma cases and their relatives. We conducted a sensitivity analysis either correcting or not correcting for IOP treatment in the <2% of individuals undergoing treatment and results were essentially unchanged.

For the UKBB glaucoma GWAS, we identified 7,947 glaucoma cases from ICD-10 diagnosis and self-reported questionnaires, and 119,318 controls who self-reported having no eye disease. We defined glaucoma cases as those who (i) had an ICD-10 diagnosis of 'primary open angle glaucoma', 'other glaucoma' or 'glaucoma, unspecified'; (ii) responded 'glaucoma' to the question 'Has a doctor told you that you have any of the following problems with your eyes?'; or (iii) responded 'glaucoma' to the question 'In the touch screen you selected that you have been told by a doctor that you have other serious illnesses or disabilities, could you now tell me what they are? (non-cancer illness). Although only a small proportion of the glaucoma cases had documented disease subtype, the proportion of non-POAG glaucoma cases in UKBB would be expected to be small (87% of glaucoma cases were POAG in a recent UK study) (M. P. Y. Chan et al. 2017). In the glaucoma case-control GWAS, we only kept each

pair of individuals with $\hat{\pi}$>0.2 and used logistic regression in PLINK (version 2.0) for the GWAS analysis (Purcell et al. 2007).

We then conducted a multitrait GWAS using the MTAG (version 1.0.7) software to combine the European descent GWAS summary statistics from UKBB glaucoma (7,947 cases, 119,318 controls), UKBB VCDR adjusted for disc diameter (N=67,040, as above), IGGC VCDR (N=23,899) and the intraocular pressure meta-analysis (N=133,492) (Figure 3.1) (Turley et al. 2018). In MTAG, GWAS summary results from related traits are used to construct the variance–covariance matrix of their SNP effects and estimation error; MTAG improves the accuracy of effect estimates by incorporating information from other genetic correlated traits. The MTAG method explicitly models sample overlap in the input studies and provides valid estimates even when sample overlap is present (Turley et al. 2018). To benchmark the increase in effective sample size relative to just using UKBB glaucoma, we calculated ($\underline{\chi 2}_{\text{MTAG}}$ -1) / ($\underline{\chi 2}_{\text{GWAS}}$-1), where $\underline{\chi 2}_{\text{MTAG}}$ and $\underline{\chi 2}_{\text{GWAS}}$ are the mean chi-squared statistics from MTAG and the UKBB glaucoma analyses, respectively (Turley et al. 2018).

We replicated the new glaucoma loci from MTAG in ANZRAG and NEIGHBORHOOD. Given our replication samples have a much smaller effective sample size than that available from our MTAG analysis, we first examined whether the direction of effect was consistent between discovery and replication cohorts. We calculated the Pearson correlation between the effect sizes estimates from discovery and replication cohorts in R. For the testing of individual putatively novel loci, given our strong prior hypothesis that a risk increasing allele discovered via MTAG would also increase risk in the replication cohorts, we performed one-sided significance tests. We applied a Bonferroni correction to correct for the number of novel loci tested.

Post GWAS analysis: ocular gene expression

Gene expression data was available from RNA extraction of 21 healthy donor eyes from 21 individuals. The original data was generated by Tiger Zhou, and has been used in analysis in a previous publication (MacGregor et al. 2018), although the gene expression data has not been published publicly yet. We analysed 63 tissues of cornea (epithelium, stroma and endothelium), trabecular meshwork, ciliary body, iris, retina, optic nerve and optic nerve head. RNA quality was assessed using Agilent Bioanalyzer 2100 RNA 6000 Nano Assay and samples were included for sequencing only if the RIN scores were greater than or equal to 3.8 and both 28S and 18S ribosomal RNA intensity peaks were prominent. RNA sequencing was done using Illumina NextSeq® 500 (San Diego, USA), followed by quality check (FASTQC v0.11.3). Trimgalore (v0.4.0) was used to trim low quality bases (Phred score < 28) and reads

shorter than 20 bases after trimming were discarded. All reads which passed every quality control step were then aligned to the human genome (GRCh38 assembly) with ≤ 2 mismatches per read. Downstream analysis was done with edgeR (version 3.22.5) (Robinson, McCarthy, and Smyth 2010). We selected genes expressed 10 times (1.5 counts per million) in at least 5 tissue samples and normalised the libraries using trimmed mean of M-values (TMM) (Robinson and Oshlack 2010). Estimating dispersions was done via Cox-Reid profile-adjusted likelihood method (using the *estimateDisp* function in *edgeR*) (Cox and Reid 1987). Differential expression was compared between optic nerve head and all other tissues via negative binomial generalised linear model using the *glmQLFit* function in *edgeR* (D. J. McCarthy, Chen, and Smyth 2012). Genes were filtered to those nearest to the identified SNPs, and the differential expression P-values were adjusted using Bonferroni correction.

Gene-based and pathway tests

We used MAGMA (v1.07) for gene-based and pathway analysis as implemented in FUMA (version 1.3.4) (de Leeuw et al. 2015; Watanabe et al. 2017). In gene-based tests, GWAS summary statistics of SNPs were mapped to 18,619 genes, and the association P values for a set of SNPs were calculated. The default parameters in FUMA were used. Bonferroni method was used for multiple testing correction ($P < 0.05/18,619$). In pathway tests, 10,678 predefined gene sets (MsigDB v6.2, curated gene sets: 4,761, GO terms: 5,917) were tested for enrichment.

Results

The following section has been previously published in two peer-reviewed manuscripts, and has been edited to fit the structure of the thesis (Craig et al. 2020; Xikun Han et al. 2019).

Optic disc size

In the discovery stage, we conducted GWAS on vertical DD in 67,040 UKBB samples, then we replicated the novel associated candidate loci in independent cohorts from the IGGC (N = 22,504) and EPIC-Norfolk (N = 6,005).

From the vertical disc diameter GWAS of 67,040 UKBB participants, we identified 91 lead significant independent SNPs (81 loci), of which 67 SNPs (66 loci) had not previously been associated with disc diameter (Figure 3.3A; detailed SNPs table is provided in the appendix). Interestingly, we also identified two genes located in the X chromosome (*EFNB1* and *ZIC3*), which play an important role in eye development (Nagai et al. 1997; Cavodeassi, Ivanovitch, and Wilson 2013). We conducted LD score regression and observed no evidence for genomic inflation (intercept = 1.05, standard error = 0.01; quantile-quantile plot provided in the

appendix). As previously reported (H. Springelkamp et al. 2017), the genetic correlation between disc diameter and VCDR was very high (rg=0.50, $P=6.18\times10^{-21}$). The genetic correlation between DD and POAG was very small (rg=0.01, P=0.78). The strong association between DD and VCDR is due to the physiologically larger vertical cup diameter and optic disc rim area found in larger optic discs (Crowston et al. 2004). A higher count of optic nerve fibres is found histologically in eyes with larger optic discs (J. B. Jonas et al. 1992), representing the larger neuroretinal rim area seen on fundoscopy. The genetic correlation of disc size between UKBB and IGGC was 0.83 ($P=1.31\times10^{-76}$).

We then replicated the identified lead vertical DD loci in IGGC and EPIC-Norfolk datasets. The correlation in effect size estimates at the lead genome-wide significant SNPs was 0.90 ($P=2.85\times10^{-33}$, Figure 3.4), indicating the identified disc diameter SNPs from UKBB could be well replicated. Of the 64 novel loci from autosomal chromosomes, 19 loci could be replicated in IGGC and EPIC-Norfolk after Bonferroni correction ($P=0.05/64=7.8\times10^{-4}$, Table 3.1), and 44 loci have nominal association (P=0.05; complete list of loci provided in the appendix). The X chromosome GWAS results are not available in the IGGC and EPIC-Norfolk cohorts. Therefore, further studies are needed to confirm the associations of these two X chromosome genes with DD.

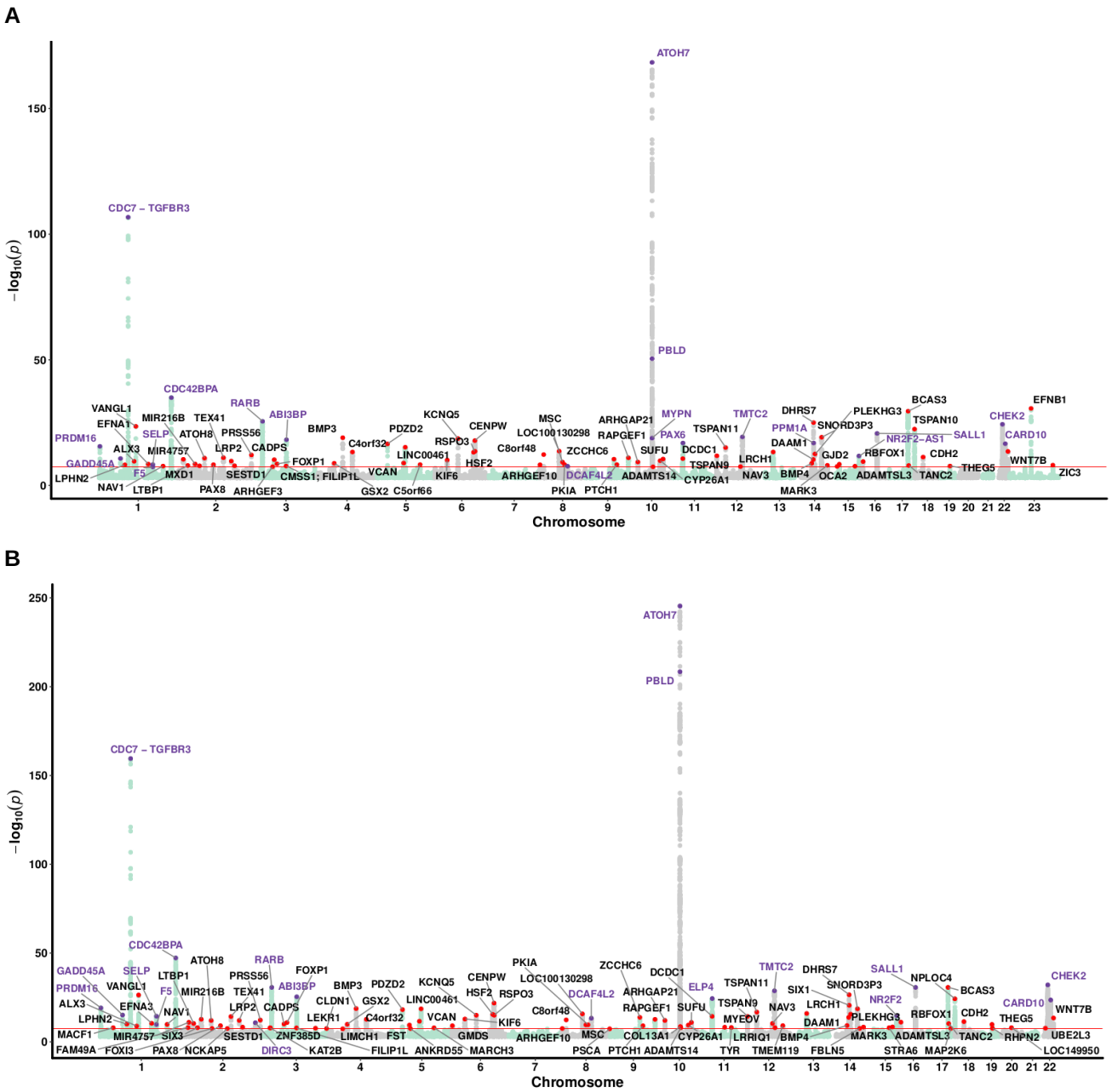

Figure 3.3. Manhattan plot of disc size genome-wide association studies using the UK Biobank dataset **(A)** and meta-analysis using UK Biobank and IGGC datasets **(B)**. Novel loci are highlighted in red dots, with the nearest gene names in black text. Known loci are highlighted in purple dots, with the nearest gene names in purple text. The red line is the genome-wide significance level ($P = 5\times10^{-8}$).

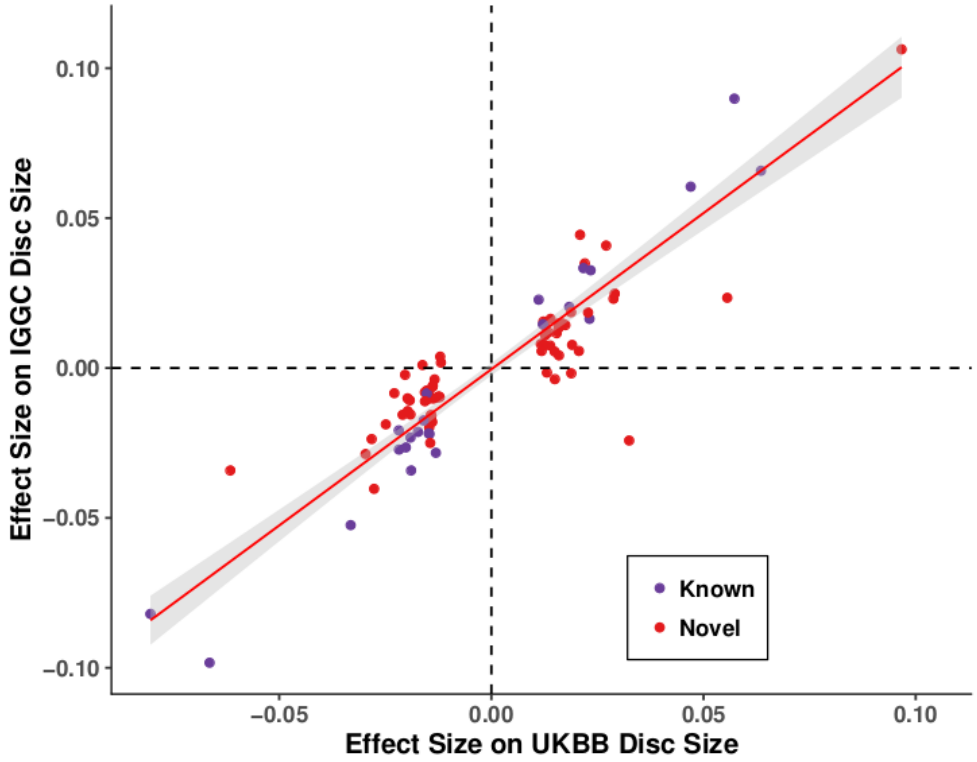

Figure 3.4. Comparison of the effect sizes for 91 genome-wide significant independent SNPs identified from UK Biobank disc size GWAS versus those in independent cohort IGGC disc size GWAS. Pearson's correlation coefficient is 0.90 (P value=2.85×10^{-33}). The red line is the best fit line, with the 95% confidence interval region in grey. Novel disc size SNPs are highlighted in red and known SNPs in purple.

GWAS: genome-wide association study; VCDR: vertical cup-to-disc ratio; IGGC: International Glaucoma Genetics Consortium; UKBB: UK Biobank; SNP: single nucleotide polymorphism.

Table 3.1. List of 19 novel disc size loci replicated in IGGC and EPIC-Norfolk datasets after Bonferroni correction.

							UKBB		META	
SNP	**CHR**	**BP**	**Nearest Gene**	**EA**	**NEA**	**FREQ**	**BETA**	**P**	**Z score**	**P**
rs12136690	1	116208944	*VANGL1*	C	T	0.76	-0.02	3.1E-24	5.40	6.7E-08
rs56412756	1	201605477	*NAV1*	C	T	0.92	0.02	2.0E-08	-3.96	7.6E-05
rs9967780	2	56234942	*MIR216B*	G	T	0.78	-0.01	3.0E-09	4.73	2.3E-06
rs4832012	2	86000500	*ATOH8*	G	C	0.49	-0.01	1.4E-11	3.69	2.3E-04
rs1365902	2	145470699	*TEX41*	T	C	0.33	-0.01	8.7E-12	-4.91	9.1E-07
rs3914468	2	170157400	*LRP2*	A	G	0.70	-0.01	2.0E-10	-3.58	3.4E-04
rs77877421	3	71182447	*FOXP1*	A	T	0.94	-0.03	2.6E-09	-3.47	5.1E-04
rs72759609	5	31952051	*PDZD2*	T	C	0.90	0.03	3.1E-17	4.02	5.9E-05
rs58531939	5	87823968	*LINC00461*	T	C	0.91	-0.03	6.3E-16	-4.55	5.3E-06
rs2092524	6	39529692	*KIF6*	G	A	0.66	-0.01	8.5E-11	4.18	3.0E-05
rs12661045	6	122682795	*HSF2*	C	T	0.70	0.02	6.1E-14	-3.46	5.5E-04
rs2152876	6	126761228	*CENPW*	G	A	0.54	-0.02	1.5E-18	5.36	8.2E-08
rs9401928	6	127298394	*RSPO3*	G	A	0.55	-0.02	2.7E-14	4.44	9.0E-06
rs6999835	8	78948855	*PKIA*	T	C	0.63	0.01	5.1E-09	3.74	1.8E-04
rs10512176	9	89252706	*ZCCHC6*	T	C	0.72	-0.01	3.5E-11	-4.07	4.8E-05
rs10764494	10	25058144	*ARHGAP21*	C	A	0.32	-0.01	4.7E-10	3.84	1.2E-04
rs76567987	12	31037655	*TSPAN11*	A	G	0.84	0.02	8.4E-16	4.01	6.1E-05
rs9534439	13	47192049	*LRCH1*	T	C	0.19	0.02	5.1E-14	4.36	1.3E-05
rs61985972	14	59550263	*DAAM1*	A	G	0.94	0.03	5.2E-11	5.02	5.2E-07

Chromosomal position is based on the NCBI RefSeq hg19 human genome reference assembly.
BETA, beta coefficient; CHR, Chromosome; EA, effect allele; FREQ, allele frequency of effect allele; NEA, non-effect allele; SNP, single nucleotide polymorphism; P, P values. UKBB, UK biobank data; IGGC, International Glaucoma Genetic Consortium; META, meta-analysis results of IGGC and EPIC-Norfolk datasets.

We subsequently conducted a GWAS meta-analysis to combine UKBB and IGGC disc size datasets, and identified 115 independent genome-wide significant SNPs from 101 loci, and an additional 26 novel disc size loci (Figure 3.3B; detailed SNPs table is provided in the appendix).

We estimated the genetic correlation between disc size and 832 traits in LD-Hub database (v1.9.0) (J. Zheng et al. 2017). We only found significant genetic correlation between disc size and myopia (UKBB data field 6147: Reason for glasses/contact lenses, rg=-0.24, $P = 5.94\times10^{-8}$) after Bonferroni correction (0.05/832). We also investigated GWAS Catalog (Morales et al. 2018), a curated collection of published genome-wide association studies, for disc size genome-wide significant SNPs. Our results showed some of the lead disc size loci had pleiotropy effects. For instance, lead SNPs in genes *CDC42BPA* and *ANKRD55* were associated with macular thickness, and lead SNPs in *ANKRD55*, *PRSS56*, *KCNQ5*, *NPLOC4*, and *BMP4* were related to myopia. Detailed results of these analyses is provided in the appendix.

Vertical cup-to-disc ratio

GWAS of VCDR (adjusted for vertical disc diameter) identified 76 statistically independent, genome-wide significant SNPs (66 loci), of which 49 SNPs (43 loci) had not previously been associated with VCDR (Figure 3.5; detailed SNPs table is provided in the appendix). Using LD score regression, we found no evidence for genomic inflation (intercept = 1.04, standard error = 0.01, quantile-quantile plot provided in the appendix). The genetic correlation between VCDR (adjusted for vertical disc diameter) and glaucoma in UKBB was 0.50 (standard error = 0.05); the correlation in effect size estimates at the 76 SNPs was 0.60 ($P=9.0\times10^{-9}$; Figure 3.6).

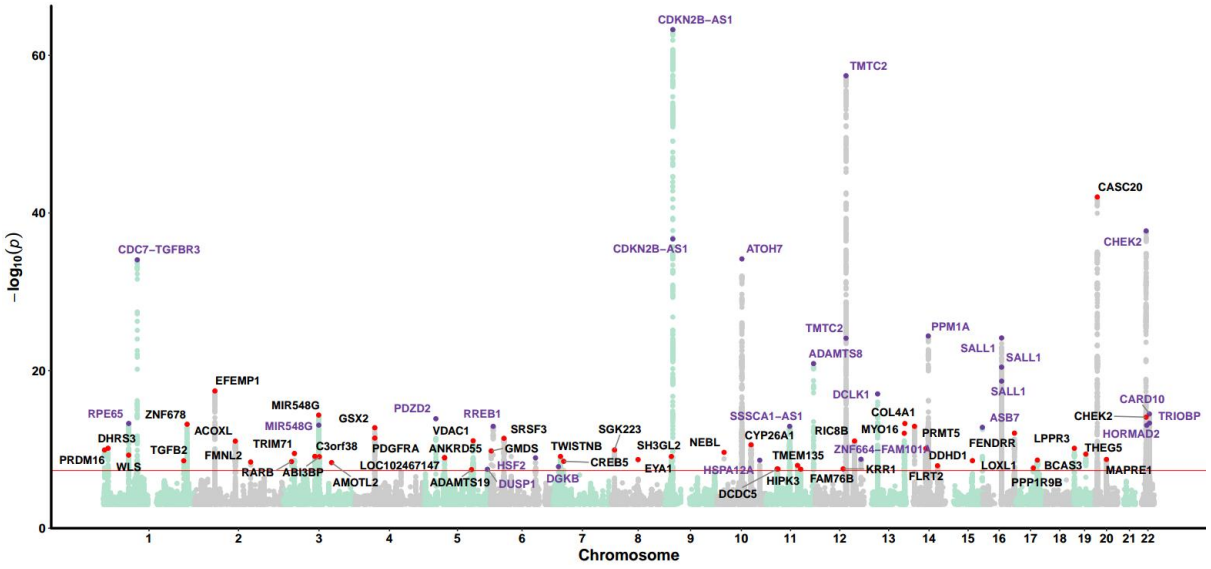

Figure 3.5. Manhattan plot for the GWAS of UKBB vertical-cup-disc-ratio (adjusted for vertical disc diameter, N = 67,040). Novel SNPs are highlighted in red dots, with the nearest gene names in black text. Known SNPs are highlighted in purple dots, with the nearest gene names in purple text. The red line is the genome-wide significance level at 5×10^{-8}.

GWAS: genome-wide association study; UKBB: UK Biobank; SNP: single nucleotide polymorphism.

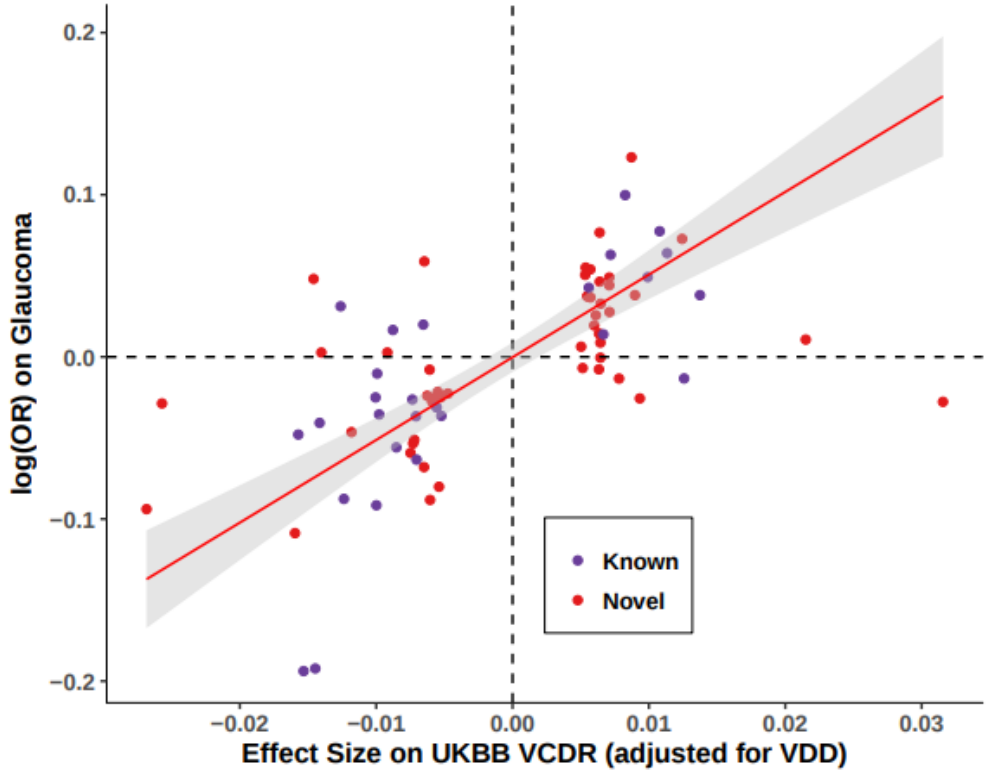

Figure 3.6. Comparison of the effect sizes for 76 UKBB VCDR (vertical DD adjusted) lead SNPs versus that in independent glaucoma cohorts. The figure shows the effect sizes for UKBB VCDR (adjusted for vertical DD) lead SNPs versus log odds ratio in meta-analysis of ANZRAG and UKBB glaucoma GWAS.

The Pearson's correlation coefficient is 0.60 (P value=9.0×10^{-9}). The red line is the best fit line with 95% confidence interval region in grey. Novel VCDR SNPs are highlighted in red and known SNPs in purple. GWAS: genome-wide association study; VCDR: vertical cup-to-disc ratio; VDD: vertical disc diameter; SNP: single nucleotide polymorphism; UKBB: UK Biobank; ANZRAG: Australian and New Zealand Registry of Advanced Glaucoma.

We further combined UKBB VCDR (adjusted for vertical disc diameter) GWAS and IGGC VCDR GWAS summary statistics using MTAG, and identified 107 independent genome-wide significant SNPs (across 90 loci) for VCDR (adjusted for vertical disc diameter) (list of SNPs is found in the appendix). As previously reported, the genetic correlation between intraocular pressure and glaucoma was high (0.71) (MacGregor et al. 2018), but as expected the genetic correlation between VCDR (adjusted for vertical disc diameter) and intraocular pressure was substantially lower (0.22, standard error = 0.03).

Multi-trait glaucoma GWAS

Given the high correlation between glaucoma and its endophenotypes, we then conducted a multivariate GWAS (with 8,002,429 SNPs after quality control) to identify 114 statistically independent SNPs (107 loci, $P < 5\times10^{-8}$) associated with glaucoma — this includes all previously published glaucoma loci as well as 49 novel loci (Figure 3.7; detailed SNPs table, and quantile-quantile plot are provided in the appendix). At the more stringent multiple testing threshold ($P < 1x10^{-8}$) suggested by a simulation study (Y. Wu et al. 2017), 95 loci reach significance, 39 of which are novel (complete list of SNPs provided in the appendix). 27 of the 49 top SNPs at these novel loci were not associated individually with any of the individual input traits at the genome-wide significance level ($P=5\times10^{-8}$), and were only found to reach this threshold for glaucoma due to the MTAG method leveraging the strong correlation between the input traits.

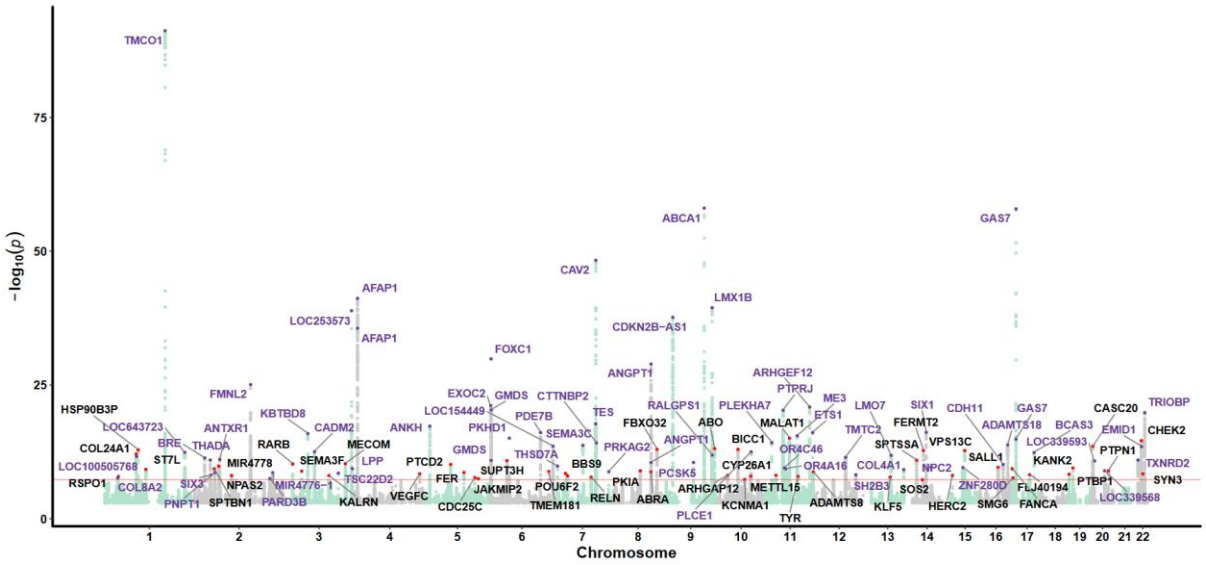

Figure 3.7. Manhattan plot displaying glaucoma-specific P values from the multi-trait GWAS (MTAG) analysis. Novel SNPs are highlighted in red dots, with the nearest gene names in black text. Known SNPs are highlighted in purple dots, with the nearest gene names in purple text. The red line is the genome-wide significance level at 5×10^{-8}.

GWAS: genome-wide association study; SNP: single nucleotide polymorphism; MTAG: multi-trait analysis of GWAS.

We then attempted to replicate the 49 novel SNPs in two independent glaucoma cohorts (ANZRAG and NEIGHBORHOOD). Given the much smaller effective sample size of these replication cohorts (versus the discovery datasets from the MTAG analysis), we did not expect all of the SNPs to be strongly associated — rather if they were genuine associations we would expect the odds ratios to be highly concordant, with some of the smaller odds ratios being individually non-significant. The concordance between the discovery cohort and our replication cohorts log odds ratios was excellent (correlation 0.88, $P=1.6\times10^{-36}$), indicating our multivariate model was successful in identifying genuine glaucoma risk loci (Figure 3.8). Of the 49 novel SNPs, nine SNPs were replicated after Bonferroni correction ($P<0.05/49=0.001$, one-sided test, Table 3.2), 26 SNPs were associated at a nominal significance level ($P<0.05$, one-sided test), and 46 (94%) were in the expected direction (the complete list is found in the appendix). Whilst the concordance between the multivariate and the glaucoma replication sample log odds ratios was high, only nine of the 49 loci were significant for glaucoma after correction for multiple comparisons, and further studies are required to replicate the remaining 40 loci for glaucoma.

Table 3.2. List of 9 novel glaucoma risk loci replicated in ANZRAG and NEIGHBORHOOD datasets after Bonferroni correction.

							UKBB		META	
SNP	**CHR**	**BP**	**Nearest Gene**	**EA**	**NEA**	**FREQ**	**OR**	**P**	**OR**	**P**
rs10796912	1	38091597	*RSPO1*	G	A	0.56	0.94	1.10E-08	0.92	1.80E-04
rs9816799	3	169222771	*MECOM*	T	C	0.56	0.93	4.50E-11	0.93	1.70E-03
rs10435033	7	39054837	*POU6F2*	G	A	0.66	1.07	8.70E-09	1.13	2.20E-06
rs17339357	8	124600906	*FBXO32*	T	A	0.93	0.86	9.20E-14	0.85	3.00E-04
rs7089636	10	60283309	*BICC1*	T	G	0.54	0.92	9.80E-14	0.87	6.80E-07
rs9530143	13	73639371	*KLF5*	G	A	0.68	1.07	1.40E-08	1.08	1.10E-03
rs2249195	15	61958029	*VPS13C*	A	C	0.57	1.08	1.60E-13	1.08	7.70E-04
rs6140009	20	6473054	*CASC20*	C	T	0.62	1.09	2.40E-14	1.12	6.10E-06
rs7273775	20	49061320	*PTPN1*	C	T	0.61	1.07	9.40E-10	1.11	5.40E-04

Chromosomal position is based on the NCBI RefSeq hg19 human genome reference assembly. CHR, Chromosome; EA, effect allele; FREQ, allele frequency of effect allele; NEA, non-effect allele; SNP, single nucleotide polymorphism; OR, odds ratio; P, P values. UKBB, UK biobank data; IGGC, International Glaucoma Genetic Consortium; META, meta-analysis results of ANZRAG and NEIGHBORHOOD datasets.

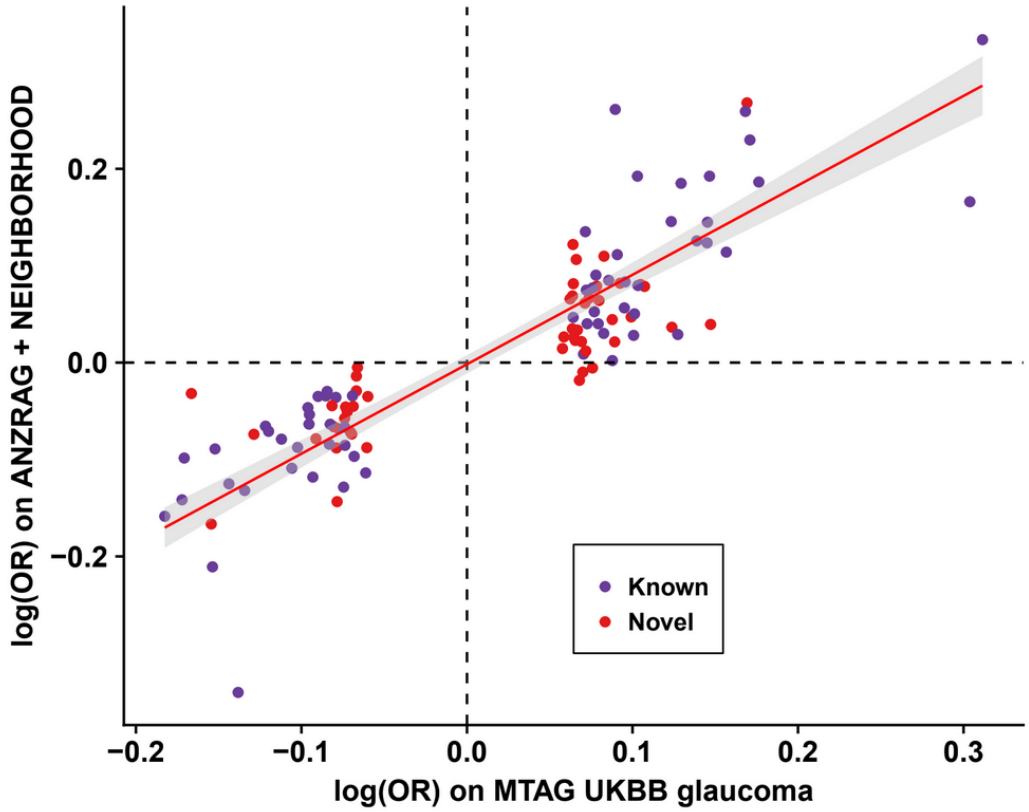

Figure 3.8. Comparison of the effect sizes (log odds ratio) for 114 genome-wide significant independent SNPs identified from the glaucoma multiple trait analysis of GWAS in the UKBB versus those in independent glaucoma cohorts (meta-analysis of ANZRAG and NEIGHBORHOOD). Pearson's correlation coefficient is 0.88 (P value=1.6×10^{-36}). The red line is the best fit line, with the 95% confidence interval region in grey. Novel glaucoma SNPs are highlighted in red and known SNPs in purple.

GWAS: genome-wide association study; UKBB: UK Biobank; ANZRAG: Australian and New Zealand Registry of Advanced Glaucoma; MTAG: multi-trait analysis of GWAS; OR: odds ratio.

Gene expression in human ocular tissues

Variants identified in the previous sections were then investigated with gene expression data to better establish their involvement in ocular development or glaucoma-related pathways at a tissue-specific level. The expression profile of the genes nearest to the identified SNPs discovered in the optic disc size meta-analysis and multitrait glaucoma GWAS were assessed in several ocular tissues: optic nerve head, optic nerve, retina, trabecular meshwork, iris, ciliary body, sclera and cornea. Only genes for which RNA expression data were available were included in the analysis.

The majority of the gene associated with optic disc size (94/106, 89%) displayed differential expression in the optic nerve head relative to all other ocular tissue (Figure 3.9A; full expression table is found in the appendix). *BCAS3* (Microtubule Associated Cell Migration

Factor), *DHRS7* (Dehydrogenase/Reductase 7) and *NPLOC4* (Nuclear Protein Localization Protein 4 Homolog) were the most significantly differentially expressed genes in the optic nerve head and were all novel discoveries. The SNP rs12147505 in *DHRS7* with no linkage disequilibrium with rs34935520 (in SIX6, $R^2 < 0.001$) (H. Springelkamp et al. 2017), had the highest magnitude of effect on disc size; it is a protein coding gene functioning as a catalyst in oxidation and reduction of a wide range of substrates (Haeseleer and Palczewski 2000). It is expressed in all ocular tissues, with highest expression in the corneal stroma followed by the optic nerve head, and suggested to be a risk locus for POAG (Puya Gharahkhani et al. 2018).

Similarly, the novel loci associated with glaucoma in the multitrait glaucoma analysis were expressed in ocular tissues, particularly the trabecular meshwork and the iris (Figure 3.9B). We examined the differential expression of the novel genes in ocular tissues likely to be involved in POAG pathogenesis, namely trabecular meshwork, ciliary body and optic nerve head, and found 6/8 (75%) of the genes differentially expressed in these tissues compared to the other eye tissues tested in this study (*KLF5*, *POU6F2*, *BICC1*, *VPS13C*, *FBXO32*, *PTPN1*). Follow-up functional studies are needed to better understand the role of these genes in glaucoma.

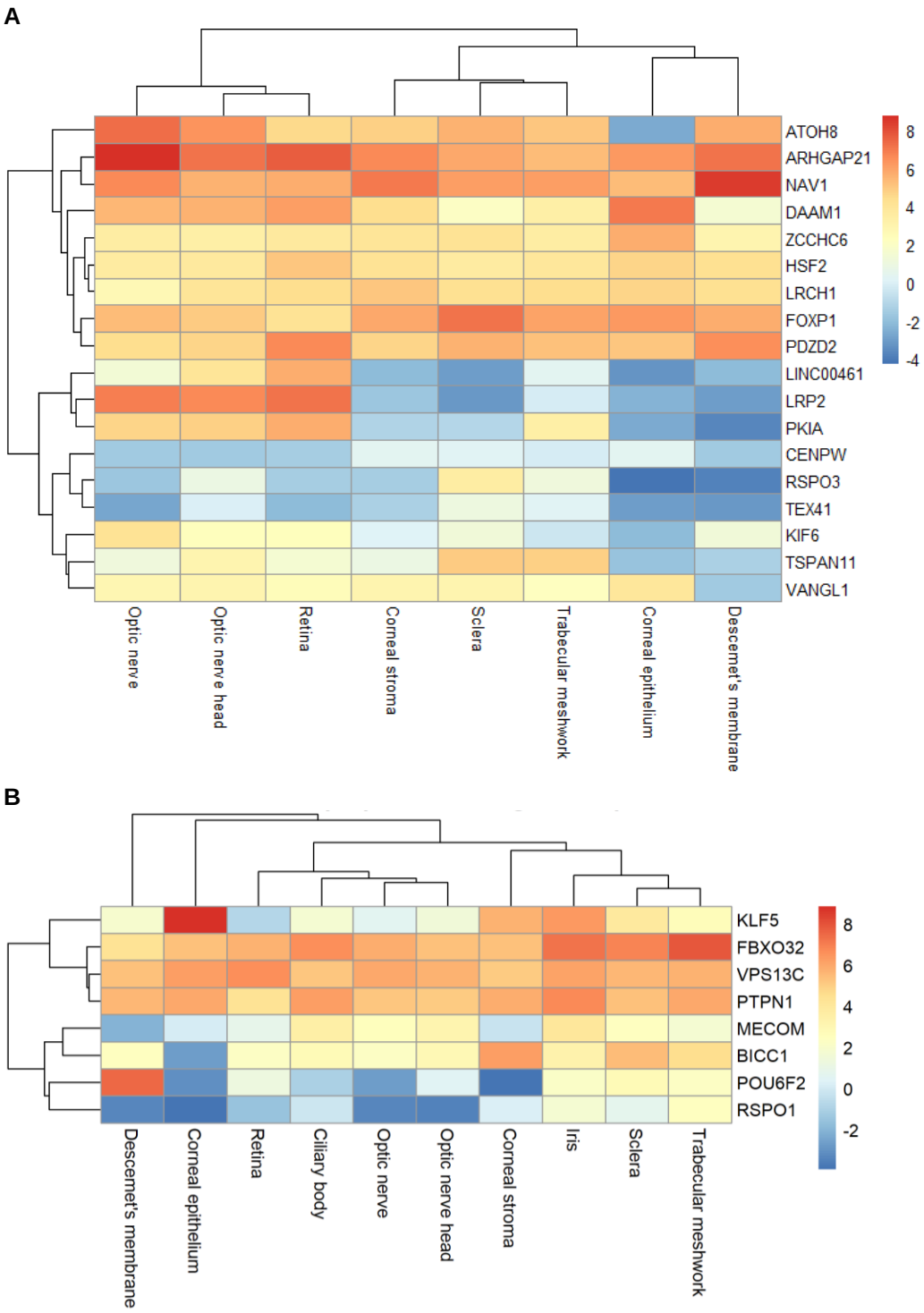

Figure 3.9. Normalised RNA-Seq expression in ocular tissue of the novel genes associated with vertical disc diameter **(A)** and multitrait glaucoma analysis **(B)** that have been reproduced after Bonferroni correction. Normalisation is done using the trimmed mean of M-values method outlined in-text. The heat plot is a measure of normalised log counts per million of the novel genes that have been replicated at Bonferroni correction in IGGC and EPIC samples for vertical disc diameter analysis, and ANZRAG and NEIGHBORHOOD for the multitrait glaucoma analysis. Genes and tissue types are clustered using complete-linkage hierarchical clustering method. Expression data for the genes *MIR216B* and *CASC20* were not available.

Gene-based and pathway analysis

We conducted a genome-wide gene-based association analysis and a gene set enrichment analysis to assess which predefined biological pathways were enriched in our optic disc size meta-analysis and multitrait glaucoma GWAS analyses. For the optic disc size, we identified additional 57 novel genes (without genome-wide significant SNPs in genes; complete list provided in the appendix). For instance, gene *THSD4* was associated with eye tail length and outercanthal width (Cha et al. 2018), and genes *RNLS*, *DENND1A*, *RASGEF1B*, *FAM150B*, and *NCOA2* were associated with myopia. Tissue expression analysis of GTEx data (V7 30 general tissue types) indicated the gene expression profiles were enriched in nerve tissue. Pathway analysis of 10,678 gene sets (MsigDB v6.2, curated gene sets: 4,761, Gene Ontology terms: 5,917) resulted in 29 significant gene sets after Bonferroni correction, which include sensory organ development, tissue development, and morphogenesis (Table 3.3). The top pathway was RAMJAUN_APOPTOSIS_BY_TGFB1_VIA_MAPK1_UP, which is a transforming growth factor-beta (TGFbeta) activated signalling pathway, involved in apoptosis and the regulation of cell growth and survival (Ramjaun et al. 2007; Saika 2006).

Table 3.3. Pathway analysis of disc size meta-analysis (list of 29 significant pathways after Bonferroni correction)

Gene set name	N GENES	BETA	SE	P-value
Ramjaun_apoptosis_by_tgfb1_via_mapk1_up	6	2.18	0.42	8.0E-08
Epithelium_development	900	0.17	0.03	1.7E-07
Regulation_of_cartilage_development	60	0.58	0.13	2.5E-06
Tissue_morphogenesis	515	0.19	0.04	4.1E-06
Morphogenesis_of_an_epithelium	383	0.24	0.05	1.1E-06
Kidney_epithelium_development	118	0.54	0.09	1.3E-09
Pathway_restricted_smad_protein_phosphorylation	13	1.36	0.3	4.0E-06
Regulation_of_mesonephros_development	23	0.98	0.22	4.4E-06
Forebrain_regionalization	24	1.05	0.21	5.0E-07
Embryo_development	864	0.16	0.03	9.0E-07
Cell_differentiation_involved_in_kidney_development	33	0.81	0.17	1.2E-06
Embryonic_organ_morphogenesis	273	0.28	0.06	3.8E-06
Nephron_epithelium_development	86	0.57	0.11	4.5E-08
Renal_tubule_development	74	0.61	0.12	8.9E-08

Organ_morphogenesis	816	0.16	0.03	2.0E-06
Tube_development	533	0.24	0.04	1.5E-09
Embryonic_morphogenesis	526	0.23	0.04	1.1E-07
Urogenital_system_development	288	0.26	0.06	2.3E-06
Mesenchyme_development	177	0.36	0.07	4.0E-07
Tube_morphogenesis	311	0.28	0.06	3.6E-07
Sensory_organ_development	481	0.2	0.04	3.6E-06
Telencephalon_regionalization	13	1.67	0.31	4.5E-08
Kidney_morphogenesis	76	0.56	0.11	4.9E-07
Nephron_development	108	0.45	0.1	1.4E-06
Circulatory_system_development	761	0.16	0.03	3.1E-06
Tissue_development	1451	0.15	0.03	8.4E-10
Metanephros_morphogenesis	27	0.87	0.19	2.4E-06
Regulation_of_ossification	166	0.33	0.07	4.4E-06
Transforming_growth_factor_beta_receptor_binding	49	0.64	0.13	8.8E-07

N GENES: number of genes in a pathway; BETA: estimated beta-coefficient of gene set in association with disc size; SE: standard error.

Using the results of the multitrait glaucoma GWAS, we found 196 genes and 14 gene sets, respectively, that were significant after Bonferroni correction (Table 3.4). The most significant pathways were also previously implicated (i.e. extracellular matrix, collagen, and circulatory system development) (Huang et al. 2019; MacGregor et al. 2018). Further studies are warranted to investigate the role of these pathways in the risk of glaucoma. The full details of the gene-based and pathway analyses are provided in the appendix.

Table 3.4. Pathway analysis of glaucoma MTAG GWAS (list of 14 significant pathways after Bonferroni correction)

Gene set name	N GENES	BETA	SE	P-value
Proteinaceous_extracellular_matrix	335	0.395	0.06	8.0E-13
Extracellular_matrix	400	0.311	0.05	4.1E-10
Collagen_trimer	84	0.659	0.11	1.8E-09
Reactome_collagen_formation	55	0.781	0.14	6.6E-09
Naba_collagens	41	0.921	0.16	7.1E-09
Response_to_laminar_fluid_shear_stress	14	1.56	0.30	7.5E-08
Pid_syndecan_1_pathway	43	0.768	0.15	2.8E-07
Naba_core_matrisome	259	0.312	0.06	6.3E-07
Kinsey_targets_of_ewsr1_flii_fusion_dn	312	0.258	0.06	1.7E-06
Circulatory_system_development	761	0.168	0.04	1.9E-06
Vasculature_development	452	0.216	0.05	2.0E-06
Extracellular_matrix_component	118	0.441	0.10	2.1E-06
Complex_of_collagen_trimers	21	1.03	0.23	2.7E-06
Extracellular_matrix_structural_constituent	71	0.571	0.13	4.5E-06

N GENES: number of genes in a pathway; BETA: estimated beta-coefficient of gene set in association with glaucoma (using a multi-trait analysis approach); SE: standard error.

Discussion

We conducted the largest GWAS of optic disc size and VCDR to date, and combined these findings with GWAS of IOP results to conduct a multitraint glaucoma GWAS. My original contribution to knowledge was identifying 101 loci associated with optic disc size, and 90 loci associated with VCDR using manual grading of the UKBB fundus photographs. A majority of the novel variants discovered were also replicated in independent datasets at nominal level. In addition, 107 loci were found to be associated with glaucoma, leveraging the correlated endophenotypes of IOP and VCDR adjusted to disc size in the discovery.

The identified optic disc size genes have important functions. For instance, the top two novel replicated genes are *VANGL1* and *CENPW*. VANGL Planar Cell Polarity Protein 1 (*VANGL1*) regulates the establishment of planar cell polarity, which plays a key role in tissue morphogenesis, embryonic development, and the development of eye tissues (Iliescu et al.

2011; Belotti et al. 2012; Wolff and Rubin 1998). *CENPW* encodes Centromere Protein W, which is related to cell cycle, mitotic state, and chromosome maintenance (Prendergast et al. 2011). The lead SNP rs2152876 in *CENPW* exhibits a pleiotropic effect, as its proxy SNPs (R^2 > 0.8) are associated with intraocular pressure (X. Raymond Gao et al. 2018), height (N'Diaye et al. 2011), hip circumference (Shungin et al. 2015), and the age onset of menarche (Elks et al. 2010). The encoded protein by *STRA6* acts as a receptor for retinol-binding protein responsible for the cellular uptake of vitamin A, which is critical to the normal development of the eyes (Casey et al. 2011). Indeed, mutations in *STRA6* impairing this function lead to severe developmental abnormalities in the eyes such as microphthalmia, anophthalmia and coloboma (Casey et al. 2011; Pasutto et al. 2007). *SIX3*, *PRSS56* and *PAX6* are also involved in eye development. *PAX6* has been labelled as the master control gene for the morphogenesis of the eye, and is regulated by the transcriptional regulator *SIX3* (Azuma et al. 2003). *BCAS3* and *RSPO3* are involved in angiogenesis, vascular support and cell migration (Jain et al. 2012; Kazanskaya et al. 2008). *BMP4* antagonises transforming growth factor-beta 2 (TGF-β2) signalling, a cytoke involved in the synthesis and deposition of extracellular matrix in the optic nerve head (Zode, Clark, and Wordinger 2009). This pathway is implicated in the pathological remodelling of the optic nerve head in glaucoma (Zode, Clark, and Wordinger 2009), and deficiency of *BMP4* results in an abnormal optic nerve with loose connective tissue (Chang et al. 2001). All together, these gene findings help us have a better understanding of the development of the eye and related traits.

Optic disc size is highly correlated with the VCDR (H. Springelkamp et al. 2017); therefore optic disc size is important for the interpretation of a glaucomatous optic disc (Hoffmann et al. 2007; Crowston et al. 2004). Clinically, adjusting VCDR to DD improves its utility as larger discs are more likely to have physiologically larger cups (J. B. Jonas et al. 2000). In clinical genetics, genes are more likely to be involved in the pathogenesis of glaucoma if associated with larger VCDR but not disc size, or VCDR adjusted to disc size. For instance, variation in the *PDZD2* gene is associated with optic cup area and VCDR (H. Springelkamp et al. 2017), and our study identifies the same variation to be strongly associated with disc size. This would suggest that the observed association with VCDR is likely due to the disc size rather than a pathological enlargement of the optic cup. Similarly, the previously reported association between *F5* and VCDR is likely related to disc size due to its larger association with disc size in our study and previously (Henriët Springelkamp et al. 2015). Indeed, when the disc size is adjusted for, Springelkamp *et al.* have reported the estimated effect size of the *F5* variant on VCDR is negligible (H. Springelkamp et al. 2017). Several of the identified disc size genes are correlated with intraocular pressure. For instance, genes *TMEM119*, *CENPW*, *LTBP1*, *TEX41*, and *PKIA* are reported to be associated with intraocular pressure (MacGregor et al. 2018; A.

P. Khawaja et al. 2018; Choquet et al. 2017; X. Raymond Gao et al. 2018), which could represent pleiotropic effects of these genes. Correlating disc size loci with the genes for glaucoma and its endophenotypes would help to identify the role of these genes in glaucoma pathogenesis.

From the multivariate GWAS, we identified 49 novel loci associated with glaucoma (nine of which were replicated after correction for multiple comparisons in independent glaucoma case-control cohorts; 26 were replicated at nominal level). Interestingly, most of the loci replicated at P<0.001 were at genes previously associated with glaucoma risk factors (myopia, central corneal thickness, IOP, and VCDR). Specifically, *RSPO1* is associated with ocular axial length (Cheng et al. 2013). *BICC1* is associated with myopia and corneal astigmatism (Pickrell et al. 2016; V. J. M. Verhoeven et al. 2013; M. C. Lopes et al. 2013). *POU6F2* modulates corneal thickness and increases glaucoma risk in animal experiments (King et al. 2018). *FBXO32*, *PTPN1*, and *VPS13C* are associated with IOP (MacGregor et al. 2018; A. P. Khawaja et al. 2018; X. Raymond Gao et al. 2018), whilst *CASC20* was identified in the VCDR (adjusted for vertical disc diameter) GWAS. These findings show that the multivariate GWAS improves power to identify novel glaucoma genes and advance our understanding of the causes of glaucoma risk.

There are some limitations for the studies presented in this chapter. A concern in MTAG method is the homogeneous assumption which could be violated for some SNPs that have no effect on one trait but non-null for other traits (i.e. it is possible that a small number of the variants may be more specific for IOP or VCDR rather than glaucoma). The homogeneity assumption has been studied in detail by Turley et al. (2018). Such possible inflation was evaluated using max False Discovery Rate (maxFDR) as recommended by Turley et al. (2018). The baseline maxFDR for MTAG glaucoma-specific input GWAS summary statistics was 0.049, and the maxFDR for MTAG glaucoma-specific output summary statistics was 0.03. As these are similar, there was no evidence of inflation due to violation of the homogeneity assumption. As recommended by the MTAG authors, replication analysis was also performed to assess the credibility of novel SNPs in two independent data sets (ANZRAG and NEIGHBORHOOD); this analysis showed there was a very good concordance between the MTAG based effect sizes and those from the glaucoma cohorts. Further research needs to be undertaken to investigate the biological mechanisms of these novel genes on glaucoma risk.

Optic nerve head phenotyping was only available for one eye in the UKBB. Due to the lengthy manual process of grading 67,040 UKBB fundus photos, DD and VCDR grading was completed on the left eye where the image quality was good, otherwise the right eye was used.

The optic disc diameter is expected to be similar. For instance, in the EPIC-Norfolk sample set (N = 6,005), the measurement of the vertical disc diameter was 2.34 ± 0.26 mm in the right eyes, compared 2.33 ± 0.26 mm in the left eyes, which is also consistent with previous studies (H. A. Quigley et al. 1990). On the other hand, VCDR asymmetry is often seen in glaucoma, and is reported to be present in about 2% of the normal population (Qiu, Boland, and Ramulu 2017). Thus, whether some individuals have a higher VCDR in the other eye and than that used in our GWAS cannot be excluded with certainty.. Ocular magnification and tilted appearance of some optic discs could also affect cup and disc size measurements; however, in practice the effects of these are expected to be small (D. F. Garway-Heath et al. 1998).

Only individuals of European ancestry were evaluated in the GWASs, hence the generalizability of the genetic findings to other populations remains unclear. For the disc diameter GWAS, the concordance in lead SNP effect sizes was very high between UKBB disc size GWAS and IGGC disc size GWAS in Asian population (Pearson's correlation coefficient 0.72). For glaucoma GWAS, further research is being conducted to investigate the glaucoma risk loci in other ethnicities. Gharahkhani et. al. (2020) have recently reported a large multi-ethnic meta-analysis of genome-wide association studies of POAG, and found the majority of POAG risk loci to have broadly consistent effects across European, Asian and African ancestries. This work identified an additional 44 POAG risk loci, as well as validating those reported in this chapter (Puya Gharahkhani et al. 2020). Interestingly, all the POAG risk variants identified in Gharahkhani et. al. were also associated with the glaucoma endophenotypes IOP or VCDR, highlighting the importance of genetic studies of these endophenotypes.

The results of these large GWAS contributed to our understanding of the biological pathways involved in the pathogenesis of POAG. These POAG risk loci are involved in sensory organ development, extracellular matrix, collagen, and circulatory system development, which may offer potential treatment targets (Puya Gharahkhani et al. 2020; Craig et al. 2020). Moreover, identifying these trait- and disease-associated common variants has paved the path to translating these risk variants to clinical application using polygenic risk scores (Torkamani, Wineinger, and Topol 2018). This approach would enable a personalised glaucoma risk prediction and stratification tool, with an aim to earlier diagnosis of glaucoma and commencement of treatment, and ultimately, saving an otherwise irreplaceable vision loss.

Chapter 4: Genetic risk prediction in glaucoma using polygenic risk scores

Published manuscripts

The majority of the contents of this chapter have been published in two peer-reviewed manuscripts in which I am a first author. Two polygenic risk scores are used for genetic risk prediction in this chapter. The clinical utility of a multi-trait glaucoma polygenic risk score was published in manuscript in *Nature Genetics* in 2020, volume 52, issue 2, pages 160–166 (Craig et al. 2020). Author contributions relating to the genetic discovery component was detailed in Chapter 3. My contributions for the clinical application of this polygenic risk score involved study concept and design (30%), data collection in the form of extracting structural and functional progression outcomes and data wrangling (85%), data analysis including association between the polygenic risk score and glaucoma phenotype (60%), data interpretation including the clinical application of the risk score (50%), drafting the manuscript (50%), and critical revision of the manuscript for important intellectual content (50%). Specific to the clinical application of the polygenic risk score, Xikun Han contributed to study concept and design (30%), data collection in the form calculating individual polygenic risk scores of the study cohorts (30%), data analysis including investigating the polygenic risk score's performance in a population-based risk stratification and myocilin-related glaucoma penetrance, data interpretation (15%), drafting the manuscript (25%), and critical revision of the manuscript for important intellectual content (25%). Other authors' contributions were detailed in Chapter 3. Specifically, Mark Hassal contributed to data analysis and interpretation of the results by supervising my work, and performing additional sensitivity analyses (10%).

Parts of the chapter relating to an intraocular pressure polygenic risk score were published in *Ophthalmology* in 2020, volume 127, issue 7, pages 910–907 (A. Qassim et al. 2020). As the first author of the manuscript, I contributed to the study concept and design (80%), data acquisition by using wrangling and summarising glaucoma phenotypes recorded in study registries (70%), data analysis including statistical analysis (100%), drafting the manuscript (90%), and critical revision of the manuscript for important intellectual content (70%). Emmanuelle Souzeau, Owen Siggs, Mark Hassall, and Jamie Craig contributed to study concept and design (20%), drafting the manuscript (10%) and critical revision of the manuscript for important intellectual content (25%). Xikun Han, Puya Gharahkhani and Stuart MacGregor contributed to generating the data collection in the form of generating the polygenic risk score (20%), and critical revision of the manuscript for important intellectual content (5%). Additionally, this manuscript is co-authored by 15 other authors who collectively

contributed to data collection by recruiting patients to the glaucoma registries, administrative and technical support, critical revision of the manuscript for important intellectual content, and supervision.

A study focused on predicting diurnal intraocular pressure profile using home tonometry was submitted to a peer-review journal in a manuscript titled “A polygenic risk score predicts intraocular pressure readings outside office hours and early morning spikes as measured by home tonometry”. The manuscript was under review at the time of writing this chapter.

Introduction

POAG is asymptomatic in the early stages, and currently approximately half of all cases in the community are undiagnosed even in developed countries (P. Mitchell et al. 1995). Better strategies to identify high-risk individuals are urgently needed (J. M. Burr et al. 2007), and more refined approaches can capitalize on the fact that POAG is one of the most heritable of all common human diseases (Chapter 1) (K. Wang et al. 2017; Sanfilippo et al. 2010; Choquet et al. 2018). Progressive vision loss from glaucoma can be slowed, or in some cases halted, by timely intervention to reduce IOP using medical therapy, laser trabeculoplasty or incisional surgery (Chapter 1) (Robert N. Weinreb and Khaw 2004). The ability to predict progression is currently crude, with delays in treatment escalation for high-risk individuals an important and inevitable consequence, as well as substantial cost and morbidity associated with overtreatment of lower risk cases. The lack of a currently cost effective screening strategy for glaucoma (J. M. Burr et al. 2007), coupled with very high heritability make glaucoma an ideal candidate disease for the development and application of a polygenic risk score to facilitate risk stratification.

IOP monitoring is a key component of the glaucoma management algorithm, but has traditionally relied on relatively scarce data obtained within office hours. These isolated IOP measurements fail to capture the dynamic IOP fluctuation occurring over the 24-hour period (Mosaed, Liu, and Weinreb 2005; Jost B. Jonas et al. 2005). Jonas et al. (2005) reported that any single IOP measurement has only a 25% probability of capturing the peak of a diurnal IOP curve. Similarly, Fogagnolo et al. (2009) reported that IOP measurements during office hours identified peak, mean, and IOP fluctuation in only 20% of glaucoma patients. Unrecognised IOP spikes may contribute to glaucomatous neurodegeneration (J. H. K. Liu et al. 2003). The phenomenon of circadian IOP fluctuation has garnered growing interest in recent years, with the expectation that treatment of currently unmeasured IOP fluctuations could be integrated into the future glaucoma treatment paradigm (Kaweh Mansouri and Weinreb 2015). Ambulatory rebound tonometry using devices such as the Icare HOME (Icare Finland Oy) can provide accurate and comparable measurements of IOP compared to Goldmann applanation tonometry (GAT), the gold standard of clinical IOP measurement (Termühlen et al. 2016; Takagi, Sawada, and Yamamoto 2017).

Glaucoma and its endophenotypes are polygenic in the normal population (Sanfilippo et al. 2010). Large GWAS have led to the discovery of more than one hundred common loci associated with glaucoma, VCDR and IOP, as reported in detail in Chapter 3. In contrast to the aforementioned monogenic variants, each single SNP contributes a very small effect size

to the risk. For instance, variants in or near the genes *TMCO1* and *CAV2*, two of the most strongly associated loci with IOP and glaucoma, are present in 10-15% of the population but account for a modest risk of glaucoma individually (odds ratio ranging between 1.1 to 1.4) (MacGregor et al. 2018). However, the combined effects of these common SNPs significantly affect the observed clinical phenotype (MacGregor et al. 2018).

To understand the impact of these common variants, the total number of variants an individual is carrying is counted and multiplied by their effect sizes, to generate a weighted polygenic risk score (PRS) (Chapter 1) (Chatterjee, Shi, and García-Closas 2016). A genetic risk stratification may then be done by calculating an aggregate score of all the SNPs an individual has associated with a trait. For instance, a person with the majority of the discovered IOP variants (a high IOP PRS) is hypothesised to have a higher IOP than someone who has only a few.

Outlined in this chapter is my original contribution to knowledge in genetic risk prediction in glaucoma using a comprehensive glaucoma PRS encompassing thousands of independent SNPs associated with glaucoma. As IOP remains the most important, and the only modifiable clinical risk factor for POAG, I additionally investigated the clinical utility of an IOP PRS that is composed of variants most stringently associated with IOP (MacGregor et al. 2018).

Methods

The following methods section has been previously published in two peer-reviewed manuscripts, and has been edited to fit the structure of the thesis (A. Qassim et al. 2020; Craig et al. 2020).

Two PRS are studied in this chapter. A comprehensive glaucoma PRS was based on the results of a multiple trait analysis of GWAS (MTAG PRS) that encompases variants assocation with glaucoma (case-control), VCDR and IOP as described in Chapter 3. Additionally, an IOP-only PRS (IOP PRS) was used to investigate the combined effects of IOP-associated risk variants using a statistically more strict SNP criteria and a recently published GWAS of IOP (MacGregor et al. 2018). The clinical application of these PRS in characterising glaucoma phenotype and predicting risk of progression was then investigated in several well-characterized large glaucoma cohorts. PRS were calculated from the summary statistics of the relevant GWAS for each cohort by selecting mutually exclusive samples for inclusion in the discovery and testing datasets to ensure no sample overlap.

Study cohorts

The MTAG PRS was derived from the GWAS summary statistics of the multiple trait glaucoma GWAS described in Chapter 3. This GWAS constitutes participants from the UKBB, and the International Glaucoma Genetics Consortium (IGGC). Details of these cohorts have been described previously in Chapters 2 and 3. The clinical application of the MTAG PRS as a risk prediction and stratification tool was then explored in ANZRAG, PROGRESSA, and the Blue Mountains Eye Study (BMES) cohorts. The former two cohorts were described in detail in Chapter 2. An additional replication dataset included advanced glaucoma cases from the UK (Southampton and Liverpool). A summary of these cohorts is shown in Table 4.1.

The ANZRAG and PROGRESSA datasets were used for clinical profiling of the MTAG and IOP PRS. In this chapter, only participants in ANZRAG with POAG were included. Similarly, for consistency and comparability to the glaucoma cohorts, only participants with established early manifest POAG in PROGRESSA were included in glaucoma-specific analyses. All PROGRESSA participants are in the early glaucoma spectrum (suspect, pre-perimetric, or early manifest glaucoma), with open angles on gonioscopy, and no secondary cause of elevated IOP or vision impairment. Thus, to harness the power of the longitudinal follow-up, additional analyses on the clinical implications of the PRS included all eligible participants with sufficient longitudinal follow-up.

A subset of the non-European UKBB was also used to evaluate the performance of MTAG PRS in a South Asian ancestry (the largest ethnic minority in UKBB, defined here as individuals self describing as Indian or Pakistani ancestry). There were 192 cases and 6,841 controls included with a homogeneous genetic ancestry which was clearly distinct from UKBB participants of European ancestry (principal component plots are attached in the appendix).

Table 4.1. Overview of study datasets

Study	Age Mean ± SD	Sex, male %	Number of participants (cases/controls)	Genotyping Array	Imputation	Imputation method
ANZRAG glaucoma (Phase 1)	74.2 ± 11.6	58%	3,147 (1,155/1,992)	Illumina Omni1M or OmniExpress	1000G phase1	IMPUTE2
ANZRAG glaucoma (Phase 2)	74.5 ± 12.2	44%	1,525 (579/946)	Illumina HumanCoreExome	HRC r1.1	Minimac3
ANZRAG glaucoma (Phase 3)	70.5 ± 15.3	26%	5,149 (1,337/3,812)	Illumina HumanCoreExome	HRC r1.1	Minimac3
UKBB glaucoma	56.95± 7.89	46%	127,266 (7,947/119,319)	Affymetrix UK BiLEVE Axiom or UK Biobank Axiom arrays	HRC r1.1	Minimac3
UKBB IOP	57.25± 7.88	47%	103,914	Affymetrix UK BiLEVE Axiom or UK Biobank Axiom arrays	HRC r1.1	Minimac3
UKBB VCDR	57.06 ± 7.89	47%	67,040	Affymetrix UK BiLEVE Axiom or UK Biobank Axiom arrays	HRC r1.1	Minimac3
IGGC IOP	Varies by sub-study	Varies by sub-study	29,578	Various Illumina and Affymetrix arrays	1000G phase1	IMPUTE2
IGGC VCDR	Varies by sub-study	Varies by sub-study	23,899	Various Illumina and Affymetrix arrays	1000G phase1	IMPUTE2
UK glaucoma (Southampton/ Liverpool)	59.03 ± 10.16	47%	3,332 (332/3,000)	Illumina Infinium Global Screening Array	HRC r1.1	Minimac3
BMES	64.02 ± 8.24	43%	1,795 (74/1,721)	Illumina Omni1M	HRC r1.1	Minimac3
PROGRESSA *	67.5 ± 9.4	41%	388 (388/0)	Illumina HumanCoreExome	HRC r1.1	Minimac3
NEIGHBORHOOD	Varies by sub-study	Varies by sub-study	37,333 (3,853/ 33,480)	Various Illumina and Affymetrix arrays	1000G phase1	Varies by sub-study

IGGC and NEIGHBORHOOD studies have several sub-studies with a wide range of participant demographics. Summary statistics of these cohorts are described in detail in previous publications (H. Springelkamp et al. 2017; Janey L. Wiggs et al. 2013).

* Summary statistics of the PROGRESSA cohort is those used in the MTAG PRS analysis only.

All samples are of genetically confirmed European ancestry.

SD: standard deviation; IOP: intraocular pressure; VCDR: vertical cup-to-disc ratio; HRC: Haplotype Reference Consortium

Replication of the clinical profiling of the MTAG PRS was performed in the Southampton and Liverpool dataset. For the IOP PRS analysis, this cohort was combined with ANZRAG POAG cases as they were recruited and phenotyped using a similar protocol. Detailed information of Southampton samples was reported previously (H. Springelkamp et al. 2017). In brief, POAG patients were recruited from the Southampton University Hospital Trust Eye Clinic and satellite regional glaucoma clinics. Each patient was examined by an experienced glaucoma specialist. Cases with advanced glaucoma (exactly matching that defined for ANZRAG) and of European ancestry were selected for the replication study. Three hundred and eight cases had trabeculectomy surgery status (as a binary indicator) available. A further set of 50 advanced POAG were recruited as part of Liverpool University study of glaucoma again with the definition of advanced POAG exactly matching the ANZRAG definition. After quality control, 332 advanced glaucoma cases from Southampton and Liverpool had genotype data available, based on Illumina Infinium Global Screening Array-24 v2.0 array genotyping. Cases were matched to 3,000 European ancestry individuals from the QSkin Sun and Health study (Olsen et al. 2012), which were genotyped on the same array.

Glaucoma risk prediction of the MTAG PRS in a population setting was examined in the BMES cohort. Detailed information of the BMES study was reported previously (P. Mitchell et al. 1995). In brief, BMES is a population-based cohort study of common eye diseases among suburban residents aged 49 years or older, living in the Blue Mountains region, west of Sydney, Australia. IOP was measured using Goldmann applanation tonometry (Haag-Streit, Bern, Switzerland) (P. Mitchell et al. 1995). DNA samples were obtained during the 5-year follow-up and ancillary surveys, which were performed between 1997 and 2000. Participants were genotyped with Human610-Quad arrays (Illumina, San Diego, CA, USA). For the MTAG PRS prediction, 74 POAG cases and 1,721 controls of European descent with genotype data were included in analysis.

Before imputation, we filtered individuals with more than 3% missing genotypes, and SNPs with call rate < 95%, minor allele frequency of <1%, and Hardy-Weinberg P value < $1x10^{-6}$. The imputation was performed using Michigan Imputation Server (Das et al. 2016). To ensure matching of cases and controls for ancestry, any non-European ethnic outliers were removed based on the first two genetic principal components (> 6 standard deviations), with European individuals from the 1000 Genomes Project Phase 3 data used as a reference population. Identity by descent was estimated using autosomal markers and only one member of each pair of related individuals ($\hat{\pi}$ >0.2) was retained for analysis.

Using home tonometry to profile short-term IOP variation

A subset of the PROGRESSA cohort were recruited to undergo home tonometry to record their short-term IOP profile, using the Icare HOME tonometer. Informed written consent was obtained from all participants, and the study was approved by the Southern Adelaide Clinical- and the Macquarie University Human Research Ethics Committees.

Each participant attended a training session conducted by a trained instructor. Participants were required to be able to appropriately position the Icare HOME tonometer, and demonstrate competence in independently generating at least two reliable measurements. Participants were instructed to measure the IOP of both eyes four times daily. The stipulated timings for IOP measurements were: early morning, midday, late afternoon, and late evening. Each measurement was to be performed seated, and concurrently for each eye. Participants were instructed to do this for five consecutive days.

The Icare HOME was then connected to a computer, and data were exported. Measurements labelled as “Rejected” by the device’s quality score were discarded as per manufacturer recommendations. IOP measurements were systematically evaluated to minimise measurement errors and artefacts. IOP measurements of >50 mmHg or <5 mmHg were excluded as such extreme measurements were more likely to be artefactual due to decentered measurements. To further exclude unreliable measurements, IOP measurements repeated within a ten minute period were grouped into “clusters”. Such clustered measurements were due to the participants repeating the IOP measurement process (observed in 54% of the eyes), and could contribute to skewed means and variance if not controlled for. Clusters with a wide IOP range (≥ 5 mmHg) suggesting poor reliability were excluded. In an effort to minimise the effect of repeated measurements on summary parameters, only the second IOP measure within each cluster was included in analyses, and other repeat measurements were discarded. To generate reliable summary parameters especially when stratified by office hours, only eyes that completed a minimum of two days with at least three IOP measurements per day after the aforementioned exclusions were included.

Mean and maximum IOP of all measurements were determined for each eye over the duration of the study. The mean IOP was also calculated for measurements made during office hours (between 09:00 and 17:00), and outside office hours (between 17:00 and 09:00) for each eye over all days in the duration of the study. Highest-recorded early-morning pressures were defined as the maximum IOP recorded between 05:00 and 09:00 at any day corresponding with the morning IOP elevation observed in glaucomatous eyes (Jost B. Jonas et al. 2005; J.

H. K. Liu et al. 2003) To assess the correlation between IOP PRS and IOP fluctuation, two parameters were defined: absolute IOP range, and standard deviation of all IOP measurements. Absolute IOP range was defined as the difference between the maximum and the minimum IOP recorded across all the days for a given eye over the course of the study (Figure 4.1).

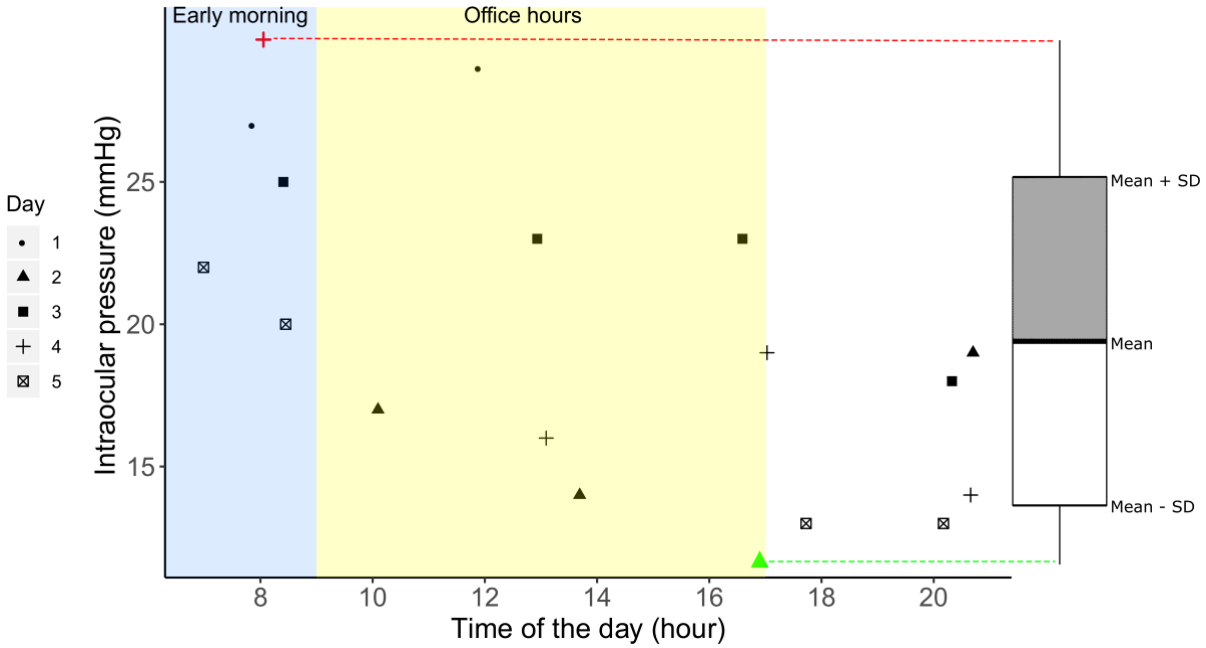

Figure 4.1. An example of the home tonometry measurement output for an eye after quality control. Each dot represents an intraocular pressure (IOP) measurement at a particular time over five days. The shapes indicate the day the measurement was taken. Office hours (0900 - 1700) and early morning (0500 - 0900) are highlighted. The unshaded region and the early morning represent the outside office hours (1700 - 0500). The box plot represents the mean and standard deviation (SD) of the IOP measurements, with the grey area representing IOP fluctuation (one SD). The absolute IOP range is shown as the difference between the maximum (red cross) and the minimum (green triangle) IOP recorded.

Polygenic risk scores: multi-trait glaucoma PRS (MTAG PRS)

The MTAG PRS was based on the estimated glaucoma odds ratios from the MTAG GWAS analysis reported in Chapter 3 (Figure 4.2A). To derive a comprehensive PRS, a range of SNP inclusion P-value thresholds were considered, applying each to the first prediction cohort (ANZRAG). The target outcome was ANZRAG advanced POAG status using 1,734 cases and 2,938 controls. PRSs were calculated in PLINK with linkage disequilibrium (LD) clumping followed by P value thresholding (PLINK version 1.90 beta, -clump-p1 1 --clump-p2 1 --clump-r2 0.1 --clump-kb 1000, and P value thresholds at 5×10^{-8}, 1×10^{-5}, 0.001, 0.05, 1) (Purcell et al. 2007). LD clumping r^2=0.1 was based on the overlap SNPs between training and target

datasets. For each PRS, Nagelkerke's pseudo R^2 and area under the curve (AUC) from the logistic regression were calculated and adjusted for the effects of sex and the first four principal components. To avoid falsely inflating prediction accuracy, the MTAG PRS threshold with the greatest predictive value in ANZRAG ($P \leq 0.001$) was subsequently used in predictions into other target sets (rather than repeatedly taking the best P-value threshold for each of the datasets).

The predictive ability of the PRS was also explored in other datasets; however, to ensure the results generalise to further cohorts, mutually exclusive samples were used for inclusion in the discovery and testing datasets to ensure no sample overlap. When required, the MTAG PRS was re-derived to ensure no sample overlap (Figure 4.2). As BMES is part of the IGGC, to avoid sample overlap when investigating the performance of the MTAG PRS over traditional risk factors in a population cohort (BMES), the MTAG PRS was rederived excluding IGGC VCDR and IOP GWAS summary results (Figure 4.2B). The target dataset was 74 POAG cases and 1,721 controls in BMES with IOP and VCDR available.

A similar approach using the UKBB cohort was performed with a target dataset of 1,421 glaucoma cases and the 3,000 controls (Figure 4.2C). In this subanalysis, 3,000 non-glaucoma participants with both IOP and VCDR available from UKBB were randomly selected, and the UKBB VCDR and IOP GWASs were re-analysed. Both the cases and controls were unrelated and had IOP and VCDR measurements, and their relatives were excluded from the dataset. The performance of the MTAG PRS was then compared to, and in combination with traditional risk factors using AUC.

The clinical utility of the MTAG PRS was also assessed in screening the general population, or in those with the commonest 'monogenic' glaucoma-associated variant (MYOC p.Gln368Ter). In this subset analysis, participants of the UKBB with other serious eye diseases were excluded, leaving data from 382,161 participants available for analysis. *MYOC* p.Gln368Ter (rs74315329) can be imputed with high accuracy from genotyping arrays (Puya Gharahkhani et al. 2015); thus, individuals with *MYOC* p.Gln368Ter variant were identified using imputation, and the risk allele (A) dosage of rs74315329 was calculated. *MYOC* p.Gln368Ter carriers were defined by setting the dosage threshold at 0.8. This identified 965 carriers, including 72 glaucoma cases. Age of glaucoma diagnosis was collected from the UKBB fields 4689 and 20009. In total, age at diagnosis information was available for 4,596 individuals. To avoid sample overlap for *MYOC* p.Gln368Ter carriers when constructing the MTAG PRS, all *MYOC* p.Gln368Ter carriers and their relatives were removed from UKBB

VCDR and IOP GWAS (Figure 4.2D). A Cox model was used to calculate the cumulative risk of glaucoma for *MYOC* p.Gln368Ter carriers, stratifying by the tertiles of PRS.

For analysis examining cumulative risk of glaucoma in the general population (i.e. in *MYOC* p.Gln368Ter non-carriers), participants were stratified by deciles of PRS. For glaucoma cases without age at diagnosis information, age at study enrollment was used as the age of diagnosis in the survival analysis. Since the VCDR and IOP GWAS samples are only from non-glaucoma cases, the prediction of glaucoma status in UKBB *MYOC* p.Gln368Ter non-carriers will not be inflated due to sample overlap (Figure 4.2D). In these Cox models, survival outcome was adjusted for sex and the first six genetic principal components.

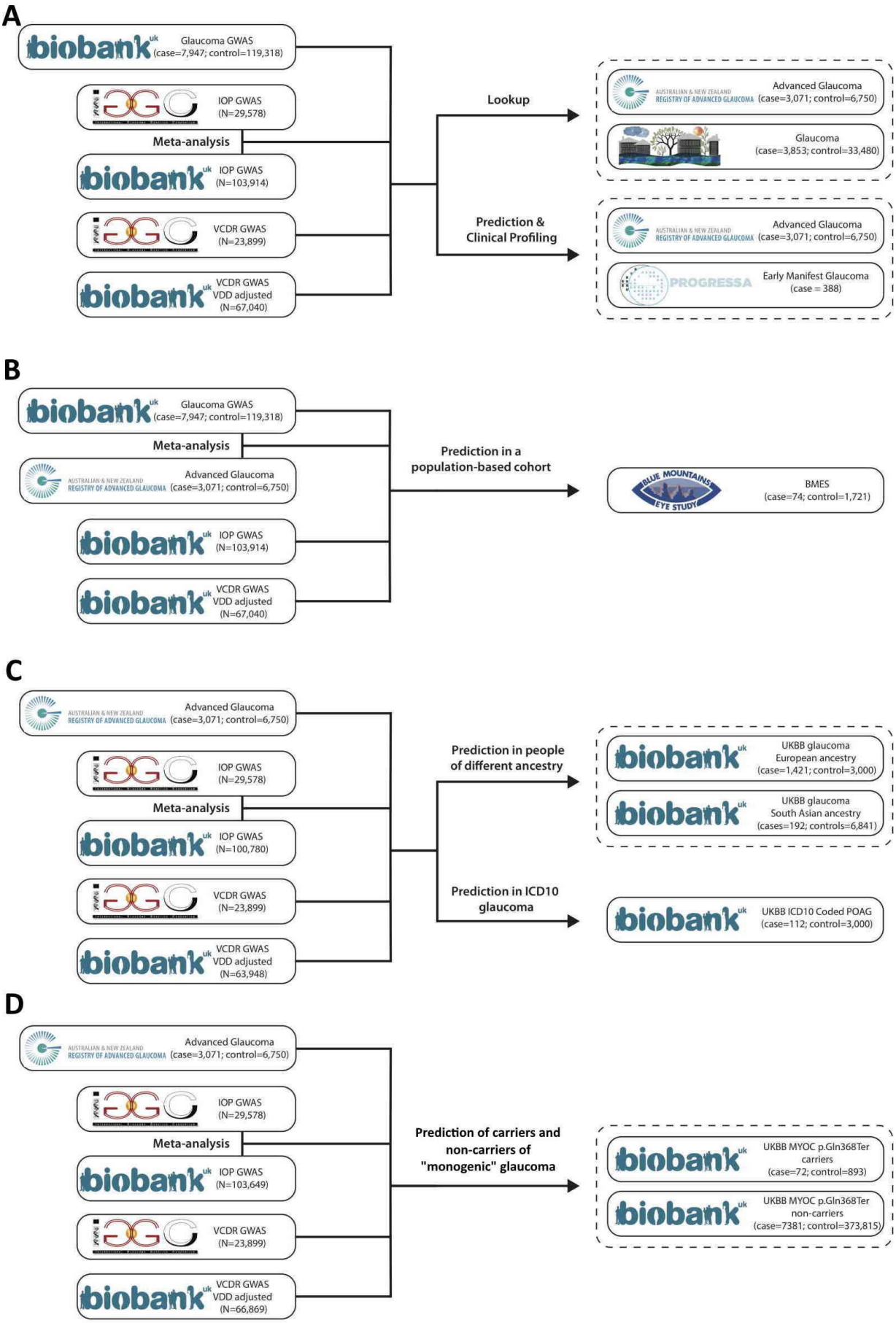
A
Glaucoma GWAS (case=7,947; control=119,318)
IOP GWAS (N=29,578)
Meta-analysis
IOP GWAS (N=103,914)
VCDR GWAS (N=23,899)
VCDR GWAS VDD adjusted (N=67,040)
Lookup
Prediction & Clinical Profiling
Advanced Glaucoma (case=3,071; control=6,750)
Glaucoma (case=3,853; control=33,480)
Advanced Glaucoma (case=3,071; control=6,750)
Early Manifest Glaucoma (case = 388)
B
Glaucoma GWAS (case=7,947; control=119,318)
Meta-analysis
Advanced Glaucoma (case=3,071; control=6,750)
IOP GWAS (N=103,914)
VCDR GWAS VDD adjusted (N=67,040)
Prediction in a population-based cohort
BMES (case=74; control=1,721)
C
Advanced Glaucoma (case=3,071; control=6,750)
IOP GWAS (N=29,578)
Meta-analysis
IOP GWAS (N=100,780)
VCDR GWAS (N=23,899)
VCDR GWAS VDD adjusted (N=63,948)
Prediction in people of different ancestry
Prediction in ICD10 glaucoma
UKBB glaucoma European ancestry (case=1,421; control=3,000)
UKBB glaucoma South Asian ancestry (cases=192; controls=6,841)
UKBB ICD10 Coded POAG (case=112; control=3,000)
D
Advanced Glaucoma (case=3,071; control=6,750)
IOP GWAS (N=29,578)
Meta-analysis
IOP GWAS (N=103,649)
VCDR GWAS (N=23,899)
VCDR GWAS VDD adjusted (N=66,869)
Prediction of carriers and non-carriers of "monogenic" glaucoma
UKBB MYOC p.Gln368Ter carriers (case=72; control=893)
UKBB MYOC p.Gln368Ter non-carriers (case=7381; control=373,815)

Figure 4.2. Overview of the MTAG PRS calculation and application in the primary **(A)**, and follow-up analyses **(B-D)**, ensuring no sample overlap. The clinical significance of the MTAG PRS was applied to advanced glaucoma cases from ANZRAG and Southampton/Liverpool datasets, and early manifest glaucoma cases from PROGRESSA **(A)**. IGGC was excluded when investigating the prediction of the MTAG PRS in the BMES to avoid sample overlap **(B)**. When investigating the prediction of MTAG PRS in UKBB, all glaucoma cases and 3000 controls with IOP/VCDR measurements as well as their relatives were excluded from UKBB VCDR/IOP GWAS **(C)**. Performance of the MTAG PRS in predicting the cumulative risk of glaucoma in UKBB *MYOC* p.Gln368Ter carriers, or the general population in UKBB (i.e. in *MYOC* p.Gln368Ter non-carriers) was assessed by excluding sample overlap from IOP and VCDR GWAS **(D)**.
GWAS: genome-wide association study; IOP: intraocular pressure; VCDR: vertical cup-to-disc ratio.

Polygenic risk scores: intraocular pressure-only PRS (IOP PRS)

The IOP derived PRS was comprised of 146 statistically independent genome-wide-significant SNPs (P value threshold at 5×10^{-8} and LD-clumping at r2 = 0.1). This statistically strict P-value threshold was used to only include variants that are most likely associated with IOP, to investigate the clinical glaucoma phenotype differences that may be attributable specifically to these genetic biomarkers of IOP and its associated pathways. This PRS is based on IOP GWAS meta-analysis which was discussed in Chapter 3, and published previously (MacGregor et al. 2018). Briefly, SNPs influencing IOP were discovered by a GWAS of cornea-compensated IOP measured by Ocular Response Analyzer in participants of the UK Biobank study (N = 103,914) (Cathie Sudlow et al. 2015; MacGregor et al. 2018). This was meta-analysed with GWAS results from the International Glaucoma Genetics Consortium (IGGC, N = 29,578) using the inverse variance weighted method (METAL software) (Loh et al. 2015). A weighted PRS was then derived for each individual in the ANZRAG study cohort using PLINK (version 1.90 beta) (Purcell et al. 2007), taking into account the effect size of each SNP using the UK Biobank GWAS summary statistics. None of the study participants in ANZRAG or PROGRESSA were part of the discovery cohort. A percentile score was then derived within the ANZRAG and the PROGRESSA cohorts. For ease of clinical interpretation, study participants were then stratified into three risk groups: the top 20% of the genetic risk score were classified as the high risk group; the middle 60% as the intermediate risk group; and the bottom 20% as the low risk group.

The IOP PRS was compared to another recently published 12-SNP unweighted POAG PRS by Fan et al. (2019). This was done for two reasons: to compare the added clinical utility of a more comprehensive PRS to a smaller one (i.e., the added benefit of including low-impact common variants); and to compare an endophenotype PRS (IOP PRS) to a glaucoma PRS

(at the time of performing this analysis, Fan et al. had the most recently published glaucoma PRS, predating the MTAG PRS by a few months). A detailed comparison between these scores is summarised in Table 4.2. Importantly, two variants near *CDKN2B-AS1* and *SIX6* included in the 12-SNP by Fan et al. are known to be strongly associated with POAG and VCDR but not with IOP (B. J. Fan et al. 2019; Kathryn P. Burdon et al. 2012; Bao Jian Fan et al. 2011). All of the remaining 10 IOP-associated variants in the 12-SNP PRS were included in the IOP PRS (MacGregor et al. 2018). Analysis using IOP PRS was aimed to describe the glaucoma phenotype influenced by all known IOP-associated variants and their biological pathways, which is why *CDKN2B-AS1* and *SIX6* ended up not being included. It is common for PRS to include thousands of SNPs (such as the aforementioned MTAG PRS), and SNP array technologies are becoming relatively easy to use and very accessible in terms of cost, justifying the inclusion of a large number of SNPs in PRS. In general, inclusion of additional low impact variants leads to better PRS models due to the genetic architecture of complex traits (Boyle, Li, and Pritchard 2017).

Table 4.2: Difference between the IOP PRS and the one reported in Fan et al. 2019, *JAMA Ophthalmology*, *137*(10), pp.1190-1194

Comparison	IOP PRS	PRS by Fan et al.
Number of SNPs	146	12
SNP selection	Associated with IOP in meta-analysis of GWAS using UK BioBank and IGGC datasets at genome-wide significance	Associated with primary open angle glaucoma in European white populations (several studies)
Phenotype measured	IOP	POAG
Inclusion of effect size of each SNP in the PRS	Yes - weighted by beta-coefficient of the meta-analysis GWAS	No.
P-value of the reported association between the PRS and age of glaucoma diagnosis, in their respective studies	2.0×10^{-5} (ANZRAG, n = 2,154)	4.0×10^{-4} (meta-analysis of NEIGHBOR and GLAUGEN, n = 2,947)

PRS: polygenic risk score; SNP: single-nucleotide polymorphism; IOP: intraocular pressure; GWAS: genome-wide association study; IGGC: international glaucoma genetics consortium; POAG: primary open angle glaucoma.

Statistical analysis

The Shapiro-Wilk test was used to assess for normality. Analysis of variance of continuous variables by PRS groups was done using Kruskal–Wallis test. Count and categorical variables were compared using Pearson's chi-squared test. For two-group comparisons, the Mann-Whitney U test was used. Logistic regression models were fitted for binary outcomes and

negative binomial regression was used for count data (e.g. the number of family members affected). The *survival* package in R was used for Cox proportional hazards models (T. Therneau and Lumley 2009). For analyses where both eyes were included, a mixed effects linear regression modeling with a random intercept for each participant to account for the inter-eye correlation was used (Q. Fan, Teo, and Saw 2011; Cnaan, Laird, and Slasor 1997). The R^2 (coefficient of determination) of the linear model was used to assess the variance of the dependent variable explained by the model, and was calculated for the mixed-effects model using the fixed-effects terms only as described by Nakagawa et al. (2017). All analysis was done using R (version 3.5.1 or version 4.0.2, RCore Team, Austria). The significance level (alpha) was set at 0.05 for two-tailed hypothesis testing.

Results of the MTAG PRS

Unless otherwise specified, the following results section has been previously published in a peer-reviewed manuscript, and has been edited to fit the structure of the thesis (Craig et al. 2020).

Optimizing prediction of glaucoma risk by combining correlated traits

The MTAG PRS was based on multiple trait analysis of GWAS data glaucoma and its endophenotypes (Figure 4.2). As well as increasing the number of SNPs that reach genome-wide significance (mean chi-squared statistic increased from 1.12 to 1.30, implying the effective sample size was 2.59 times larger than if UKBB glaucoma cases and controls were used alone), the multivariate model improved the power of risk prediction by reducing the error in the estimate of the effect size for every SNP (Turley et al. 2018). The discriminatory power of the MTAG-derived PRS was first evaluated in the ANZRAG cohort of advanced glaucoma cases. This analysis showed that SNPs with MTAG P values ≤0.001 (corresponding to 2,673 uncorrelated SNPs after LD-clumping at $r^2 = 0.1$ and P value threshold at 0.001) had the highest Nagelkerke R^2 (13.2%) and AUC (0.68, 95% CI: 0.67–0.70) (Table 4.3). The MTAG PRS has better prediction ability than any of the input traits alone (Table 4.4). Based on this, the P value threshold at 0.001 was used for all the remaining prediction target sets (PROGRESSA, BMES, UKBB).

Table 4.3. Discriminatory power of MTAG PRS in the ANZRAG cohort of advanced glaucoma.

P value thresholds	Nagelkerke R^2	AUC (95% confidence interval)
5×10^{-8}	9.7%	0.66 (0.64,0.67)
1×10^{-5}	12.1%	0.68 (0.66,0.69)
0.001	13.2%	0.68 (0.67,0.70)
0.05	9.2%	0.65 (0.63,0.67)
1	6.9%	0.63 (0.62,0.65)

Sex and first four principal components were adjusted when calculated Nagelkerke R^2 and AUC.
AUC: area under the receiver operator curve

Table 4.4. The prediction value of MTAG PRS and each trait alone in the ANZRAG cohort of advanced glaucoma.

Methods	Sample size	Nagelkerke R^2
MTAG method[1]	-	0.13
LDpred[2]	-	0.10
IOP alone[3]	133,492	0.09
Glaucoma alone[4]	Cases = 7,947 Controls = 119,318	0.06
VCDR (disc-diameter adjusted) alone[5]	67,040	0.03

[1] The MTAG method with LD-clumping and P value threshold is the main analysis reported in this section. The reported prediction value was for SNPs with P values ≤ 0.001.
[2] The LDpred method is based on the summary statistics of MTAG output for glaucoma reported in Chapter 3. The infinitesimal prior (LDpred-inf), and models with different fraction of causal variants (0.1, 0.01, and 0.0001) were tested. The best prediction value is at the fraction of causal variants of 0.1.
[3] The training dataset was intraocular pressure meta-analysis of UK biobank (N = 103,914) and IGGC (N =29,578) GWAS. The best prediction value was at the threshold of P value ≤ 1×10^{-5}.
[4] The training dataset was UK Biobank glaucoma GWAS (7,947 cases and 119,318 controls). The best prediction value was at the threshold of P value ≤ 1×10^{-5}.
[5] The training dataset was UK biobank VCDR (adjusted for disc diameter) GWAS (N = 67,040). The best prediction value was at the threshold of P value ≤ 1×10^{-4}.
MTAG: multi-trait analysis of GWAS; GWAS: genome-wide association study; IOP: intraocular pressure; VCDR: vertical cup-to-disc ratio; LD: linkage disequilibrium.

The MTAG-derived PRS was effective at separating advanced glaucoma individuals in terms of risk, with a clear dose-response over deciles (Figure 4.3A). In ANZRAG, individuals in the top decile of the PRS had 14.9-fold higher risk (95% CI 10.7–20.9) relative to the bottom decile, with even better discrimination for the more common high-tension glaucoma (odds ratio = 21.5, 95% CI 12.5–37.0) than normal-tension glaucoma (Figure 4.4). The dose-response of

the PRS was replicated in a smaller UK advanced glaucoma dataset (Southampton and Liverpool); the top versus bottom PRS decile had odds ratio = 11.6 (95% CI 6.0–25.3) (Figure 4.3B), with again better discrimination for high-tension glaucoma (odds ratio = 12.9, 95%CI 6.2–31.3). While comparing the top and bottom deciles shows the dose-response across deciles, one can also consider the risk in the high PRS individuals versus all others; when this is done in ANZRAG, the odds ratio is 4.2 and 8.5 in the top 10% and 1%, respectively, of individuals versus all remaining individuals (Table 4.5).

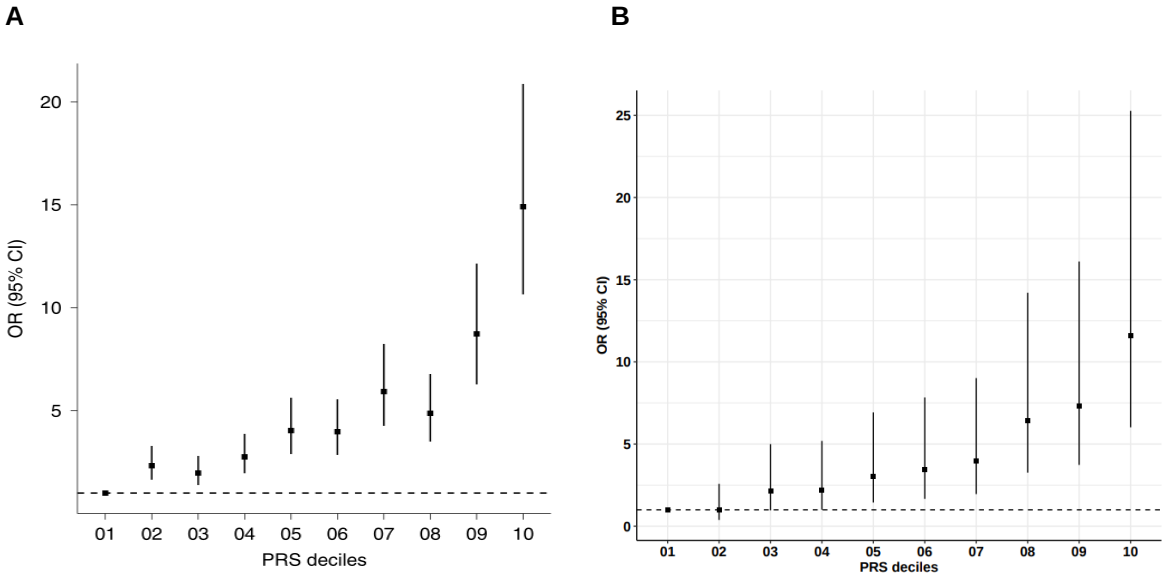

Figure 4.3. The odds ratio (OR) of developing advanced glaucoma in the ANZRAG cohort **(A)** (with 1,734 advanced glaucoma cases and 2,938 controls) for each PRS decile, and replication in the UK Southampton/Liverpool cohort (with 332 advanced glaucoma cases and 3,000 controls). The square dots are the OR values (adjusted for sex and the first four principal components) and the error bars are 95% confidence interval. The dashed line is the reference at the bottom PRS decile (OR=1).
PRS: polygenic risk score; OR: odds ratio.

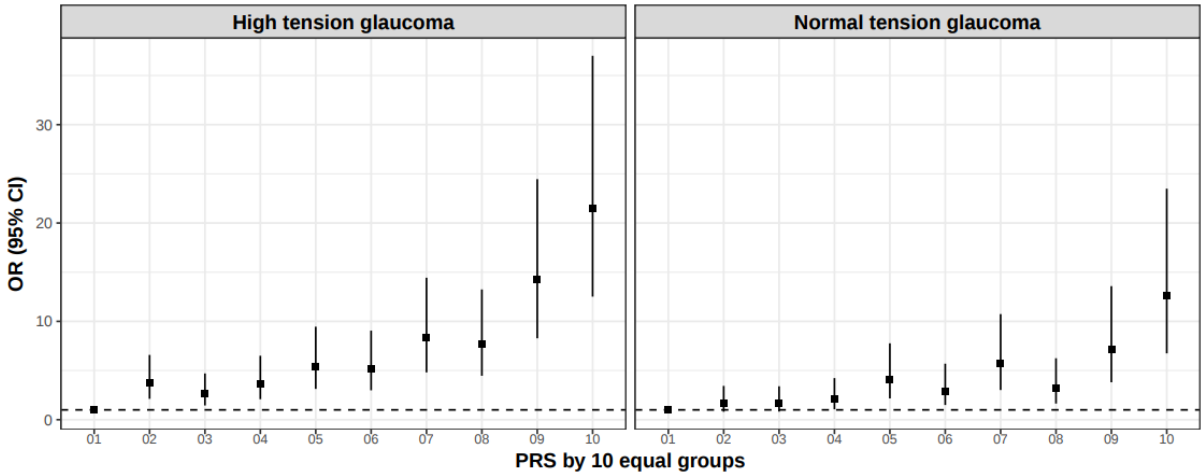

Figure 4.4. MTAG PRS prediction in high tension glaucoma and normal tension glaucoma. The OR (95%CI) of MTAG PRS in ANZRAG advanced glaucoma cohort (left panel: 709 high tension glaucoma cases and 1,991 controls; right panel: 330 normal tension glaucoma cases and 1,991 controls). The square dots are the OR values and the error bars are 95% CI. The dashed lines are referenced at the bottom PRS decile (OR = 1).

PRS: polygenic risk score; OR: odds ratio.

Table 4.5. The odds ratio of a high MTAG PRS relative to the remainder.

High PRS	Reference group	OR	95% CI	P value
Top 50% of distribution	Remaining 50%	2.94	2.60 - 3.34	1.5E-64
Top 20% of distribution	Remaining 80%	3.61	3.11 - 4.20	3.7E-63
Top 10% of distribution	Remaining 90%	4.20	3.43 - 5.17	1.4E-42
Top 5% of distribution	Remaining 95%	4.47	3.36 - 6.00	5.3E-24
Top 2% of distribution	Remaining 98%	5.65	3.55 - 9.37	2.2E-12
Top 1% of distribution	Remaining 99%	8.49	4.16 - 19.69	4.7E-08

Odds ratios were calculated by comparing the high PRS group with the remainder of the population in a logistic regression model adjusted for the effects of sex and the first four principal components of ancestry.

PRS: polygenic risk score; OR: odds ratio; CI: confidence interval

MTAG PRS performance in individuals carrying high penetrance variants

Previous studies indicated that PRS modifies the penetrance of rare *BRCA1/2* deleterious variants for breast, ovarian, and prostate cancers.(Kuchenbaecker et al. 2017; Lecarpentier et al. 2017) Although the MTAG-derived PRS only contains common variants, given it indexes general glaucoma risk, it was hypothesized that it could stratify individuals carrying known high-penetrance glaucoma variants. Pathogenic *MYOC* gene variants account for 2-4% of POAG cases among most populations, the most common disease causing variant being

p.Gln368Ter (rs74315329) (Hewitt, Mackey, and Craig 2008). Penetrance is age-related and is lower in population-based than family based studies.(Hewitt, Mackey, and Craig 2008; X. Han et al. 2019) It was hypothesised that this difference in penetrance could be due to enrichment of common glaucoma associated variants in families modifying age related penetrance. Within UKBB, 965 *MYOC* p.Gln368Ter carriers were identified based on imputation (Puya Gharahkhani et al. 2015). Figure 4.5 shows the cumulative risk of glaucoma in p.Gln368Ter carriers, stratifying by MTAG PRS tertiles. For p.Gln368Ter carriers in the lowest tertile MTAG PRS, glaucoma risk remained very low (2%) up to age 60. In contrast, the highest tertile MTAG PRS group had substantially increased risk of early diagnosis, reaching a 6-fold increase in absolute risk of glaucoma by age 60, relative to the lowest MTAG PRS tertile (considering whole age range, hazard ratio=3.4, 95%CI: 1.7-6.6). This supports the utility of PRS in optimizing risk stratification and prediction, and early screening for patients carrying high penetrance *MYOC* variants in the presence of high MTAG PRS scores.

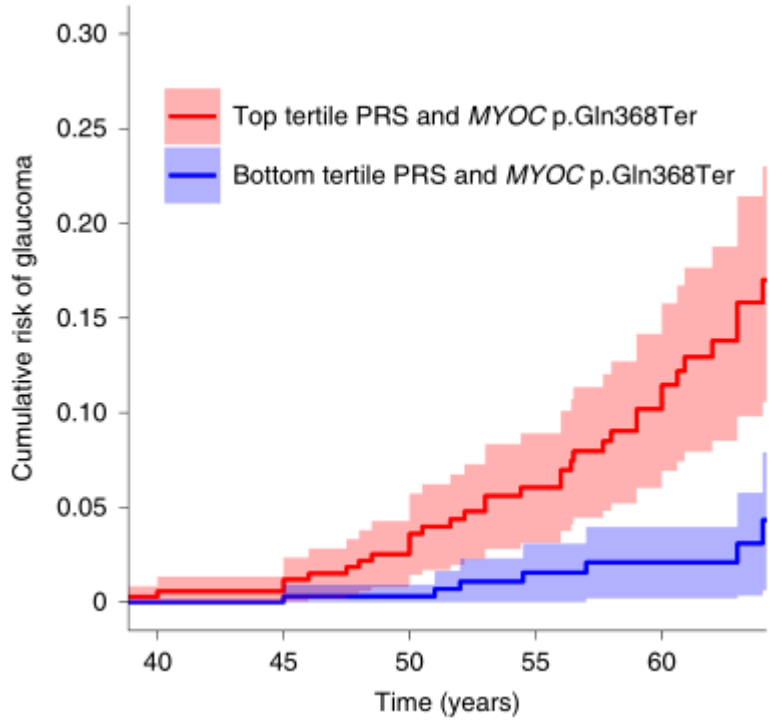

Figure 4.5. Cumulative risk of glaucoma in UKBB *MYOC* p.Gln368Ter carriers stratified by the MTAG PRS (adjusted for sex and first six genetic principal components). The cumulative risk of tertiles (with 95% CIs) of the MTAG PRS are displayed given the relatively small number of *MYOC* p.Gln368Ter carriers (n = 965).

PRS: polygenic risk score; MTAG: multi-trait analysis of genome-wide association studies

Potential for glaucoma risk score in screening in the general population

A general population screening scenario was considered using UKBB (PRS was re-derived to ensure no sample overlap, Figure 4.2D), where the 965 *MYOC* p.Gln368Ter carriers were excluded. Over the 40-69 year old age range for individuals sampled in UKBB, glaucoma prevalence increased from 0.1% at age 40, reaching 3% (95% CI 2.9–3.1%) by age 64. The MTAG-derived PRS stratified UKBB participants very effectively; for those in the top PRS decile, 3% prevalence (prevalence in general population) is reached by age 59, whilst it takes an additional 10 years for this disease prevalence to be reached for people in the bottom PRS decile. Alternatively, the prevalence can be well stratified by PRS deciles (Figure 4.6).

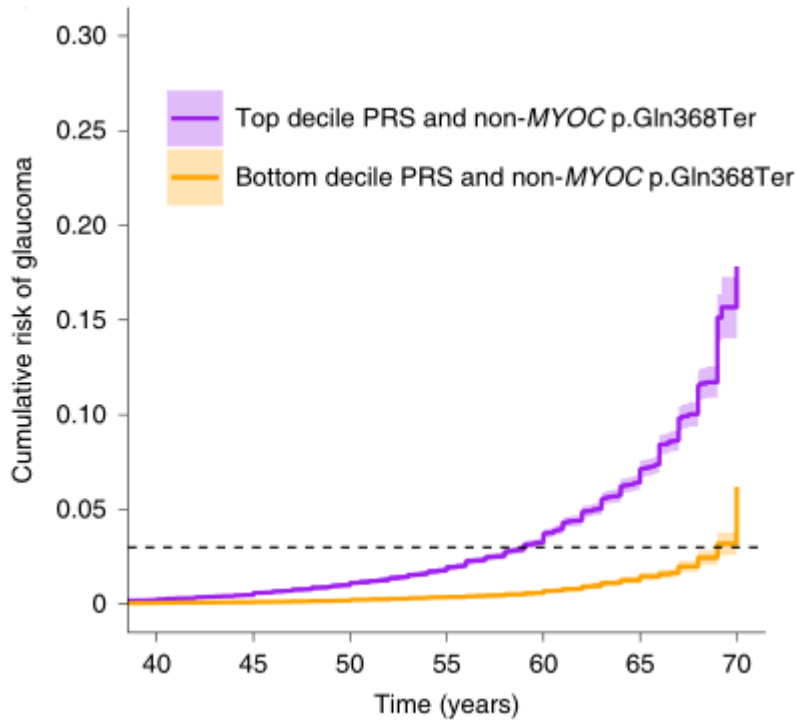

Figure 4.6. Cumulative risk of glaucoma for people in the top and bottom decile (with 95% CIs) of MTAG PRS of the UKBB participants who do not have the *MYOC* p.Gln368Ter variant (adjusted for sex and first six genetic principal components). The dashed line is the reference line of cumulative risk at 3%. PRS: polygenic risk score; MTAG: multi-trait analysis of genome-wide association studies

To benchmark the performance of the MTAG-derived PRS with traditional risk factors, the AUC were computed in datasets for which this was possible: BMES, UKBB glaucoma (broad glaucoma definition), and UKBB POAG (ICD-10 definition) (Figure 4.7, Table 4.6; PRS was re-derived to ensure no sample overlap). In the BMES, MTAG PRS provided additional predictive ability beyond that imparted by traditional risk factors (age, sex, and self-reported family history), with a significant change in the AUC (from 0.73 to 0.80, P=0.002, Figure 4.7). Clear improvement in prediction using this PRS is also observed in people of South Asian

ancestry (Table 4.6), though this analysis was underpowered to further explore this findings across other groups.

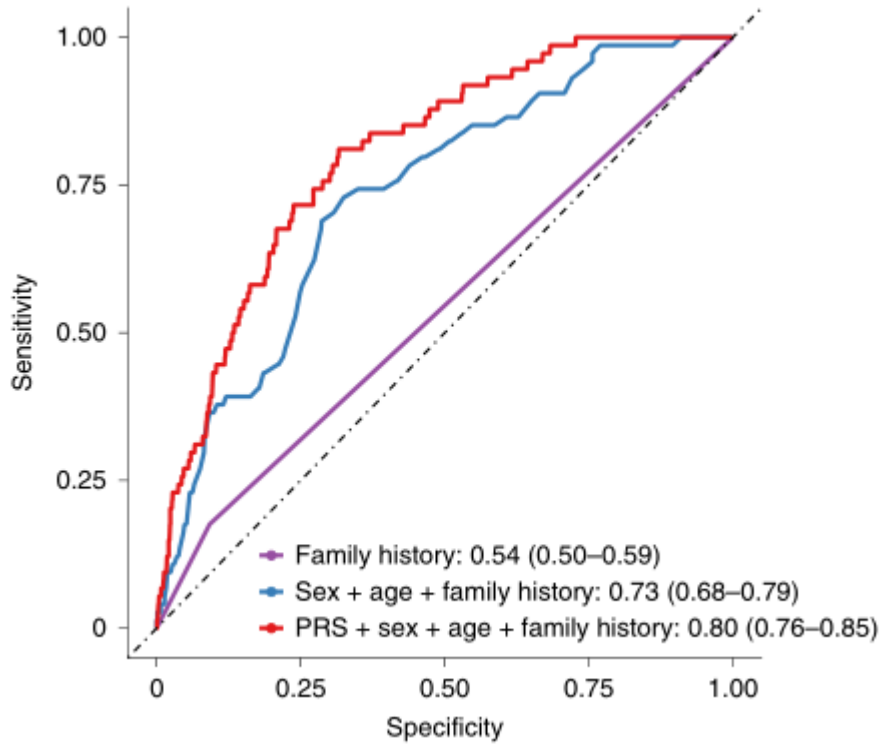

Figure 4.7. AUCs of MTAG PRS in the BMES cohort. The MTAG-derived PRS provided additional predictive ability on top of traditional risk factors (age, sex, and self-reported family history; DeLong test P = 0.002). The AUC is based on a logistic regression model with the coefficients for age, sex, family history and PRS estimated from the BMES data.

PRS: polygenic risk score; MTAG: multi-trait analysis of genome-wide association studies

Table 4.6. Prediction value of MTAG PRS in BMES and UKBB

Target	Models	AUC[95% CI]	P(AUC change)
BMES	Model 1	0.71[0.66,0.77]	N/A
	Model 2	0.72[0.67,0.78]	2.7E-03
	Model 3	0.79[0.75,0.84]	
	Model 4	0.81[0.76,0.86]	5.9E-03
	Model 5	0.86[0.82,0.89]	
	Model 6	0.86[0.82,0.90]	0.02
	Model 7	0.88[0.85,0.92]	
UKBB POAG (European Ancestry)	Model 1	0.67[0.63,0.72]	N/A
	Model 2	0.71[0.67,0.76]	2.8E-04
	Model 3	0.76[0.72,0.81]	
	Model 4	0.78[0.74,0.83]	2.2E-03
	Model 5	0.81[0.78,0.85]	
	Model 6	0.88[0.85,0.91]	0.06
	Model 7	0.89[0.85,0.92]	
UKBB glaucoma (European Ancestry)	Model 1	0.66[0.64,0.68]	N/A
	Model 2	0.70[0.68,0.71]	7.9E-20
	Model 3	0.75[0.73,0.76]	
	Model 4	0.76[0.75,0.78]	8.7E-12
	Model 5	0.79[0.78,0.80]	
	Model 6	0.82[0.80,0.83]	7.4E-07
	Model 7	0.83[0.81,0.84]	
UKBB glaucoma (South Asian Ancestry)	Model 1	0.64[0.59,0.68]	
	Model 2	0.73[0.70,0.77]	9.6E-03
	Model 3	0.76[0.73,0.79]	

Model 1: PRS; Model 2: sex + age; Model 3: PRS + sex + age; Model 4: sex + age + IOP; Model 5: PRS + sex + age + IOP; Model 6: sex + age + IOP + VCDR; Model 7: PRS + sex + age + IOP + VCDR

P value from comparing the AUC of two correlated models with and without PRS. Details of the training samples of the target datasets to construct PRS are available in Figure 4.2. There was no sample overlap between each of the training and target datasets.

AUC: area under the curve; CI: confidence interval; IOP: intraocular pressure; VCDR: vertical cup-to-disc ratio; PRS: polygenic risk score.

A previous study examined the cost-effectiveness requirements for glaucoma screening and highlighted the key age 50-60 bracket (J. M. Burr et al. 2007). In the BMES data, screening only those with a top decile PRS identified 40% of all early onset cases in the age 50-60 bracket (40% of the 10 cases, P=0.013). Such individuals represent a set of individuals likely to benefit from referral for immediate clinical assessment — with skilled clinical examination, retinal imaging, and visual fields. This result was replicated in the UKBB POAG ICD10 cohort, where the top 10% MTAG PRS screening identified 29% of 24 cases aged 50-60, (P=0.0075). In this way, PRS-based screening would satisfy the cost-effectiveness requirements of Burr et al. (2007), identify a meaningful proportion of cases, and capture those cases most at risk of severe disease.

These results suggest the MTAG PRS has clinical utility in identifying high-risk individuals that may benefit from detailed clinical examination. Family members of individuals with glaucoma are at a significantly higher risk of developing glaucoma themselves compared to the normal population (J. M. Tielsch et al. 1994). Thus, it was hypothesised that this risk was mediated by the POAG-associated common variants captured in the MTAG PRS. The self-reported number of family members affected by glaucoma was investigated in ANZRAG as stratified by the MTAG PRS (Figure 4.8). There was a linear dose-response relationship, whereby individuals with a higher MTAG PRS had more family members affected by glaucoma ($P=3.5\times10^{-9}$), with the highest decile risk group having twice as many members affected relative to the lowest decile risk (Figure 4.8).

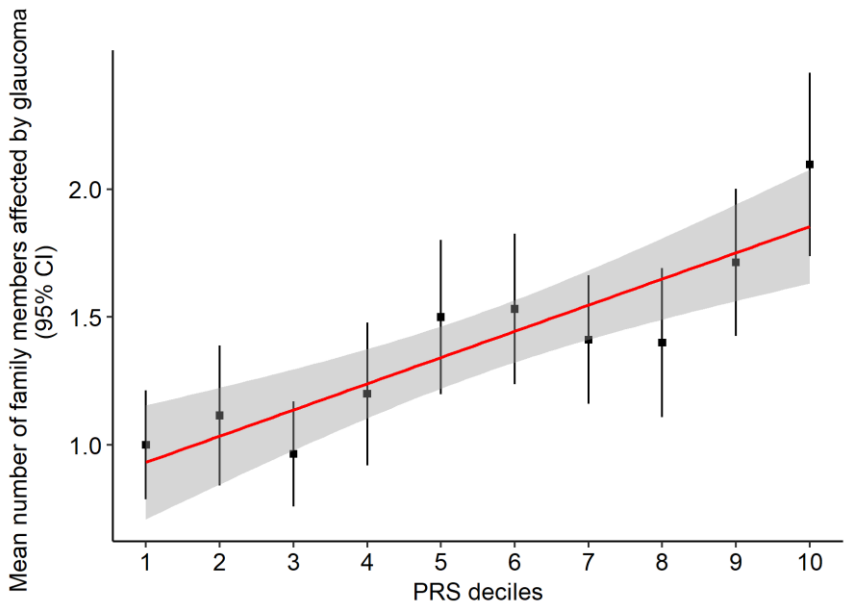

Figure 4.8. Mean number of family members affected by glaucoma per MTAG PRS decile. A total of 1,392 ANZRAG cases had accurate family history information. The square dots are the observed mean number of family members affected by glaucoma with error bars reflecting the 95% confidence intervals. The red line is the line of best fit based on linear regression model ($P = 3.5\times10^{-9}$).
PRS: polygenic risk score; MTAG: multi-trait analysis of genome-wide association studies; CI: confidence interval.

Clinical implications of the glaucoma risk score

The predictive power of the PRS was evaluated in advanced glaucoma; in 1,336 ANZRAG advanced POAG cases with accurate age at diagnosis information available, the MTAG PRS was significantly associated with age at diagnosis of POAG ($P = 1.8\times10^{-5}$). Individuals in the top 10% of the MTAG PRS distribution (N = 134) were on average diagnosed 7 years younger than people in the bottom 10% (N = 134) (mean age of diagnosis of 62.8 [SD 15.7] years compared to 55.7 [SD 13.0] years respectively). There was a dose-response relationship between the MTAG PRS and the age of glaucoma diagnosis in this cohort (Figure 4.9A).

RNFL thinning is a major structural change evident in early stage glaucoma (Na et al. 2012) In the early manifest glaucoma (PROGRESSA) cohort, the PRS predicted both the proportion lost, and the rate of loss of peripapillary RNFL. Given that glaucomatous loss of retinal ganglion cells generally progresses unequally between eyes, with some quadrants of the retina damaged more rapidly than others, the most affected quadrant of the most affected eye was analysed in individuals with early manifest glaucoma and greater than two years of longitudinal optical coherence tomography data (Poinoosawmy et al. 1998) The PRS was significantly associated with the proportion of RNFL lost from baseline to most recent review, even after adjustment for known risk factors; age, IOP and RNFL thickness at presentation (P

= 0.004; Figure 4.9B). Expressed in terms of rate of loss, each decile change in PRS was associated with an accelerated progression rate of 0.05 µM/year, which was twice the rate of thinning per mmHg (approximately 1 decile change for IOP) of baseline IOP (0.022 µM/year).

Incisional surgery for glaucoma (trabeculectomy) is highly effective at reducing IOP, but has significant complications which can adversely impact vision (Robert N. Weinreb and Khaw 2004). Trabeculectomy is performed either when IOP is unable to be controlled with medical or laser therapy, or when there is progressive visual field loss despite well controlled IOP. Participants with a high MTAG PRS were more likely to have undergone surgery for glaucoma (Figure 4.9C). In the ANZRAG cohort of POAG cases, a higher PRS was associated with requiring trabeculectomy more often, even after adjustment for maximum recorded IOP and age ($P=3.6\times10^{-6}$), the odds ratio of requiring trabeculectomy in either eye for individuals in the top MTAG PRS decile was 1.78 (95% CI 1.07–3.00) compared to the bottom decile. A very similar trend was observed in the UK replication (Southampton/Liverpool) samples, despite the smaller sample size (126 recorded trabeculectomies in 332 cases [38%]; MTAG PRS linear trend P=0.057).

Figure 4.9. Panel **(A)** shows the mean age at diagnosis (years) for each decile of MTAG PRS in the ANZRAG cohort (linear regression $P=1.8\times10^{-5}$). A total of 1,336 cases had accurate age at diagnosis information. The mean age at diagnosis was calculated for each decile of MTAG PRS, adjusted for sex and the first four principal components in a linear regression model. The square dots are the regression-based mean age at diagnosis, with error bars for 95% confidence intervals. The red line is the line of best fit, with 95% confidence intervals in grey. Panel **(B)** shows the proportion of preserved baseline retinal nerve fibre layer for PROGRESSA participants with early manifest glaucoma plotted against PRS decile (N=388; linear regression P=0.004). The square dots are the retinal nerve fibre layer proportions, with error bars showing 95% confidence intervals. The remaining retinal nerve fibre layer proportion is calculated for the most affected quadrant of the most affected eye of each participant — as determined on optical coherence tomography scans at baseline and latest follow-up scan. Panel **(C)** displays the proportion of participants requiring trabeculectomy in either eye in the ANZRAG POAG cohort (linear regression $P=3.6\times10^{-6}$). There were 1,360 cases with records of surgical treatment status. The square dots represent the observed average proportion of cases in each decile of PRS who required

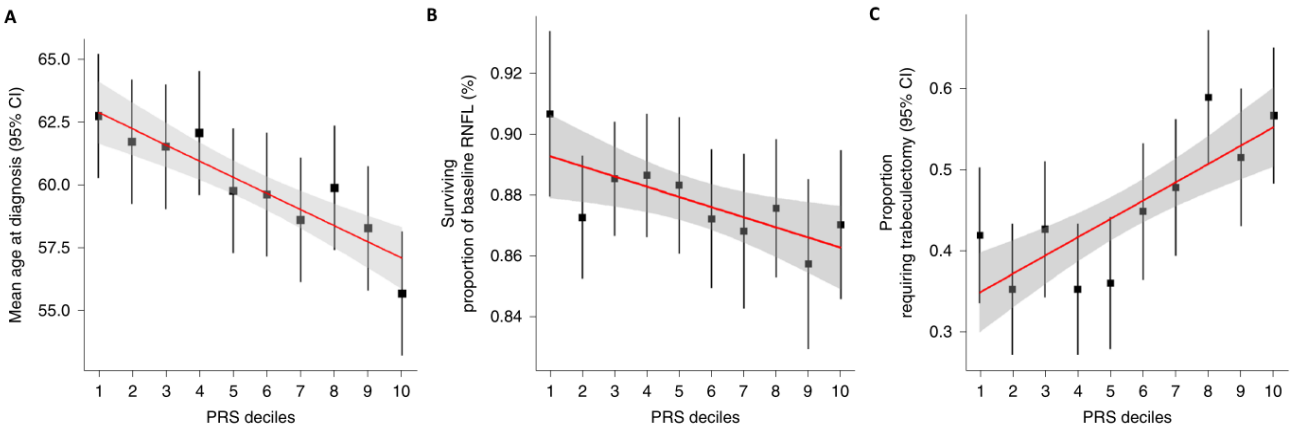

trabeculectomy, with 95% confidence interval bars. The line of best fit is shown in red, with 95% confidence interval shaded in grey.

PRS: polygenic risk score; MTAG: multi-trait analysis of genome-wide association studies; CI: confidence interval.

Identifying high-risk individuals in reference to a population cohort

The following subsection has not been published in a peer-reviewed journal. I am a co-author on a manuscript inclusive of these that is currently being drafted for submission. The following section is my original contribution and was replicated in this section for relevance (i.e., my contribution of the design, analysis, drafting, and critical revision of this segment is at 100%).

Another approach of identifying individuals at the highest risk of developing glaucoma is using a PRS cut-off in reference to a 'normal' population cohort. For population controls, 17,642 genotyped individuals from the population-based QSkin cohort were used. QSkin is a prospective cohort of men and women aged 40–69 years, randomly sampled from the population of Queensland, Australia in 2011 (Olsen et al. 2012). Using this method of an unselected 'control' population reference, the threshold for 'high polygenic risk' was set as the top 5% of the QSkin cohort. This cohort is also ancestrally-matched to PROGRESSA cohort. The top 5% of a control cohort cut-off is chosen to represent the highest-risk individuals that could be potentially targeted in an unselected population study. Indeed, the top 5% of the population PRS distribution corresponds to 11.3% of the PROGRESSA cohort (Figure 4.10A), suggesting that PROGRESSA recruitment strategy has already captured some of genetic risk captured by the PRS (i.e., glaucoma suspicious optic nerve head appearance; details provided in Chapter 2). In these validation results, all PROGRESSA participants with sufficient follow-up were included regardless of baseline perimetric glaucoma status.

Individuals with early manifest glaucoma and glaucoma suspects were more likely to have a higher glaucoma PRS, with the top 5% of the population PRS distribution capturing 11.3% of

the PROGRESSA cohort. Individuals in the top 5% of the population PRS distribution were more likely to have a first-degree relative with glaucoma than the bottom 95% (56% vs 37% respectively; $P=2.4x10^{-4}$), and had a higher treatment intensity as measured by the mean number of prescribed IOP-lowering drops or selective laser trabeculoplasty (SLT) procedures (mean [SD] pf 1.51 [1.3] treatments vs 1.07 [1.2] treatments respectively; $P=1.5x10^{-4}$).

Longitudinal visual field progression was investigated as the primary outcome in this analysis, adjusting for age, gender and baseline visual field mean deviation using a Cox proportional hazards regression model. The PROGRESSA criteria for visual field progression was detailed in Chapter 2. Briefly, visual field progression was defined by a modified Hodapp-Parish-Anderson criteria; i.e., two consecutive reliable field tests showing a new visual field defect, defined by 3 contiguous test locations showing pattern standard deviation (PSD) < 5%, one of which was at < 1%, in the same visual field zone (nasal, paracentral, Bjerrum's, or temporal areas). If the glaucoma hemifield test was “Outside Normal Limits” or the global PSD was below 5% in both visual field tests, then test locations being < 5% on PSD was considered sufficient. All visual field data available were utilised for this analysis including those predating PROGRESSA enrollment. If both eyes had progressed, then the eye with the earlier time to progression was used.

A total of 829 individuals had sufficient reliable visual field follow-up (≥ 4 fields) with a mean follow-up time of 8.4 ± 4.1 years and a median of 11 visual field examinations. The mean baseline visual field mean deviation was -1.1 dB (SD 2.0), which was not different between the top 5% and the bottom 95% genetic groups at baseline (P = 0.10). Despite higher treatment intensity, the top 5% PRS group had a greater likelihood of visual field progression relative to the bottom 95% PRS group (hazard ratio = 1.4, 95% CI 1.1–1.8, P = 0.009), with a median time to visual field progression approximately 2 years earlier (4.1 [95% CI 3.1–6.5] vs 5.9 [95% CI 5.5–6.7] years) (Figure 4.10B).

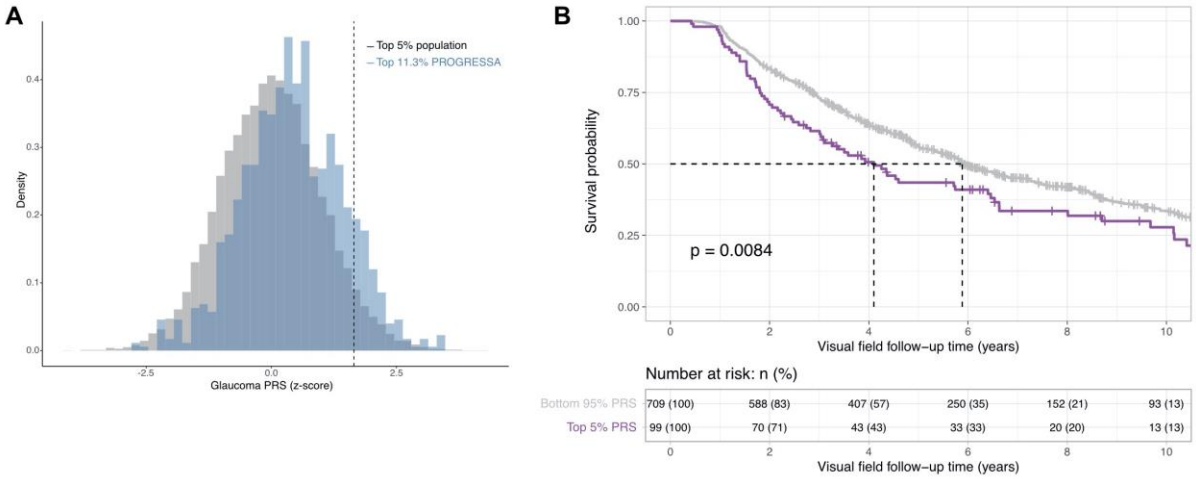

Figure 4.10. Visual field progression in early manifest glaucoma participants and glaucoma suspects, stratified by genetic risk. **(A)** Distribution of scaled PRS values (z-scores) for the PROGRESSA cohort of early manifest glaucoma and glaucoma suspects, relative to an unselected control population. **(B)** Individuals in the top 5% of the population PRS distribution (i.e., 11.3% of PROGRESSA) showed accelerated visual field loss relative to the bottom 95% population PRS group in the PROGRESSA cohort. The dashed lines represent the median survival time for each group; the P-value was calculated by log-rank test of the survival distributions (not adjusted for covariates and only including one eye per individual).
PRS: polygenic risk score.

An alternative analysis approach is including both eyes, if eligible. Using this approach, a total of 1,563 eyes were included, with 717 visual field progression end-points (46%). A mixed-effect Cox proportional hazards regression model with a random intercept per eye was used to account for the inter-eye correlation, and adjusting for age, gender and baseline visual field mean deviation. The findings of this model support the aforementioned primary analysis, with eyes in the top 5% of the population PRS having 1.48-fold higher risk of visual field progression compared to eyes in the bottom 95% of the PRS (95% CI 1.12 – 1.96; P = 0.0052).

A similar analysis was performed for structural progression, using the rate of RNFL thinning of all eligible eyes in PROGRESSA. A minimum of 2 years and 4 OCT scans were required to generate an RNFL rate of thinning. A positive rate of RNFL change, corresponding to a non-pathological inter-scan thickness variation was set to 0. The rate of RNFL thinning in the superior and inferior quadrants of the peripapillary RNFL were measured for each eye. A subgroup of the PROGRESSA cohort has undergone optic disc OCT imaging using Spectralis OCT (Heidelberg Engineering, GmbH, Dossenheim, Germany). A multi-level mixed-effect linear regression model was fitted with the rate of quadrant RNFL thinning as the outcome measure, and a random intercept per participant, then per eye, to account for inter-eye and inter-quadrant rate of RNFL thinning correlation. The top 5% genetic risk group was the

predicting variable, adjusting for age and gender. Additionally, the rates of RNFL thinning measured by the Spectralis OCT is comparable, but not interchangeable to that measured by the Cirrus OCT (Saks et al. 2020). Therefore the model was additionally adjusted for the OCT device type (Heinze, Wallisch, and Dunkler 2018).

RNFL rates of thinning was available for 3,546 quadrants of 1,777 eyes, from 896 individuals. Of these, 114 individuals (12.7%) were in the top 5% of the population PRS. Individuals in the top 5% of the PRS had accelerated rates of RNFL thinning by 0.19 µm per year (95% CI 0.017–0.362; P = 0.031) compared to the bottom 95%, after adjustment for age and gender and OCT device type. Individuals in the top 5% of the PRS were 1.6-fold more likely to be fast RNFL progressors, defined by a rate of quadrant RNFL thinning exceeding 1 µm/year, relative to the bottom 95% group (odds ratio 95% CI 1.27–1.95; P = 0.006 using a generalised mixed-effect linear regression model).

Results of the IOP-only PRS

The following results section has been previously published in a peer-reviewed manuscript, and has been edited to fit the structure of the thesis (A. Qassim et al. 2020).

The clinical phenotype of POAG as stratified by IOP PRS

The prediction ability of the IOP derived PRS was first assessed in the ANZRAG cohort. A total of 2,154 eligible POAG participants from ANZRAG with mean age at recruitment of 77.4 (SD 13.2) years were included. That is, only participants of European ancestry with POAG were included and participants with variants in the known POAG genes (*MYOC*, *OPTN* and *TBK1*) were excluded to isolate the clinical impact of common SNPs most strongly associated with IOP (i.e., at a strict GWAS P-value threshold). In this section, the 381 cases recruited from the UK who were ethnically matched to the ANZRAG cohort (N = 290 from Southampton and N = 91 from Liverpool, as defined in the methods) were combined with the ANZRAG POAG cohort. The majority of the study cohort (N = 1,664; 77%) had advanced glaucoma, defined by a Humphrey 24-2 visual field mean deviation < -15 dB in the worse eye, or loss of at least two of the central visual field points on the pattern deviation map (detailed in Chapter 2). A summary of the glaucoma phenotype across the three genetic risk groups is summarised in Table 4.7.

Table 4.7: Summary of the glaucoma phenotype across genetic risk groups in ANZRAG

Clinical characteristic	Low	Intermediate	High	p
Number	410	1313	431	-
Gender, male (%)	192 (46.8)	622 (47.4)	185 (43.0)	0.286
Age of diagnosis, years	62.90 (15.32)	61.39 (14.16)	59.16 (13.80)	**<0.001**
Family members affected	0.99 (1.56)	1.16 (1.53)	1.45 (1.89)	**0.001**
High-tension glaucoma (%)	251 (74.3)	867 (79.1)	298 (84.7)	**0.003**
Maximum recorded IOP, mmHg	25.54 (9.17)	26.08 (8.63)	27.25 (9.14)	**0.005**
VCDR	0.87 (0.11)	0.86 (0.12)	0.87 (0.13)	0.32
Visual field MD, dB	-16.87 (9.04)	-16.12 (9.15)	-16.91 (9.25)	0.179
Incisional surgery rate* (%)	151 (39.8)	507 (43.7)	186 (49.5)	**0.026**
Bilateral incisional surgery* rate (%)	65 (17.2)	259 (22.3)	100 (26.6)	**0.007**

Low risk group represents the first quintile of the IOP genetic risk score and the high risk is the highest quintile. Values displayed are mean (standard deviation) for continuous variables and N (%) for categorical variables. Number of family members is self reported up to the fourth degree. VCDR, MD and treatment values are recorded at the time of referral. P values represent the statistical significance of the analysis of variance (difference between any two groups) for continuous variables (Kruskal–Wallis test) or Chi-squared test for categorical variables. High-tension glaucoma is defined by a maximum IOP >21 mmHg.

* The majority of the incisional surgeries in this dataset were trabeculectomies. Other surgeries include tube shunt surgery, deep sclerectomy and two cases of Xen Gel implants.

IOP: intraocular pressure; VCDR: vertical cup-to-disc ratio; MD: mean deviation.

The high IOP genetic risk group had a significantly higher maximum IOP by 1.3 mmHg (95% CI 0.32 – 2.7 mmHg; $P = 5.5x10^{-3}$) compared to the intermediate and low genetic risk groups. The maximum IOP was not statistically significantly different in the intermediate group relative to the low risk group (mean difference of 0.54 mmHg, 95% CI -1.5 – 0.47 mmHg; P = 0.08). Similarly, the high genetic risk group was more likely to present as high tension glaucoma, defined by a maximum IOP above 21 mmHg (odds ratio = 1.9; 95% CI 1.3 – 2.8; $P = 7.9x10^{-4}$ relative to the low-risk group). Further analysis by decile groups of the IOP PRS shows a continuous variant dose-response relationship between higher IOP PRS and maximum IOP, signifying the cumulative effects of the common IOP variants (Figure 4.11A).

The mean age of glaucoma diagnosis was significantly different across the IOP genetic risk groups ($P = 1.3x10^{-4}$). The high IOP genetic risk group were diagnosed with glaucoma on average 2.2 (SD 0.80) years earlier than the intermediate group ($P = 5.5x10^{-3}$) and 3.7 (SD 1.0) years than the low genetic risk group ($P = 2.4x10^{-4}$). The high risk group were more likely to have family members affected by glaucoma relative to the low risk group (odds ratio = 1.6,

95% CI 1.2 – 2.1. P = $1.1x10^{-3}$). The number of self-reported family members affected by glaucoma was also higher in the high IOP PRS group compared to the intermediate (mean difference of 0.29 members, SD 0.1, P = $5.2x10^{-3}$) and low risk groups (mean difference of 0.46 members, SD 0.11, P = $1.8x10^{-4}$). Furthermore, there was a linear relationship between the IOP PRS and the number of family members affected by glaucoma which highlights the importance of these variants and their impact on the development of glaucoma (Figure 4.11B).

There was no significant difference between the Humphrey visual field mean deviation or VCDR between the IOP PRS groups (P = 0.18). However, the high genetic risk group were more likely to require an incisional surgery for the management of their glaucoma relative to the intermediate and low risk groups (odds ratio = 1.3, 95% CI = 1.0 – 1.6; P = 0.049 and odds ratio = 1.5; 95% CI = 1.1 – 2.0; P = $7.9x10^{-3}$ respectively). Further, the high IOP PRS group were more likely to require bilateral incisional surgeries than the intermediate and low risk groups (odds ratio = 1.4, 95% CI = 1.0 – 1.8; P = 0.020).

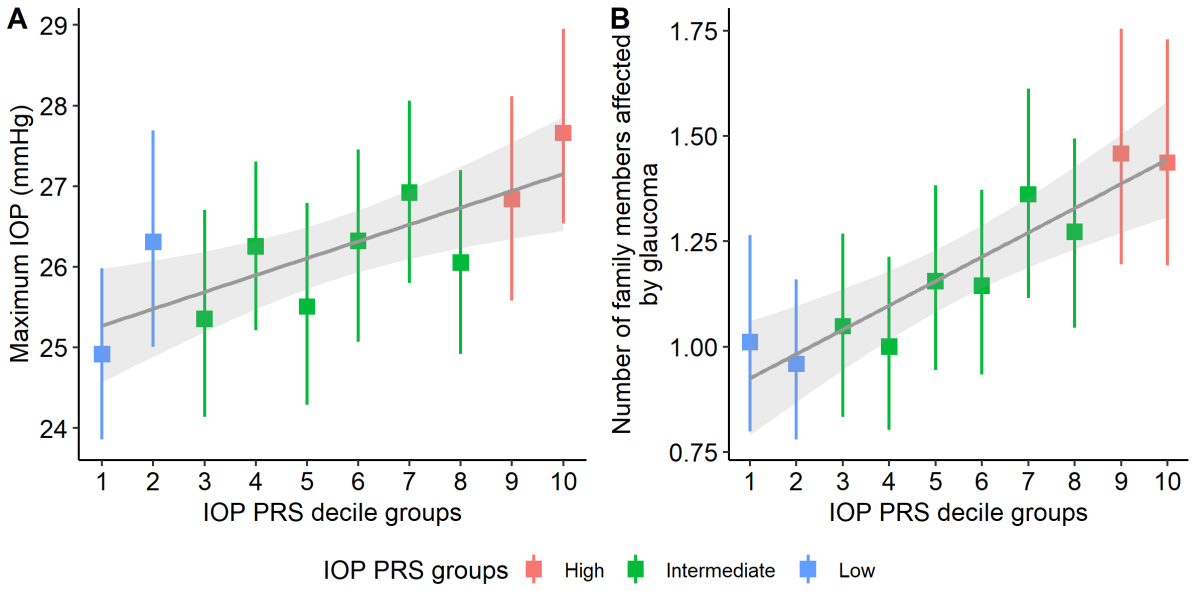

Figure 4.11. A continuous variant dose-response relationship between IOP PRS and **(A)** the maximum recorded IOP in the ANZRAG cohort (P = $1.9x10^{-3}$ for linear model trend); **(B)** the mean number of family members affected by glaucoma (P = $1.3x10^{-5}$ for negative binomial generalised linear model trend). The squares represent the mean values for each PRS decile group, and the error bars represent the 95% confidence interval of the mean. The grey line is the line of best fit with the 95% confidence interval lightly shaded around the line.

IOP: intraocular pressure; PRS: polygenic risk score.

As ANZRAG is a large registry with over a 100 clinicians contributing to the registry, a concern may be that the association with surgical outcomes are influenced by the referring clinicians. It is possible that there was inter-clinician variability in likelihood and timing of surgical intervention for glaucoma management, or the selection of cases to refer to the registry. However, given the large number of clinicians involved in the registry, such inter-clinician variance will likely be evenly distributed. A sensitivity analysis was performed to address this concern.

In a statistical sense, the referring clinician can be considered a random variable not accounted for by other study factors. The clinicians involved in the registry can be considered to be a random selection of "pool of possible clinicians" who have referred to the registry.(Cnaan, Laird, and Slasor 1997; Hubbard et al. 2010) Thus to test the effects of the referring clinician, a mixed-effects model was developed with the number of eyes with incisional surgery per participant as the outcome, the IOP PRS groups as the fixed effect, and the referring clinician as a random intercept. The variance explained by the referring clinician random effect was 0.072 (SD 0.26) with a residual variance of 0.62 (SD 0.79). This suggests some contribution of the referring clinician to the outcome of the number of surgeries. In this model, the magnitude of effect of IOP PRS and statistical significance remained very similar: in the aforementioned fixed-effects only model, the odds ratio of high-risk IOP PRS group to have undergone an incisional surgery was 1.48 compared to low-risk group (P = 0.008); in the mixed-effects model accounting for the random effect of the referring clinicians, the odds ratio of high-risk vs low-risk group to have undergone incisional surgery was 1.42 (P = 0.020). While the estimated effect size of the PRS was largely similar, the mixed-effects model was statistically a better fit (Akaike information criterion 2555 vs 2626; P < 0.001).

Replication of the phenotype in an early manifest glaucoma cohort

For replication, an independent cohort of early perimetric POAG participants (N = 624), with an average age of 69.5 (SD 10) years, were stratified into three risk groups based on the same absolute numerical IOP PRS cut-off used above. This was sampled from the larger PROGRESSA cohort, to maintain a consistent POAG cohort definition. Thus, only PROGRESSA participants with established perimetric glaucoma, defined by two consecutive reliable visual field examinations with Glaucoma Hemifield Test "Outside Normal Limits", pattern standard deviation <5%, or a cluster of 3 contiguous points depressed <5% in the pattern standard deviation map, at least one of which is <1%, were included (details of the PROGRESSA visual field grading protocol is described in Chapter 2). There was no sample overlap between this group and those from ANZRAG reported above.

There was a similar association of increasing maximum IOP, number of family members affected, and treatment intensity (Table 4.8 and Figure 4.12). The high risk group had more than twice as many family members affected as the low risk group, and were more likely to require more intensive medical therapy to control their disease (P = 0.013). There was no significant association between the PRS and the length of follow-up (P = 0.65).

Table 4.8. Summary of the glaucoma phenotype across genetic risk groups in the replication cohort (PROGRESSA)

Clinical characteristic	Low	Intermediate	High	p
Number	144	378	102	-
Gender, male	68 (47.2)	159 (42.1)	37 (36.3)	0.228
Number of family members affected	0.60 (1.21)	0.88 (1.19)	1.27 (1.81)	**0.001**
Maximum recorded IOP, mmHg	19.31 (5.36)	21.08 (5.80)	21.03 (5.20)	**<0.001**
VCDR	0.73 (0.10)	0.74 (0.10)	0.72 (0.10)	0.119
Visual field MD, dB	-3.17 (2.94)	-3.35 (3.10)	-2.79 (2.73)	0.442
Number of glaucoma drops or SLT*	1.06 (1.18)	1.36 (1.35)	1.35 (1.26)	**0.033**
Required 2 or more medications or SLT*	33 (22.9)	133 (35.2)	39 (38.2)	**0.013**

Risk group stratification is based on IOP genetic risk score cut-offs as calculated and used in the primary cohort (ANZRAG). Values displayed are mean (standard deviation) for continuous variables and N (%) for categorical variables. Number of family members is self-reported. VCDR, MD and treatment intensity are at the last clinic visit recorded in the study database. P values represent the statistical significance of the analysis of variance for continuous variables (Kruskal–Wallis test) or Chi-squared test for categorical variables.

* SLT was counted as equivalent to 1 glaucoma medication.

IOP: intraocular pressure; VCDR: vertical cup-to-disc ratio; MD: mean deviation; SLT: selective laser trabeculoplasty.

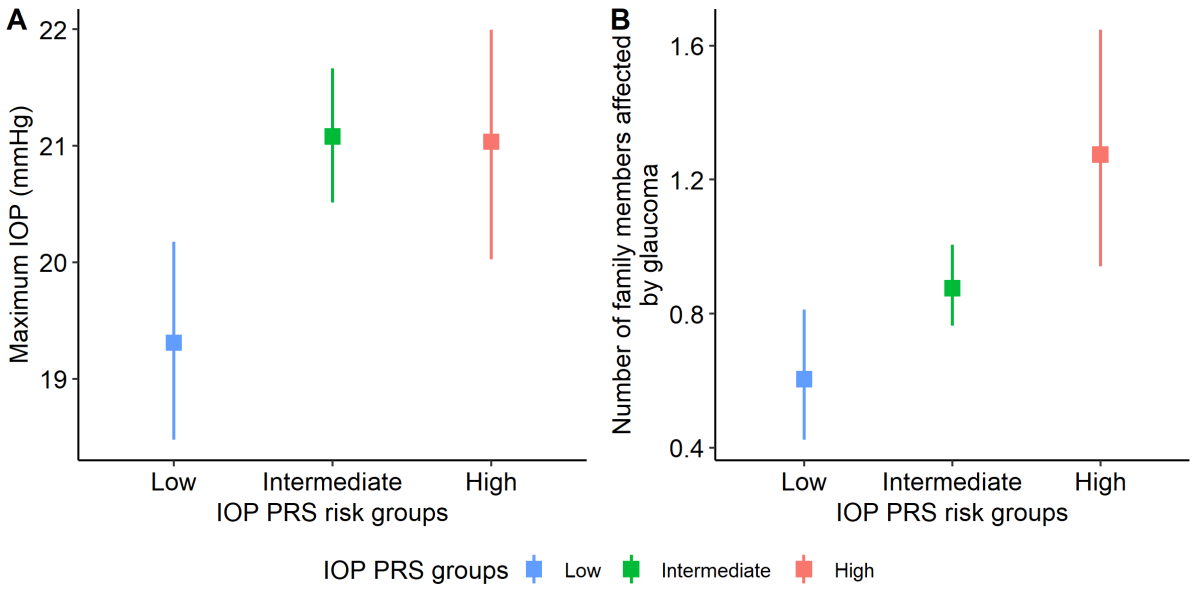

Figure 4.12. Replication of the **(A)** maximum IOP recorded ($P = 5.0x10^{-4}$ for one-way analysis of variance) and **(B)** the number of family members affected by glaucoma ($P = 1.0x10^{-3}$ for one-way analysis of variance) in an independent cohort of early POAG participants (N = 624). The squares represent the mean values for each PRS group, and the error bars represent the 95% confidence interval of the mean.

IOP: intraocular pressure; PRS: polygenic risk score; POAG: primary open angle glaucoma.

In ANZRAG and PROGRESSA, family history was self-reported and recorded for affected relatives up to the fourth degree by the referring clinician. Where applicable, the family tree of affected individuals was recorded and reviewed by the registry staff before recording the number of family members affected by glaucoma in the registry. In the ANZRAG study, relatives who are reported to be affected by glaucoma are examined and invited for recruitment to ANZRAG. While relatives were not used in the reported PRS analyses for genetic similarity, a high accuracy of the reported family members history was found as it is often validated by the treating clinicians. The correlation between the database recorded number of family members affected by glaucoma, and the number of family members examined and proven to have glaucoma and subsequently enrolled in ANZRAG is high (Pearson's product-moment correlation 0.54, 95% CI 0.49 – 0.58; $P < 2 \times 10^{-16}$). While the validity of patient-reported family history of glaucoma has not been extensively validated in glaucoma, Mitchell et al. (2002) have reported estimated biases in the Blue Mountain Eye Study. Despite possible recall and survival biases and community under-diagnosis of glaucoma, the trend of higher number of family members affected by glaucoma held true in the replication dataset. This suggests that the association is likely real, however the effect size estimated by the PRS may be under or overestimated.

Comparative performance to a 12-SNP POAG PRS

A recently reported PRS associated with POAG in European white populations was associated with a younger age of glaucoma diagnosis (B. J. Fan et al. 2019). For comparison, this PRS was calculated in the primary cohort (ANZRAG, N = 2,154) (Table 4.2). The IOP PRS was more strongly associated with the age of glaucoma diagnosis ($P = 2.0x10^{-5}$) than the 12-SNP PRS reported by Fan *et al*. ($P = 2.6 \times 10^{-4}$) and explained a greater variance of this outcome (R^2 of linear regression 0.89% vs 0.65% respectively; Table 4.9). The 12-SNP PRS was not associated with the maximum IOP recorded (P = 0.45), and explained less variance in the need for incisional surgery outcome compared to the IOP PRS (R^2 of linear regression 0.53% vs 0.79% respectively; Table 4.9). Due to the inclusion of two VCDR-associated POAG risk variants near *CDKN2B-AS1* and *SIX6*, the 12-SNP PRS was associated with a higher VCDR but not the IOP PRS (Table 4.9).

Table 4.9: Association between the PRS reported in our manuscript and that reported by Fan et al. 2019, *JAMA ophthalmology*, *137*(10), pp.1190-1194, in ANZRAG cohort (n = 2,154).

Variable	P-value		R-squared	
	IOP PRS	Fan et al. PRS	IOP PRS	Fan et al. PRS
Age of glaucoma diagnosis	2.0×10^{-5}	2.6×10^{-4}	0.89%	0.65%
Maximum IOP	0.002	0.45	0.47%	0.03%
VCDR	0.74	4.8×10^{-4}	0%	0.83%
Incisional surgeries	1.0×10^{-4}	1.5×10^{-3}	0.79%	0.53%

IOP: intraocular pressure; PRS: polygenic risk score; POAG: primary open angle glaucoma.

Prediction of short-term diurnal IOP profile

The following section has been submitted to a peer-reviewed journal and was under review at the time of writing.

Study sample characteristics

Ambulatory IOP data were collected from August 2016 until December 2019 from a total of 473 eyes of 239 participants trained in the use of the Icare HOME tonometer who had genotyping data available. The same tonometer model and participant training protocol was used throughout the study period. IOP data were downloaded from the devices, and was systematically evaluated for errors as described in the methods. All eligible eyes of each participant were included in the study. CCT was used as a covariate in all of the following home tonometry analyses as it significantly affects IOP measurements, particularly when

using rebound tonometry (Figure 4.13).(Takagi, Sawada, and Yamamoto 2017; Termühlen et al. 2016)

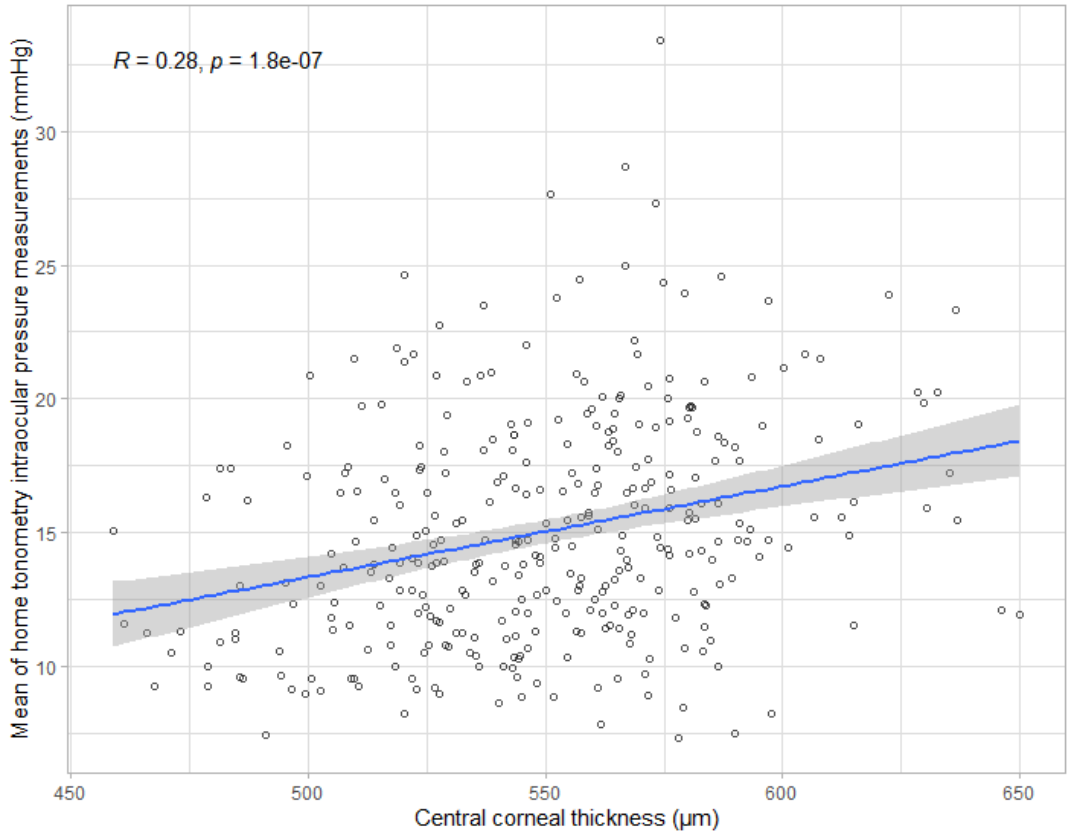

Figure 4.13. Correlation between central corneal thickness and home tonometry measurements in the study dataset. Each dot represents the values for an eye. The blue line is the linear line of best fit, with the grey shading representing the 95% confidence interval. The R value displayed on the top left is the Pearson's correlation coefficient, and P-value is the statistical significance of this correlation.

The main exclusion criteria was participants not completing sufficient measurements (i.e., having less than two days with at least 3 measurements; 129 eyes, 27%) which excluded 61 participants who had no other eligible eyes. After assessing the quality of the data, 336 eyes from 177 participants met the study inclusion criteria. One participant with two eligible eyes was excluded for being related to another participant to avoid inflating genetic association results. Thus 334 eyes were used in the analyses (Figure 4.14). Participants had a mean of 3 reliable measurements per day.

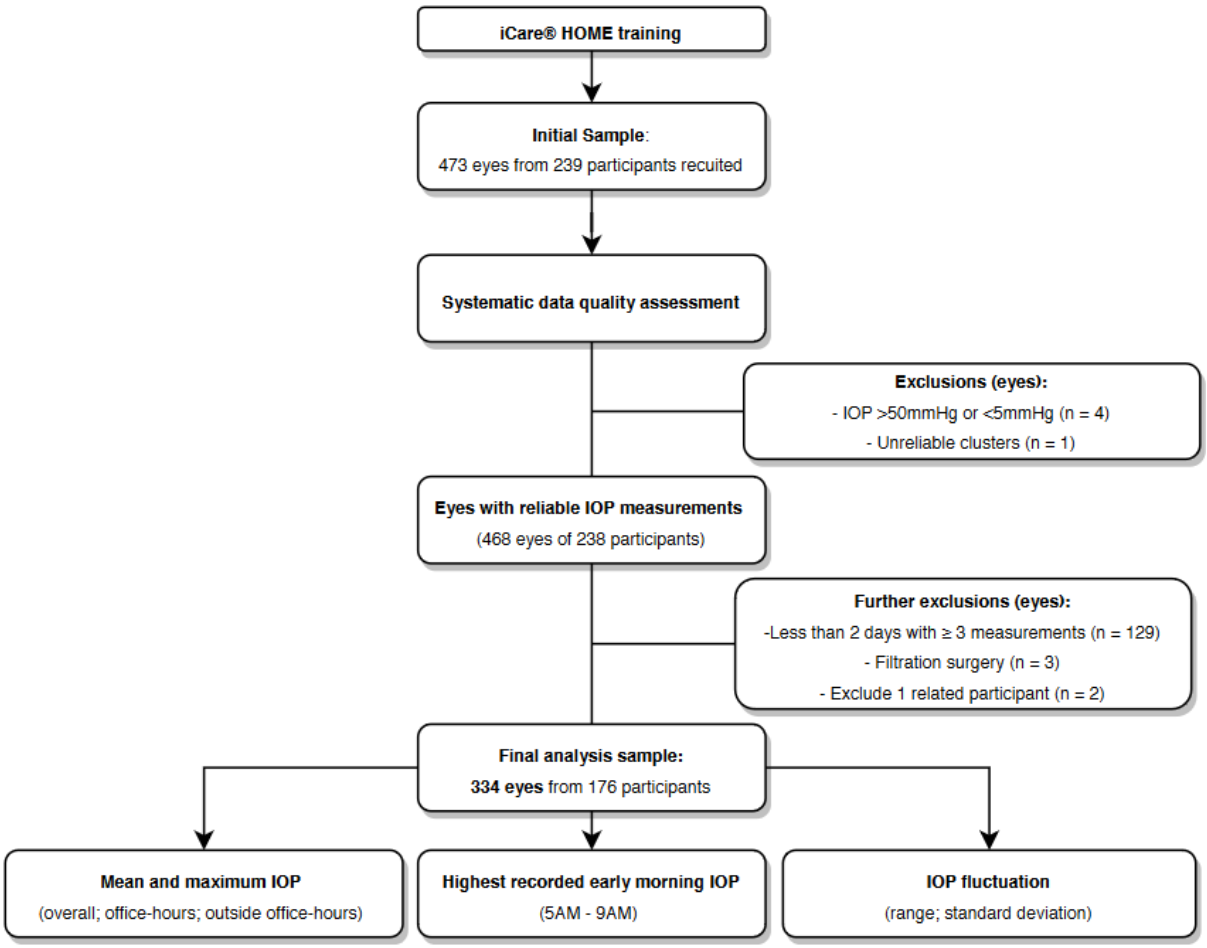

Figure 4.14. Flowchart of the home tonometry study design
IOP: intraocular pressure.

For clinical interpretation, the study cohort was stratified into three risk groups based on the quintile distribution of the IOP PRS relative to a control population: the lowest 20% of the sample PRS was considered low-risk, the middle 60% as intermediate risk, and the highest 20% as high-risk (A. Qassim et al. 2020). The control population included 17,642 genotyped individuals from the population-based QSkin cohort, a cohort of randomly sampled individuals aged 40–69 years from Queensland, Australia (Olsen et al. 2012). The clinical and demographic characteristics of the study participants are summarised in Table 4.10.

Table 4.10: Clinical cohort characteristics stratified by intraocular pressure polygenic risk score (IOP PRS)

Characteristic	Low risk	Intermediate risk	High risk	P-value
Number of eyes / participants (No.)	33	194	107	-
Gender, male (No., %)	15 (46%)	104 (54%)	51 (48%)	0.49
Age, years	65.1 (8.9)	63.7 (9.1)	64.4 (10.0)	0.64
Central corneal thickness, µm	550 (46)	551 (34)	546 (33)	0.51
Vertical cup-to-disc ratio	0.68 (0.11)	0.70 (0.12)	0.70 (0.13)	0.69
Eyes on topical glaucoma medications (n, %)	16 (49%)	83 (43%)	54 (51%)	0.42
Visual field mean deviation, dB	-0.81 (2.1)	-0.84 (2.3)	-1.28 (2.6)	0.27

Summary statistics values are mean (standard deviation) unless otherwise stated. P-values were obtained using Kruskal-Wallis rank sum test.

Age was negatively correlated to maximum IOP (including the highest recorded early morning IOP), and IOP fluctuation (P = 0.031 and P = 0.006) (Table 4.11). These associations were modest (Pearson's correlation coefficient: -0.10 to -0.20), although persisted after adjustment for gender, CCT, and the number of topical glaucoma medications. Thus age was included as a covariate in the following regression analyses (Heinze, Wallisch, and Dunkler 2018). Gender was not significantly correlated with any home tonometry parameters.

Table 4.11. Effect of age on home tonometry parameters.

Home tonometry parameters (mmHg)	Estimated change per 10 years older age	Standard error	P-value	R2 (%)
Highest recorded early morning IOP	-1.43	0.46	**0.006**	4.95
Mean IOP	-0.47	0.33	0.174	1.1
Maximum IOP	-1.16	0.49	**0.031**	2.7
Mean IOP during office hours	-0.50	0.35	0.174	1.1
Mean IOP outside office hours	-0.41	0.33	0.211	0.8
Absolute IOP range	-1.28	0.40	**0.006**	4.30
IOP fluctuation (standard deviation)	-0.34	0.11	**0.006**	4.17

Models were fitted using mixed effect linear regression with age as the predicting variable. Pseudo-R^2 values represent the variance explained by the model, and were calculated with fixed-effects only as detailed in the methods. IOP: intraocular pressure.

IOP PRS effectively stratifies short-term IOP profile

Increasing IOP PRS correlated strongly with higher mean- and maximum-IOP measurements across all time-periods (Table 4.12). The magnitude of effect of this association was greatest for the highest-recorded IOP in the early morning. Participants stratified within the highest IOP PRS quintile had a highest-recorded IOP in the early morning increase of 4.3 mmHg (95% CI 1.4–7.3 mmHg; P = 0.005; Figure 4.15A) compared to the lowest risk quintile. The mean outside office hours IOP was 2.7 mmHg higher in the highest IOP PRS quintile relative to the lowest-risk (95% CI 0.61–4.7 mmHg; P = 0.013; Figure 4.15B). Similarly, the mean inside office hour IOP was higher by 2.9 mmHg (95% CI 0.72–5.1 mmHg; P = 0.011; Figure 4.15C). The IOP PRS accounted for 14% of the variance in the mean diurnal IOP, and 19% of the highest recorded early-morning IOP, with adjustment for CCT and age. A model inclusive of the IOP PRS was significantly better compared to a model using CCT and age alone, in predicting the overall mean IOP, and the highest recorded early-morning IOP (additional R^2 of 7% and 9% respectively; P <0.001).

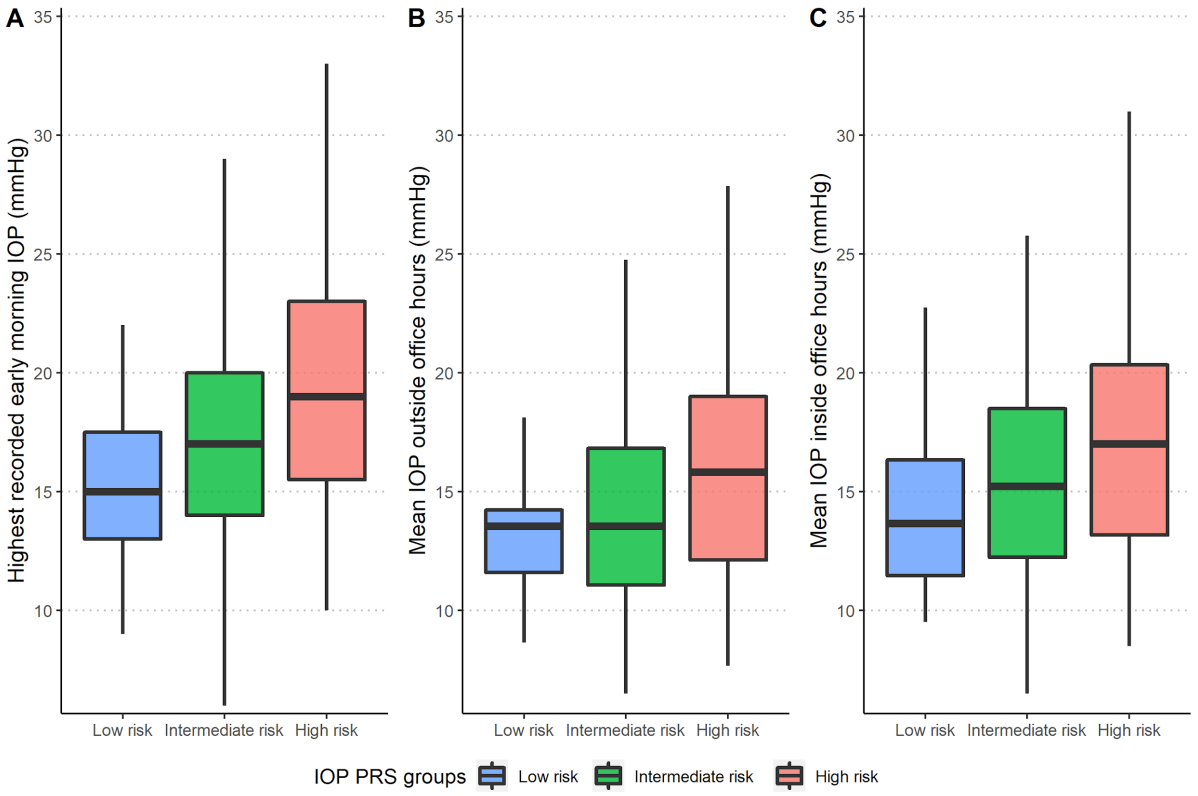

Figure 4.15. Comparison of home tonometry IOP profile stratified by IOP PRS. Box plot comparison of **(A)** the highest recorded early morning (5AM – 9AM) intraocular pressure (IOP), and **(B)** the mean IOP outside (5PM – 9AM) and **(C)** inside office hours (9AM – 5PM) between three groups of IOP-derived genetic risk score (P ≤0.001 for trend using linear mixed effect model adjusting for age and central corneal thickness). The box plot represents the median and the first and third quartiles.
IOP: intraocular pressure; PRS: polygenic risk score.

Table 4.12. Summary of the home tonometry IOP parameters stratified by the IOP PRS groups.

Circadian IOP parameters (mmHg)	Low risk (n=33)	Intermediate risk (n=194)	High risk (n=107)	P-value
Highest recorded early morning IOP*	15.2 (3.5) [9.0–22.0]	17.3 (5.0) [6.0–33.0]	20.2 (7.2) [10.0–46.0]	<0.001
Mean IOP	13.5 (2.9) [9.0–20.9]	14.6 (3.8) [7.3–24.4]	16.3 (5.0) [8.2–33.4]	<0.001
Maximum IOP	19.3 (4.8) [11.0–36.0]	21.1 (6.5) [11.0–50.0]	22.5 (7.2) [10.0–47.0]	0.001
Mean IOP during office hours	14.3 (3.4) [9.5–22.8]	15.3 (4.0) [6.5–25.8]	17.2 (5.5) [8.5–33.5]	<0.001
Mean IOP outside office hours	13.0 (2.5) [8.6–19.0]	14.1 (4.0) [6.5–28.8]	15.7 (4.9) [7.7–33.3]	0.002
Absolute IOP range	11.1 (4.4) [5.0–26.0]	11.9 (6.0) [3.0–42.0]	12.6 (5.8) [3.0–35.0]	0.009
IOP fluctuation (standard deviation)	3.3 (1.3) [1.3–6.9]	3.4 (1.5) [1.2–10.4]	3.7 (1.7) [1.2–9.2]	0.008

Values represent the mean (standard deviation) for each PRS group, followed by the range. P-values are of a mixed effect linear regression model using the IOP PRS as a continuous score as the predicting variable and the circadian IOP parameters as the outcome variable while adjusting for age and CCT. The P-values are adjusted for multiple testing using Benjamini & Hochberg false discovery rate.(Benjamini and Hochberg 1995; Glickman, Rao, and Schultz 2014).

* Early morning IOP data was available for N = 301 eyes (90%).

IOP: intraocular pressure; CCT: central corneal thickness; PRS: polygenic risk score.

The IOP PRS identified individuals who had IOP spikes in the early morning hours that were not otherwise detected during in-office hours. Early morning IOP spikers were defined as having a higher early morning IOP than the highest recorded IOP during office hours, which was observed in 87 eyes (26%). Stratified by the PRS, individuals in the highest PRS quintile were more likely to be early morning IOP spikers (36%) relative to the intermediate (27%) and low (11%) risk groups (linear regression P = 0.019). Participants in the highest IOP PRS quintile were 5.4-fold more likely to be early morning IOP spikers compared to the lowest risk quintile (odds ratio 95% CI 1.3–23.6; P = 0.023).

The IOP PRS correlated with IOP fluctuations as defined by the standard deviation of all IOP measurements and IOP range (linear regression P = 0.009 and P = 0.008 respectively). However, measurement of short-term fluctuation using variance is strongly confounded by maximum IOP measurements (Pearson's correlation coefficient 0.82; P <0.001). Thus, when

the maximum recorded IOP was included in the model, the IOP PRS, CCT, and age were not significantly associated with IOP fluctuation as measured by either the standard deviation or the absolute range.

Topical glaucoma medications are expected to change the circadian IOP profile (J. H. Liu, Kripke, and Weinreb 2004). We performed a sensitivity analysis using eyes that were not on topical glaucoma medications at the time of home tonometry measurements. The IOP PRS remained associated with all the variables reported in Table 4.12 (Table 4.13). In the medication free subgroup, the highest IOP PRS quintile had a higher highest-recorded early morning IOP by 4.7 mmHg (95% CI 1.2–8.3; P = 0.012), and mean outside office hour IOP by 2.4 mmHg (95% CI 0.66–6.1 mmHg; P = 0.019) than the low risk quintile. A sensitivity analysis including a binary covariate for whether an eye has perimetric glaucoma was also performed (Table 4.14). The results show that whether a participant had established perimetric glaucoma did not impact the results of the IOP PRS significantly. Perimetric glaucoma eyes had a lower mean in-office hour IOP by 1.15 mmHg (SD 0.4), which may be due to topical glaucoma treatment, consistent with results from Table 4.13. Nonetheless, the association of the IOP PRS remained consistent.

Table 4.13. Sensitivity analysis using medication naive eyes.

Circadian IOP parameters (mmHg)	**Full cohort (n=334 eyes)**		**Medication naïve cohort (n=181 eyes)**	
	β coefficient (standard error)	**P-value**	**β coefficient (standard error)**	**P-value**
Highest recorded early morning IOP	1.74 (0.4)	<0.001	1.7 (0.49)	0.001
Mean IOP	1.1 (0.28)	<0.001	1.16 (0.38)	0.003
Maximum IOP	1.46 (0.43)	0.001	1.62 (0.51)	0.002
Mean IOP during office hours	1.26 (0.3)	<0.001	1.45 (0.4)	0.001
Mean IOP outside office hours	0.94 (0.29)	0.001	0.95 (0.38)	0.015
Absolute IOP range	0.96 (0.36)	0.009	1.04 (0.46)	0.025
IOP fluctuation (standard deviation)	0.28 (0.1)	0.006	0.3 (0.13)	0.020

β coefficient represents change in home tonometry parameter per 1 standard deviation increase in IOP PRS. Multivariable mixed effect linear regression models were fitted to the home tonometry parameters as the outcome measures, with the standardised IOP PRS (i.e., converted to Z-scores for ease of interpretation) as the predicting variable, while adjusting for CCT and age.

IOP: intraocular pressure; CCT: central corneal thickness; PRS: polygenic risk score.

Table 4.14. Sensitivity analysis including a binary indicator of perimetric glaucoma status.

Circadian IOP parameters (mmHg)	IOP PRS (scaled to Z-score)		Perimetric glaucoma (binary indicator)	
	β coefficient (standard error)	P-value	β coefficient (standard error)	P-value
Highest recorded early morning IOP	1.74 (0.39)	1.8E-05	-0.52 (0.54)	0.33
Mean IOP	1.1 (0.28)	1.3E-04	-0.56 (0.34)	0.10
Maximum IOP	1.46 (0.43)	0.001	-0.49 (0.65)	0.45
Mean IOP during office hours	1.27 (0.29)	2.8E-05	-1.15 (0.4)	0.004
Mean IOP outside office hours	0.94 (0.29)	0.001	-0.3 (0.34)	0.39
Absolute IOP range	0.96 (0.36)	0.009	-0.21 (0.63)	0.74
IOP fluctuation (standard deviation)	0.28 (0.1)	0.006	-0.09 (0.16)	0.60

β coefficients represent change in home tonometry parameter per 1 standard deviation increase in PRS, or if an eye has perimetric glaucoma. Multivariable mixed effect linear regression models were fitted to the home tonometry parameters as the outcome measures, with the standardised IOP PRS (i.e., converted to Z-scores for ease of interpretation) as the predicting variable, while adjusting for perimetric glaucoma status, CCT and age.

IOP: intraocular pressure; CCT: central corneal thickness; PRS: polygenic risk score.

Added utility of the IOP PRS in addition to the in-clinic IOP measurements

It is previously reported that in-office hours IOP characterises circadian IOP parameters in some but not all individuals with glaucoma (Fogagnolo et al. 2009). The added utility of the IOP PRS in predicting home tonometry parameters was investigated by including the clinician measured GAT IOP done at Icare Home training visit in a multiple variable model. IOP measurements performed in-clinic (including by GAT) correlate with home tonometry measurements, particularly when performed within a short period after the in-clinic measurement. This correlation is expected to be weaker if the in-clinic IOP measurement was from a more distant timeframe. For instance, when predicting the mean home tonometry IOP using the most recent available GAT IOP (whenever it may be), the R^2 was 20%, which improves to 23% if only GAT IOP measurements within 30 days were included. Conversely, if the GAT IOP measurement was that at study enrollment to the PROGRESSA study (which variably predates home tonometry assessment), the R^2 of predicting mean home tonometry IOP dropped to 10%. In contrast, PRS risk stratification could potentially be implemented at any stage, including at primary care or community optometry settings, without detailed ophthalmic assessment.

For this analysis, only participants who have performed the home tonometry within 30 days of the last recorded in-clinic GAT were included (n = 277 eyes; 83%). After accounting for the most recent in-clinic GAT IOP, CCT, and age, IOP PRS remained significantly associated with the highest-recorded IOP in the early morning, with an increase of 3.6 mmHg in the high IOP PRS quintile (95% CI 0.72–6.5; P = 0.017) relative to the lowest. The IOP PRS remained associated with the mean IOP outside office hours, and mean IOP during office hours (linear regression using continuous PRS, P = 0.010 and 0.001 respectively) after adjustment for GAT IOP, CCT and age. Inclusion of clinician measured GAT-IOP improved the variance explained in mean IOP to 31%. A model inclusive of the IOP PRS performed better than that with a recent GAT IOP, CCT and age alone (additional R^2 of 4%; P = 0.005).

Comparison to a multitrait glaucoma PRS

The performance of the IOP PRS was compared to the aforementioned, more comprehensive MTAG PRS, which in addition to IOP, includes variants associated with VCDR and glaucoma diagnosis (Craig et al. 2020). The IOP-only PRS was more strongly associated with circadian IOP parameters than the multitrait glaucoma PRS (Figure 4.16). For instance, for each one standard deviation higher IOP PRS, there was an associated increase of 1.74 mmHg (SD 0.40) highest recorded early morning IOP (P < 0.001) compared to 0.95 mmHg (SD 0.41) for the multitrait glaucoma PRS (P = 0.043). The IOP PRS explained more variance of the mean IOP measured during the whole study compared to the multitrait glaucoma PRS (13.5% vs 9.9% respectively).

Figure 4.16. Relative performance of the IOP PRS and a multi-trait glaucoma PRS in predicting home tonometry IOP profile

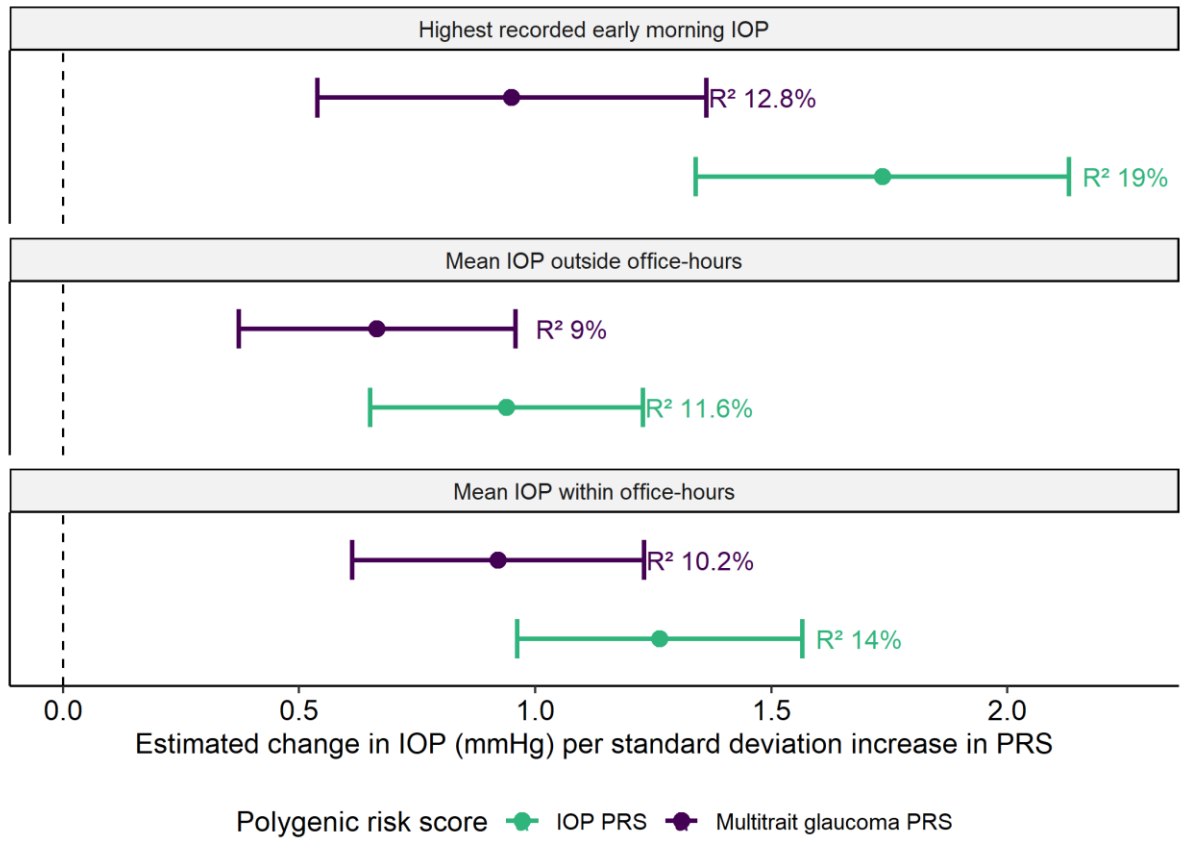

The dots represent the estimated mean change in IOP per standard deviation increase in PRS (scaled beta-coefficients) in a linear model using the home tonometry parameters as outcomes. The error bars represent standard errors of the estimate. The variance explained (R^2) by each PRS model is also displayed. All models were adjusted for central corneal thickness and age.
IOP: intraocular pressure; PRS: polygenic risk score.

Discussion

Common genetic variants associated with both glaucoma and IOP have been identified via large GWAS, and combined into risk scores that are effective at risk stratifying individual patients. Individuals in the top MTAG PRS decile were at 15-fold increased risk of advanced glaucoma, and at 21.5-fold increased risk of advanced high tension glaucoma, relative to the bottom decile. This was a substantial improvement over previously reported PRS risk profiling in glaucoma, including the IOP-only PRS whereby top decile individuals had a 5.6-fold increased risk of advanced glaucoma relative to the bottom (MacGregor et al. 2018). The MTAG-derived PRS was validated in independent samples, confirming its high predictive ability.

The aetiology of complex diseases depends on both environmental and genetic factors, thus PRS alone will never achieve the very high predictive power (e.g. AUC >0.9) required for accurate population screening (Dudbridge 2013). A glaucoma PRS will be primarily useful for stratifying individuals into risk groups; for example in the BMES data, screening the top decile of the MTAG PRS in individuals between 50-60 years old identifies 40% of the cases. Moreover, as argued by Khera et al. (2018), individuals with a high PRS for glaucoma are likely to be at a similar risk to individuals carrying rare "high penetrance" *MYOC* variants (X. Han et al. 2019). Finally, the PRS performance for glaucoma is particularly noteworthy given the clinical implications of identifying at-risk individuals and the prevention of irreversible blindness with readily available treatment proven to be effective at preventing or minimising visual loss.

Whilst current treatments are effective in preventing or reducing POAG progression (D. F. Garway-Heath et al. 2015), many patients are not diagnosed before irreversible damage to visual function has already occurred. Earlier diagnosis of glaucoma can reduce glaucoma blindness, and this work demonstrates that people with a higher PRS require earlier clinical assessment. In the UKBB, individuals in the top MTAG PRS decile reach an equivalent absolute risk for glaucoma 10 years earlier than people in the bottom decile. In advanced glaucoma cases, individuals in the top decile were diagnosed 7 years earlier than those in the bottom decile. Similarly, the MTAG-derived PRS was associated with significantly earlier disease onset in UK Biobank *MYOC* p.Gln368Ter carriers who are at high disease risk. This is of particular importance to genetic testing in POAG as it shows the additive effects of both rare and common variants in the development of glaucoma. Therefore, a clinical genetic risk stratification strategy in glaucoma would ideally incorporate both rare variants and PRS, as both contribute to the genetic architecture of glaucoma (refer to Chapter 1; this concept is discussed in further detail in Chapter 7).

Previous studies in glaucoma risk profiling using common genetic variants were limited by the inclusion of a small number of risk variants and a lack of validation cohorts. *TMCO1* was one of the earliest reported genes to be associated with POAG in common variant studies, and remains one of the most strongly associated variants with IOP and POAG (K. P. Burdon et al. 2011; MacGregor et al. 2018; A. P. Khawaja et al. 2018) A variant in the *TMCO1* gene was reportedly associated with conversion from ocular hypertension to glaucoma in non-Hispanic whites in a subgroup of The Ocular Hypertension Treatment cohort who underwent genotyping (Scheetz et al. 2016). In another study, individuals homozygous for a variant near *TMCO1* were reported to have a younger age of POAG onset (Sharma et al. 2012). The clinical utility of genetic risk scores is now rapidly expanding due to the accelerated discovery of disease-

associated loci as larger GWAS are conducted. Fan et al. (2019) reported an unweighted PRS inclusive of 12-SNPs associated with POAG, two of which (those near *CDKN2B-AS1* and *SIX6*) are known to be associated with POAG and VCDR but not IOP (K. P. Burdon et al. 2011; H. Springelkamp et al. 2017), to be associated with a younger age of glaucoma diagnosis. Similarly, Mabuchi et al. (2020) reported an unweighted PRS inclusive of 17-SNP associated with IOP to be associated with a younger age of glaucoma diagnosis, but not with a family history of glaucoma, in a cohort of Japanese individuals. Prior studies included even fewer risk variants and reported only a modest risk of the development of POAG (Y. C. Tham et al. 2015; Nannini et al. 2018; F. Mabuchi et al. 2017) The markedly improved genetic risk prediction inferred by the more comprehensive PRS reported in this chapter supports the fact that inclusion of additional low impact variants leads to better PRS models for complex traits (Boyle, Li, and Pritchard 2017). Thus, larger GWAS of POAG and its endophenotype could further improve the performance of the PRS in the future.

The MTAG-derived PRS was able to stratify people with early manifest glaucoma or glaucoma suspects who are at higher probability of disease progression (using both structural and functional progression end-points). Furthermore, it was predictive of the likelihood of requiring surgical intervention, which is highly effective at reducing IOP, but carries substantial treatment morbidity meaning it should always be targeted specifically to those at higher risk of disease progression and blindness. Of note, individuals in the high PRS groups were more likely to progress despite the more observed higher treatment intensity. Given the pragmatic study design in PROGRESSA, it is unknown whether the higher treatment intensity was in response to clinicians detecting progression, or whether the PRS captured additional risk of progression that was not responsive to traditional IOP-lowering therapies. The latter hypothesis stems from the fact that the MTAG PRS encompses genetic variants associated with optic neuropathy (i.e., higher VCDR) independent of IOP (e.g. *CDKN2B-AS1* locus) which may correspond to IOP-independent neurodegenerative biological pathways. The outcomes of my project highlight the ability of the MTAG PRS to identify patients who are the most at risk of early glaucoma onset and disease progression and who would benefit the most from timely and more invasive interventions.

Previous evidence showed that optic nerve head insult caused by unrecognised IOP spikes — such as those occurring early-morning and outside office hours — may contribute to glaucomatous neurodegeneration (J. H. K. Liu et al. 2003). Diurnal change and fluctuation in IOP has been previously reported in glaucomatous eyes (Asrani et al. 2000; J. H. K. Liu et al. 2003; Mona S. Awadalla et al. 2020). Liu et al. (2003) have reported an early-morning IOP increase in glaucomatous eyes which was not seen in controls . However, the current methods

of IOP assessment are limited to the time of measurement and are a poor measure of an individual's IOP profile, maximum and fluctuations (Mosaed, Liu, and Weinreb 2005; Jost B. Jonas et al. 2005). Our IOP PRS was able to address some of these limitations. Indeed, in a subset of patients who underwent home tonometry, the IOP PRS was most strongly associated with higher early-morning IOP, as well as a higher mean IOP both during and outside office hours, which remained independently associated after adjusting for a recent in-clinic IOP measurement. Similarly, individuals in the high IOP PRS quintile were 5.4-fold more likely to be early morning IOP spikers compared to the lowest risk quintile.

Additional IOP measurements outside office hours may offer clinical utility in the management of glaucoma. Asrani et al. (2000) have reported that short-term IOP fluctuation was an independent risk factor for glaucoma progression. Similarly, diurnal IOP parameters and 24-hour IOP fluctuation measured by a contact lens sensor were recently reported to be associated with glaucoma progression (Moraes et al. 2018; Tojo, Hayashi, and Otsuka 2020). Barkana et al. (2006) have reported that in a study of 32 patients with progressive glaucoma not attributable to their in-office hours IOP, the majority (69%) had a higher peak and fluctuation in IOP outside office hours, which informed a treatment change in 19 (59%) of the cases. Our findings highlight further the clinical utility of genetic markers in stratifying patients at high risk of IOP fluctuation and glaucoma progression. Whether the genetic prediction of a likelihood to have early-morning IOP spikes or greater short-term IOP fluctuation will be informative in clinical care of glaucoma patients requires further research. The current evidence supports IOP PRS stratification may be used to prompt clinicians to obtain additional IOP measurements (e.g. outside office hours, or early-morning either in-clinic or via home tonometry), the results which may guide further clinical intervention.

Despite the clinically modest difference in the maximum IOP between the high and low IOP genetic risk groups (between 1–2 mmHg), there was a strong relationship between the IOP PRS and treatment intensity. In a glaucoma registry, the incisional surgery rate was 50% in the high IOP PRS group compared to 38% in the low risk group. Similarly, in an early glaucoma cohort, 38% of the high IOP PRS group required 2 or more medications or SLT for glaucoma management compared to 23% in the low IOP PRS risk group. This may be attributable to two factors. Clinicians are more aggressive in IOP-lowering treatments when there is evidence of progressive visual field loss, regardless of the IOP measurements in-clinic (R. N. Weinreb et al. 2007; Clement, Bhartiya, and Shaarawy 2014). Thus, treatment is sometimes initiated or escalated without confirmatory observation of elevated IOPs (e.g. in cases with central vision-threatening glaucoma). Furthermore, IOP measured during clinic hours is routinely performed either in the morning or afternoon, which may not be reflective of an individual's diurnal IOP

profile, as introduced in the beginning of the chapter (Mosaed, Liu, and Weinreb 2005; Jost B. Jonas et al. 2005).

While the MTAG PRS generally outperformed the IOP PRS in glaucoma risk prediction and clinical phenotyping, the IOP PRS may offer further insight into an individual's chronic exposure to higher IOP than sporadic clinic measurements, and the impact of IOP fluctuations or spikes. Interestingly, while combining multiple traits (such as vertical cup-to-disc ratio, and glaucoma status; the MTAG PRS) to generate a more comprehensive glaucoma PRS significantly improves glaucoma risk and phenotype stratification, the IOP PRS provided a comparatively better association with outside office hours and early morning IOP profiling. This highlights the clinical utility of a trait-specific PRS in addition to a comprehensive disease risk PRS, depending on the desired prediction and use of the PRS data.

The research reported in this chapter has several strengths. A large population cohort was utilised to derive the genetic risk scores, incorporating all the known and novel risk variants associated with POAG, IOP, and VCDR. For the IOP-only PRS, a strict genome-wide threshold was used to characterise the clinical glaucoma phenotype that is most attributable to the genetic biomarkers of IOP and its associated pathways. The primary analysis was conducted in cohorts independent of the GWAS discovery cohort, and the results were validated in independent cohorts across the clinical POAG spectrum allowing further generalisability of the findings. For investigating the diurnal IOP profile using home tonometry , a subset of well-characterised PROGRESSA participants were enrolled from four clinics across the early glaucoma spectrum. However, as patient-driven IOP measurements are prone to artefactal recordings, a systematic and objective approach was undertaken to exclude unreliable measurements and generate robust summary parameters.

A limitation of the genetic risk prediction using the currently available glaucoma PRS is that genetic risk scores are limited by the genetic pool of the discovery cohort. Thus, the results reported are limited to the ethnicities of the European ancestry individuals of the UK Biobank study which matched the prediction target cohorts. The clinical utility of the PRS in risk profiling and improved prediction accuracy over and above traditional risk factors was performed in homogeneous groups (as defined by genetic principal components) of either European or South Asian ancestries. The performance of the PRS in other populations should be tested to investigate the generalisability of these findings. However, further analyses including individuals from non-European background are underway. For example, a large multi-ethnic meta-analysis of POAG GWAS has thus far identified an additional 69 novel risk loci for POAG (Puya Gharahkhani et al. 2020). Additionally, the performance of the PRS in aiding clinical

decision making and guiding earlier treatment needs to be evaluated prospectively in a longitudinal intervention study, with participants randomised to have their PRS provided or withheld from their treating specialist. Finally, IOP lowering treatments will significantly affect IOP measurements and fluctuations, as well as glaucoma progression, and will confound the analysis in comparison to treatment naive newly presenting cases. It is encouraging that the PRS was positively associated with several progression outcomes, and diurnal IOP profile despite this.

The home tonometry study has some additional limitations. While the Icare HOME tonometer provides valid ambulatory IOP measurements, it does not provide continuous IOP monitoring which may be better suited to assess IOP fluctuations. Furthermore, nocturnal IOP which has been reported to be elevated in glaucoma (Mosaed, Liu, and Weinreb 2005), were not investigated in the home tonometry study. Frequent and reliable measurements are also operator dependent, and further confounding factors include posture, fluid intake and systemic blood pressure, although these factors are not expected to correlate with the PRS. Rebound tonometry is significantly affected by CCT, thus CCT was used as a covariate in all home tonometry-specific analysis (Takagi, Sawada, and Yamamoto 2017; Termühlen et al. 2016).

An aggregate score of common genetic risk variants provide an effective means of genetic risk profiling in glaucoma. Genetic risk scores presented in this chapter were shown to be predictive of: 1) increasing risk of advanced glaucoma; 2) glaucoma status significantly beyond traditional risk factors; 3) earlier age of glaucoma diagnosis; 4) high levels of absolute risk in persons carrying high penetrance glaucoma variants; 5) increasing likelihood of disease progression in early stage disease in both structural and functional measures; 6) increasing likelihood of incisional glaucoma surgery in advanced disease and medical treatment in early disease; and 7) a higher early-morning IOP and outside office hour mean IOP, as well as a higher risk early-morning IOP spikes. Glaucoma PRS has good predictive power across a range of clinical cohorts. Its application will facilitate the rational allocation of resources through clinical screening and timely treatment in high-risk patients using IOP-lowering therapies, with reduced clinical monitoring costs in lower risk groups.

Chapter 5: Clinical interventions in reducing intraocular pressure in early glaucoma

Published manuscripts

The contents of this chapter have been published in two peer-reviewed manuscripts in which I am a first author. The effects of two established clinical interventions in lowering intraocular pressure in glaucoma were investigated. The role of selective laser trabeculoplasty in reducing the mean and fluctuation of short-term intraocular pressure was published in a manuscript in *Clinical and Experimental Ophthalmology*, volume 48, issue 3, pages 328–333 (Mona S. Awadalla et al. 2020). My contributions to this manuscript involved the study concept and design (50%), data collection in the form data wrangling and generating a tidy dataset (50%), data analysis including statistical analysis (100%), data interpretation including the clinical application of the results (50%), drafting the manuscript (50%), and critical revision of the manuscript for important intellectual content (50%). Mona Awadalla contributed equally to the manuscript including study concept and design (40%), data collection in the form recruiting participants for home tonometry (50%), data interpretation (40%), drafting the manuscript (50%), and critical revision of the manuscript for important intellectual content (40%). Thi Nguyen contributed to technical and material support, and data collection by assisting in the recruitment and training of the study participants. Mark Hassall, John Landers, and Jamie Craig contributed by supervision, obtaining funding, and critical revision of the manuscript for important intellectual content.

The study investigating the role of cataract surgery in reducing intraocular pressure was published in a manuscript in *Clinical and Experimental Ophthalmology*, volume 48, issue 4, pages 442–449 (Ayub Qassim, Walland, et al. 2020). My contributions to this manuscript involved the study concept and design (80%), data collection in the form case note review and data extraction from electronic database (90%), data analysis including statistical analysis (100%), data interpretation including the clinical role of cataract surgery in the management of glaucoma (85%), drafting the manuscript (90%), and critical revision of the manuscript for important intellectual content (85%). Mark Walland contributed to data interpretation and critical revision of the manuscript for important intellectual content. John Landers and Paul Healey contributed to study design. Mona Awadalla, Thi Nguyen, Jason Loh, Angela Schulz, and Bronwyn Ridge contributed to technical and material support, and assisted in data collection. All authors contributed to critical revision of the manuscript for important intellectual content. All senior authors contributed to obtaining funding, patient recruitment and study design. Additionally, John Landers and Jamie Craig contributed to supervision.

Introduction

Elevated IOP is the most important risk factor for the development and progression of POAG (Sultan, Mansberger, and Lee 2009; Anders Heijl et al. 2002; Gordon et al. 2002). Normal IOP may be defined by population studies as the value within two standard deviations of the mean encompassing 95% of the normal population, or approximately 10–21 mmHg (Hollows and Graham 1966; Bonomi et al. 1998). These population studies did not take into account systemic and ocular features that are now known to influence IOP measurements (Nakano et al. 2005; Memarzadeh et al. 2008; Jost B. Jonas et al. 2011; M. P. Y. Chan et al. 2016). For instance, in the UK Biobank cohort of 110,573 individuals, IOP was positively assocaited with older age, male sex, higher systolic blood pressure, faster heart rate, greater myopia, and colder season (M. P. Y. Chan et al. 2016). Despite this, lowering IOP is highly effective in slowing the onset and progression of glaucoma, and remains the only demonstrably therapeutic treatment for POAG (Conlon, Saheb, and Ahmed 2017; Jost B. Jonas et al. 2017).

For patients with glaucoma, the therapeutic IOP target is individually determined depending on the disease severity, the rate of progression and the vision-related quality of life (Conlon, Saheb, and Ahmed 2017). Additionally, short- and long-term fluctuations in IOP may be associated with glaucoma progression (Asrani et al. 2000; J. Caprioli and Coleman 2008; Boel Bengtsson et al. 2007). Thus, accurate and frequent IOP measurements at different time points are imperative. Both topical medical therapy and SLT are effective and commonly used to treat POAG (Wong et al. 2015; D. F. Garway-Heath et al. 2015). Filtration surgery is a more widely effective means of lowering IOP but carries higher morbidity compared to medical or laser therapy and thus is commonly reserved for more recalcitrant disease not responding to other therapies (Joseph Caprioli et al. 2016; Feiner, Piltz-Seymour, and Collaborative Initial Glaucoma Treatment Study 2003).

Several studies have demonstrated the role of SLT in reducing IOP in patients with glaucoma either as a primary or an adjunctive treatment. In a recent observer-masked, randomised controlled trial of SLT in treatment-naive patients, target IOP was achieved in 75% of the eyes at 36 months, without the need for IOP-lowering medications (Gus Gazzard et al. 2019; A. Garg et al. 2019). In a pragmatic retrospective analysis of real-world SLT data from 5 ophthalmology practices in the UK, Khawaja et. al. (2020) reported the success rate of SLT in lowering IOP to be 70%, 45%, and 27% of eyes at 6, 12, and 24 months post-SLT, respectively. This difference is attributable to the different study designs, cohort characteristics, and treatment targets (Anthony P. Khawaja et al. 2020; G. Gazzard et al. 2018). Nonetheless, evidence from previous meta-analyses support the clinical IOP-lowering

effects of SLT to be similar to that of topical medications (X. Li, Wang, and Zhang 2015; Wong et al. 2015). However, the effect of SLT on short-term diurnal IOP profile has not been investigated, and a clinical concern for post-SLT IOP spike often mandates additional clinical appointments to measure IOP (Hirabayashi, Ponnusamy, and An 2020; A. Garg et al. 2019).

While cataract surgery is not a procedure for IOP lowering in open angle glaucoma, several studies have reported a reduction of IOP following cataract surgery in patients with open angles (Hayashi et al. 2001; Shingleton et al. 2006; Mansberger et al. 2012). The prevalence of POAG and cataract are strongly associated with older age, and thus both conditions commonly coexist (Paul Mitchell et al. 1996; McCarty et al. 1999). A recent meta-analysis of the studies on the effects of phacoemulsification on IOP has identified the lack of a control group, medication use and washout, and the loss to follow-up as sources of bias which potentially undermine certain conclusions in the reported literature (Masis et al. 2018).

Outlined in this chapter is my original contribution to knowledge in characterising the effects of SLT on short-term diurnal IOP profile using home tonometry, and providing a patient-centered follow-up strategy post SLT. Additionally, I investigated the role of cataract surgery in reducing IOP in a prospectively monitored early glaucoma cohort, using a pragmatic, case-controlled study design, aiming to address the current gaps in the literature.

Methods

The following methods section has been previously published in two peer-reviewed manuscripts, and has been edited to fit the structure of the thesis (Ayub Qassim, Walland, et al. 2020; Mona S. Awadalla et al. 2020).

In this chapter, IOP-lowering effects of SLT and cataract surgery were investigated in participants enrolled in the PROGRESSA study. For SLT study, the feasibility and efficacy of Icare HOME tonometer (Icare Finland Oy) as an initial method for IOP follow-up after SLT was investigated, and the time-course of IOP reduction following SLT was characterised (Mona S. Awadalla et al. 2020). For the cataract study, the longitudinal IOP-lowering effects of cataract surgery was investigated, and the clinical predictors of a greater IOP reduction were identified (Ayub Qassim, Walland, et al. 2020).

Study cohort

Participants were sampled from the PROGRESSA study, described in detail in Chapter 2. Briefly, individuals with optic disc features suspicious or probable for glaucoma (glaucoma suspects), and those with early manifest glaucoma were followed-up longitudinally with

detailed clinical examination every 6 months. Treatment was at the discretion of the treating ophthalmologist, in keeping with the current guidelines (NHMRC 2010).

The effects of SLT on diurnal IOP profile was investigated in a subgroup of PROGRESSA participants who underwent SLT between September 2016 and December 2018, and were recruited to perform home tonometry monitoring before and after SLT. Only participants with established early manifest glaucoma were enrolled for SLT treatment. Early manifest glaucoma was defined as patients who had reproducible visual field loss in glaucomatous regions with mean deviation better than -6 dB, described in detail in Chapter 2. SLT was administered either as an initial treatment or as an adjuvant due to insufficient control of IOP despite maximum tolerated topical medications at the discretion of the treating clinician. SLT was performed by a glaucoma specialist with a Q-switched Nd:YAG laser (Ellex Solo, Ellex Medical Pty. Ltd., Adelaide, Australia) using Latina SLT gonio lens (Ocular Instr., Bellevue, Washington) to visualize the trabecular meshwork. The initial energy was set to 1.0-1.2 mJ and titrated the minimum energy required to generate visible bubbles from the trabecular meshwork with each laser pulse. A 360° SLT was performed in all cases with approximately 100 non-overlapping spots spread throughout 360°. None of the participants had any other eye surgery or laser procedure during the one week follow-up period post SLT.

The effects of cataract surgery on long-term IOP was investigated in a subgroup of PROGRESSA participants who who had undergone cataract surgery via phacoemulsification with intraocular lens implant in either eye during their period of longitudinal monitoring, and had at least one visit 6-months post procedure. The indication for surgery was a visually significant cataract interfering with vision. Surgical technique and IOP management was at the discretion of the treating glaucoma specialist. Case notes were then reviewed to record the pre-treatment maximum IOP, and the preoperative ocular biometry: anterior chamber depth and axial length (IOL Master, Carl Zeiss, Germany). A matched sample of the PROGRESSA cohort who had not undergone any ocular surgery during their follow-up were selected as controls for this investigation. These were enrolled and followed up under the same protocol. To account for confounding factors that could affect IOP measurements over time, the control group were matched to the cases (who underwent cataract surgery) by age, gender, duration of study follow-up, baseline IOP at enrolment, and treatment intensity during follow-up.

Home tonometry assessment for the SLT group

Each participant attended an Icare HOME training session, as described in Chapter 4. Certification was only achieved when the patients were able to position the Icare HOME appropriately and generate two reliable Icare HOME measurements independently.

Participants were requested to perform four measurements per day (morning, afternoon, evening and before bedtime) for 1 week prior to and following SLT. All measurements were instructed to be taken in a seated and upright position. A single IOP reading on the same day after SLT was requested to note any post-SLT IOP spikes. For the early morning reading, participants were advised to wait for 30 minutes after waking. To protect patient privacy and so as not to alter patient measurement behaviour, the recorded IOP data was only visible when connected to a computer with the Icare LINK or Icare EXPLORE software and Icare CLINIC browser.

Data were exported from Icare LINK software and Icare CLINIC browser for analysis. Only the eye treated with SLT was included for each patient. If there were multiple measurements at one time, the last consecutive measurement was selected, and other repeated measurements were discarded. Any IOP recorded less than 5 mmHg and more than 50 mmHg suggestive of measurement errors or artefacts were excluded. IOP fluctuation was defined as the standard deviation of all IOP measurements before or after SLT. Outcome measures were the change in the mean IOP, maximum IOP and IOP fluctuation before and after SLT.

Statistical analysis

All statistical analyses were performed using R (version 3.5.1, RCore Team, Austria). Analysis on the effects of SLT on diurnal IOP profile was performed using a paired comparison of the outcome variables (home tonometry summary parameters) before and after SLT. Mixed-effects linear models were used to account for paired nature of the data (Q. Fan, Teo, and Saw 2011). Only the eye that has undergone SLT was included in the analysis for each patient.

Analysis on the effects of cataract surgery on long-term IOP was performed on all eligible eyes, using a case-control design. Controls were matched by dissimilarity matrix calculation using the *cluster* (version 2.0.7.1) (Maechler et al. 2019) and *e1071* (version 1.7.0.1) (Meyer et al. 2019) packages in R. Analysis of variance between the cases and controls was done using Kruskal–Wallis test for continuous variables and Chi-squared test for categorical variables. To account for the correlated nature of these measurements, a mixed-effects linear model with random intercepts per patient was used (Q. Fan, Teo, and Saw 2011). Longitudinal IOP measurements from each visit were used in the primary analysis; within-eye correlation was adjusted for using two-level random intercepts per patient then per eye. In the case-control analysis, the mean difference between all the IOP measurements before and after cataract surgery was used for the cases. For the controls, the median visit per patient (e.g. visit 5 of visits 1 through 9) was used as the point in time to calculate the “change in IOP”. To

account for the random effects of the clinic sites, the recruitment and follow-up site was used as another random intercept in the models.

All mixed-effect models were fitted using the *lme4* package in R (version 1.1.20) (Bates et al. 2015). Hypothesis testing of the models were performed using Satterthwaite's degrees of freedom method implemented in the *lmerTest* package (Kuznetsova, Brockhoff, and Christensen 2017). The pseudo-R2 of the mixed-effects models were calculated based on the fixed-effects only as described by Nakagawa et al. (2017). The cut-off of statistical significance (alpha level) was set at P = 0.05.

Effects of selective laser trabeculoplasty on diurnal IOP profile

The following results section has been previously published in a peer-reviewed manuscript, and has been edited to fit the structure of the thesis (Mona S. Awadalla et al. 2020).

Fourteen eyes from 14 patients were included in the study, comprising nine males and five females. The mean age was 65.0 (SD 11.0) years with a range of 42 to 77 years old. All patients had primary open-angle glaucoma; of whom seven had no previously documented IOP above 21 mmHg (i.e., normal tension glaucoma). Six patients had SLT as an initial treatment while eight patients had SLT after failure of maximum tolerated topical anti-glaucomatous medication to adequately control IOP. Only two patients had a previously recorded maximum IOP below 22 mmHg (i.e., 'normal tension' glaucoma). Patient demographics and ocular parameters are shown in Table 5.1. All patients were able to obtain IOP measurements successfully. An example for post-SLT reduction is presented in Figure 5.1, and the remaining case figures can be found online in the published manuscript appendix.

Table 5.1. Demographic and clinical features of the study participants

Baseline clinical characteristic	Summary statistics
Age in years	65.0 (11.0)
Sex male: female	9:5
Best corrected visual acuity (LogMAR)	0.1 (0.1)
Spherical equivalent in diopters	−0.9 (1.9)
Central corneal thickness in mm	560 (43.2)
Number of glaucoma medications prior to SLT	2 (2)

Note: Summary statistics represent the mean (SD) for continuous variables, and the count for discrete variables.

SLT: selective laser trabeculoplasty

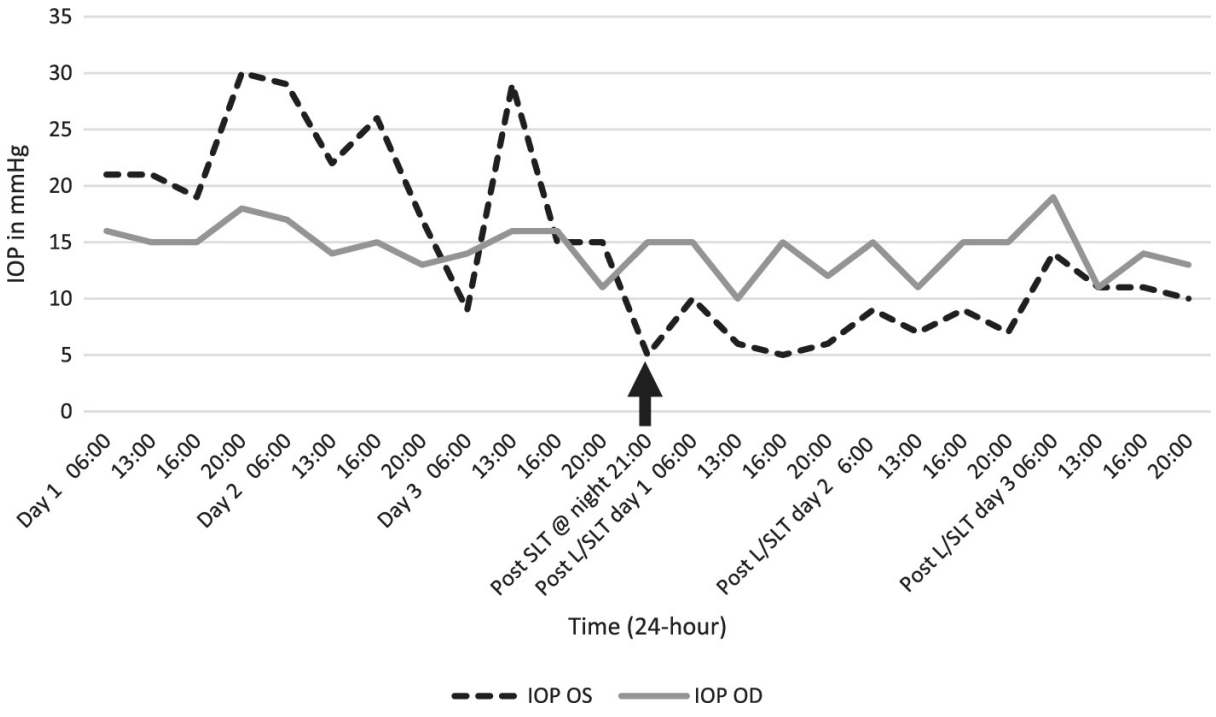

Figure 5.1. Changes in intraocular pressure (IOP) before and after selective laser trabeculoplasty (SLT). The presented example is for a 42-year-old male patient who had SLT in the left eye (black dot line). The arrow points to the first IOP measurement post-SLT.

OD: right eye; OS: left eye; L/SLT: SLT in the left eye; SLT: selective laser trabeculoplasty; IOP: intraocular pressure

There was a significant reduction in mean IOP of the whole post-SLT period by 5.12 mmHg (95% CI 3.75–6.50 mmHg, P < 0.001). Similarly, the maximum IOP was lower post-SLT by 6.14 mmHg (95% CI 3.07–9.21, P < 0.001) (Table 5.2). The magnitude of effect and the statistical significance remained unchanged in multiple variable models including age, sex and central corneal thickness.

There was also an overall reduction in the IOP fluctuation as measured by the standard deviation of all IOP measurements (1.07 mmHg lower post-SLT, 95% CI 0.24–1.89 mmHg, P = .021). In the multiple variable model, age was associated with lower fluctuation alongside SLT (0.066 mmHg lower SD per year older, 95% CI 0.02–0.11 mmHg, P = 0.015). Gender and central corneal thickness were not significant. Data showing IOP measurements throughout the day are presented in Figure 5.2. There were no adverse effects or IOP spikes recorded in the treated eyes after SLT.

Table 5.2. Preoperative and postoperative summary home tonometry results.

Home tonometry parameter	Pre-SLT	Post-SLT	P-value
Mean IOP, mmHg	17.6 (3.79)	12.5 (4.20)	< 0.001
Maximum IOP, mmHg	26.3 (6.58)	20.1 (8.54)	< 0.001
IOP fluctuation, mmHg	4.35 (1.26)	3.29 (1.61)	0.021

Values are mean (standard deviation). IOP fluctuation was defined as the standard deviation of all IOP measurements pre or post SLT P-values are obtained using a mixed-effect linear regression comparison between the pre- and post-SLT measurements.

SLT: selective laser trabeculoplasty; IOP: intraocular pressure

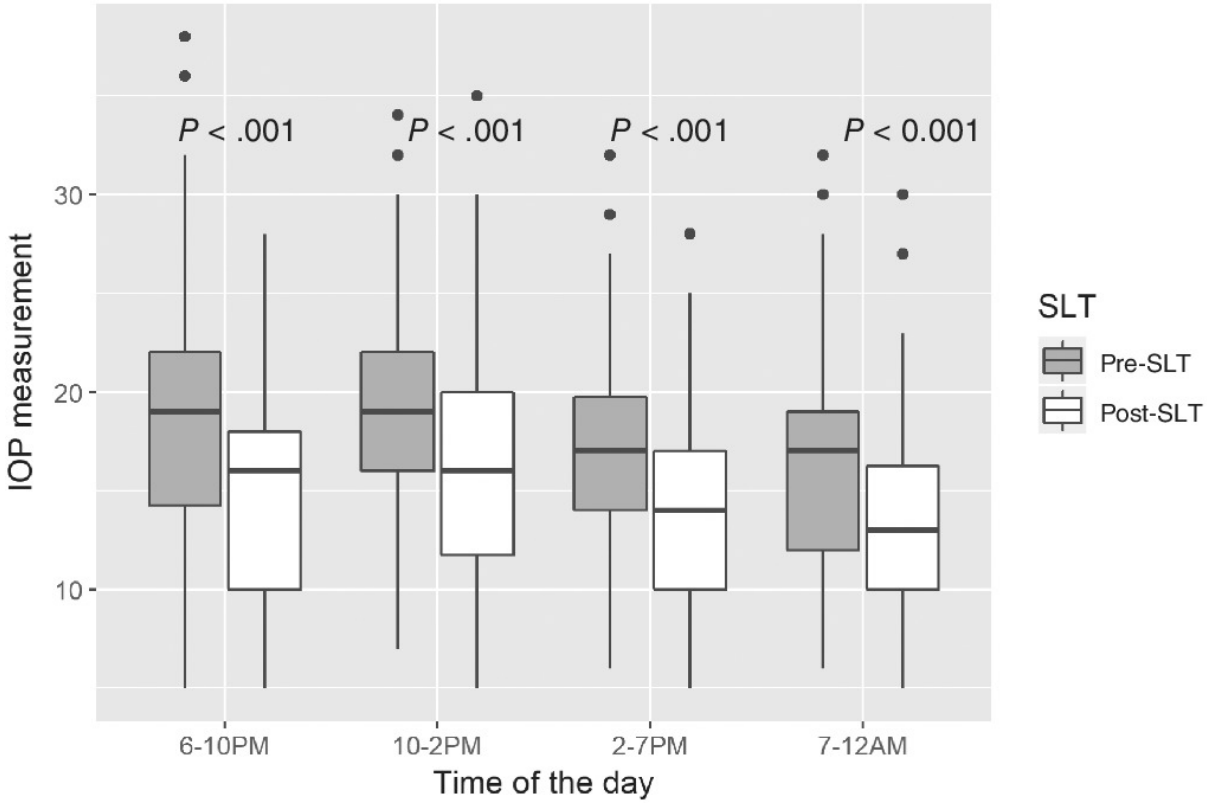

Figure 5.2. Boxplot distribution of intraocular pressure (IOP) measurements using the Icare HOME tonometer at different time points in the day pre- and post-SLT. There is a significant reduction in the IOP median and quartiles at all timepoints post-SLT. *P* values represent the statistical significance of a paired Kruskal-Wallis rank sum test between pre- and post-SLT at each time period.
IOP: intraocular pressure; SLT: selective laser trabeculoplasty

The role of phacoemulsification cataract surgery in reducing IOP

The following results section has been previously published in a peer-reviewed manuscript, and has been edited to fit the structure of the thesis (Ayub Qassim, Walland, et al. 2020).

In total, 171 eyes of 108 patients from 8 clinics across Australia met the case eligibility criteria for this study. All cases were enrolled in PROGRESSA and underwent cataract surgery electively during routine follow-up. The mean (SD) age of the patients at the time of cataract extraction was 72.8 (6.8) years. Cases had clinical data recorded for 3.9 (3.4) years before the operation with a mean follow-up time of 2.7 (1.7) years post procedure. The majority of our patients had at least one year of follow-up (n = 145, 85%). Follow-up rates at 18 and 24 months post procedure were 73% (n = 125) and 59% (n = 100) respectively. Five eyes (2.9%) underwent trabeculectomy surgery at a later date due to progressive glaucoma not responding to medical treatment. IOP measurements following the trabeculectomy were not included in the analysis.

For the control group, 171 eyes from 144 participants enrolled in PROGRESSA who have not undergone cataract surgery, were matched to the cases, and followed-up by the same protocol. As cataract surgery was indicated for visually significant cataracts, there was a significant difference in the best corrected visual acuity between the cases (prior to cataract surgery) and the controls (median [interquartile range] 6/9.5 [4.5] vs 6/7.6 [3.5] respectively; P = $3.3x10^{-8}$). The distribution of the cataract density of the cases and the controls using The Lens Opacities Classification System III is presented in Figure 5.3. Detailed clinical and demographic characteristics of the study cohort is summarised in Table 5.3

Table 5.3 Clinical and demographic characteristics of study participants

Baseline characteristics	Cases	Controls	P-values
Number: eyes / patients	171 / 108	171 / 144	-
Gender, male (%)	56 (51.9)	69 (47.9)	0.62
Age at recruitment, years	69.2 (6.8)	69.0 (6.5)	0.93
Study follow-up duration, years	4.8 (1.4)	4.43 (1.5)	0.05
Number with 5 year follow-up, patients (%)	55 (50.9)	58 (40.3)	0.12
Pseudoexfoliation syndrome, patients (%)	5 (4.6)	4 (2.8)	0.66
Central corneal thickness, µm	546 (35)	538 (31)	0.05
IOP at recruitment, mmHg	16.7 (4.2)	16.5 (3.6)	0.90
Maximum recorded IOP, mmHg	20.6 (5.8)	20.4 (5.2)	0.88
Vertical cup-to-disc ratio	0.71 (0.12)	0.67 (0.13)	0.01
Visual field mean deviation, dB	-2.72 (3.95)	-2.38 (3.14)	0.65
Number of glaucoma medications	1.0 (1.0)	0.9 (0.9)	0.52
Selective laser trabeculoplasty, eyes (%)	57 (34.1)	43 (25.1)	0.09
Number of treatment naive patients (%)	27 (25.0)	43 (29.9)	0.47

Values displayed are mean (standard deviation) for continuous variables and N (%) for categorical variables. P values represent the statistical significance of the analysis of variance for continuous variables (Kruskal–Wallis test) or Chi-squared test for categorical variables.

IOP: intraocular pressure.

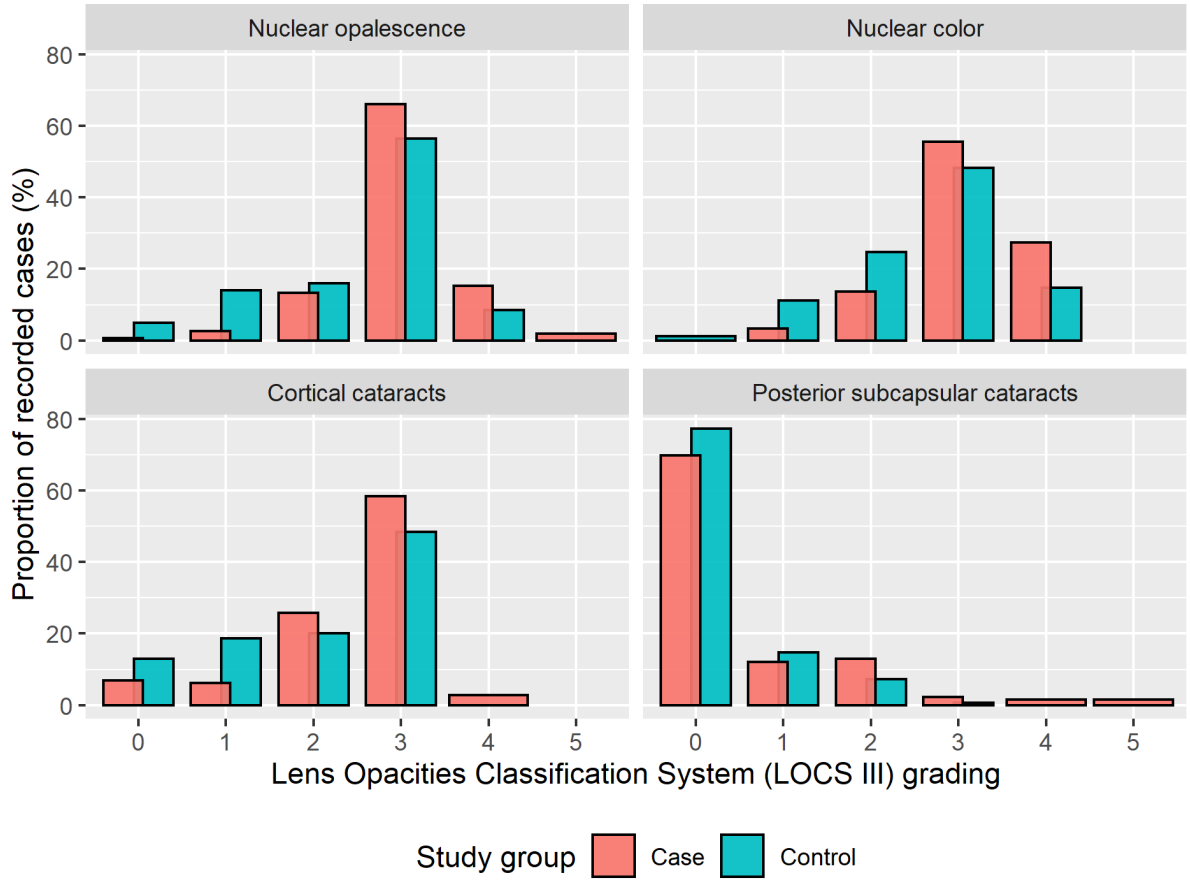

Figure 5.3. Cataract grading using the The Lens Opacities Classification System III of the cases and controls. This data was available for 153 cases and 164 controls.

Using the longitudinal data of all IOP measurements, cataract surgery reduced the mean IOP by 2.22 mmHg (95% CI: 1.93–2.52 mmHg; $P < 2x10^{-16}$). The effect was most pronounced in the first 18 months after cataract surgery then diminished to some extent although remaining below pre-operative mean measurements (Figure 5.4A). The magnitude of reduction differed between eyes, with 59 eyes (34%) achieving at least 3 mmHg reduction within two years of cataract surgery, and 34 eyes (20%) having no, or a positive, change in IOP. A breakdown of the change in IOP per eye within two years of the cataract surgery is summarised in Table 5.4 and Figure 5.5. In individuals who had cataract surgery in both eyes (n = 63), there was a moderate correlation in the magnitude of IOP reduction between the eyes (Pearson's product-moment correlation = 0.52; 95% CI = 0.32– 0.69; $P = 8.7x10^{-6}$). Ongoing glaucoma management was at the discretion of the treating clinicians and was individualised to each patient. Thus, only 5 eyes (3%) stopped at least one glaucoma medication post cataract surgery. Escalation in medical treatment was similar between the cases (29 eyes) and controls (27 eyes; P = 0.9).

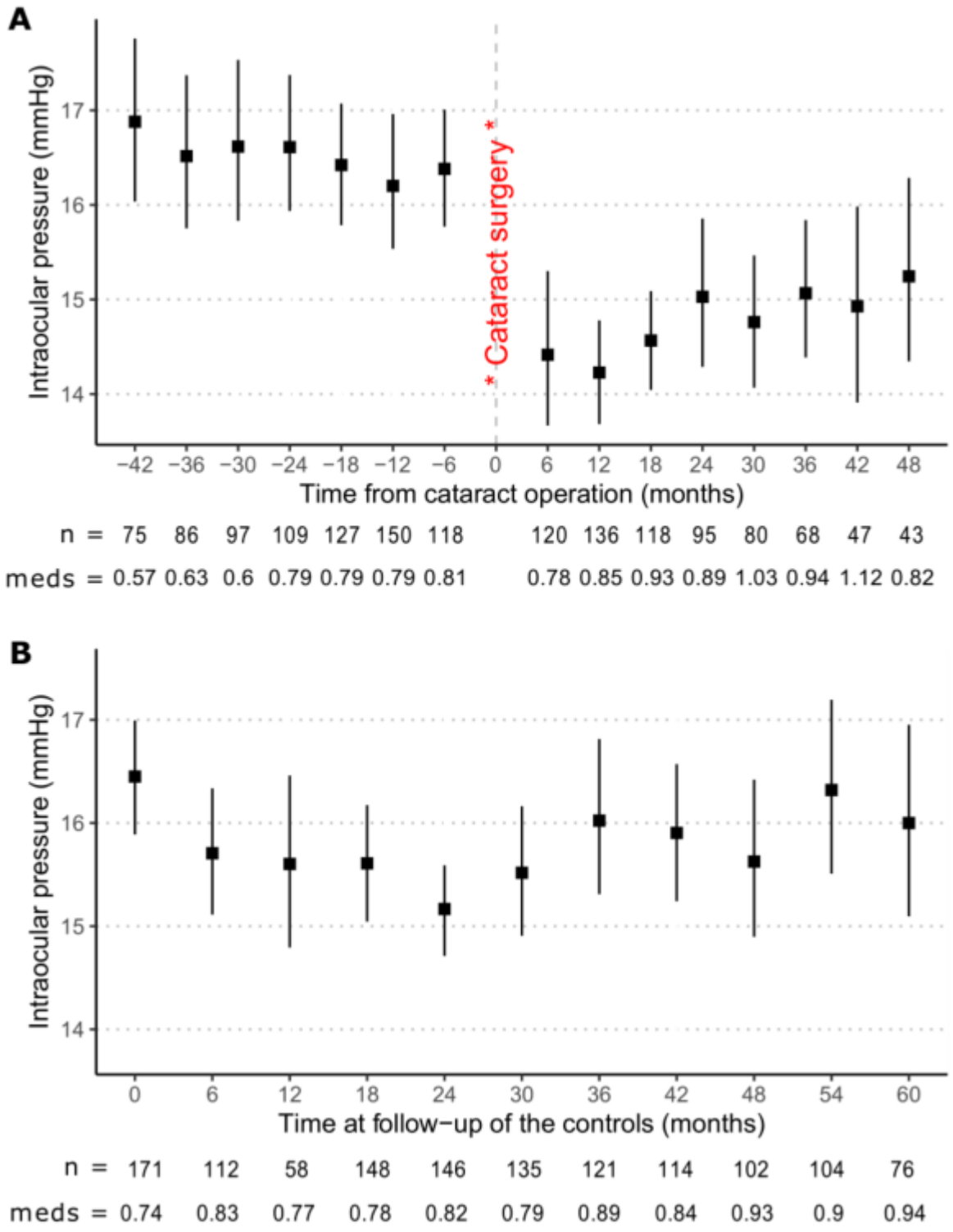

Figure 5.4. Longitudinal change in intraocular pressure (IOP) after cataract surgery **(A)** in the cases n = 171, and **(B)** in the control group n = 171. The square dot represents the mean IOP at each time point, and the error bars represent the 95% confidence interval of the mean. The number of eyes with IOP data recorded and the mean number of topical glaucoma medications at each time point is reported below each figure. For the control group, the median visit used to calculate the 'change in IOP' is individualised for each person (relative to the number of visits for that person) and is not apparent in the plot in panel B.

Table 5.4. Number and percent of eyes with the corresponding two-year mean change in intraocular pressure following cataract surgery

Two-year absolute change in IOP after cataract surgery	Number of eyes	Percent of eyes
At least -6 mmHg	7	4.1%
-6 up to -5 mmHg	11	6.4%
-5 up to -4 mmHg	15	8.8%
-4 up to -3 mmHg	19	11%
-3 up to -2 mmHg	33	19.3%
-2 up to -1 mmHg	23	13.5%
-1 up to 0 mmHg	29	17%
No or positive change	34	19.9%

IOP: intraocular pressure.

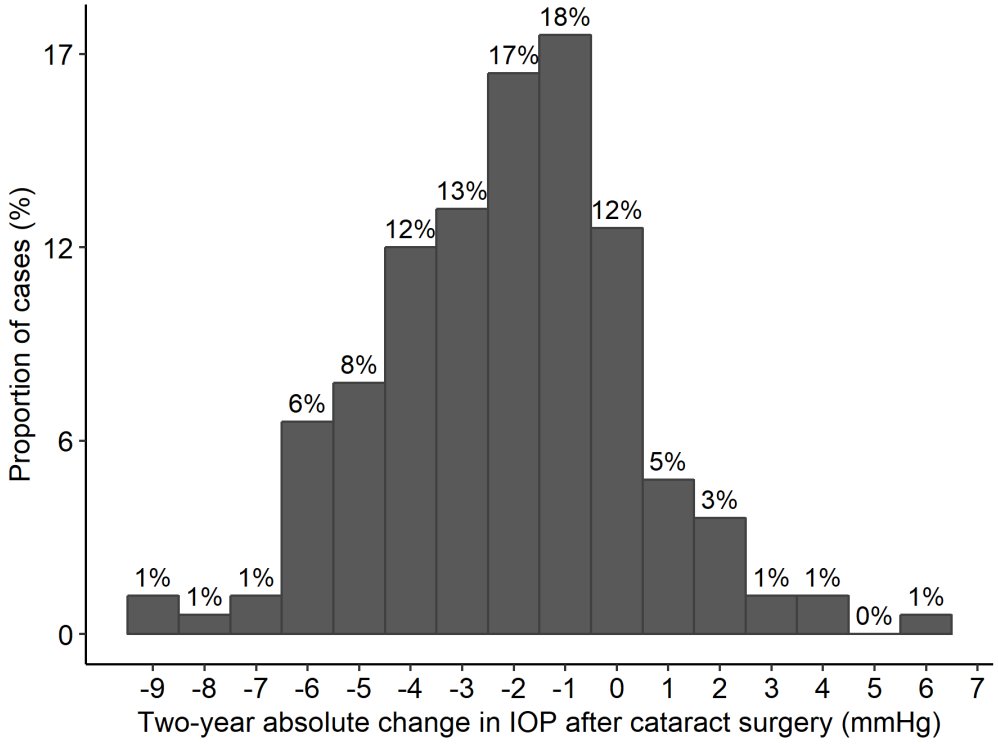

Figure 5.5. Histogram of the absolute change in intraocular pressure (IOP) within 2 years after cataract surgery in the PROGRESSA cohort (N = 171 eyes).

IOP: intraocular pressure.

To further isolate the effect of cataract surgery from the change of IOP over time, a case-control analysis was conducted, comparing the change in IOP in those who underwent cataract surgery (i.e. the group reported above) to matched controls (no cataract surgery; N = 171 eyes) (Figure 5.4B). The controls had similar age, gender, IOP at enrolment, duration of follow-up, and medical treatment compared to the cases (Table 5.3). Compared to the controls, and accounting for the intereye correlation of IOP and the clinic site as a random effect, cataract surgery reduced IOP by 1.75 mmHg (95% CI 1.15–2.33 mmHg; P = $1.6x10^{-8}$) (Figure 5.4).

To identify predictors of the change in IOP for inclusion in a multiple variable model, univariate linear regressions were performed with the following variables: gender, age at operation, maximum recorded IOP prior to the operation, baseline IOP at study enrollment, central corneal thickness, axial length, anterior chamber depth, history of pseudoexfoliation syndrome, and the number of topical glaucoma medications prior to the operation (Table 5.5). Variables with P-values < 0.2 were then used in a multiple variable model. When the maximum recorded IOP was limited to two years prior to cataract surgery, the strength of the association and the goodness-of-fit of the change in IOP improved significantly with 23% of the variance in the postoperative IOP change explained compared to 7% when the all-time maximum IOP was used. Thus the two-year maximum IOP was included in the multiple variable model. Interestingly, preoperative anterior chamber depth and axial length were not associated with the change in IOP postoperatively (Figure 5.6).

Table 5.5. Univariate linear mixed-effects models of the clinical predictors of the intraocular pressure reduction following cataract surgery in PROGRESSA (N = 172 eyes).

Variable used in the univariate model	Estimate	Standard error	P-value	R^2
Gender, male	-0.83	0.44	**0.06**	**2.7%**
Age at operation, years	0.02	0.03	0.55	0.3%
Maximum recorded IOP prior to operation, mmHg	-0.13	0.04	**$1.1x10^{-03}$**	**7.3%**
Maximum IOP in the last 2 years prior to cataract operation, mmHg	-0.28	0.04	**$3.3x10^{-10}$**	**22.5%**
Baseline study IOP, mmHg	-0.05	0.04	**0.18**	**1.3%**
Central corneal thickness, µm	0.00	0.01	0.69	0.1%
Preoperative axial length, mm†	-0.09	0.22	0.68	0.1%
Preoperative anterior chamber depth, mm‡	-0.24	0.65	0.71	0.1%
Pseudoexfoliation syndrome, positive history	-0.42	1.09	0.70	0.1%
Number of glaucoma medications preoperatively	0.84	0.23	**$4.4x10^{-04}$**	**8.4%**

R^2 is the variance explained by the fixed effects only of the generalized linear mixed-effects model (i.e. pseudo-R2) as described by Nakagawa et al. (2017). Estimate refers to the estimated change in IOP per unit increase in the variable, based on the linear regression model. Boldface P-values and R^2 represent variables that are subsequently included in the multivariable model (i.e., P < 0.1 as per the methods).

† Axial length was missing for 5 cases

‡ Anterior chamber depth was missing for 12 cases

IOP: intraocular pressure.

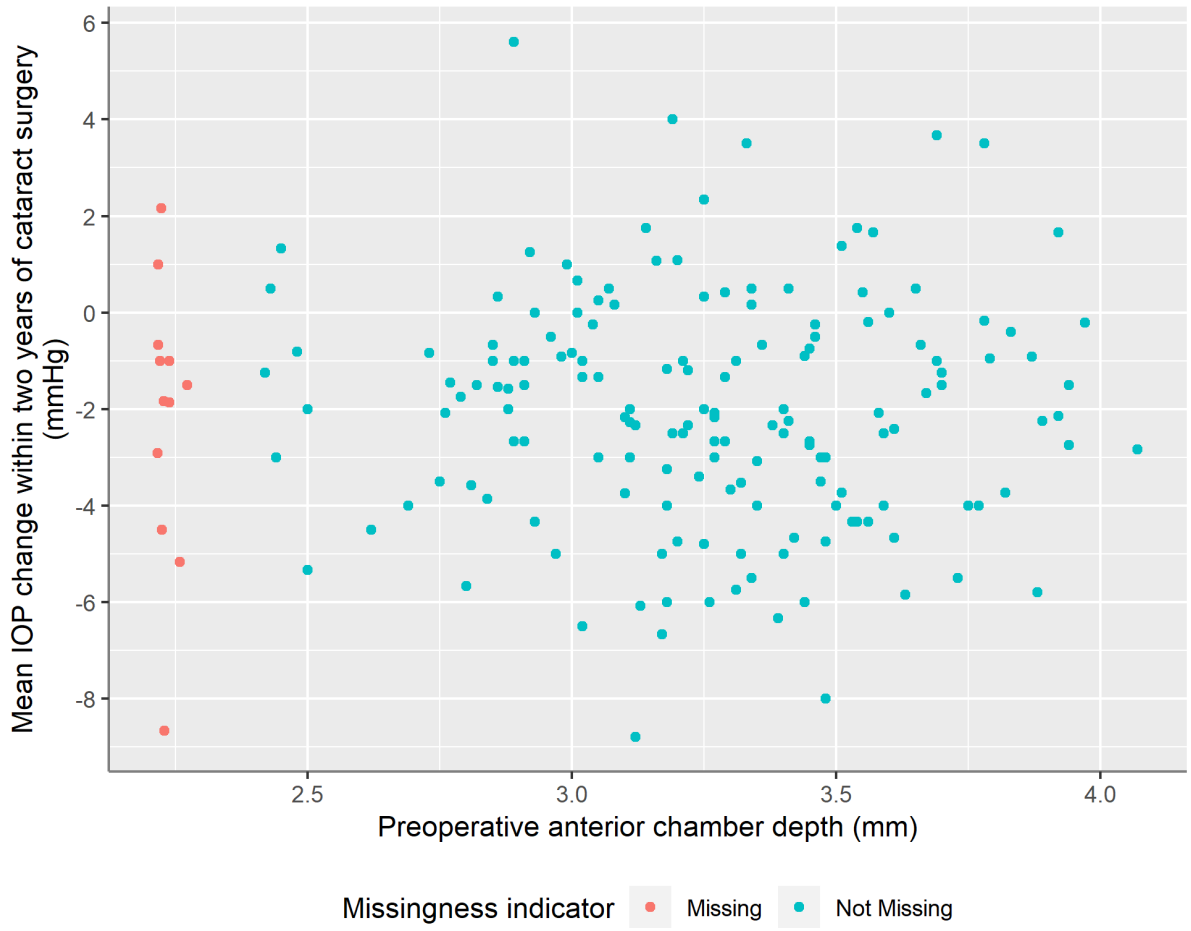

Figure 5.6. Scatter plot of the preoperative anterior chamber depth and observed two-year mean change in intraocular pressure following cataract surgery. Each blue point represents an eye (N = 159). Red points (N = 12) are cases with missing preoperative anterior chamber depth. These are plotted on the left margin of the plot to assess for missingness bias. The missing cases appear to be missing-at-random. A line of best fit is not shown as it was non-significant with a near-zero slope (Table 5.5).

In the multiple variable model, elevated preoperative IOP was strongly predictive of a larger reduction in IOP post cataract surgery (Table 5.6). For each 1 mmHg higher maximum preoperative IOP (in the preceding 2 years), there was an estimated reduction of 0.33 mmHg (95% CI: 0.23–0.42 mmHg) of IOP post cataract surgery ($P = 1.4x10^{-10}$). The number of glaucoma medications preoperatively was inversely associated with the change in IOP. That is, patients who were on more intensive glaucoma medical therapy experienced a lower reduction in IOP than those with fewer topical glaucoma drops (Figure 5.7). Finally, male participants experienced an estimated 1 mmHg (95% CI: 0.30–1.7 mmHg) greater reduction in IOP than females ($P = 7.5x10^{-3}$).

Table 5.6. Multiple variable model of clinical predictors of IOP reduction following cataract surgery.

Variable	Estimated change in postoperative IOP	Standard error	P-value
Number of glaucoma medications preoperatively, mmHg	0.77	0.21	3.0×10^{-4}
Maximum IOP in the last 2 years prior to cataract operation, mmHg	-0.33	0.048	1.4×10^{-10}
Baseline study IOP, mmHg	0.073	0.037	0.05
Gender, male	-1.01	0.37	7.5×10^{-3}

Results are the coefficients of a linear mixed-effects model with the post cataract change in IOP as the response and the variables as fixed predictors. The model random effects were the patients (to account for the intereye correlation) and clinic site. Pseudo-R-squared (fixed effects only) = 35%.
IOP: intraocular pressure.

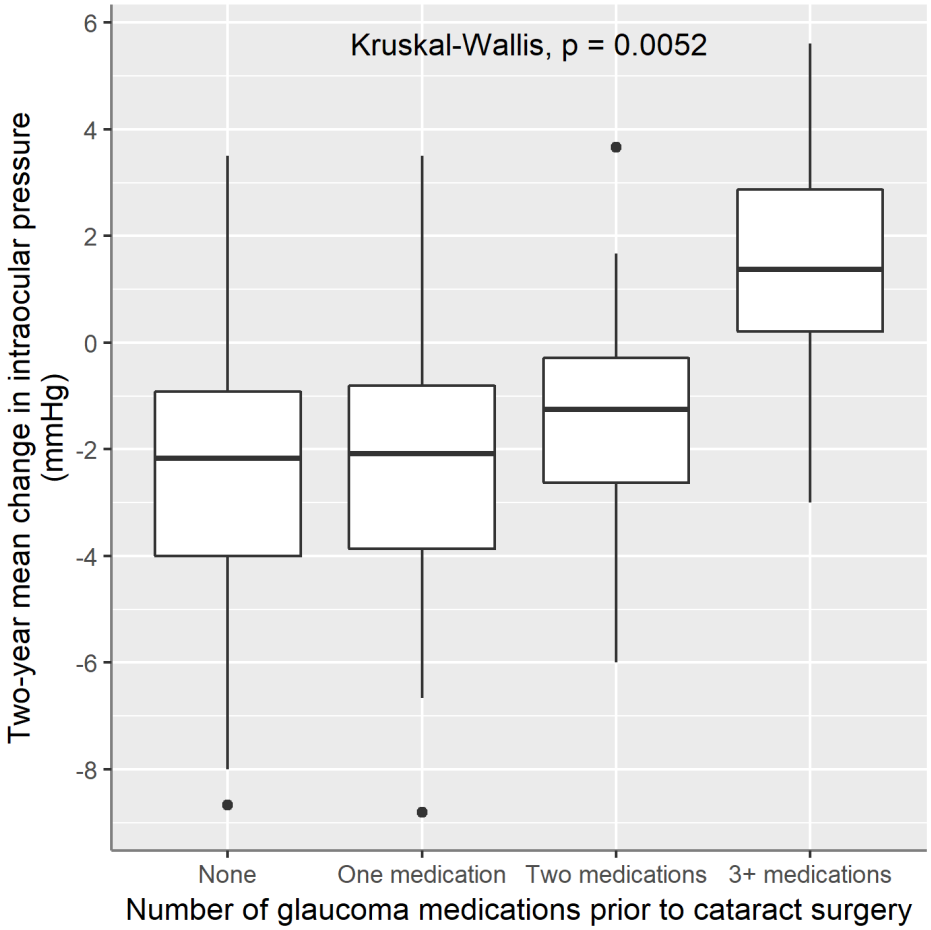

Figure 5.7. Boxplot of the observed two-year mean change in intraocular pressure following cataract surgery based on the number of preoperative glaucoma medications.

The impact of high preoperative IOP on the expected postoperative reduction in pressure was further investigated (Figure 5.8). Eyes with 2-year preoperative maximum IOP of at least 24 mmHg (N = 16) had a mean IOP reduction of 4.03 (SD 3.27) mmHg in the first 2 years, with 13 of the eyes (81%) experiencing at least 3 mmHg reduction. The outlier in the top right of Figure 5.8 was a patient with POAG and a persistently high IOP despite maximal medical therapy (4 medications). The cataract operation was done in anticipation of a trabeculectomy which was done 6 months later (no post-trabeculectomy IOP data was included in the analysis).

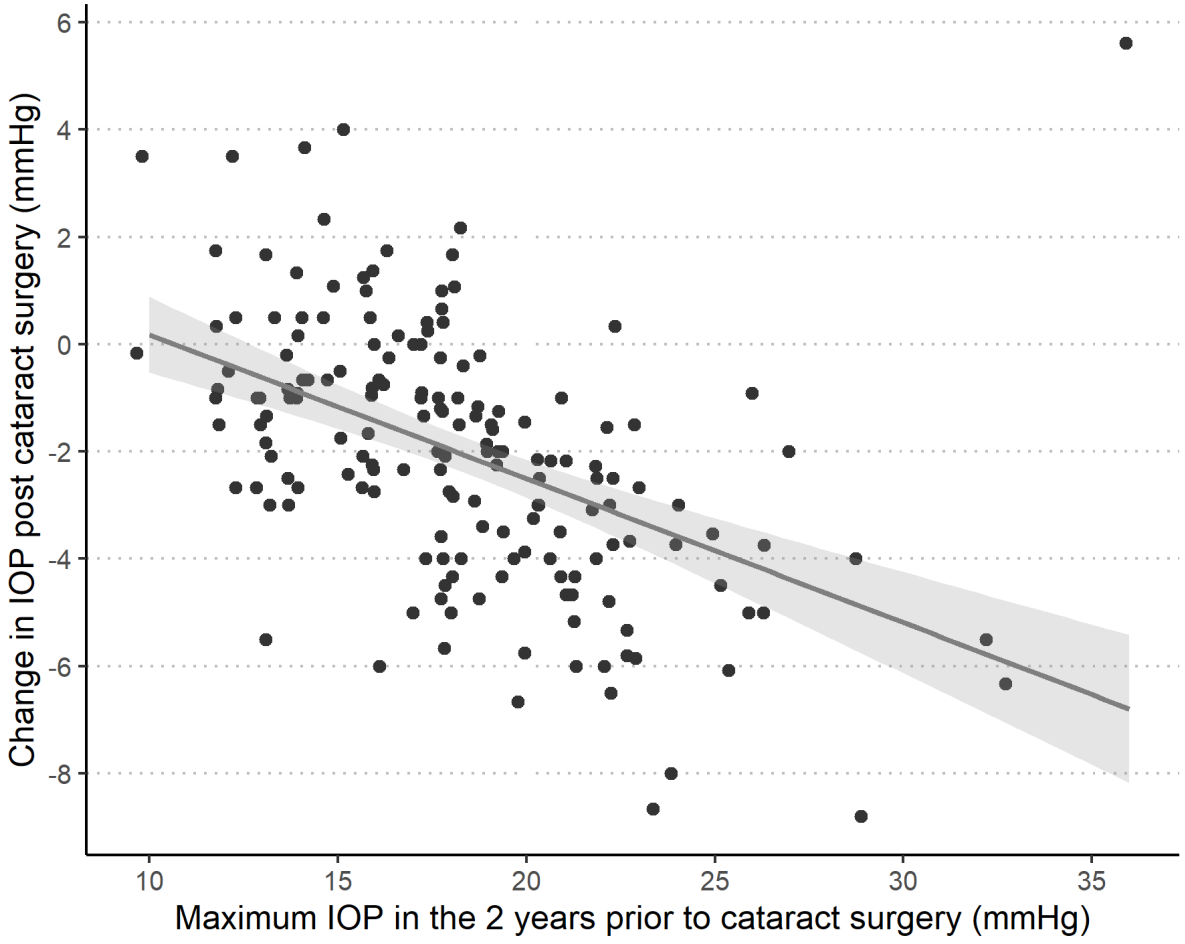

Figure 5.8. Observed difference in the mean intraocular pressure (IOP) within two years post cataract surgery. Each point represents a study eye. The grey line is the line of best fit with the 95% confidence interval shaded in light grey (P-value for trend = 3.3×10^{-10}).

To improve the generalisability of these results, various sensitivity analyses were performed. Topical medications used to treat glaucoma will invariably affect the IOP changes measured during follow-up. To account for this important covariate, a subgroup analysis on medication naive participants was performed — i.e., those who have not been on any topical ocular

hypotensive drops during the study period (N = 43 eyes). In this subgroup, cataract surgery was associated with a mean reduction of IOP of 2.4mmHg (95% CI 1.9–2.9 mmHg; $P < 2x10^{-16}$). Only one eye had prior peripheral iridotomy and had a mean reduction of 3.8 mmHg. Exclusion of this case did not change the results. Eyes with pseudoexfoliation syndrome may experience IOP reduction via a different mechanism than POAG eyes. Seven eyes had pseudoexfoliation syndrome; the mean IOP reduction in this subgroup was 2.7 mmHg (95% CI 1.2–4.1 mmHg; $P = 4.7x10^{-4}$). This change in IOP was not statistically significantly different than the rest of the study cohort (P = 0.6).

Discussion

A relative or absolute reduction in the clinically measured IOP is the cornerstone of glaucoma management (Jost B. Jonas et al. 2017). Effective IOP-lowering can be achieved with either topical medications, laser trabeculoplasty, or surgical interventions (Conlon, Saheb, and Ahmed 2017). In the initial investigation reported in this chapter, the Icare HOME tonometer was effective in closely monitoring IOP post-SLT, showing a reduction in IOP by 63% on the first day and the results remained consistent in 80% of the participants over the duration of the study. IOP fluctuation was also reduced by 24%, which may have an additional neuroprotective role as higher short-term IOP fluctuations have been reportedly associated with glaucoma progression (Asrani et al. 2000; Carlos Gustavo De Moraes et al. 2018; Y. W. Kim et al. 2020; Tojo, Hayashi, and Otsuka 2020).

The association of short-term IOP fluctuation with glaucoma progression was reported in a prospective study by Asrani et al. (2000), who developed a patient-administered home tonometer and studied the diurnal IOP profile of 64 POAG patients. A higher IOP fluctuation, defined as either the standard deviation of all IOP measurements or the absolute range, were predictive of glaucoma progression even after adjustment for clinical covariates over a mean follow-up of 5 years (Asrani et al. 2000). More recently, diurnal IOP-related variation has been more closely studied using a contact lens sensor that measures corneoscleral junction dimensional changes, which correspond to IOP variations (K. Mansouri and Shaarawy 2011; Mottet et al. 2013). For instance, Kim et al. (2020) reported that a cohort of 30 normal tension glaucoma patients had a significantly higher 24-hour contact lens sensor measurement fluctuation than healthy controls. Other contact lens sense parameters were reported by De Moraes et al. (2018) to correlate with a faster rate of visual field progression. Whether the SLT-induced reduction in the short-term IOP fluctuation confers additional advantage in the management of glaucoma is not known and is a subject identified for further study using the PROGRESSA cohort

SLT has been increasingly utilised either in conjunction with, or instead of, topical medical therapies in the management of early glaucoma (Szigiato et al. 2015; Jampel et al. 2014; Campbell et al. 2008). For example, a study on the trends of bilateral laser trabeculoplasty in Canada from 2000 to 2013 found that the rate had dramatically increased from 15.3 per 1000 individuals with open-angle glaucoma to 74.7 in the study time period (Szigiato et al. 2015). Recently, results from the Laser in Glaucoma and ocular HyperTension (LiGHT) study, a randomised controlled trial comparing first-line treatment of POAG or ocular hypertension with SLT versus medication, were reported (Gus Gazzard et al. 2019). This trial has shown that first-line SLT treatment is more cost-effective than eye drops, with a similar mean IOP reduction and health-related quality of life (Gus Gazzard et al. 2019; A. Garg et al. 2019). Additionally, repeat SLT was found to be a safe and effective treatment option, maintaining medication-free IOP control in 67% of the eyes that failed initial SLT therapy, with no adverse events (Anurag Garg et al. 2020). While the global and pointwise rates of visual field progression were similar between the SLT and medication groups, secondary analysis shows that moderate or fast visual field progression was more common in the medically treated eyes compared to the SLT group (risk ratio 1.55) (Wright et al. 2020). These results support the use of SLT as a first-line treatment option in the management of POAG, which can be safely monitored by patient-administered home tonometry particularly in patients residing in remote and rural areas, where it can assess the effect of SLT on lowering IOP without the need for clinic attendance. This is facilitated by patients being able to upload their IOP data to a cloud service provided by Icare by connecting the tonometer to a compatible computer or smartphone.

While cataract surgery is not used solely to reduce IOP in POAG, concomitant cataract and glaucoma is common (although this is becoming increasingly less common in developed countries) (Bernth-Petersen and Bach 1983). In the original investigation reported in this chapter, the effects of cataract surgery on IOP in early POAG patients was demonstrated in a “real world” setting from 8 clinics in Australia. Patients were enrolled in the study for glaucoma monitoring, and the treatment of cataract was based on visually significant cataract symptoms and clinical assessment. This pragmatic approach is consistent with the clinical opinion that cataract grading (e.g. Lens Opacities Classification System) should not influence the decision to operate, as this is based largely on visual symptoms; rather, cataract grading is relevant to operative planning, and remains a valid research tool.

The reduction in IOP after cataract surgery was statistically significant, and although persisted for the duration of follow-up, it was most pronounced in the first 18 months. A third of the cases

had at least 3 mmHg of mean IOP reduction at 2 years. Patients with higher IOP before the operation, and those on fewer glaucoma medications had a larger reduction in IOP. The latter finding suggests that cataract surgery is subject to the so-called 'law of diminishing returns', in producing a lesser yield of IOP-lowering benefit in those already on treatment (Camras, Toris, and Tamesis 1999). This may be explained by medications already increasing aqueous outflow and limiting the added benefit of lensectomy in contributing to this pathway of IOP reduction. Further research can explore this further by examining the interaction with different classes of medications (e.g. prostaglandin analogues reduce IOP primarily via increasing uveoscleral outflow, while beta-blockers reduce aqueous secretion) (T. Li et al. 2016; Goel et al. 2010).

Nonetheless, cataract surgery in this cohort was not intended to modify the glaucoma medical therapy, therefore there were only a few patients who had their glaucoma medications reduced. However, the findings of this study suggest that clinicians could consider reducing the topical medication burden in patients with mild high tension glaucoma or ocular hypertension. In this cohort, eyes with preoperative IOP ≥ 24 mmHg had a mean IOP reduction of 4.03 mmHg with 81% experiencing at least 3 mmHg reduction, results which are comparable to single-agent medical therapy or SLT (D. F. Garway-Heath et al. 2015; A. Garg et al. 2019; T. Li et al. 2016).

These results are consistent with previously published studies on the effect of cataract surgery on IOP in glaucoma (Hayashi et al. 2001; Shingleton et al. 2006; Masis et al. 2018; Melancia, Abegão Pinto, and Marques-Neves 2015). In a study of 55 eyes with POAG, Shingleton et al. (2006) reported a mean reduction of 1.4 ± 3.3 mmHg at the three-year follow-up post cataract surgery, which had persisted at their last follow-up appointment (mean of 5 years). Hayashi et al. (2001) observed a mean reduction of 4.3 ± 4.2 mmHg in 68 eyes with POAG at 1 year post cataract surgery, which has persisted for patients followed up to 2 years. This larger effect size may be attributable to the relatively higher preoperative IOP in this study (mean of 20.7 mmHg) (Hayashi et al. 2001). Other studies have demonstrated a comparable reduction in ocular hypertensives and normal eyes without glaucoma (Mansberger et al. 2012; Pohjalainen et al. 2001). Cataract surgery may therefore be a useful treatment option in the management in early high tension glaucoma patients with comorbid cataracts. Unlike primary angle closure suspects, there is currently no evidence to support cataract surgery as a primary IOP-lowering intervention.

Microinvasive glaucoma surgery (MIGS) has recently been introduced as a treatment option for early glaucoma (Conlon, Saheb, and Ahmed 2017). The currently available devices are

usually inserted during cataract surgery. The effect of combined MIGS and cataract surgery relative to cataract surgery alone has been reported in several studies (Fernández-Barrientos et al. 2010; Craven et al. 2012; Vold et al. 2016; Antonio M. Fea 2010; Antonio Maria Fea et al. 2015; Pfeiffer et al. 2015). Of note, these comparative studies only recruited eyes with high tension glaucoma, where this investigation and previous studies show that cataract removal is most likely to be efficacious as standalone surgery without MIGS. Furthermore, the results of MIGS studies are often reported after medication washout, which whilst valid as a trial tool, is less relevant in a clinical scenario where IOP reduction from the treated IOP is the therapeutic aim (Masis et al. 2018).

For instance, Craven et. al. (2012) reported that cataract surgery alone reduced IOP by 7.5 mmHg at 24 months post procedure. In this high tension POAG cohort, the mean pre-procedure IOP was 25.2 mmHg after medication washout period, thus regression to the mean is expected. This study additionally compared the IOP changes of cataract surgery alone to combined cataract surgery with iStent insertion (Glaukos Corporation, California, United States), a commonly used MIGS device that establishes a direct route to Schlemm's canal, bypassing the trabecular meshwork. At 24 months post-op, the iStent group had only a modestly lower washout IOP than the cataract only group (17.1 ± 2.9 mmHg vs 17.8 ± 3.3 mmHg respectively), which was not statistically significant (Craven et al. 2012). The iStent group, however, required fewer ocular hypotensive medications. Similarly, Pfeiffer et. al. (2015) reported 9.2 mmHg IOP reduction at 12 months post cataract surgery in their high tension POAG cohort (mean baseline IOP of 26.6 mmHg). The effect size has diminished at 24 months to a net IOP reduction of 7.4 mmHg, consistent with the results that the effect of cataract surgery on IOP may reduce in some patients over time (Masis et al. 2018; Pfeiffer et al. 2015). In this study, the IOP reduction effects of cataract surgery alone was compared to a combined operation with Hydrus Microstent (Ivantis, Inc) insertion, a trabecular meshwork bypass device that extends and dilates Schlemm's canal over 3 clock hours (Pfeiffer et al. 2015). At 12 months medication-free follow-up, the Hydrus Microstent group had a modest 0.8 mmHg lower IOP compared to cataract surgery alone group that was statistically significant (16.6 ± 2.8 mmHg vs 17.4 ± 3.7 mmHg respectively) (Pfeiffer et al. 2015). The difference widened however at 24 months to 2.3 mmHg (16.9 ± 3.3 mmHg vs 19.2 ± 4.7 mmHg respectively), which suggests that MIGS may provide additional IOP-lowering effects particularly when the effect of cataract surgery start to diminish (Pfeiffer et al. 2015).

The mechanism of the IOP reduction seen after cataract surgery may partly be related to the anatomical changes due to the crystalline lens removal. Issa et al. (2005) have developed an index for predicting the reduction in IOP post cataract surgery in non-glaucomatous eyes.

Elevated preoperative IOP and shallower anterior chamber depth (ACD) were both predictive of greater IOP reduction post-operatively, consistent with the experience in angle closure eyes (Issa 2005). The ratio of preoperative IOP to preoperative ACD was positively correlated to the magnitude of IOP reduction and there was at least 4 mmHg IOP reduction in those with a ratio higher than 7.0. The role of ACD is likely related to the effect of lens thickness on this parameter (Issa 2005). It should be noted that gonioscopy was not performed on the participants of this study. In the study reported in this chapter (Ayub Qassim, Walland, et al. 2020), all participants had open angles by gonioscopy and there was no correlation found between the ACD or axial length and the change in IOP. This suggests that ACD is not a crucial predictor of IOP reduction post cataract surgery in those with open angles by clinical examination.

Using anterior segment optical coherence tomography in open angle glaucoma patients undergoing cataract operation, Lin et al. (2017) reported the angle-opening distance, iris thickness, iris area and the lens vault (the area between the anterior pole of the phakic lens and the line between the two scleral spurs) were associated with greater IOP reduction post surgery, although other studies have failed to use such parameters to predict IOP lowering after cataract surgery (A. W. Zhou et al. 2010). Lensectomy is also speculated to possibly improve aqueous drainage by providing posterior traction on the ciliary body and scleral spur resulting in widening of the trabecular meshwork and Schlemm's canal (Poley et al. 2009).

In pseudoexfoliation syndrome, reversal of anterior chamber shallowing due to zonular laxity as well as anterior chamber lavage of pseudoexfoliation syndrome material have been postulated as reasons for greater IOP lowering in pseudoexfoliation syndrome cataract patients, and one cannot exclude the possibility that such lavage and simple trabecular meshwork stretching may contribute to the transitory nature of the IOP lowering after routine cataract surgery (Wishart, Spaeth, and Poryzees 1985). Finally, the phacoemulsification ultrasound may improve trabecular meshwork aqueous drainage. DeVience et al. (2017) reported that intraoperative phacoemulsification time was associated with greater IOP reduction in normal eyes. This is supported by an *in-vitro* study of phacoemulsification ultrasound on trabecular meshwork cells activating cellular pathways leading to improved aqueous outflow and lower IOP (N. Wang et al. 2003). This stress-mediated pathway may be similar to the effects of laser trabeculoplasty on the trabecular meshwork (Bradley et al. 2000; N. Wang et al. 2003). Both phacoemulsification ultrasound and SLT induce the the secretion of IL-1 and TNF-α, which are involved in remodelling of the juxtacanalicular extracellular matrix and possibly decreased aqueous outflow resistance (Bradley et al. 2000; N. Wang et al. 2003). If this is the primary pathway by which phacoemulsification cataract surgery leads to a

reduction in IOP, then it is possible that any anticipated IOP reduction by cataract surgery will be diminished in patients who have recently undergone SLT procedure. However, this remains an unanswered question and further research is needed to elicit the interaction between phacoemulsification cataract surgery and laser trabeculoplasty in reducing IOP.

The studies reported in this chapter have several strengths and some limitations. Participants were sampled from the PROGRESSA cohort, with a homogenous enrollment criteria including open angles on gonioscopy, and no secondary causes of vision impairment. Treatment with SLT, or cataract extraction were at the discretion of the treating senior ophthalmologist; this pragmatic design reflects the current clinical practice in the management of early glaucoma patients and improves the generalisability of the reported findings. In the cataract study, the results were obtained from a prospective follow-up of a large sample size from multiple clinics and specialists, with statistical modelling that utilises this longitudinal data and adjusted for several covariates including the clinic site. Nonetheless, given that all of the participants were sampled from PROGRESSA with early open angle glaucoma, the results are not directly applicable to non-glaucomatous eyes or those with secondary open angle or angle-closure types of glaucoma. As treatment was not standardised by a protocol, patients were treated per their glaucoma specialists, which may confound the reported results. The sample size for the cataract study was sufficiently large to perform a sub-analysis to address this, which supported the primary findings. Whether the cataract density and type may have been a contributing factor to the IOP reduction post surgery cannot be excluded, although the reported results were adjusted for ocular variables, and clinic sites. Interestingly, cataract grading in the study cohort regressed to the mean (i.e., the majority of the cases and controls were graded in the mean grade of nuclear color and opalescence of 3), suggesting that the Lens Opacities Classification System may not be an accurately applied clinical grading in this setting. In the study investigating post-SLT diurnal IOP profile, participants were followed-up for a relatively short period of one week. While this early change is likely predictive of longer term outcome (Johnson, Jatz, and Rhee 2006), a longer follow-up and larger sample size may be needed to elucidate the sustained effect of this intervention on IOP reduction, and to evaluate the low incidence of IOP spikes post-SLT. Finally, as discussed in the previous chapter, assessment of short-term IOP fluctuation is confounded by its strong correlation to the mean and maximum IOP recorded in a time period. Thus whether a reduction in IOP fluctuation is clinically relevant requires further research (Konstas et al. 2018). Regardless, the results reported in the SLT study provide supporting evidence for the use of patient-administered home tonometry in monitoring the effect of SLT on IOP.

The results reported in this chapter provide further evidence on the clinical utility of laser trabeculoplasty and cataract surgery in reducing IOP. The clinical application of home tonometry using the Icare HOME was demonstrated in the setting of post SLT IOP monitoring, which will be highly relevant as SLT continues to increase in popularity as a cost-effective first-line treatment option in glaucoma (Gus Gazzard et al. 2019). There was also a consistent but a small magnitude of the IOP reduction post cataract surgery, and it will remain a point of debate as to whether this magnitude of reduction is clinically useful in glaucoma care, particularly if as a deliberate surgical intervention for progressive glaucoma.

Chapter 6: Corneal biomechanics as a risk factor of glaucoma progression

Published manuscripts

The contents of this chapter have been published in a peer-reviewed manuscript in which I am a first author. At the time of writing, the manuscript has been published online (in-press) in *Ophthalmology* (Ayub Qassim, Mullany, et al. 2020). My contributions to this manuscript involved the study concept and design (85%), data collection (100%), data analysis including statistical analysis (100%), data interpretation including the clinical application of the results (85%), drafting the manuscript (85%), and critical revision of the manuscript for important intellectual content (85%). All other authors collectively contributed to data interpretation and critical revision of the manuscript for important intellectual content. Mark Hassall, Owen Siggs and Jamie Craig additionally contributed to supervision.

Introduction

POAG is an optic neuropathy which results in asymptomatic and progressive vision loss if left untreated. POAG, which is the most common type of glaucoma, is characterised by retinal neurodegeneration in the presence of an open iridocorneal angle, with no secondary cause for elevated IOP. POAG is the result of accelerated retinal ganglion cell apoptosis which is mediated by a relatively high IOP (Leske et al. 2007; Robert N. Weinreb, Aung, and Medeiros 2014). Despite the importance of IOP elevation in its pathophysiology, POAG can also manifest and progress in individuals with IOP measurements consistently within the 'normal' range.

IOP causes mechanical stress (applied force) and strain (deformation) at the optic nerve head, where the retinal ganglion cell axons leave the orbit, making a 90° turn and traversing the sclera via the lamina cribrosa. In turn, this applied force and deformation is thought to interrupt orthograde axonal transport, ultimately leading to cellular injury and apoptosis (Burgoyne et al. 2005; Chidlow, Wood, and Casson 2017; Harry A. Quigley 1981). The biomechanical responses of the optic nerve head to IOP-mediated stress and strain have been hypothesised to play an important role in the pathogenesis of POAG (Boote et al. 2020). Computational models predict that scleral stiffness is the most important determinant of the biomechanical stress at the optic nerve head, being the main load-bearing tissue in the eye (Boote et al. 2020; Sigal, Flanagan, and Ross Ethier 2005). Stiffer sclerae which have been reported in glaucomatous eyes, have been shown in animal models to be associated with optic nerve head deformation and neuroretinal rim shear (Boote et al. 2020; Coudrillier et al. 2012; Jin et al. 2018; H. A. Quigley, Brown, and Dorman-Pease 1991).

CCT is a corneal clinical parameter that has been long recognised to be integral to glaucoma management, as it confounds IOP measurements obtained using traditional applanation and rebound tonometry techniques (J. Liu and Roberts 2005; Copt, Thomas, and Mermoud 1999). More recently, *in vivo* studies have implicated various biomechanical properties of the cornea as important risk factors in POAG (B. N. Susanna, Ogata, Daga, et al. 2019; C. N. Susanna et al. 2018; Vinciguerra et al. 2020; Miki et al. 2019). In addition to confounding IOP measurement accuracy (B. N. Susanna, Ogata, Jammal, et al. 2019), biomechanical properties measured at the cornea have been hypothesised to reflect the biomechanical properties of the posterior part of the eye that are in structural continuum with the corneal and scleral tissue, such as the peripapillary sclera and the lamina cribrosa. The notion that corneal biomechanics may be inextricable from whole-eye biomechanics was demonstrated by Nguyen et al. who observed *ex vivo* that radial tension applied to sclera resulted in dynamic

changes in corneal biomechanical response to corneal air-puff deformation (B. A. Nguyen et al. 2020).

Using newer clinical tools such as the Corvis ST (Oculus Optikgeräte GmbH, Wetzlar, Germany), many biomechanical parameters can be measured at the cornea. Various indices representing viscoelastic features such as stiffness (the force required to deform an object) can be extrapolated from high speed photo series mapping corneal deformation responses to the application of a calibrated air puff (Roberts et al. 2017). To date, most studies using such tools to investigate corneal biomechanics in glaucoma have assessed corneal hysteresis (the net energy loss occurring in an object through a deformation) measured by the Ocular Response Analyser (Reichert Instruments, USA), which does not correlate directly to corneal stiffness (Dupps 2007). To the best of our knowledge, no studies have investigated corneal stiffness as a potential risk factor for the development or progression of POAG.

In this study, we investigated the association between baseline corneal stiffness parameters measured using the Corvis ST and clinical features of disease progression in a cohort of POAG suspects. We hypothesised that higher corneal stiffness parameters would be associated with a greater risk of glaucoma progression.

Methods

Study participants

This study was an evaluation of participants defined as 'glaucoma suspects' at enrolment into the PROGRESSA study. PROGRESSA is a longitudinal, multi-centre Australian study monitoring glaucoma progression (Chapter 2). The current study sampled participants from a single centre in South Australia who were under the care of one of two glaucoma specialists. Enrolment into PROGRESSA stipulated that participants demonstrate open angles on gonioscopy, no secondary causes of elevated IOP, and the absence of other vision-affecting ophthalmic conditions, including any corneal diseases.

A 'glaucoma suspect' was defined by the presence of an optic nerve head which appeared suspicious for glaucoma (i.e., disc damage likelihood scale score of 1 or greater) (Bayer et al. 2002), and a normal visual field test. IOP was not used in the definition of a glaucoma suspect. Baseline assessment of the optic disc was performed by the treating glaucoma specialist on a dilated pupil, and visual field testing was undertaken using Humphrey Visual Field (HVF) 24-2 SITA Standard perimetry assessment (Humphrey Field Analyzer; Carl Zeiss Meditec; Dublin, CA). OCT was available to the treating glaucoma specialist but was not directly used

as part of the recruitment criteria. A normal visual field was defined by a normal pattern standard deviation (i.e., >5%) and a normal glaucoma hemifield test on a reliable visual field. Visual field reliability was defined by fixation losses and false positive rates of less than 33%, and only reliable visual fields were assessed.

This study adhered to the tenets of the Declaration of Helsinki, and followed the National Health and Medical Research Council statement of ethical conduct in research involving humans. Informed written consent was obtained from all participants, and the study was approved by the Southern Adelaide Clinical Human Research Ethics Committee.

Baseline corneal biomechanics assessment

Baseline corneal biomechanical assessments were performed using Corvis ST before clinical examination (i.e., prior to the installation of any eye drops, applanation, or pupil dilation). The air puff generated by the Corvis ST is not expected to impact ocular biometry or IOP. This device captures high-speed serial images of a corneal deformation response to a calibrated air puff using a Scheimpflug camera (Hong et al. 2013). Approximately 140 images at the horizontal meridian of the cornea are captured and used by the software for analysis (Corvis ST software, Oculus, database version 6.08r22, scan review version 1.3r1727). Only measurements passing the software quality assessment (i.e., recorded as a quality score "OK") were used.

The Corvis ST air puff results in corneal deformation which can be evaluated at key stages relative to the baseline corneal position (Figure 6.1): the inward applanation as the cornea flattens when transitioning from the default convex to concave shape (A1); and the point of the highest concavity where the cornea is at highest deformity (HC). The whole eye movement is also measured and accounted for when measuring the corneal deflection amplitudes, allowing for isolation of the corneal component of the deformation response (Aoki et al. 2018).

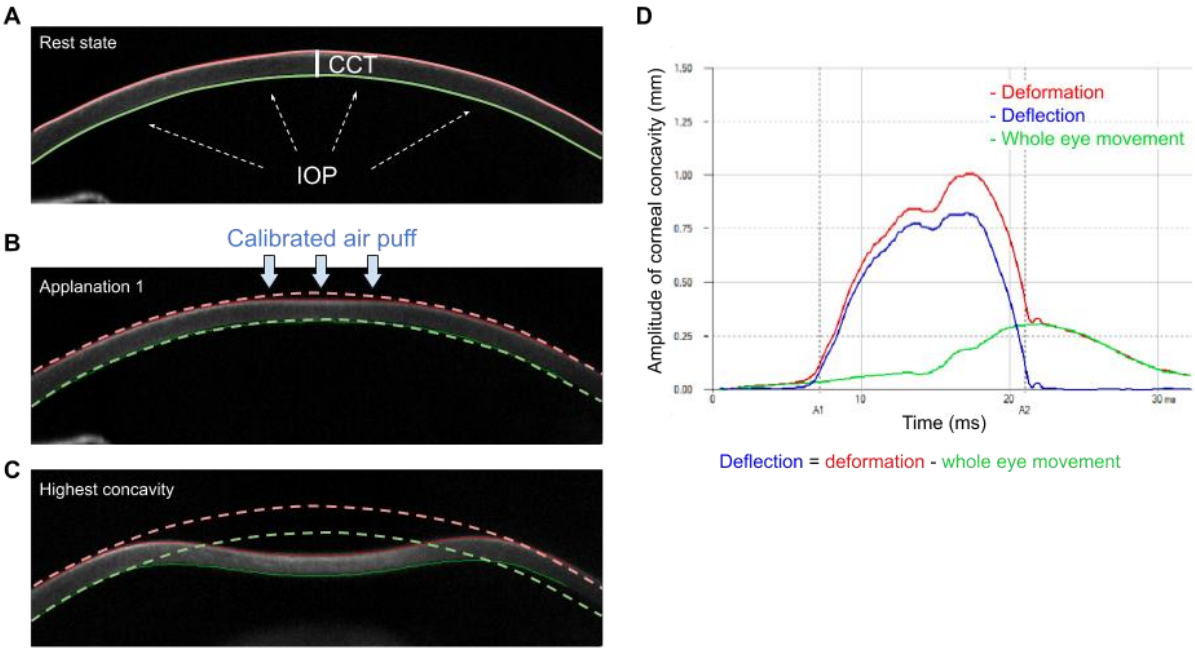

Figure 6.1. Corneal deformation response to a calibrated air puff recorded by the Corvis ST. Relative to its rest state **(A)**, the cornea deforms inwards to initial applanation **(B)** until the point of highest concavity **(C)** before returning back to its rest state. The corneal deformation amplitude consists of the inwards corneal deflection, plus the whole eye movement **(D)**. The reported stiffness parameters (SP-A1 and SP-HC) represent the applied force to the cornea (the difference between the applied air pressure from the tonometer and intraocular pressure) divided by the corneal deflection amplitude in reference to first applanation and highest concavity, and represented as mmHg/mm. The dashed curves in panels B and C refer to the corneal position at rest.
IOP: intraocular pressure; CCT: central corneal thickness.

The Corvis ST analysis software measures numerous inter-correlated parameters which pose analytical challenges due to multicollinearity and multiple testing (Vinciguerra et al. 2016). We have chosen to investigate the stiffness parameters as they are the only parameters experimentally derived to measure the mechanical stiffness of the cornea in response to a calibrated air puff, while accounting for the whole eye movement and intraocular pressure (Roberts et al. 2017; Aoki et al. 2018). Furthermore, these stiffness parameters correlate well with several corneal biomechanical properties measured by the Corvis ST (Roberts et al. 2017), and the corneal resistance factor measured by the Ocular Response Analyser (Fujishiro et al. 2020). Stiffness is defined by the extent to which a material resists deformation in response to an applied force. Thus, a cornea with greater stiffness will deform less in response to an air puff. The formulae and experimental design by which these stiffness parameters were calculated have been detailed previously (Roberts et al. 2017). Briefly, the applied force on the cornea is the pressure of the air puff generated by the Corvis ST minus the biomechanically corrected IOP (bIOP). Corneal deflection is measured in millimeters at A1

and HC relative to its rest state, accounting for the whole eye movement (Figure 6.1). bIOP is algorithmically calculated based on a finite element modeling to be less affected by corneal parameters (Joda et al. 2016). In an *ex-vivo* study, bIOP was reported to correlate well with the 'true' IOP that was experimentally applied via a syringe pump to the globe and recorded by a pressure transducer (Eliasy et al. 2018). Baseline optical CCT measurements were also performed by the Corvis ST, which have been shown to be repeatable and accurate compared to ultrasound pachymetry (Reznicek et al. 2013). Corvis ST CCT is measured by a software evaluation of the CCT derived using anatomical corneal boundaries determined from a cross-sectional image acquired at the rest state (Figure 6.1A). Stiffness parameter at first applanation (SP-A1) was exported from the Corvis ST analysis software, and was not provided to the treating clinicians at clinical appointment. Stiffness parameter at highest concavity (SP-HC) is not directly measured by the software, but we sought to investigate it as it has been reported in the literature recently.(Vinciguerra et al. 2020) We derived SP-HC using other exported parameters: SP-A1, maximum deflection amplitude and deflection amplitude at first applanation (Roberts et al. 2017).

$$Stiffness\ parameter\ (mmHg/mm) = \frac{Applied\ force\ to\ the\ cornea}{Corneal\ displacement} = \frac{Adjusted\ air\ pressure\ valve - biomechanical\ corrected\ IOP}{Corneal\ deflection\ amplitude\ at\ a\ set\ point}$$

Longitudinal follow-up

Participants were followed-up every 6 months with clinical examination, OCT, and HVF. The first visit with a Corvis ST measurement was considered the baseline visit. Clinical examination included visual acuity, optic nerve head examination and IOP as measured by Goldmann applanation tonometry (GAT). Baseline refraction, as spherical equivalent, was obtained using an autorefractor and a measurement prior to cataract surgery was recorded, if applicable. Treatment at each visit was at the discretion of the treating glaucoma specialist. HVF assessment at each visit was done using 24-2 SITA Standard protocol. Spectral domain OCT was acquired by a CIRRUS SD-OCT device (Software Version 9.5; Carl Zeiss, Meditec; Dublin, CA). Average and quadrant peripapillary RNFL thickness were downloaded for each optic disc cube scan. We additionally acquired macular GCIPL thickness for the superior and inferior sections of the macular cube scans. Scans with a quality score <6 were excluded as per the manufacturer's recommendation. Additionally, scans with segmentation errors and artefacts affecting thickness measurements were excluded.

Structural progression for each eye was assessed by the annual rate of change of the OCT RNFL thickness for the superior and inferior quadrants (Figure 6.2A). A prospective rate of

thickness change was calculated using linear regression, with the baseline set at the date of Corvis ST scan. We therefore excluded scans acquired prior to Corvis ST data acquisition. A minimum of 4 scans over 2 years was used as the cut-off to generate reliable rates. As early glaucoma changes are typically asymmetrical, we selected the rate of the faster progressing quadrant for analyses. Positive rates of RNFL change, which were considered to represent non-pathological inter-examination variation, were set to 0. A similar approach was used to generate the average macular GCIPL rates of thinning as a secondary structural outcome (Figure 6.2B). For clarity and ease of interpretation, we report the rate of RNFL or GCIPL thinning as a positive value; for example, a rate of thinning of 1 µm per year is equivalent to a rate of thickness change of -1 µm/year.

Functional progression for each eye was assessed by the permutation analyses of pointwise linear regression (PoPLR) method implemented in the R package *visualFields* (version 0.6) (Marin-Franch and Swanson 2013; O'Leary, Chauhan, and Artes 2012). A minimum of 4 reliable HVF exams were required, with reliability defined by a fixation loss and a false positive rate less than 33%. False negatives were not used for exclusion (B. Bengtsson and Heijl 2000). PoPLR has been validated as a sensitive and accurate method to detect glaucomatous visual field progression at a relatively earlier timeframe than other methods (O'Leary, Chauhan, and Artes 2012; Rabiolo et al. 2019; Saeedi et al. 2019). Briefly, pointwise linear regression of the total deviation (i.e. adjusted for age-related threshold sensitivity changes) is calculated for each visual field location, then the overall statistical significance of the change is calculated. The observed chronological order of HVF changes is compared to 5,000 permutations of the fields, allowing an assessment of progression that is individualised to the patient's data (Figure 6.2C). A PoPLR P-value < 0.05 was considered a significant progression. To improve specificity, we defined functional progression as two consecutive visits with a significant PoPLR.

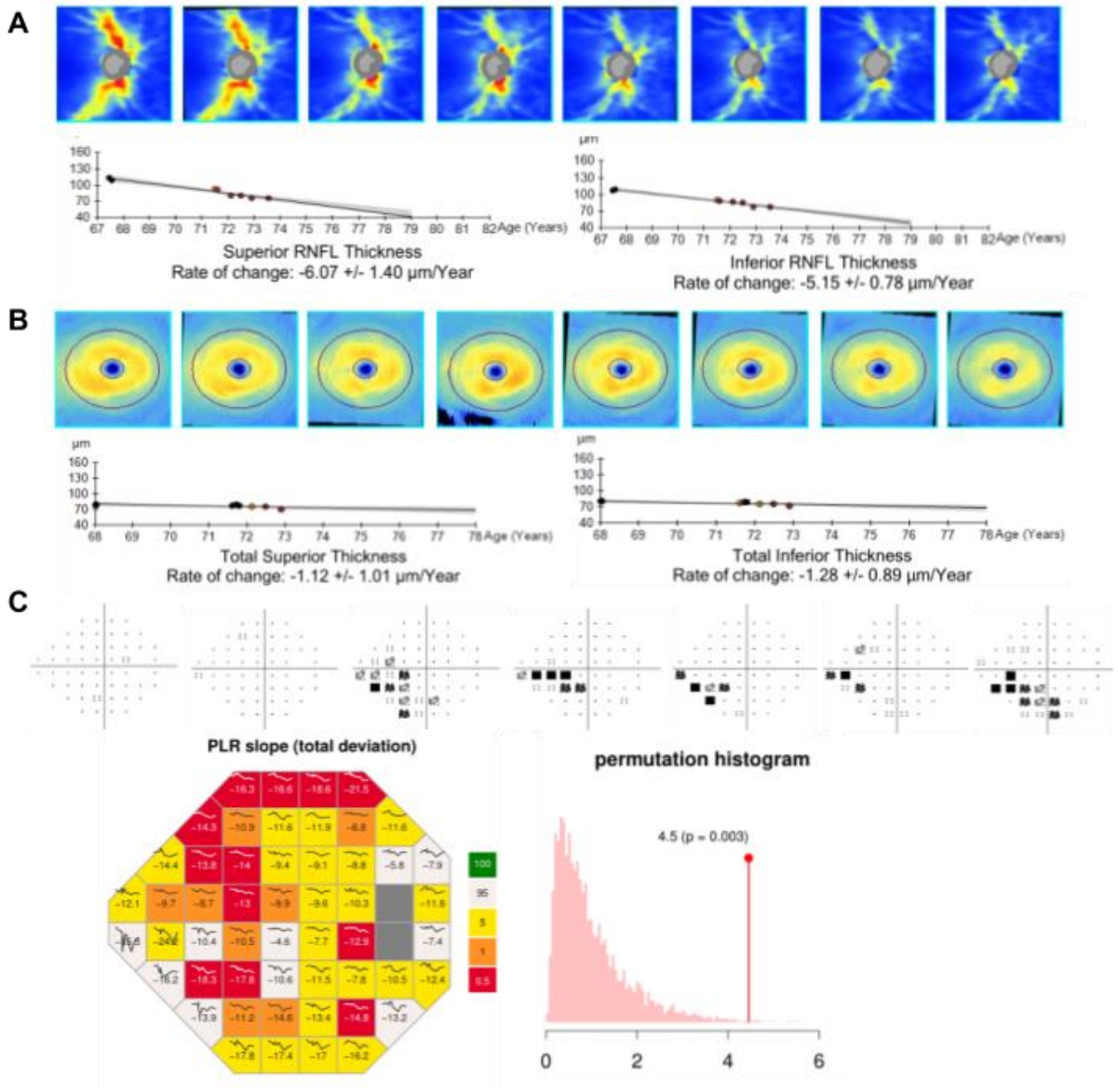

Figure 6.2. Study progression outcomes. Structural progression is measured by the rate of OCT peripapillary RNFL **(A)** and macular GCIPL **(B)** thinning. Functional progression is measured by PoPLR method **(C)**, where the pointwise linear regression (bottom left) of the observed visual fields (top) is compared to 5,000 permutations of the visual field examinations (bottom right). Progression occurs when the observed visual field sequence is significantly different to the permutations (P<0.05) in two consecutive visits.

OCT: optical coherence tomography; RNFL: retinal nerve fibre layer; GCIPL: ganglion cell inner plexiform layer; PoPLR: permutation analyses of pointwise linear regression; PLR: pointwise linear regression.

Statistical analysis

Statistical analyses were performed in R (version 4.0.2, RCore Team, Austria). Both eyes, if applicable as glaucoma suspects, were included in the study. Exploratory correlation analysis

was first performed using Pearson's product moment correlation. Statistical inference was performed using mixed effects linear regression modeling with a random-intercept per patient to account for inter-eye correlation (Q. Fan, Teo, and Saw 2011). Models were fitted using the *lme4* package (version 1.1.21) (Bates et al. 2015), and hypothesis testing of the model was performed using Satterthwaite's degrees of freedom method (*lmerTest* package, version 3.1.2). In addition to stiffness parameters, we included *a priori* variables that may be associated with glaucoma progression, and used stepwise backward elimination to select the most statistically relevant variables in the model (Heinze, Wallisch, and Dunkler 2018). Visual field progression was assessed using a survival model. Mixed-effect Cox proportional hazard regression model was used for visual field progression outcome accounting for inter-eye correlation (using *coxme* package, version 2.2.16) (T. M. Therneau, Grambsch, and Shane Pankratz 2003). Standardised coefficients (i.e., per 1 standard deviation increase in a variable) were reported for stiffness parameters and CCT for ease of variable comparison and model interpretation. The cut-off for statistical significance (alpha level) was set at P=0.05.

Results

Baseline Data

Our cohort included 371 eyes from 228 patients who met the inclusion criteria as glaucoma suspects with a baseline Corvis ST examination. The mean age of the participants was 62.4 years (SD 11.4), and 95 participants (42%) were male. The majority (92%) of our cohort were of Caucasian ethnicity. Detailed characteristics of the cohort are summarised in Table 6.1. We validated the Corvis ST CCT measurements through comparison with CCT values obtained using ultrasound pachymetry (Pachmate DGH55; DGH Technology Inc, Exton, PA). There was no statistically significant difference in CCT values obtained between the two modalities (mean difference of 1.3 µm; 95% CI = -4.0 to 6.6; P = 0.64). We proceeded to use Corvis ST CCT measurements in our analyses.

Table 6.1. Baseline cohort characteristics

Characteristic	Summary statistics
Number of eyes (patients)	371 (228)
Gender, male (n, %)	95 (42%)
Age, years	62.4 (11.4)
Central corneal thickness, µm	550 (37)
Vertical cup-to-disc ratio	0.62 (0.13)
Intraocular pressure (Goldmann Applanation Tonometry)	15.7 (3.2)
Intraocular pressure (Corvis ST, unadjusted)	15.8 (2.3)
Biomechanically corrected intraocular pressure	14.3 (2.7)
Spherical equivalent	-0.1 (2.4)
Average baseline OCT RNFL thickness, µm	84.4 (9.8)
Number of eyes that had cataract surgery (n, %)	42 (11%)
Number of eyes on topical glaucoma medications (n, %)	85 (23%)

Values are mean (standard deviation) unless otherwise stated.

OCT: optical coherence tomography; RNFL: retinal nerve fibre layer

Corvis stiffness parameters

The mean SP-A1 was 112 mmHg/mm (SD 19) and mean SP-HC was 15.4 mmHg/mm (SD 4.9). There was a significant positive correlation between both stiffness parameters and the IOP (as measured by GAT or Corvis ST), with a stronger correlation for SP-HC than SP-A1 (Table 6.2): that is, eyes with a higher IOP also had higher stiffness parameters, as might be expected due to the increased resistance to inward corneal deformation by the air puff (Figure 6.3A). Furthermore, some correlation is expected as IOP is part of the formula used in calculating the stiffness parameters (Roberts et al. 2017). Similarly, both stiffness parameters were positively correlated with higher CCT, consistent with thicker corneas having greater resistance to deformation than thinner corneas (Figure 6.3B). Age and refractive error were not correlated with either stiffness parameter (Table 6.2), nor was there a correlation between prior cataract surgery and either stiffness parameter. Additionally, there was no association between either of the baseline stiffness parameters (SP-A1 or SP-HC) and the baseline average peripapillary RNFL thickness, or the average GCIPL thickness (linear mixed effect P-values > 0.05). As expected, the two stiffness parameters were highly correlated with each other (Pearson's correlation coefficient 0.85; P <0.001).

Table 6.2. Pearson's correlation between stiffness parameters and some key characteristics

Measurement	SP-A1		SP-HC	
	Correlation coefficient	P-value	Correlation coefficient	P-value
bIOP	0.47	<0.001	0.66	**<0.001**
IOP (GAT)	0.49	<0.001	0.56	**<0.001**
CCT	0.61	<0.001	0.56	**<0.001**
Spherical equivalent	0	0.90	0.066	0.23
Age	0.016	0.76	-0.060	0.25

Correlation analyses were done using Pearson's method. SP-A1: stiffness parameter at first application; SP-HC: stiffness parameter at highest concavity; bIOP: biomechanically corrected intraocular pressure; CCT: central corneal thickness;; GAT: Goldmann Applanation Tonometry

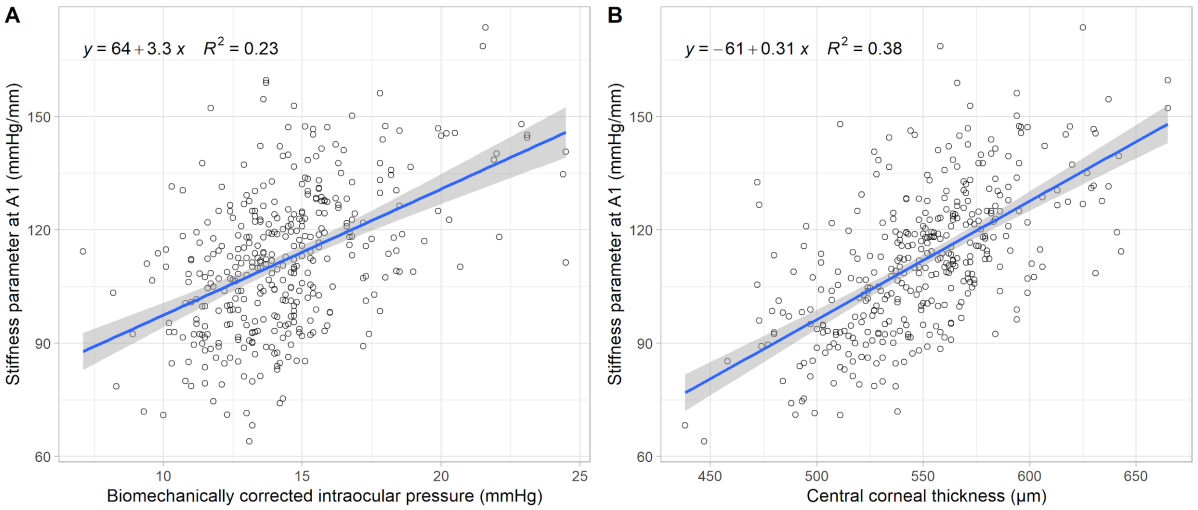

Figure 6.3. A higher corneal stiffness parameter (measured at A1; SP-A1) is found in eyes with a higher intraocular pressure **(A)** or central corneal thickness **(B)**. The blue line represents the linear line of best fit (equation shown above), and the grey shade represents the 95% confidence interval of the linear model. The R-squared value of the linear model is shown in each panel.

Structural progression

The mean OCT follow-up time was 4.2 years (SD 0.8) since the baseline Corvis ST examination. The mean rate of RNFL thinning in the fastest-progressing quadrant was 1.27 µm per year (SD 1.4). We proceeded to include baseline Corvis ST SP-A1, CCT, age, gender, history of cataract surgery, and spherical equivalent as predicting variables for the rate of RNFL thinning, and used stepwise backward elimination method to select the most optimum

method. We could not include IOP as a covariate as it was internally adjusted for in the stiffness parameters formulae, thus a statistical adjustment would not be valid (Anthony P. Khawaja, Crabb, and Jansonius 2013). The final model included SP-A1, CCT and age as the predicting variables.

Both baseline stiffness parameters were significantly associated with a faster rate of RNFL thinning after adjustment for CCT and age, which were also significant predictors (Table 6.3). The results indicate that higher stiffness parameters and a thinner CCT are predictors of a faster rate of RNFL thinning, adjusting for age. In univariate analyses, neither baseline IOP measured by GAT, nor Corvis ST (bIOP) were significantly associated with RNFL thinning (β = 0.042 and 0.057 µm/year change inRNFL per 1 mmHg respectively; P = 0.090 and 0.050 respectively).

Table 6.3. Predictors of the rate of OCT RNFL thinning using mixed-effect multivariable regression models with either stiffness parameters while adjusting CCT and age.

Variable (standardised)	Estimated change in RNFL rate of thinning (µm/year)	Standard error	P-value
Model 1 (for stiffness parameter at first applanation)			
SP-A1 per 19 mmHg/mm	0.34	0.09	<0.001
CCT per 37 µm	-0.25	0.10	0.004
Age per 10 years	0.19	0.07	0.012
Model 2 (for stiffness parameter at highest concavity)			
SP-HC per 4.9 mmHg/mm	0.27	0.09	0.003
CCT per 37 µm	-0.22	0.10	0.022
Age per 10 years	0.21	0.01	0.005

Standardised coefficients (per 1 standard deviation change in variables) are reported for SP-A1 and CCT for ease of interpretation.

SP-A1: stiffness parameter at first application; SP-HC: stiffness parameter at highest concavity; CCT: central corneal thickness.

We explored the apparent synergistic effects of stiffness parameters and CCT further. Using univariate models, higher SP-A1 was associated with a faster rate of RNFL thinning (β = 0.20; P = 0.011), while SP-HC and CCT were not (β = 0.15 and -0.08; P = 0.065 and 0.30 respectively). To visualise this relationship, we grouped the cohort in relation to their mean CCT and SP-A1 measurements (Figure 6.4). Eyes with a thinner CCT (lower than the cohort mean of 550 µm) and a higher SP-A1 (higher than the cohort mean of 112 mmHg/mm) had a faster rate of RNFL thinning by 0.72 µm per year relative to the group with thicker CCT and

lower SP-A1 (95% CI 0.17–1.28 µm/year; P = 0.011). We additionally used the rate of loss in the average circumpapillary RNFL as the outcome measure with findings consistent with our primary results (Table 6.4). We then defined eyes as fast RNFL progressors if the rate of RNFL thinning was faster than 1 µm/year, which is significantly faster than the age-related RNFL thinning (Chauhan et al. 2020). Eyes with thinner CCT and a higher SP-A1 were at 2.9-fold higher likelihood of being fast RNFL progressors relative to the rest (odds ratio 95% CI 1.4–6.1; P = 0.006).

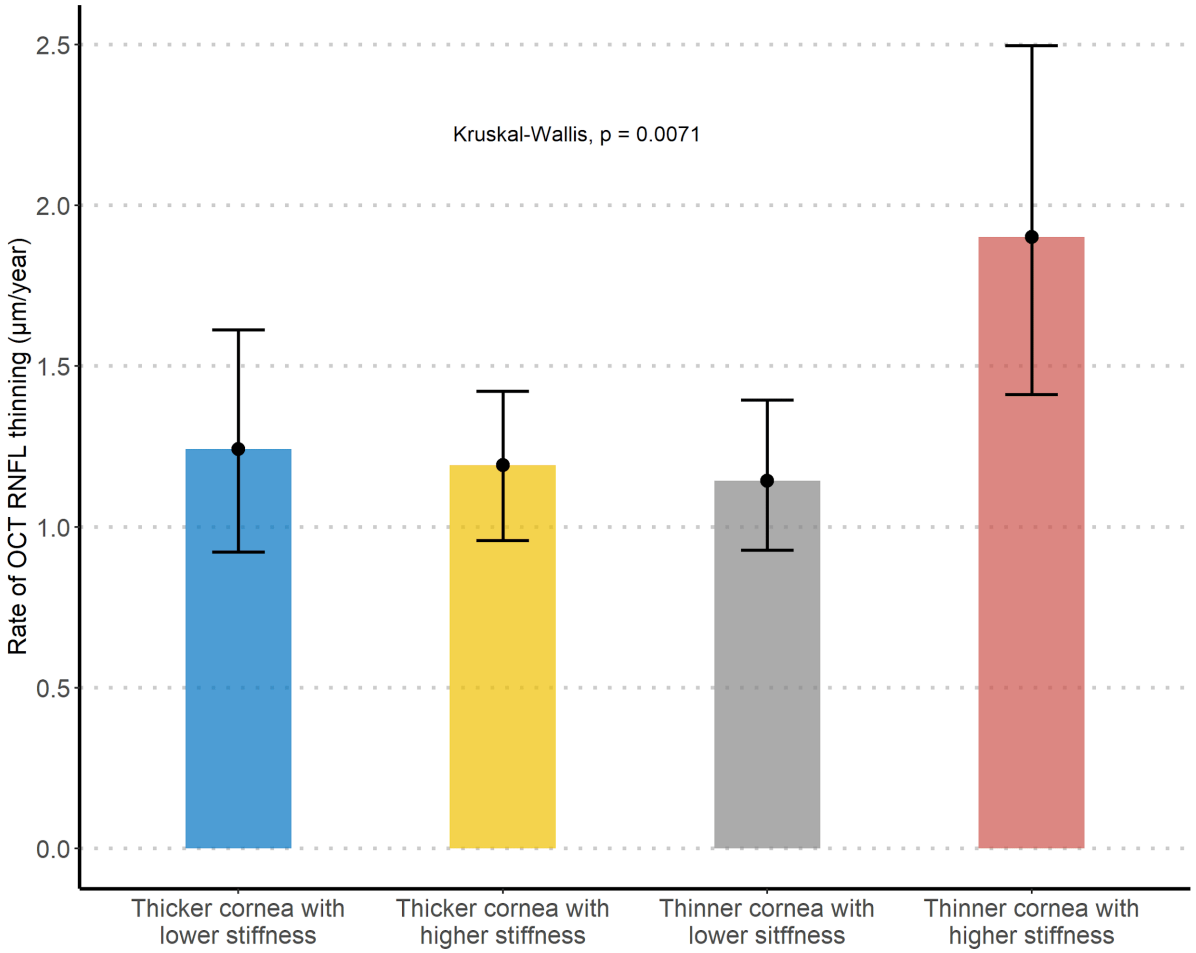

Figure 6.4. Prospective rate of OCT RNFL thinning grouped by corneal biomechanical properties. Thickness refers to CCT and stiffness refers to SP-A1. Grouping is in reference to the mean value for CCT (550 µm) and SP-A1 (112 mmHg/mm) in the study dataset. The dot and the bar represent the mean rate of RNFL thinning per group and error bars represent the 95% confidence interval of the mean. A groupwise analysis of variance using Kruskal-Wallis test is reported. However, statistical inference requires accounting for the inter-eye correlation, as reported in-text.

OCT: optical coherence tomography; RNFL: retinal nerve fibre layer; SP-A1: stiffness parameter at first application; CCT: central corneal thickness.

Table 6.4. Univariable and multivariable models predicting the rate of OCT average circumpapillary RNFL thinning using mixed-effect regression models with either stiffness parameters as the predicting variables.

Variable (standardised)	Estimated change in average RNFL rate of thinning (µm/year)	Standard error	P-value
Univariable model 1 (for stiffness parameter at first applanation)			
SP-A1 per 19 mmHg/mm	0.098	0.040	0.016
Univariable model 2 (for stiffness parameter at highest concavity)			
SP-HC per 4.9 mmHg/mm	0.073	0.042	0.085
Multivariable model 1 (for stiffness parameter at first applanation)			
SP-A1 per 19 mmHg/mm	0.16	0.047	<0.001
CCT per 37 µm	-0.14	0.053	0.007
Age per 10 years	0.09	0.040	0.022
Multivariable model 2 (for stiffness parameter at highest concavity)			
SP-HC per 4.9 mmHg/mm	0.13	0.048	0.006
CCT per 37 µm	-0.11	0.051	0.029
Age per 10 years	0.10	0.040	0.011

Standardised coefficients (per 1 standard deviation change in variables) are reported for SP-A1 and CCT for ease of interpretation.

SP-A1: stiffness parameter at first application; SP-HC: stiffness parameter at highest concavity; CCT: central corneal thickness.

Given the correlation between stiffness parameters and CCT (Table 6.2 and Figure 6.3B), we assessed for the statistical validity of our model with SP-A1, CCT and age. In addition to the aforementioned variables, we added an interaction term between SP-A1 and CCT, to assess the co-dependent effect of these variables in the model. The interaction term was not significant in predicting the rate of RNFL thinning (P = 0.17), and this model was not significantly better than the additive model (Akaike information criterion 1279.3 vs 1279.2; P = 0.16). We also assessed for multicollinearity in the additive model using variance inflation factor, which did not show any significant variable collinearity (variance inflation factor of SP-A1, CCT and age < 1.5) (Akinwande, Dikko, and Samson 2015).

We sought to validate our structural progression findings by examining the rate of macular GCIPL thinning. Macular scans with machine segmentation errors or artefacts interfering with the rate of GCIPL thinning were excluded as previously described (Mona S. Awadalla et al. 2018). Reliable longitudinal GCIPL thickness was available for 355 eyes (96%) from 220

participants, with a mean rate of average GCIPL thinning of 0.45 µm per year (SD 0.44). A higher SP-A1 and lower CCT were associated with a faster rate of GCIPL thinning (β = 0.063, and -0.069; P = 0.035 and 0.031 respectively). The model using SP-HC was not significantly associated with the rate of GCIPL thinning (P = 0.12). Using the aforementioned groupings in Figure 6.4, eyes with a higher SP-A1 and a thinner CCT had a rate of GCIPL thinning 0.066 µm/year faster than eyes with thicker CCT and lower SP-A1, however this was not statistically significant (P = 0.46).

Functional progression

There were 333 eyes from 205 patients that had at least 4 reliable visual fields (90% of total eyes) for functional progression analysis, with a mean follow-up time of 4.2 years (SD 0.9). The median number of HVF examinations per eye was 7 HVF tests (interquartile range 5–8). Seventy seven eyes (23%) have reached the visual field progression end-point. We verified that our structural progression marker (rate of RNFL thinning in the worst quadrant) was strongly associated with the functional progression end-point (two consecutive fields with significant progression by PoPLR criteria) using a survival analysis (hazard ratio for each 1 µm RNFL thinning per year = 1.3; 95% CI = 1.2–1.5; P < 0.001).

A higher SP-A1 was associated with a greater risk of visual field progression in a multivariable model including CCT and age (Table 6.5). Consistent with our structural progression findings, eyes with a higher stiffness parameter SP-A1 and lower CCT were at greatest risk of visual field progression. This apparent synergistic risk is shown in Figure 6.5: eyes with a higher SP-A1 and thinner CCT (relative to the cohort mean, as defined above) were at a 3.7-fold greater risk of visual field progression relative to those with a lower SP-A1 and thicker CCT (hazard ratio 95% CI 1.3–10.5; P = 0.014). However, stiffness parameter SP-HC was not associated with visual field progression (Table 6.5). Neither baseline IOP measured by GAT, nor Corvis ST (bIOP) were significantly associated with visual field progression in univariate analyses (hazard ratio = 1.03 and 1.07; P = 0.52 and 0.14 respectively).

Table 6.5. Variables associated with the risk of visual field progression using a mixed-effect multiple variable Cox hazard models

Variable	Hazard ratio	95% CI	P-value
Model 1 (for stiffness parameter at first applanation)			
SP-A1 per 19 mmHg/mm	1.57	1.17–2.11	0.002
CCT per 37 µm	0.67	0.50–0.91	0.010
Age per 10 years	1.42	1.12–1.82	0.005
Model 2 (for stiffness parameter at highest concavity)			
SP-HC per 4.9 mmHg/mm	1.27	0.95–1.71	0.11
CCT per 37 µm	0.78	0.58–1.04	0.090
Age per 10 years	1.46	1.14–1.88	0.003

Standardised coefficients (per 1 standard deviation change in variables) are reported for SP-A1 and CCT for ease of interpretation.SP-A1: stiffness parameter at first application; SP-HC: stiffness parameter at highest concavity; CCT: central corneal thickness.

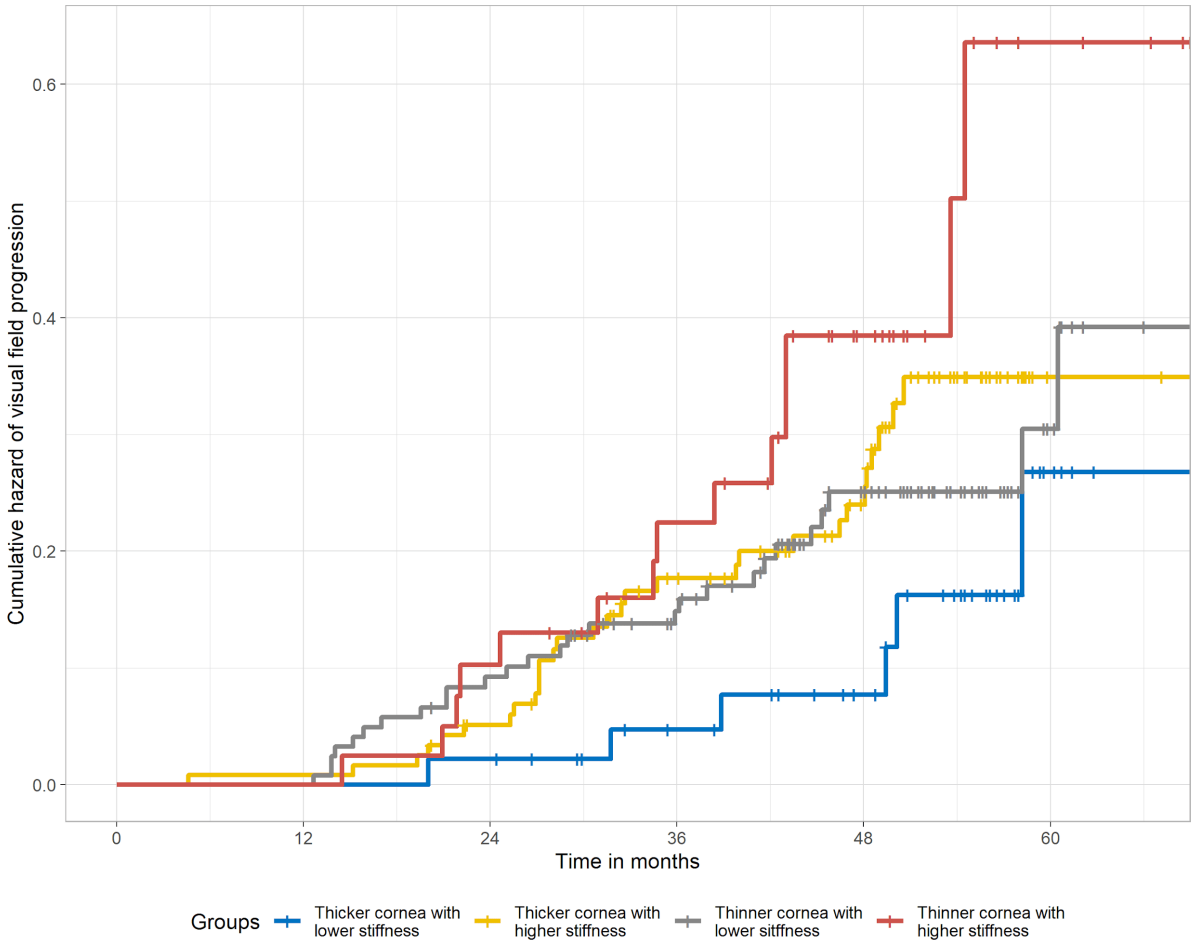

Figure 6.5. Prospective cumulative risk of visual field progression grouped by corneal biomechanical properties. Thickness refers to CCT and stiffness refers to SP-A1. Grouping is in reference to the mean value for CCT (550 µm) and SP-A1 (112 mmHg/mm) in the study dataset.
SP-A1: stiffness parameter at first application; CCT: central corneal thickness.

Effect of glaucoma medications

Topical glaucoma medications, particularly prostaglandin analogues, are known to affect corneal thickness and biomechanics (Amano et al. 2019; Georgalas et al. 2013). We explored whether the stiffness parameters were different in eyes on topical medications. In our study, 85 eyes (23%) were on topical IOP-lowering medications at the time of the baseline Corvis ST examination. Treatment was at the discretion of the treating glaucoma specialists, and in the majority of the cases was due to ocular hypertension (but with a normal visual field as described above). Prostaglandin analogues were the most commonly prescribed topical medication (74 eyes), followed by beta-blockers (28 eyes), carbonic anhydrase inhibitors (12 eyes), and alpha agonists (5 eyes). Twenty-three eyes were on more than one topical medication.

There was no significant difference in either stiffness parameter between eyes on any topical medication and treatment naive eyes ($P > 0.05$) after adjustment for CCT (Table 6.6). We then examined whether stiffness parameters were different by individual classes of medications. To avoid confounding results, we excluded eyes on more than one topical medication. Only topical prostaglandin analogues (53 eyes) and beta-blockers (7 eyes) were prescribed as monotherapies in sufficient numbers for this analysis. There were no significant differences in either stiffness parameter and the aforementioned medication classes (Table 6.6).

Table 6.6. The effect of topical glaucoma medications on stiffness parameters at baseline examination using mixed-effect multivariable linear regression models. All models included bIOP and CCT as covariates.

Group	SP-A1			SP-HC		
	Estimated difference in SP-A1	Standard error	P-value	Estimated difference in SP-HC	Standard error	P-value
Any topical medication	0.66	2.1	0.75	-0.71	0.56	0.21
Prostaglandin analogue monotherapy*	0.57	2.5	0.82	-0.77	0.70	0.27
Beta-blocker monotherapy*	1.08	6.0	0.86	0.81	1.6	0.61

* Participants on more than one medication were excluded; total eyes = 348.

SP-A1: stiffness parameter at first application; SP-HC: stiffness parameter at highest concavity; bIOP: biomechanically corrected intraocular pressure; CCT: central corneal thickness

We proceeded to perform a sensitivity analysis of our primary structural and functional outcomes using the number of topical glaucoma eyes as a covariate. We evaluated a

multivariable model using SP-A1, CCT and age as the predicting variables since it was consistently associated with progression in our analyses. Adjusting for the number of glaucoma medications, eyes with a higher SP-A1 and lower CCT had a faster rate of RNFL thinning (β =0.34, $P < 0.001$; and β = -0.29, $P = 0.005$, respectively). In this multivariable model, the number of glaucoma medications at baseline was not significantly associated with the RNFL rate of thinning (β = 0.005; $P = 0.97$). A similar analysis using each class of medication as a binary covariate yielded similar results. Using the number of medications as a covariate, eyes with a higher SP-A1 and lower CCT were at a higher risk of visual field progression (hazard ratio = 1.53, $P = 0.004$; and hazard ratio = 0.69, $P = 0.014$ respectively). In this multivariable model, the baseline number of glaucoma medications did not reach statistical significance (hazard ratio = 1.2, $P = 0.23$). Using each class of medication as a covariate did not change this association.

Added utility of corneal biomechanics to longitudinal IOP measurements

The positive correlation between the stiffness parameters and IOP at baseline (Table 6.2 and Figure 6.3A) pose a question regarding the independent role of corneal biomechanics as risk factors for glaucoma progression. To better understand the added clinical utility of the baseline SP-A1 and CCT measurements, we additionally examined the mean follow-up IOP measured using GAT as a predictor for our outcome measures. As expected, there was a linear positive association between the baseline IOP and the mean follow-up IOP (Pearson's correlation coefficient 0.75; $P < 0.001$; Figure 6.6A). Adjusting for the baseline IOP however, neither CCT nor SP-A1 at baseline were associated with the mean follow-up IOP ($P > 0.05$; Figure 6.6B).

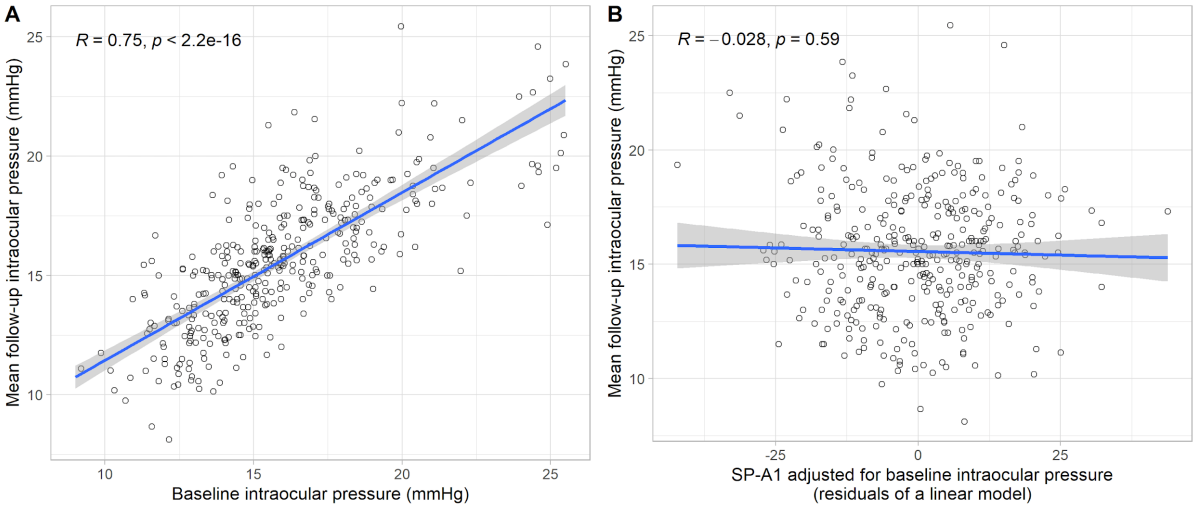

Figure 6.6. Association of the baseline intraocular pressure **(A)** and SP-A1 **(B)** to the mean follow-up intraocular pressure. A higher baseline intraocular pressure is positively associated with a higher follow-up mean intraocular pressure. Adjusting for this correlation, baseline SP-A1 is not associated with the mean follow-up IOP. Visualisation of this adjustment in panel **(B)** is done by plotting the residuals of a linear model (SP-A1 predicted by IOP) on the x-axis (i.e. SP-A1 adjusted to intraocular pressure). The blue lines represent the linear line of best fit with the grey shade representing the 95% confidence interval of the linear model. Pearson's correlation coefficient (R) and P-value are also shown for each panel.

We proceeded to include the mean follow-up IOP as a covariate for our outcome measures, alongside baseline SP-A1, CCT and age (Table 6.7). In these multivariable analyses, a higher SP-A1 and a thinner CCT remained associated with a faster rate of RNFL thinning, and a higher risk of visual field progression (P ≤ 0.01; Table 6.7). While SP-A1 is not independent of IOP, these results support that the association of a higher SP-A1 and a thinner CCT as risk factors for glaucoma progression are not solely attributable to IOP.

Table 6.7 Sensitivity analyses of the study outcome measures using mean follow-up IOP as a covariate.

Outcome	Variable	Estimated change in RNFL rate of thinning (µm/year)	Standard error	P-value
RNFL	SP-A1 per 19 mmHg/mm	0.27	0.11	**0.013**
	CCT per 37 µm	-0.26	0.10	**0.013**
	Age per 10 years	0.19	0.07	**0.009**
	Mean follow-up IOP per 1 mmHg	0.041	0.035	0.25
	Variable	**Hazard ratio**	**95% confidence interval**	**P-value**
HVF	SP-A1 per 19 mmHg/mm	1.78	1.22–2.58	**0.003**
	CCT per 37 µm	0.64	0.47–0.88	**0.006**
	Age per 10 years	1.40	1.10–1.79	**0.007**
	Mean follow-up IOP per 1 mmHg	0.94	0.84–1.06	0.31

The RNFL outcome refers to the rate of RNFL thinning per annum measured by OCT, using a multivariable linear mixed-effect model. The HVF outcome refers to the time to visual field progression by PoPLR criteria using a mixed-effect multivariable Cox hazard model. Standardised coefficients (per 1 standard deviation change in variables) are reported for SP-A1 and CCT for ease of interpretation. Boldface P-values are statistically significant.

IOP: intraocular pressure; RNFL: retinal nerve fibre layer; GCIPL: ganglion cell inner plexiform layer; SP-A1: stiffness parameter at first applanation; CCT: central corneal thickness; HVF: Humphrey visual field; OCT: optical coherence tomography; PoPLR: permutation analysis of pointwise linear regression.

Discussion

Corneal biomechanics are emerging as an increasingly important risk factor for the development and progression of POAG (C. N. Susanna et al. 2018; B. Zhang et al. 2019; Felipe A. Medeiros et al. 2013; Miki et al. 2019). In this study, we demonstrated an association between baseline corneal stiffness parameters and prospective glaucoma progression, measured by structural and functional end-points in a cohort of glaucoma suspects. Eyes with higher corneal stiffness parameters had more rapid thinning of RNFL and GCIPL, and were more likely to have progressive visual field loss. This association was most pronounced in subjects with thinner CCT and higher stiffness parameters, suggesting a synergistic effect between corneal thickness and stiffness parameter on glaucoma progression (Figure 6.7).

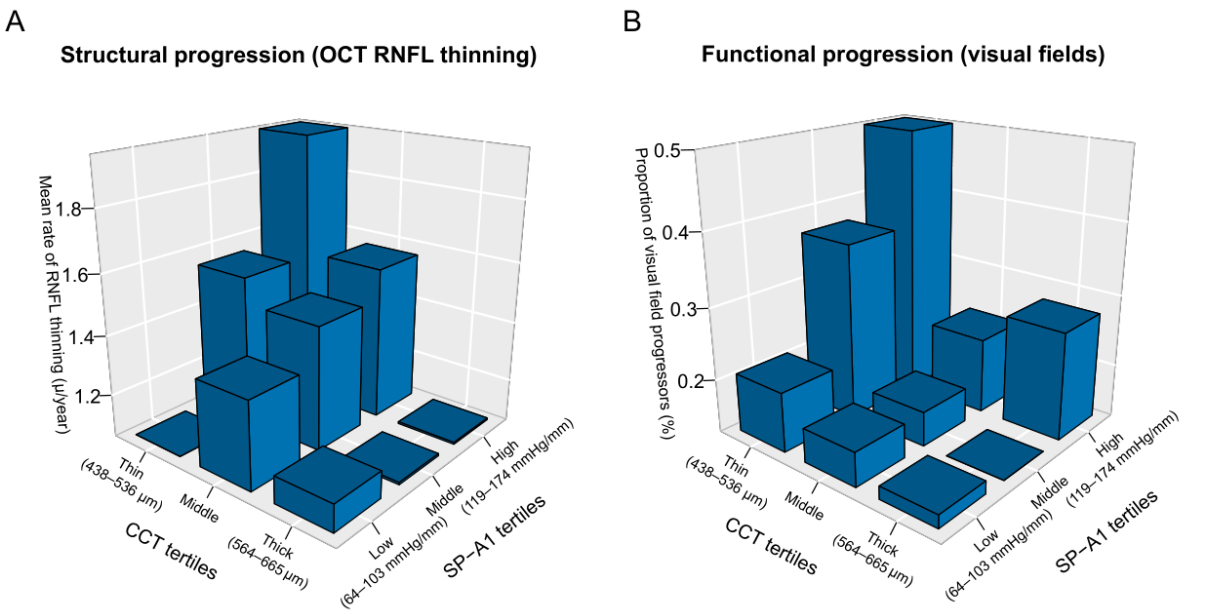

Figure 6.7. The synergistic effects of the baseline stiffness parameter (SP-A1) and CCT as risk factors for glaucoma progression in glaucoma suspects. Our cohort of 371 glaucoma suspect eyes were divided into SP-A1 and CCT tertiles, then the main structural **(A)** and functional **(B)** outcome measurements were summarised for each group. The combination of a thin cornea and a high SP-A1 infer a higher risk of OCT and visual field progression.

The corneal stiffness parameters are measured *in vivo* by the corneal deformation response to a calibrated air puff while accounting for the biomechanically corrected IOP. Higher stiffness parameters are seen in eyes with a thicker CCT and higher IOP, where the cornea deforms to a lesser magnitude to the applied force (air puff) (Fujishiro et al. 2020; Roberts et al. 2017). In agreement with the previously reported literature, stiffness parameters were independent of age (Fujishiro et al. 2020). Therefore, it is important to adjust for CCT when analysing corneal stiffness parameters (Heinze, Wallisch, and Dunkler 2018). While stiffness parameters and CCT are positively correlated, these variables confer additive risks in the opposite direction (Figure 6.7). That is, the highest risk of progression is seen amongst those with a lower CCT but a higher stiffness parameter (SP-A1). This phenotype may represent a distinct biological subgroup in which an unusually vulnerable optic nerve head is indirectly assessed through a coexisting thin, stiff cornea. Our results show that measurements of corneal stiffness parameter and CCT can be thought of as a composite corneal risk factor for structural and functional glaucoma progression. Additionally, using longitudinal IOP measurements, we have shown the risk associated with a higher stiffness parameter and a thinner CCT cannot be solely explained by their correlation with IOP. This supports the added clinical utility of the corneal biomechanics as a risk factor for glaucoma progression that may be independent of IOP (B. N. Susanna, Ogata, Jammal, et al. 2019). Though mean follow-up IOP was not statically significant in this multivariable analysis, ostensibly due to the pragmatic 'real-world'

study design (i.e., including the effects of clinical interventions), this does not diminish the importance of IOP as a glaucoma risk factor.

A higher corneal stiffness is postulated to reflect a higher peripapillary scleral stiffness, and thus greater optic nerve head vulnerability. Coudrillier et al. (2012) have reported that glaucomatous eyes exhibited a stiffer response at the peripapillary, but not mid-posterior, sclera compared to normal eyes . Nguyen et al. (2020) has demonstrated that Corvis ST corneal stiffness parameters were associated with scleral mechanical properties and stiffness using human donor eyes, whereby chemically stiffened sclerae had higher stiffness parameters than control; stiffness parameter at the highest concavity showed a stronger association than that at the first applanation . Vinciguerra et al. (2020) reported that eyes with normal tension glaucoma had lower corneal stiffness parameters than normal eyes at both first applanation and highest concavity . However, this result is confounded by a lower IOP and CCT in the normal tension glaucoma subgroup, which contribute to the lower stiffness parameters observed, in addition to topical medication usage. In our study, stiffness parameter at first applanation was more informative than at highest concavity, as it was consistently associated with both structural and functional progression end-points.

In addition to corneal thickness, other corneal biomechanical properties have also been studied in glaucoma. Corneal hysteresis measures the viscoelastic damping of corneal tissues in response to an air puff, and is found to be lower in eyes with glaucoma (B. Zhang et al. 2019). Lower corneal hysteresis is also a risk factor for the development and progression of glaucoma (Felipe A. Medeiros et al. 2013; C. N. Susanna et al. 2018). Hysteresis is a different biomechanical property of the cornea compared to those measured by the Corvis ST, and thus a direct comparison cannot be made to our findings. Several dynamic corneal response parameters measured by the Corvis ST, such as applanation time and velocity, and deformation amplitude, were previously reported to be different in glaucomatous eyes compared to normal eyes (W. Wang, Du, and Zhang 2015; Jung et al. 2017; Miki et al. 2019). However, these studies were limited by a lack of prospective follow-up, univariate analysis and confounding topical treatment. Numerous additional Corvis ST parameters are reported by the software, however this pose an analytical challenge in three ways: a majority of these parameters are tightly correlated with IOP and CCT, which limits their added clinical utility (Figure 6.8); the multicollinearity between the variables pose a statistical challenge in regression models; and controlling for Type 1 errors for several parameters (e.g. using Bonferroni method) limits the statistical power of identifying a predictive parameter with a high statistical confidence. Nonetheless, these findings support the importance of corneal biomechanics in glaucoma pathogenesis.

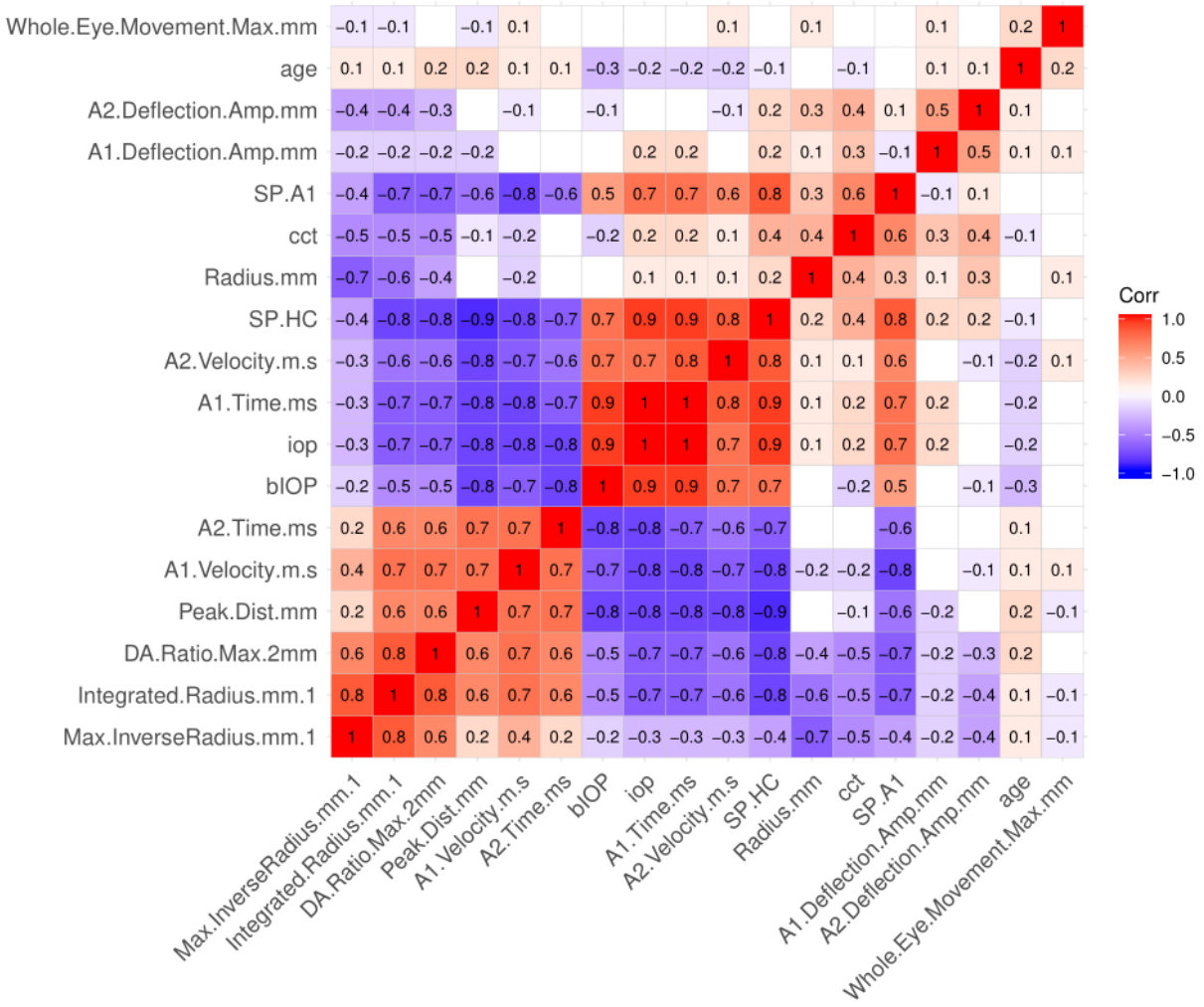

Figure 6.8. Correlation plot between selected Corvis ST parameters showing a high inter-correlation within the parameters, and with intraocular pressure (IOP) and central corneal thickness (CCT).

Our study has several strengths and some weaknesses. We used a large sample of glaucoma suspect eyes with a well-characterised diagnosis of open angles and normal visual fields at baseline. We investigated baseline Corvis ST corneal stiffness parameters in predicting prospective progression outcomes using both structural and functional endpoints, and utilised both eyes in our statistical analyses while accounting for the inter-eye correlation. Furthermore, we accounted for the effect of CCT, which was demonstrated to be important for interpreting the findings (Heinze, Wallisch, and Dunkler 2018). We performed sensitivity analysis accounting for the use of topical glaucoma medications, the results of which supported our primary findings. Nonetheless, a limitation of our study was that participants were treated at the discretion of the treating clinician, which is expected to slow or delay progression outcomes. While we showed that eyes on topical glaucoma medications did not have significantly different stiffness parameters to treatment-naive eyes, we did not perform

sequential Corvis ST assessments prior to and post commencement of topical medications to study this relationship more closely. Further research is needed to examine the effect of topical glaucoma medications on corneal biomechanics as measured by Corvis ST, including medication class, duration of treatment, and longitudinal nature of any changes. We only included baseline parameters in assessing prospective progression markers in our analysis; it is possible that including longitudinal measurements may have a different effect on progression. While our aim was to assess the baseline predictive utility of corneal stiffness parameters, further studies on longitudinal measurements of corneal biomechanical properties may be useful. We have however performed a sensitivity analysis including the mean follow-up IOP as a covariate, the results of which showed our findings were robust, and support an added clinical utility of the corneal biomechanics. Our cohort was primarily of Caucasian ethnicity; validation in other ethnicities is required. Finally, a thinner CCT is a well recognised risk factor for glaucoma, and this may have independently informed clinical treatment decisions. However, our results show that higher stiffness parameters are synergistic with lower CCT as progression risk factors. Clinician knowledge of the CCT value is expected to diminish its effect on prospective progression (e.g. by earlier intervention), therefore the "true" effect of a lower CCT may be even stronger. Moreover, stiffness parameters were not available to the clinicians during consultations, and were not used in management decisions.

In conclusion we demonstrate that higher corneal stiffness parameters are predictive of OCT and visual field progression in glaucoma suspect eyes, which appear to be synergistic with lower CCT as progression risk factors. Eyes with a higher stiffness parameter and a thinner CCT are at the highest risk of progression. This provides further evidence for the importance of corneal biomechanical factors in stratifying risk of progression in glaucoma suspect eyes.

Chapter 7: Discussion and conclusion

In a recent World Health Organisation systematic review, approximately 161 million people worldwide were estimated to either be blind or have low vision not attributable to refractive errors (Foster and Resnikoff 2005; Resnikoff et al. 2004). Vision impairment and blindness has a tremendous economic impact, with an estimated societal cost of US$5–10 billion attributable to blindness in developed economies (Pezzullo et al. 2018; Frick et al. 2007; Chakravarthy et al. 2017). Additionally, visually impaired individuals have significantly lower quality of life, particularly in the domains of mobility and self-care, with an estimated loss of over 200,000 quality-adjusted life years attributable to blindness (Frick et al. 2007; Khorrami-Nejad et al. 2016). The cause of blindness varies amongst different regions and age groups globally; however, glaucoma remains the leading cause of irreversible blindness worldwide (Flaxman et al. 2017). In 2015, an estimated 2.9 million people worldwide were blind due to glaucoma, and this is expected to have increased to 3.2 in 2020 (Flaxman et al. 2017).

Glaucoma is a hypernym that encompasses several optic neuropathies with common and characteristic features of structural and functional loss, mediated by raised IOP (Casson et al. 2012). The broad definition of what constitutes glaucoma (which often logically distils to “glaucoma is glaucoma”) and the mostly asymptomatic natural history makes glaucoma a challenging disease from an epidemiological, clinical and research perspective (Casson et al. 2012). The spectrum of clinical presentations of glaucoma ranges from asymptomatic pre-clinical retinal ganglion cell loss, to a rapidly progressing and vision-threatening disease that leads to blindness within a few months if left untreated (Robert N. Weinreb, Aung, and Medeiros 2014). Treatment options for glaucoma are safe, widely available, and highly effective in slowing down or stopping otherwise irreversible vision loss (Jost B. Jonas et al. 2017). This creates a window of opportunity that makes glaucoma an ideal target for early detection and risk stratification (Gottlieb, Schwartz, and Pauker 1983). The work presented in this thesis is focused on primary open-angle glaucoma (POAG), the most common subtype of glaucoma in Australia and worldwide (Y.-C. Tham et al. 2014).

Genetic risk prediction in glaucoma

Polygenic risk scores

Genome-wide association studies (GWAS) have proliferated over the past decade, the results of which have dramatically advanced our understanding of the genetic architecture of common complex diseases such as POAG (Visscher et al. 2017; Claussnitzer et al. 2020). Since the first glaucoma GWAS reported 10 years ago (Thorleifsson et al. 2010), more than a hundred

independent glaucoma-associated single nucleotide polymorphisms (SNPs) have been identified (Chapter 3) (Craig et al. 2020). This significant advancement in identifying disease-associated common variants is attributable to improved analytical techniques that effectively utilise the correlation between SNPs and traits (Loh et al. 2015; Turley et al. 2018); larger sample size cohorts that have well characterised phenotypes, such as population biobanks (C. Sudlow et al. 2015); and open-access publication and data sharing of previous GWAS summary statistics which allows for pooled meta-analyses of new and existing datasets (H. Springelkamp et al. 2017). The results of such GWAS have implications in improving our understanding of the biological pathways underpinning common complex diseases, genetic risk prediction, and identifying potential therapeutic targets (Visscher et al. 2017).

Common complex disease GWAS were initially met with great skepticism (Visscher et al. 2012; McClellan and King 2010; Crow 2011). A primary concern was that early GWAS had failed to identify a majority of the genetic variants that would explain the heritability of common diseases, leading to the concept of 'missing heritability' (Crow 2011; Manolio et al. 2009). However, more recent GWAS — best exemplified by the results reported in Chapter 3 — have continued to exponentially uncover new loci that are associated with glaucoma and its heritable endophenotypes at a statistically stringent threshold (Craig et al. 2020; MacGregor et al. 2018). Statistical power analyses show that sample size remains a key limitation for identifying low frequency or low effect size genetic variants (Figure 7.1) (Park et al. 2010). For example, one model estimated the sample size needed to identify a variant with a minor allele frequency of 5% and effect size (odds ratio) of 1.1 at a genome-wide significance threshold of 5×10^{-8} in GWAS to be 88,300; under the same assumptions, a rarer variant with a minor allele frequency of 1% was estimated to need more than quadruple the sample size at 422,300 individuals (Chapman et al. 2011). The genome-wide significance threshold was derived from Bonferroni correction of P-value using the estimated number of common (minor allele frequency > 5%) independent variants in the genome reported by International HapMap Consortium in 2015 (150 variants per 500 kilobase pairs in European population, extrapolated to the 3.3 gigabase genome) (Fadista et al. 2016; International HapMap Consortium 2005). One suggested method to address this sample size limitation is to lower the P-value threshold of a statistically significant variant, allowing additional SNPs to be identified at a "suggestive", rather than genome-wide significant, level of statistical confidence (Fadista et al. 2016). Indeed, our multi-trait glaucoma polygenic risk score (PRS) showed improved discriminatory power and could explain more variance when additional SNPs below the genome-wide significance threshold were included in the score, suggesting a higher signal-to-noise ratio using less stringent P-value thresholds (Chapter 4) (Craig et al. 2020). A similar trend has been reported across several other diseases (Khera et al. 2018), suggesting the 'missing

heritability' gap will continue to narrow as larger sample sizes are amassed and better statistical association methods are developed (Turley et al. 2018).

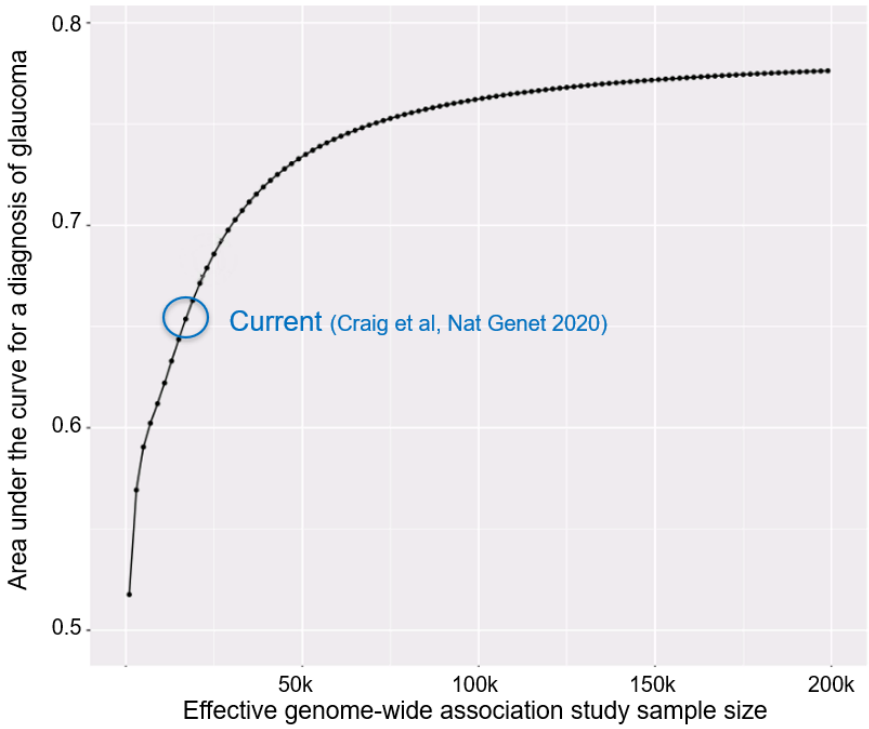

Figure 7.1. Effective genome-wide association study sample size needed to improve the predictive ability of a glaucoma genetic risk score. The model is obtained using genetic effect-size distribution inference from summary-level data (GENESIS) software (Y. Zhang et al. 2018). The current model of genetic risk prediction of glaucoma (without including age, sex, or ocular measurements in the model) has an area under the receiver operator curve of 0.67 (as detailed in Chapter 4) (Craig et al. 2020). This is expected to continue to improve with increasingly large sample sizes, particularly through the development of multiple international biobanks. This figure was generated by Professor Stuart Macgregor, and reused with permission.

Rare and common variants

Glaucoma is a good example of a common complex disease that is associated with both rare variants (minor allele frequency < 1%) of large effect size, and common variants (minor allele frequency > 1%) of small effect size. Rare genetic variants in *MYOC*, *OPTN* and *TBK1* account for about 6% of POAG risk in the general population (A. P. Khawaja and Viswanathan 2018). It is not currently known how much additional risk can be ascribed to rare genetic variants in other genes. However, my research has shown (as detailed in Chapters 3 and 4) that common variants in aggregate (using PRS approach) account for a significant risk to the development of glaucoma (AUC of glaucoma diagnosis in an independent cohort = 0.79; 95% CI 0.75–0.84, adjusted to age and gender) (Craig et al. 2020). For example, individuals in the top decile of

our glaucoma PRS (i.e., those carrying the majority of glaucoma-associated common variants) had a 14.9-fold higher risk (95% CI 10.7–20.9) of glaucoma relative to the bottom decile. Alternatively, when using the remaining 90% of the study cohort as the reference group, the top decile group had a 4.2-hold higher risk of developing glaucoma (95% CI 3.43–5.17) (Chapter 4) (Craig et al. 2020). This common variants based risk prediction in glaucoma is significantly better than those reported in other conditions such as coronary artery disease, diabetes and breast cancer, whereby the odds ratio of the top decile to the remaining 90% is between 2.32 and 2.89 (Khera et al. 2018). Of note, some of the difference can be attributable to the study design since our target dataset was a glaucoma case-control dataset, as opposed to the population subset used by Khera et al. (2018). Nonetheless, it is evident that common genetic variants account for a substantial risk of glaucoma, in keeping with the relatively higher heritability of glaucoma compared to most common complex diseases (K. Wang et al. 2017).

The large-scale identification of rare genetic variants is not currently feasible using the genotyping arrays commonly used in GWAS — instead, these variants are typically identified through genome (including Sanger or targeted sequencing) and exome sequencing. Rare genetic variants tend to be in poor linkage disequilibrium with more common variants identified via genotyping, since linkage disequilibrium (commonly measured as r^2) is closely related to allele frequency (Wray 2005). Thus, it is likely that causal rare variants that confer a significant risk of glaucoma in some individuals are not readily captured in the current glaucoma PRS models. Some 'unobserved' rare variants can be derived from genotyping data using statistical imputation techniques that could theoretically identify variants with minor allele frequencies as low as 0.1% (S. McCarthy et al. 2016; Browning and Browning 2007). For example, Gharahkhani et al. (2015) used genotyping imputation on array data to identify a rare yet well established pathogenic variant in the *MYOC* gene, p.Gln368Ter (allele frequency of 0.1–0.3% in populations of European ancestry), with a positive predictive value of 96%. Using this approach, Han et. al. (2019) reported the penetrance of p.Gln368Ter in a population-setting to be 7.6% in patients with glaucoma, and 24.3% in patients with ocular hypertension. Interestingly, as reported in Chapter 4, common variants seem to influence the penetrance of *MYOC* p.Gln368Ter, highlighting the additive role of common and rare variants in glaucoma (Craig et al. 2020).

In the future, GWAS using low-coverage whole genome sequencing will likely replace the current SNP array method, particularly as sequencing costs become more affordable (Visscher et al. 2017). A subgroup of 50,000 individuals from the UK Biobank are already planned to undergo whole genome sequencing, the data of which will be publicly released in the next few years. The advantage of a more comprehensive sequencing in glaucoma can be

seen on the role of *LOXL1* gene in pseudoexfoliation. While common variants in this gene are strongly associated with pseudoexfoliation glaucoma in some studies (Thorleifsson et al. 2007), other studies have shown a 'flipped' association (i.e., protective effect of the variants) (J. L. Wiggs and Pasquale 2014; Williams et al. 2010). Efforts of understanding the role of *LOXL1* in pseudoexfoliation glaucoma using deep sequencing of the gene has led to the identification of a rare (minor allele frequency of 0.002%) strongly protective variant (p.Tyr407Phe) in this gene (resistance odds ratio = 25) (Aung et al. 2017). Clinical implementation of genetic risk stratification for glaucoma should ideally include both rare and common variants, with whole genome sequencing being the most comprehensive testing strategy to achieve this.

Using whole genome sequencing data, the contribution of rare variants to disease risk can be better quantified, although GWAS using this approach will still require exponentially larger sample sizes to reach genome-wide significance thresholds (Visscher et al. 2017). However, whole genome or exome sequencing data can also be used for burden testing of rare variants across a gene, identifying gene-based associations that cannot be inferred from GWAS (Kiezun et al. 2012), and dramatically reducing the multiple-testing penalty (from ~1,000,000 common variants to only ~20,000 genes). This is based on the assumption that multiple rare variants across a gene independently contribute to the observed risk, a phenomenon commonly observed in 'monogenic' causes of a disease (E. Souzeau et al. 2013). One recent example of this is the identification of the potential protective role of *ANGPTL7* in glaucoma, possibly via a loss of interaction or function (Tanigawa et al. 2020). Using the UK Biobank genotyping data, a rare (minor allele frequency = 0.8%) missense variant (p.Gln175His) in *ANGPTL7* was found to be associated with a 34% reduction of risk of glaucoma (Tanigawa et al. 2020). While hypothesis-free gene-based burden testing would be limited by current sample sizes of whole exome and genome sequencing data (with notable exception of the afortmenioted *ANGPTL7* variants), this strategy has been effective in family-based studies where segregation of rare variants with large effects is more likely (Siggs et al. 2020, 2019). The recent release of exome sequencing data of 200,000 individuals from the UK Biobank will be a key next step in gene-based analyses in glaucoma. This approach may be of a higher yield in the setting of glaucoma with a low PRS derived from common variants, whereby rare variants may explain the genetic predisposition to glaucomatous optic neuropathy. Such rare variants may be additive to common variants as we reported with *MYOC* p.Gln368Ter (Craig et al. 2020), or independent to previously identified common variants as observed with *LOXL1* p.Tyr407Phe (Aung et al. 2017).

Genetic risk and disease pathogenesis

A primary aim of genetic studies of common diseases is uncovering new biological pathways leading to disease pathogenesis. Translating GWAS results to functional outcomes is challenging, as the majority of identified variants are in the non-coding regions of the genome. Functional annotation platforms such as FUMA (Functional Mapping and Annotation of Genome-Wide Association Studies) have been a major step forward in identifying biological pathways that correspond to SNP or gene sets (Watanabe et al. 2017; de Leeuw et al. 2015). Using the results of the multi-trait GWAS of glaucoma, my research identified several biological pathways that could be highly relevant to glaucoma pathogenesis (Chapter 3) (Craig et al. 2020). For instance, two key pathways identified were circulatory system development and vasculature development, suggesting a potential role of vasculopathies in the development or pathogenesis of glaucoma (Craig et al. 2020). This hypothesis was supported in a follow-up collaborative work where we identified cardiovascular disease history, and particularly hypertension, to be significantly associated with a thinner macular ganglion-cell complex, and an important risk factor for structural and functional progression of glaucoma (odds ratio for hypertension = 1.9, 95% confidence interval 1.2–3.2) (H. Marshall et al. 2020). In an observational cross-sectional study of 109 glaucoma patients, relative nocturnal hypertension was significantly associated with glaucoma (adjusted odds ratio of nondipping blood pressure = 2.0, 95% confidence interval 1.3–3.1) (Yoshikawa et al. 2019). Nondipping nighttime blood pressure pattern was defined as a reduction of less than 10% in the mean nocturnal blood pressure compared to the mean daytime blood pressure (Yoshikawa et al. 2019). In light of the growing understanding of the link between cardiovascular diseases and glaucoma, I am leading recruitment for a study to investigate the prevalence of nocturnal hypoxia and obstructive sleep apnoea in individuals with early glaucoma, and their potential association with glaucoma progression. Further research is needed to establish a potential causative relationship between cardiovascular diseases and glaucoma, and whether treatment of hypertension or cardiovascular diseases helps mitigate glaucoma progression.

Another translational potential of the circulatory and vasculature development pathways is in investigating treatment targets focused on vasculogenesis. For instance, our gene-based analysis has highlighted Angiopoietin 1 (*ANGPT1*) and Angiopoietin 2 ligand (*ANGPTL2)* to be significantly associated with glaucoma, both of which were first identified in the UKBB IOP GWAS (Craig et al. 2020; MacGregor et al. 2018). Angiopoietin and the related *TEK* pathway are involved in IOP homeostasis via their role in vascular and lymphatic development, and rare variants in the *TEK* and *ANGPT1* genes have been associated with primary congenital glaucoma (Souma et al. 2016; B. R. Thomson et al. 2014, 2017). Mice models have shown

the ANGPT-TEK pathway to be essential for the normal development and integrity of Schlemm's canal, and a loss of function in this pathway leads to insufficient aqueous humor outflow and glaucoma (J. Kim et al. 2017; Souma et al. 2016; B. R. Thomson et al. 2014). Therapeutic targeting of this pathway may offer novel treatment options for ocular hypertension or glaucoma, and this is currently being explored by multiple biotechnical companies, one of which has completed phase II trials with a topical *TEK* activator (Benjamin R. Thomson et al. 2020; Q. D. Nguyen et al. 2020).

A fertile area of current research is investigating the apparent pervasive pleiotropy observed in our GWAS findings and as reported in other diseases (Pickrell et al. 2016; Xikun Han et al. 2019; Craig et al. 2020). My research identified several optic disc size loci that were also associated with macular thickness or myopia (Xikun Han et al. 2019). Similarly, Gao et al. (2019) reported pleiotropy between macular thickness and neurological diseases including Alzheimer's disease. Additional functional research is needed to correlate our genetic findings in glaucoma and its endophenotypes to the underlying biological and molecular mechanisms. Functional studies will be able to identify the potentially shared molecular basis by which these loci influence multiple disease risk, which would enhance our knowledge on the shared genetic pathway of common complex diseases, and offer therapeutic targets. Additionally, pleiotropy could be leveraged to infer causal relationship between diseases or traits using Mendelian randomisation studies. Simcoe et al. (2020) have recently used this approach to demonstrate a causal relationship between corneal biomechanics, namely corneal hysteresis and corneal resistance factor, and IOP, supporting the clinically observed intricate interconnection between these traits. Another Mendelian randomisation study investigated the previously reported link between glaucoma and Alzheimer's disease (Vickers et al. 2002; Mancino et al. 2018; Margeta et al. 2020), and failed to show a causal relationship between the two diseases (Budu-Aggrey et al. 2020). It should be noted that this study (not peer-reviewed and published only in a preprint server at the time of writing) did not use the full list of glaucoma-associated SNPs identified by our multi-trait GWAS (Craig et al. 2020), and thus likely underestimates the genetic risk of glaucoma (Budu-Aggrey et al. 2020). Our understanding of pleiotropy and the shared impact of some risk loci across several diseases will continue to improve as additional disease- and trait-associated variants are identified. Further functional research is needed to better understand the biological implications of our GWAS findings.

Newer analytical methods provide a platform for *in silico* follow-up functional investigation of GWAS results. This is accomplished by utilising gene expression data, chromatin contacts maps, protein–protein interactions or other genomic annotations (Won et al. 2016; Visscher et al. 2017; Chimusa et al. 2019). One particularly interesting strategy is integrating the results

of expression quantitative trait loci studies with GWAS results to identify associations between complex traits or diseases and gene transcription (Gusev et al. 2016; Zhu et al. 2016; Gamazon et al. 2015). This approach, aptly called a transcriptome-wide association study, allows prioritising candidate causal genes at GWAS loci (Wainberg et al. 2019). One study applied this method to five complex traits or diseases and found that about two-thirds of the identified candidate genes were not the nearest annotated gene to the top GWAS SNP, an approach commonly used to identify relevant genes post GWAS (Zhu et al. 2016). Our approach to post-GWAS *in silico* functional analysis was examining ocular tissue gene expression of the nearest genes to our lead SNPs (Chapter 3). We should that the majority (75%) of the novel glaucoma genes identified through our multi-trait GWAS had differential expression in tissues most likely involved in IOP hemostasis or POAG pathogenesis, namely trabecular meshwork and the iris. This provides a basic overview of a gene's involvement in glaucoma pathogenesis, particularly if the gene is highly expressed in tissues involved in aqueous outflow pathway or in the optic nerve head (Chapter 3) (Craig et al. 2020; Xikun Han et al. 2019). However, further research using newer methods such as transcriptome-wide association studies may highlight novel candidate genes that may be associated with glaucoma, and prioritise genes for functional follow-up studies.

Clinical utility of polygenic risk scores

In stark contrast to functional and biological translational research, genetic disease risk prediction, including PRS, does not require knowledge of the specific molecular pathways underlying the risk loci. By including 2,673 uncorrelated SNPs that may be associated with glaucoma in a composite score, we developed a 'functionally agnostic' tool of glaucoma risk stratification that has translational and clinically meaningful outcomes (Chapter 4) (Craig et al. 2020). Our glaucoma PRS was was highly predictive of risk of development of advanced glaucoma (odds ratio = 15 in the top PRS decile vs the bottom), earlier age of glaucoma diagnosis in those affected, and a higher likelihood of disease progression in early stage disease in both structural and functional measures. Additionally, the glaucoma PRS was 'predictive' of clinicians treatment intensity in both early and advanced glaucoma (number of topical IOP-lowering medications and likelihood of incisional surgery, respectively). Treatment escalation can be thought of as a subjective composite measure of disease progression as assessed by the treating clinician's assessment of the risk of vision loss (Conlon, Saheb, and Ahmed 2017). Genetic disease risk prediction can be regarded as a distinct aim of GWAS that supplements the aforementioned functional studies in translating the genetic findings to imparting clinical utility (Visscher et al. 2017).

Common complex diseases are often diagnosed late in life with a long period of preclinical or 'asymptomatic' disease. A key advantage of PRS risk stratification is the ability to identify individuals before they develop symptoms or irreversible pathology, and in some cases also predict the risk of progression (Craig et al. 2020; Ding et al. 2017; Tedja et al. 2018; MacGregor et al. 2018; Seddon and Rosner 2019). Risk stratification is best utilised where early low-risk intervention can alter the natural history of a disease and improve quality of life, as has been reported across a range of cardiovascular conditions (Khera et al. 2016; Mega et al. 2015; Rutten-Jacobs et al. 2018; T. Wang et al. 2018). In addition, lifestyle modification (such as increasing time outdoors for myopia, or smoking cessation and dietary modification for age-related macular degeneration) and earlier or more frequent screening strategies can be an effective means of minimising vision loss associated with glaucoma. POAG represents an ideal case scenario for the clinical utility of PRS: 1) it is one of the most heritable common human diseases (K. Wang et al. 2017); 2) it has a prolonged asymptomatic disease phase; 3) it leads to irreversible vision loss if left untreated or diagnosed late (A. P. Khawaja and Viswanathan 2018); 4) it has good outcomes with early, cost-effective, and low-risk treatment that can effectively halt vision loss (D. F. Garway-Heath et al. 2015; Gus Gazzard et al. 2019); 5) there are highly sensitive and non-invasive screening methods available using OCT (V. Kansal et al. 2018); and 6) highly predictive PRS are available for the risk of developing POAG, and characterising its phenotype (Craig et al. 2020; A. Qassim et al. 2020).

Polygenic risk testing for glaucoma can benefit several groups of patients, highlighting broad clinical utility. Currently, single-gene genetic testing can be performed in patients with early onset glaucoma to identify individuals and their relatives at a higher risk of glaucoma (E. Souzeau et al. 2017). Individuals carrying variants in genes known to cause early-onset glaucoma such as *MYOC* can benefit from genetic counselling and a personalised approach to screening and management. Further, our research has shown that common variants for POAG may influence the penetrance of incompletely penetrant 'monogenic' variants (Craig et al. 2020). PRS-based risk stratification will be more effective in combination with known demographic and clinical risk factors and may be best applied to older individuals (50 years or older), those with a family history of glaucoma, or who may have optic disc features suspicious of developing glaucoma (A. P. Khawaja and Viswanathan 2018). In addition, PRS may improve the triage of glaucoma suspect referrals by identifying high-risk individuals prior to specialist review, optimise resource allocation in the face of an ageing global population and increasing glaucoma prevalence, and potentially also form part of targeted glaucoma screening programs (A. P. Khawaja and Viswanathan 2018).

Under current guidelines, new glaucoma suspects are referred from Optometrists on the basis of elevated IOP or findings suspicious for glaucoma on optic disc assessment, or in recent years, abnormal findings on OCT retinal nerve fibre layer analysis (leading to a surge in referrals with many false positives). In the absence of a clear reproducible glaucomatous visual field defect, the Royal Australian and New Zealand College of Ophthalmologists RANZCO and NHMRC guidelines recommend a period of monitoring to assess baseline IOP, and disease progression. For glaucoma suspects, six monthly longitudinal reviews are recommended, which for lower risk cases would occur in the optometry setting. Conservatively, if 5-10% of Australians over 65 are classified as glaucoma suspects,(Healey and Mitchell 2015) and at a review cost of $250 (inclusive of visual field and retinal imaging), the cost of these reviews is estimated at >$300 million per annum if all such individuals were to be monitored according to guidelines.(Dirani et al. 2011) Immediate treatment is not generally advocated, particularly in the absence of IOP elevation. There is no strong evidence-base regarding appropriate monitoring frequency, and what should trigger initiation of treatment.

In health care systems with finite resources, targeting high risk individuals with low-risk interventions, and minimising screening and interventions in low-risk individuals, will improve the cost-benefit ratio of these strategies and optimise resource allocation. There will be a significant clinical and economical advantage to targeted screening strategies to individuals at high risk of developing a disease, while saving resources spent on screening low-risk individuals. Several studies have shown using a PRS would significantly improve targeting at-risk individuals in cancer screening settings (Fantus and Helfand 2019; Mavaddat et al. 2019; Weigl et al. 2018). The current NHMRC guidelines recommend screening for at-risk individuals using established clinical and demographic glaucoma risk factors such as age, IOP, and family history, although the optimal combination of risk factors has not been defined (NHMRC 2010). The NHMRC glaucoma screening guidelines also includes ascenstory-specific recommendations, such as earlier age of screening for individuals of African descent (NHMRC 2010). Of note, while family history can capture some of the genetic risk of a disease, it is often incomplete, imprecise, and strongly confounded by shared environmental risk factors (S. A. Lambert, Abraham, and Inouye 2019).

PRS are an increasingly effective and accurate measure of the genetic component of disease risk, which typically outperforms self-reported family history in glaucoma and other diseases such as age-related macular degeneration and inflammatory bowel disease (Neema Ghorbani Mojarrad, Williams, and Guggenheim 2018; S. A. Lambert, Abraham, and Inouye 2019; Craig et al. 2020; C. B. Do et al. 2012). Additionally, sporadic cases with no known family history of

a disease would also benefit from genetic risk prediction. For example, in the Blue Mountain Eye Study, only 15.7% of the glaucoma cases reported a first-degree family history of glaucoma, which itself is likely inflated by recall bias of previously diagnosed cases (as opposed to newly diagnosed cases in this population study) (Paul Mitchell et al. 2002). Nonetheless, PRS is not aimed at replacing clinical history or screening programs as it is not a diagnostic test; rather PRS can serve to improve risk stratification, screening, and clinical decision making in combination with traditional risk factors. As explored in Figure 7.1, genetic risk variants would not achieve definitive diagnostic capacity anytime soon, and optimal screening strategy would incorporate known glaucoma risk factors.

As reported in detail in Chapter 4, our glaucoma PRS was effective in identifying at-risk individuals at an earlier age, using a subset cohort of the UKBB (Craig et al. 2020). Individuals in the top PRS decile reached 3% glaucoma prevalence (prevalence in general population) by age 59, whilst it takes an additional 10 years for this disease prevalence to be reached for people in the bottom PRS decile. Additionally, our glaucoma PRS provided additional predictive ability beyond that imparted by traditional risk factors (age, sex, and self-reported family history) in an independent cohort (Craig et al. 2020). A glaucoma PRS — in combination of other risk factors such as age, IOP, and optic nerve head appearance — could be used to reduce the screening intensity of low-risk individuals, which would translate to potential savings in excess of $50 million per annum, without increased risk. Conversely, early intervention in the higher risk cases is likely to reduce visual morbidity and blindness in older age in these individuals with further cost savings related to maintaining independence, work and driving years, and reducing falls.(Montana and Bhorade 2018) These cost savings need to be balanced against the cost of personalising care using genetic stratification, and further research is needed in using PRS to develop an economically viable screening strategy in ophthalmology and glaucoma.

PRS can be readily generated from public GWAS summary statistics, and easily updated as newer and larger studies are completed (Samuel A. Lambert et al. 2020). Since the germline genome is fixed, once generated genomic data can be queried simultaneously at any time with any number of disease-specific PRS. This is particularly beneficial in the fast-paced GWAS literature, where new risk variants are continuously being reported, and can be used to generate new and improved PRS. However, a potential drawback in clinical practice would be the requirement to re-accredit and re-validate each iteration of the test. Furthermore, additional research is needed on how best to counsel patients on the risk of multiple diseases and the ethical challenges this imposes. For example, a PRS-based platform can generate disease risk for tens of diseases simultaneously (such as that currently implemented by

www.impute.me). Would specialists interested in a specific disease risk (e.g. glaucoma) mask the report to exclude other 'unintended' risk estimates? The discussion surrounding consent for such a test would need to emphasise 'material risk' for each patient, and this is likely significantly different for each individual particularly in disease-prevention settings (Skene and Smallwood 2002). One approach could be a tiered analysis during the lifetime of the individual for different diseases, based on other relevant acquired risks (notably age), and the availability of effective lifestyle modifications or other interventions.

Glaucoma PRS is effective in identifying high-risk individuals, and infers risk of disease progression in those with early disease (Craig et al. 2020). Since early intervention is highly effective in halting glaucomatous optic neuropathy progression, the PRS-based risk stratification can be used to guide intervention in at-risk individuals (e.g. high-risk glaucoma suspects). This may be similar to the recommendations from the OHTS study, whereby the decision to treat ocular hypertensive individuals is guided by a validated risk stratification tool, with a suggested threshold for treatment initiation of 15% risk of progression at 5-years (F. A. Medeiros et al. 2005). Nonetheless, there is still a need for prospective studies to test the clinical validity and utility of a glaucoma PRS in routine clinical practice. The design of such studies will need to involve stratification of disease risk based on PRS, in addition to known risk factors of disease progression, such as IOP and neuroretinal rim width. Further investigations will need to assess the impact of preventative measures to assess the clinical utility of PRS in glaucoma by randomisation of high-risk patients into treatment and control (standard of care) arms. The aim of this individualised-treatment approach would be to reduce the risk of vision loss in those at the highest-risk of progression. Conversely, low-risk patients may be followed less frequently resulting in economical benefit. The implementation of PRS in ophthalmic practice can be done at the general practitioner level (primary prevention or multiple disease risk stratification), optometrists (screening of high-risk individuals, or risk stratifying glaucoma suspects) and specialists (prognostic and phenotypic risk stratification); however, further research is needed in this area.

There are still some additional challenges to the implementation of PRS testing in the clinical setting. To date, a disproportionate majority of the large-scale GWAS — and thus the PRS derived from them — have been performed in populations of European ancestry (Martin et al. 2019). The effect size of disease-associated genetic variants can vary between different populations; therefore, the predictive power of a PRS derived from a majority European ancestry cohort can be lower when applied to other ethnicities (Martin et al. 2019). For example, while our glaucoma PRS derived from a cohort of European ancestry was predictive of glaucoma risk in South Asian individuals, it had a slightly better predictive power in an

independent cohort of European ancestry (AUC of 0.76, 95% CI: 0.73 – 0.79 vs AUC 0.79, 95% CI: 0.75 – 0.84 respectively) (Chapter 4) (Craig et al. 2020). Validation studies and mixed-ancestry GWAS are essential for the effective translation of PRS to clinical practice and health equity. This is already underway for glaucoma, and I have been involved in subsequent GWAS of mixed-ethnicities to bridge this gap (results are not published at the time of writing). Furthermore, there is little consensus on the best methodology to calculate PRS, or the analysis methods used to report findings (Witte, Visscher, and Wray 2014). This limits ease of comparison, replication and validation of the currently published scores (Witte, Visscher, and Wray 2014). An evidence-based and consistent analysis approach as well as detailed reporting of the variants and methods used to generate each score will address these issues. This is currently being addressed by the active development of The Polygenic Score Catalog, an online repository of published PRS with full annotation of variants, weights, and reported performance metrics (Samuel A. Lambert et al. 2020). Finally, PRS research should aim to address clinical questions on the utility of the score in a disease-specific manner (such as risk of progressive vision loss in glaucoma), rather than focusing solely on statistical prediction accuracies (such as area under the receiver operating characteristic curve).

In summary, we showed that glaucoma PRS is effective in identifying individuals at high-risk of developing progressive glaucomatous optic neuropathy. This PRS is additionally informative on the penetrance of the commonest 'monogenic' POAG-associated variant in the *MYOC* gene. The findings implicate an added clinical and economical utility in incropraite genetic risk stratification into disease prediction and prognostication models. A prospective trial using a PRS-inclusive risk matrix demonstrating a benefit of earlier intervention in high-risk individuals, and a lower frequency of screening in low-risk individuals is needed to apply PRS into clinical practice. Clinicians and genetic counsellors are then needed to communicate genetic risk to patients in a personalised manner with actionable monitoring frequencies and life-style or pharmacological intervention suggestions. This implementation however, will require additional clinician education, updated guidelines, and end-user engagement.

Clinical risk prediction in glaucoma

Glaucoma interventions

Elevated IOP is the single most important risk factor for the development and progression of POAG, particularly since IOP remains the only known modifiable risk factor (Conlon, Saheb, and Ahmed 2017). Results from the landmark Collaborative Initial Glaucoma Treatment Study showed that the topical IOP-lowering medications and trabeculectomy were equally effective in preventing glaucomatous visual field progression (Musch et al. 2009), while quality of life

scores and rates of cataract surgery were significantly better in the medication group (Janz et al. 2001; Lichter et al. 2001). This is consistent with trends of less invasive treatments being increasingly favored for the management of glaucoma over the past decade (Conlon, Saheb, and Ahmed 2017). This is exemplified by the growing use of minimally-invasive implantable glaucoma drainage devices for lowering IOP, collectively termed microinvasive glaucoma surgery (MIGS) (Chadha et al. 2019; Conlon, Saheb, and Ahmed 2017).

MIGS is commonly performed in conjunction with cataract surgery, where the risks of intraocular surgery (such as infection, bleeding, or macular oedema) have already been justified (Conlon, Saheb, and Ahmed 2017). This new class of glaucoma procedures are considered an alternative to topical medications for the management of early to moderate glaucoma or ocular hypertension (Megevand and Bron 2020; Poitras et al. 2019). However, there is currently limited and short-term evidence on the safety, efficacy and cost-effectiveness of these new surgical techniques, particularly when compared to traditional IOP-lowering options such as topical medications (Megevand and Bron 2020). For instance, the additional IOP-lowering benefits of MIGS compared to that obtained from cataract surgery alone was reported to be small or non-significant in randomised controlled trials (Fernández-Barrientos et al. 2010; Craven et al. 2012; Vold et al. 2016; Antonio M. Fea 2010; Antonio Maria Fea et al. 2015; Pfeiffer et al. 2015). My original contribution to the literature was delineating the IOP-lowering effects of phacoemulsification cataract surgery in a prospective, multicentre, matched case-control study (Chapter 5) (Ayub Qassim, Walland, et al. 2020). Cataract surgery alone achieved a clinically significant IOP reduction of 3 mmHg in a third of the eyes, with the greatest benefit seen in those with a higher preoperative IOP and fewer topical glaucoma medications. This study serves as a benchmark on the expected IOP reduction from cataract surgery, particularly in the context of high-tension glaucoma or ocular hypertension where the magnitude of IOP reduction was greatest (Ayub Qassim, Walland, et al. 2020; Masis et al. 2018). Nonetheless, the IOP-lowering effect of cataract surgery alone may be short-lived, and as such there may be a potential advantage of MIGS in maintaining longer-term reductions in IOP (Ayub Qassim, Walland, et al. 2020; Masis et al. 2018; Pfeiffer et al. 2015). Additional clinical experience and reports of long-term outcomes of the MIGS trials is needed to guide the clinical application of MIGS in routine glaucoma care.

The shift towards less invasive glaucoma treatment options is further supported by the recently published findings from the LiGHT study, which showed equivalent health-related quality of life at 3 years and IOP-lowering efficacy between SLT and topical medications as first-line POAG treatment options (Gus Gazzard et al. 2019). SLT is an attractive treatment option for glaucoma due to its lower cost compared to the long term use of topical medications (Gus

Gazzard et al. 2019), and the possibility of maintaining drop-free IOP control in a majority of POAG patients (up to two-thirds of the eyes 18 months with no adverse outcomes) (Anurag Garg et al. 2020). Despite its general effectiveness, some POAG patients may continue to progress after SLT, and in some cases, repeat SLT treatment may be required (Anurag Garg et al. 2020). One of the key outcomes of this thesis was demonstrating the clinical utility of patient-administered home tonometry during the post-SLT follow-up period (Chapter 5) (Mona S. Awadalla et al. 2020). In a pilot study, we demonstrated that patients were able to effectively self-measure their IOP using a home tonometer, with resulting data readily accessible by the treating clinicians (Mona S. Awadalla et al. 2020). This is of particular relevance to patients living in remote areas, where this approach could replace follow-up visits to assess IOP response and save on travel costs. A major limitation is the need to train patients on using the home tonometer to be able to generate reliable measurements. However, in our experience this could be overcome by careful instructions (including print material), and patient engagement in the process and outcome of the research. Moreover, device reliability and ease of use are expected to improve with subsequent iterations of home tonometry devices, particularly with the increasing uptake of these devices in clinical practice.

IOP fluctuation

Another utility of home tonometry is measuring the diurnal IOP profile, which is thought to be an important risk factor for glaucoma progression (Asrani et al. 2000; J. H. K. Liu et al. 2003). IOP measurements in-clinic represent the value of IOP at a ‘snapshot in time’ and do not necessarily reflect the short- and long-term variations in IOP (K. Mansouri et al. 2020). A more comprehensive and accurate IOP profile would be highly valuable in guiding glaucoma therapeutic interventions, which are currently limited to the infrequent IOP readings made mostly during office hours (K. Mansouri et al. 2020). While home tonometry is relatively affordable and accurate, it has several drawbacks that limit its widespread use. Rebound tonometry is significantly affected by corneal biomechanics, and results are particularly unreliable in the extremes of corneal thickness (Takagi, Sawada, and Yamamoto 2017; Termühlen et al. 2016). Additionally, the reliability of IOP measurements is highly dependant on the operator; from our experience and those from previous studies, nearly a third of patients were unable to generate a completely reliable set of measurements over a few days (Chapter 4) (Ayub Qassim, Awadalla, et al. 2020; Asrani et al. 2000). Finally, obtaining nocturnal IOP measurements — which is known to increase relative to daytime, particularly in individuals with POAG — is particularly difficult and currently not possible without sleep interruption (J. H. K. Liu et al. 2003). Although instructing patients in optimal device usage may be initially labour-intensive, home tonometry could replace the previously used strategy of an overnight hospital admission for obtaining a diurnal IOP profile (Barkana et al. 2006).

Continuous measurements of ambulatory IOP-related patterns can be better achieved using a contact lens sensor technology such as the Triggerfish telemetric device (SENSIMED AG, Lausanne, Switzerland) (Ittoop et al. 2016). This system measures the corneal curvature changes (in electronic units of millivolt equivalents) in response to variations in IOP, and offers the potential of estimating a nearly uninterrupted 24-hour IOP profile (K. Mansouri and Shaarawy 2011). Thus, such a contact lens sensor system overcomes most of the limitations of portable home tonometry in measuring diurnal IOP profile. However, there are several barriers to the clinical utility of continuous IOP monitoring using a contact lens sensor. Importantly, the measured signal output of Triggerfish telemetry does not directly correlate to IOP measurements made by Goldmann applanation tonometry (Cutolo et al. 2019; Pajic, Pajic-Eggspuchler, and Haefliger 2011). A contact lens sensor does not measure the same phenomenon as applanation tonometry; rather, it indirectly estimates IOP-related patterns by measuring changes in the ocular surface dimensions that are most likely attributable to IOP (K. Mansouri et al. 2020). This is further confounded by the limited reproducibility of the contract lens sensor output curves. In one study, reproducibility of Triggerfish signal patterns over a one week interval was estimated using Pearson's correlation to be 0.59, indicating a moderate reproducibility (K. Mansouri et al. 2012). These limitations are apparent when using a contact lens sensor to monitor the effects of IOP-lowering interventions. Several studies have reported either no, or very small changes in the contract lens sensor output curves after SLT, phacoemulsification, or initiation of topical medications (Kaweh Mansouri, Medeiros, and Weinreb 2015; Tojo, Oka, et al. 2014; Aptel et al. 2017; Tojo, Otsuka, et al. 2014). Furthermore, adverse effects of using the device, such as blurred vision and conjunctival hyperemia, are very common (reported in more than 80% in one study) and may further limit routine clinical utility (K. Mansouri et al. 2012). While contract lens sensors remain a valuable research tool, these limitations need to be addressed prior to a wider clinical adoption.

Newer technologies of measuring diurnal IOP profile would allow a better understanding of the role of IOP fluctuation on glaucoma progression. One novel approach is by using an implantable telemetric sensor, such as the recently developed prototype wireless IOP transducer (Implandata Ophthalmic Products GmbH, Hannover, Germany) (Melki, Todani, and Cherfan 2014). Preliminary reports indicate an acceptable safety profile, and accurate measurements of IOP with a good correlation to applanation tonometry (Melki, Todani, and Cherfan 2014; Enders et al. 2019; Koutsonas et al. 2015).

An alternate approach is using genetic risk scores as biomarkers of the risk of higher IOP, including outside office hours (Chapter 4) (Ayub Qassim, Awadalla, et al. 2020). In an original

investigation, I reported that a higher IOP PRS was a significant predictor of higher mean IOP, maximum IOP, highest recorded early-morning IOP, and IOP fluctuation, even after adjusting for recent in-clinic Goldmann applanation tonometry measurements (Chapter 4) (Ayub Qassim, Awadalla, et al. 2020). Additionally, eyes in the highest PRS quintile were 5.4-fold more likely to be early-morning IOP spikers than the lowest quintile. These results suggest that an IOP PRS can be used to provide an insight into the diurnal IOP profile, requiring more detailed clinical phenotyping, the results of which may guide additional interventions to improve IOP control (Ayub Qassim, Awadalla, et al. 2020).

Corneal biomechanics

Progressive glaucomatous neurodegeneration can occur despite good IOP control (Jost B. Jonas et al. 2017). This has led researchers to investigate IOP-independent ocular and systemic risk factors of glaucoma onset and progression (Ernest et al. 2013). Corneal biomechanics were one of the earliest recognised risk factors that gained increased attention following the results of the OHTS study, where individuals with a lower CCT were at a significantly higher risk of developing glaucoma (Gordon et al. 2002, 2007). The notion that CCT was independent of elevated IOP as a risk factor for glaucoma has been strongly debated in the literature (Sng, Ang, and Barton 2017; Belovay and Goldberg 2018; Brandt 2007; Gordon and Kass 2018). Despite this, it is thoroughly accepted that corneal biomechanics including CCT are important in glaucoma management, regardless of whether they merely influence tonometric IOP measurements, or are truly independent markers of optic nerve head vulnerability (H. A. Quigley 2019; Brandt 2004). Importantly, central corneal thickness, as measured by ultrasound pachymetry, is only one of many biomechanical properties of the cornea.

Recent technical advances have allowed *in vivo* measurement of several corneal biomechanical properties. Corneal hysteresis — a measure of the corneal viscous damping of an applied airpuff as captured by the Ocular Response Analyser (Reichert Inc, Buffalo, New York) — has gained considerable traction as a novel risk factor of glaucoma development and progression (Chapter 1) (B. Zhang et al. 2019; C. N. Susanna et al. 2018; Felipe A. Medeiros et al. 2013). It is hypothesised that a less deformable or a stiffer cornea is unable to disperse the IOP-mediated stress in the anterior chamber effectively, leading to a greater stress on the optic nerve head. Additionally, corneal stiffness may be an indirect measure of stiffness in the lamina cribrosa and peripapillary sclera, the primary site of retinal ganglion cell axon vulnerability as they exit the globe (Harry A. Quigley 1981). It should be noted that these hypotheses have not been proven histologically, and are based on the anatomical continuum between these tissues, the similarity in their extracellular composition, and other correlations

made using posterior segment OCT images (K. M. Lee et al. 2019; Lanzagorta-Aresti et al. 2017; Zimprich et al. 2020). Furthermore, corneal hysteresis is a dynamic measurement that is influenced by IOP, age, sex, and ethnicity, and is not directly a measurement of corneal rigidity, stiffness, or elasticity (B. Zhang et al. 2019; Dupps 2007). Ultimately however, the clinical utility of any static or dynamic corneal biomechanical property (such as CCT or corneal hysteresis, respectively) depends on the evidence of their utility in guiding clinical management.

In my original contribution to knowledge, I reported that a higher corneal stiffness parameter (SP-A1) was synergistic with lower CCT as risk factors of glaucoma progression (Chapter 6) (Ayub Qassim, Mullany, et al. 2020). The corneal stiffness parameter can be measured using a high-speed Scheimpflug camera (Corvis ST, Oculus Optikgeräte GmbH, Wetzlar, Germany) which measures the dynamic corneal deformation response to an airpuff (Hong et al. 2013; Roberts et al. 2017). This work has significant implications for the clinical care of early glaucoma patients. The corneal stiffness parameter is not traditionally accounted for when CCT is measured by ultrasound pachymetry. Our results show that measurements of corneal stiffness parameter and CCT can be thought of as a composite corneal risk factor of structural and functional glaucoma progression (Chapter 6) (Ayub Qassim, Mullany, et al. 2020). These findings support the clinical utility of corneal biomechanics in the management of early glaucoma patients, and that such biomechanical properties may infer glaucoma risk that is not solely attributable to IOP. Additionally, Corvis ST may be a preferred tool for early glaucoma screening as it measures IOP, CCT, corneal stiffness parameter, and biomechanically-corrected IOP in a single test (Joda et al. 2016; Roberts et al. 2017).

Corneal biomechanical properties will most likely be implemented into routine glaucoma care in the future. It is increasingly apparent that corneal biomechanical factors such as hysteresis and stiffness offer additional utility in risk stratifying glaucoma patients (Gaspar, Pinto, and Sousa 2017). Moreover, there is a growing understanding that traditional IOP measurements made using applanation or rebound tonometry are far more limited than previously thought (Gerassimos Lascaratos et al. 2014; Founti et al. 2020; B. N. Susanna, Ogata, Daga, et al. 2019; Brandt 2004). Biomechanically-adjusted IOP is superior to traditional applanation tonometry in several ways: it is a better estimate of an experimentally-derived ‘true’ anterior chamber IOP (Eliasy et al. 2018); it is a statistically better predictor of glaucoma progression (B. N. Susanna, Ogata, Daga, et al. 2019; Founti et al. 2020; Gerassimos Lascaratos et al. 2014); it has a greater repeatability and reproducibility (Kotecha et al. 2010; Hong et al. 2013; B. T. Lopes et al. 2017); and it is less affected by corneal diseases such as keratoconus, or refractive surgery (Bao et al. 2020; Mollan et al. 2008).

Corneal biomechanical measurement devices have not yet been widely adopted in glaucoma care. This is likely attributable to the somewhat recent development and commercialisation of these devices, and the evolving literature supporting their use. There is also a relatively high barrier of upfront device purchase costs compared to traditional tonometers. Undoubtedly, the role of corneal biomechanics in glaucoma management will continue to be better understood in coming years. Further research results will likely continue to emerge since the Ocular Response Analyser was the tonometer used in two recent landmark trials in ophthalmology: the UK Biobank Eye and Vision Consortium, and The United Kingdom Glaucoma Treatment Study (D. F. Garway-Heath et al. 2013; Chua et al. 2019). This will help address the gaps in knowledge regarding the clinical utility of corneal biomechanics in glaucoma management, such as the effects of medications or ocular surgeries; the utility of longitudinal measurements; replication of the findings in other cohorts; and the validation of its use in different ethnicities or glaucoma subtypes. Nonetheless, given the high reliability and repeatability of corneal biomechanical properties (B. T. Lopes et al. 2017), and the added accuracy of corneal-compensated IOP to traditionally measured IOP (e.g. Goldmann applanation), it is likely that advanced tonometers such as the Corvis ST or ORA will be a part of the standard of glaucoma care in the future.

Conclusion

Glaucomatous optic neuropathy is a heterogeneous group of disorders that can lead to progressive and irreversible vision loss. Our understanding of glaucoma and its clinical and genetic risk factors has markedly evolved over the last two decades (H. A. Quigley 2019, 1999). For example, it is now accepted that raised IOP is only one of several factors that lead to the development and progression of glaucomatous optic neuropathy. However, the lack of a standardised definition of glaucoma diagnosis and progression is still one of the key challenges in glaucoma research (H. A. Quigley 2019). Without a uniform agreement on which parameters constitute ‘glaucoma’, we will not be able to effectively compare published studies, leaving us not truly knowing if all participants had the same disease. Fortunately, there is an ongoing effort to achieve this goal in an active discussion currently involving 176 international glaucoma experts (Iyer, Vianna, et al. 2020). This consensus definition aims to incorporate both structural and functional indicators of glaucomatous optic neuropathy, utilising the recent advancements in retinal imaging technology using OCT in the criteriation (Iyer, Vianna, et al. 2020).

Once glaucoma is diagnosed, the next challenge lies within estimating the risk and quantitative rate of disease progression and vision loss. We know from large longitudinal cohort studies that only a minority of individuals with glaucoma have a rapidly progressive disease course that leads to statutory blindness (Saunders et al. 2014; Chauhan et al. 2014; A. Heijl et al. 2013). Similarly, data from the landmark glaucoma treatment trials show that a majority of untreated early glaucoma patients or ocular hypertensives do not progress at all, or do so at a very slow rate (Kass et al. 2002; Leske et al. 2003, 2007; D. F. Garway-Heath et al. 2015). There is currently a gap in our ability to identify individuals before they develop glaucoma, and in those who do develop glaucoma, to predict which patients will progress rapidly. As a consequence, clinicians are left routinely reviewing all early glaucoma patients and glaucoma suspects for several years before being able to establish a trend. This poses a significant burden to the health care system, consuming resources which could be better used on fast progressors requiring more urgent management.

In my PhD thesis, I approached this key issue from two directions. My original contribution to knowledge was contributing to the largest glaucoma genome-wide association study to date, and identifying novel glaucoma-associated gene variants, gene sets, and biological pathways (Chapter 3) (Craig et al. 2020; Xikun Han et al. 2019). In a subsequent translational effort, I demonstrated the clinical utility of a glaucoma polygenic risk score in identifying individuals at the highest-risk of developing glaucoma, glaucoma progression, and having early-morning IOP spikes (Chapter 4) (Ayub Qassim, Awadalla, et al. 2020; A. Qassim et al. 2020; Craig et al. 2020). From the clinical direction, I quantified the IOP-lowering effects of phacoemulsification cataract surgery in early glaucoma, and identified clinical predictors of clinically-significant postoperative IOP reduction (Chapter 5) (Ayub Qassim, Walland, et al. 2020). Finally, I demonstrated the importance of the SP-A1 corneal stiffness parameter as a novel risk factor for progression in glaucoma suspects that acts synergistically with lower CCT (Chapter 6) (Ayub Qassim, Mullany, et al. 2020).

We are now approaching a new era of glaucoma risk stratification and screening. Our expanded knowledge of clinical and genetic risk factors of glaucoma development and progression facilitate focusing our finite resources on a subgroup of individuals who are most likely to benefit from screening, close follow-up, and early intervention. While IOP remains the only modifiable risk factor, researchers remain hopeful of introducing neuroprotective agents in the glaucoma management algorithm (Robert N. Weinreb et al. 2018; Krupin et al. 2011; Hui et al. 2020). With earlier detection, improved risk stratification, and personalised treatment, we ultimately hope to eliminate the global burden of blindness and vision loss from glaucoma. Combined with recent advances in retinal imaging, telemedicine, and artificial intelligence, it

is time to re-evaluate our approach for glaucoma screening and referral pathways (Tan et al. 2020). We ought to move away from relying on absolute IOP cut-offs (e.g. 21 mmHg) and subjective optic nerve head assessments in guiding our decision making for risk stratifying glaucoma suspects or early glaucoma patients (H. A. Quigley 2019; Iyer, Boland, et al. 2020; Vessani et al. 2009). We now have unprecedented access to enormous and well-characterized genomic, transcriptomic, metabolomic and other 'omics' datasets, along with paired phenotypic data involving hundreds of thousands of individuals (The All of Us Research Program Investigators 2019; C. Sudlow et al. 2015; Raina et al. 2009; Z. Chen et al. 2011). New analytical approaches such as deep neural networks (a branch of machine learning) allows efficient use of such 'big data', expanding the scope of artificial intelligence to automated analysis of fundus photographs, OCTs and other imagery (Asaoka et al. 2019; P. Wang et al. 2019; Gulshan et al. 2016). The future of glaucoma research is very promising, with the combination of these resources bringing us a step closer to precision and personalised medicine (Figure 7.2) (Moroi et al. 2019; R. Chen and Snyder 2013; Rajkomar, Dean, and Kohane 2019).

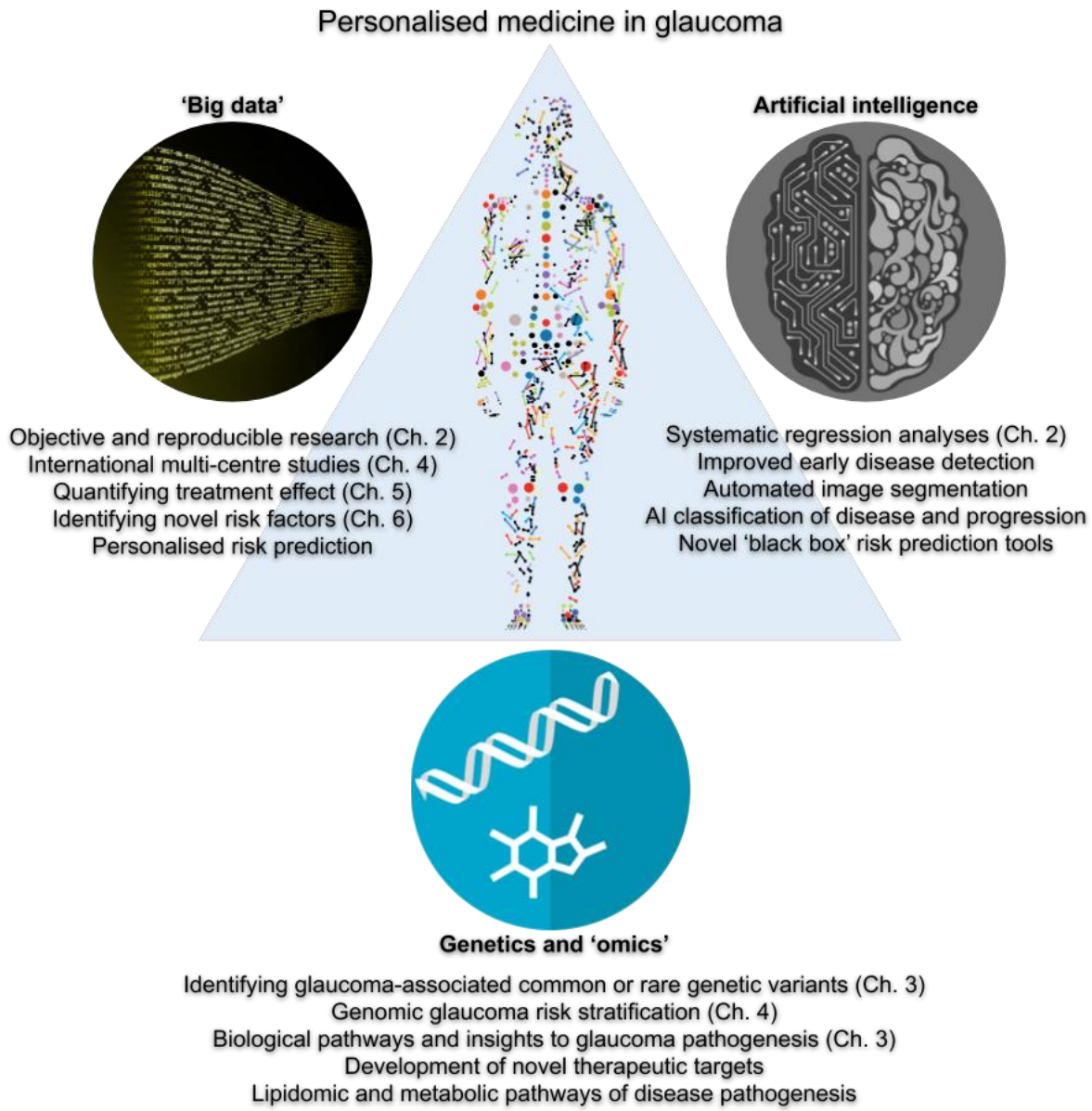

Figure 7.2. Transition to the era of precision and personalised medicine in glaucoma care will be powered by research in genomics, multi-omics, machine learning, and big data. Images used in this figure were freely available for reuse and distribution without restriction or attribution under Creative Commons Zero license (CC0 1.0 Universal).

Bibliography

Abecasis, G. R., D. Altshuler, A. Auton, L. D. Brooks, R. M. Durbin, R. A. Gibbs, M. E. Hurles, and G. A. McVean. 2010. “A Map of Human Genome Variation from Population-Scale Sequencing.” *Nature* 467 (7319). https://doi.org/10.1038/nature09534.

Abe, Ricardo Y., Alberto Diniz-Filho, Linda M. Zangwill, Carolina P. B. Gracitelli, Amir H. Marvasti, Robert N. Weinreb, Saif Baig, and Felipe A. Medeiros. 2016. “The Relative Odds of Progressing by Structural and Functional Tests in Glaucoma.” *Investigative Ophthalmology & Visual Science* 57 (9): OCT421.

“Advanced Glaucoma Intervention Study.” 1994. *Ophthalmology*. https://doi.org/10.1016/s0161-6420(94)31171-7.

Akagi, T., L. M. Zangwill, L. J. Saunders, A. Yarmohammadi, P. I. C. Manalastas, M. H. Suh, C. A. Girkin, J. M. Liebmann, and R. N. Weinreb. 2017. “Rates of Local Retinal Nerve Fiber Layer Thinning before and after Disc Hemorrhage in Glaucoma.” *Ophthalmology* 124 (9). https://doi.org/10.1016/j.ophtha.2017.03.059.

Akinwande, Michael Olusegun, Hussaini Garba Dikko, and Agboola Samson. 2015. “Variance Inflation Factor: As a Condition for the Inclusion of Suppressor Variable(s) in Regression Analysis.” *Open Journal of Statistics* 05 (07): 754–67.

Alward, W. L., Y. H. Kwon, K. Kawase, J. E. Craig, S. S. Hayreh, A. T. Johnson, C. L. Khanna, et al. 2003. “Evaluation of Optineurin Sequence Variations in 1,048 Patients with Open-Angle Glaucoma.” *American Journal of Ophthalmology* 136 (5). https://doi.org/10.1016/s0002-9394(03)00577-4.

Alward, W. L. M., C. van der Heide, C. L. Khanna, B. R. Roos, S. Sivaprasad, J. Kam, R. Ritch, et al. 2019. “Myocilin Mutations in Patients With Normal-Tension Glaucoma.” *JAMA Ophthalmology* 137 (5). https://doi.org/10.1001/jamaophthalmol.2019.0005.

Amano, Shiro, Ryohei Nejima, Kenji Inoue, and Kazunori Miyata. 2019. “Effect of Topical Prostaglandins on the Biomechanics and Shape of the Cornea.” *Graefe’s Archive for Clinical and Experimental Ophthalmology*. https://doi.org/10.1007/s00417-019-04435-7.

Anand, A., C. G. De Moraes, C. C. Teng, C. Tello, J. M. Liebmann, and R. Ritch. 2010. “Corneal Hysteresis and Visual Field Asymmetry in Open Angle Glaucoma.” *Investigative Ophthalmology & Visual Science* 51 (12). https://doi.org/10.1167/iovs.10-5580.

Aoki, Shuichiro, Hiroshi Murata, Masato Matsuura, Yuri Fujino, Shunsuke Nakakura, Yoshitaka Nakao, Yoshiaki Kiuchi, and Ryo Asaoka. 2018. “The Effect of Air Pulse-Driven Whole Eye Motion on the Association between Corneal Hysteresis and Glaucomatous Visual Field Progression.” *Scientific Reports* 8 (1): 868.

Aptel, Florent, Cécile Musson, Thierry Zhou, Antoine Lesoin, and Christophe Chiquet. 2017. “24-Hour Intraocular Pressure Rhythm in Patients With Untreated Primary Open Angle Glaucoma and Effects of Selective Laser Trabeculoplasty.” *Journal of Glaucoma* 26 (3): 272–77.

Ariani, F., I. Longo, P. Frezzotti, C. Pescucci, F. Mari, A. Caporossi, R. Frezzotti, and A. Renieri. 2006. “Optineurin Gene Is Not Involved in the Common High-Tension Form of Primary Open-Angle Glaucoma.” *Graefe’s Archive for Clinical and Experimental Ophthalmology = Albrecht von Graefes Archiv Fur Klinische Und Experimentelle Ophthalmologie* 244 (9). https://doi.org/10.1007/s00417-005-0079-3.

Asaoka, Ryo, Hiroshi Murata, Kazunori Hirasawa, Yuri Fujino, Masato Matsuura, Atsuya Miki, Takashi Kanamoto, et al. 2019. “Using Deep Learning and Transfer Learning to Accurately Diagnose Early-Onset Glaucoma From Macular Optical Coherence Tomography Images.” *American Journal of Ophthalmology* 198 (February): 136–45.

Asrani, Sanjay, Ran Zeimer, Jacob Wilensky, David Gieser, Susan Vitale, and Kim Lindenmuth. 2000. “Large Diurnal Fluctuations in Intraocular Pressure Are an Independent Risk Factor in Patients With Glaucoma.” *Journal of Glaucoma* 9 (2): 134–42.

Atwal, P. S., M. L. Brennan, R. Cox, M. Niaki, J. Platt, M. Homeyer, A. Kwan, et al. 2014. "Clinical Whole-Exome Sequencing: Are We There Yet?" *Genetics in Medicine: Official Journal of the American College of Medical Genetics* 16 (9). https://doi.org/10.1038/gim.2014.10.

Aulchenko, Yurii S., Stephan Ripke, Aaron Isaacs, and Cornelia M. van Duijn. 2007. "GenABEL: An R Library for Genome-Wide Association Analysis." *Bioinformatics* 23 (10): 1294–96.

Aung, T., M. Ozaki, M. C. Lee, U. Schlötzer-Schrehardt, G. Thorleifsson, T. Mizoguchi, R. P. Igo, et al. 2017. "Genetic Association Study of Exfoliation Syndrome Identifies a Protective Rare Variant at LOXL1 and Five New Susceptibility Loci." *Nature Genetics* 49 (7). https://doi.org/10.1038/ng.3875.

Aung, T., T. Rezaie, K. Okada, A. C. Viswanathan, A. H. Child, G. Brice, S. S. Bhattacharya, O. J. Lehmann, M. Sarfarazi, and R. A. Hitchings. 2005. "Clinical Features and Course of Patients with Glaucoma with the E50K Mutation in the Optineurin Gene." *Investigative Ophthalmology & Visual Science* 46 (8). https://doi.org/10.1167/iovs.04-1133.

Awadalla, Mona S., Jude Fitzgerald, Nicholas H. Andrew, Tiger Zhou, Henry Marshall, Ayub Qassim, Mark Hassall, et al. 2018. "Prevalence and Type of Artefact with Spectral Domain Optical Coherence Tomography Macular Ganglion Cell Imaging in Glaucoma Surveillance." Edited by Laura J. Frishman. https://doi.org/10.1371/journal.pone.0206684.

Awadalla, Mona S., Ayub Qassim, Mark Hassall, Thi T. Nguyen, John Landers, and Jamie E. Craig. 2020. "Using Icare HOME Tonometry for Follow-up of Patients with Open-angle Glaucoma before and after Selective Laser Trabeculoplasty." *Clinical & Experimental Ophthalmology* 48 (3): 328–33.

Awadalla, M. S., J. H. Fingert, B. E. Roos, S. Chen, R. Holmes, S. L. Graham, M. Chehade, et al. 2015. "Copy Number Variations of TBK1 in Australian Patients with Primary Open-Angle Glaucoma." *American Journal of Ophthalmology* 159 (1). https://doi.org/10.1016/j.ajo.2014.09.044.

Azuma, Noriyuki, Yuki Yamaguchi, Hiroshi Handa, Keiko Tadokoro, Atsuko Asaka, Eriko Kawase, and Masao Yamada. 2003. "Mutations of the PAX6 Gene Detected in Patients with a Variety of Optic-Nerve Malformations." *American Journal of Human Genetics* 72 (6): 1565–70.

Bailey, Jessica N. Cooke, Stephanie J. Loomis, Jae H. Kang, R. Rand Allingham, Puya Gharahkhani, Chiea Chuen Khor, Kathryn P. Burdon, et al. 2016. "Genome-Wide Association Analysis Identifies TXNRD2, ATXN2 and FOXC1 as Susceptibility Loci for Primary Open-Angle Glaucoma." *Nature Genetics* 48 (2): 189–94.

Bao, F., W. Huang, R. Zhu, N. Lu, Y. Wang, H. Li, S. Wu, et al. 2020. "Effectiveness of the Goldmann Applanation Tonometer, the Dynamic Contour Tonometer, the Ocular Response Analyzer and the Corvis ST in Measuring Intraocular Pressure Following FS-LASIK." *Current Eye Research* 45 (2). https://doi.org/10.1080/02713683.2019.1660794.

Barkana, Yaniv, Sarah Anis, Jeffrey Liebmann, Celso Tello, and Robert Ritch. 2006. "Clinical Utility of Intraocular Pressure Monitoring Outside of Normal Office Hours in Patients With Glaucoma." *Archives of Ophthalmology*. https://doi.org/10.1001/archopht.124.6.793.

Bates, Douglas, Martin Mächler, Ben Bolker, and Steve Walker. 2015. "Fitting Linear Mixed-Effects Models Using lme4." *Journal of Statistical Software* 67 (1). https://doi.org/10.18637/jss.v067.i01.

Bayer, Atilla, Paul Harasymowycz, Jeffrey D. Henderer, William G. Steinmann, and George L. Spaeth. 2002. "Validity of a New Disk Grading Scale for Estimating Glaucomatous Damage: Correlation with Visual Field Damage." *American Journal of Ophthalmology*. https://doi.org/10.1016/s0002-9394(02)01422-8.

Bearpark, H., L. Elliott, R. Grunstein, S. Cullen, H. Schneider, W. Althaus, and C. Sullivan. 1995. "Snoring and Sleep Apnea. A Population Study in Australian Men." *American Journal of Respiratory and Critical Care Medicine* 151 (5). https://doi.org/10.1164/ajrccm.151.5.7735600.

Beckers, Henny J. M., Jan S. A. G. Schouten, Carroll A. B. Webers, Rikkert van der Valk, and Fred Hendrikse. 2008. “Side Effects of Commonly Used Glaucoma Medications: Comparison of Tolerability, Chance of Discontinuation, and Patient Satisfaction.” *Graefe’s Archive for Clinical and Experimental Ophthalmology = Albrecht von Graefes Archiv Fur Klinische Und Experimentelle Ophthalmologie* 246 (10): 1485–90.

Begg, I. S., S. M. Drance, and V. P. Sweeney. 1971. “Ischaemic Optic Neuropathy in Chronic Simple Glaucoma.” *The British Journal of Ophthalmology* 55 (2). https://doi.org/10.1136/bjo.55.2.73.

Behjati, S., and P. S. Tarpey. 2013. “What Is next Generation Sequencing?” *Archives of Disease in Childhood. Education and Practice Edition* 98 (6). https://doi.org/10.1136/archdischild-2013-304340.

Belotti, Edwige, Tania M. Puvirajesinghe, Stéphane Audebert, Emilie Baudelet, Luc Camoin, Michel Pierres, Lea Lasvaux, Géraldine Ferracci, Mireille Montcouquiol, and Jean-Paul Borg. 2012. “Molecular Characterisation of Endogenous Vangl2/Vangl1 Heteromeric Protein Complexes.” *PloS One* 7 (9): e46213.

Belovay, G. W., and I. Goldberg. 2018. “The Thick and Thin of the Central Corneal Thickness in Glaucoma.” *Eye* 32 (5). https://doi.org/10.1038/s41433-018-0033-3.

Bengtsson, B. 1976. “The Variation and Covariation of Cup and Disc Diameters.” *Acta Ophthalmologica* 54 (6): 804–18.

Bengtsson, B., and A. Heijl. 2000. “False-Negative Responses in Glaucoma Perimetry: Indicators of Patient Performance or Test Reliability?” *American Journal of Ophthalmology*. https://doi.org/10.1016/s0002-9394(00)00758-3.

Bengtsson, Boel, M. Cristina Leske, Leslie Hyman, and Anders Heijl. 2007. “Fluctuation of Intraocular Pressure and Glaucoma Progression in the Early Manifest Glaucoma Trial.” *Ophthalmology* 114 (2): 205–9.

Benjamini, Yoav, and Yosef Hochberg. 1995. “Controlling the False Discovery Rate: A Practical and Powerful Approach to Multiple Testing.” *Journal of the Royal Statistical Society. Series B, Statistical Methodology* 57 (1): 289–300.

Bernth-Petersen, Peter, and Elsa Bach. 1983. “EPIDEMIOLOGIC ASPECTS OF CATARACT SURGERY: III: Frequencies of Diabetes and Glaucoma in a Cataract Population.” *Acta Ophthalmologica* 61 (3): 406–16.

Blumberg, D., A. Skaat, and J. M. Liebmann. 2015. “Emerging Risk Factors for Glaucoma Onset and Progression.” *Progress in Brain Research* 221. https://doi.org/10.1016/bs.pbr.2015.04.007.

Boer, Johannes F. de, Barry Cense, B. Hyle Park, Mark C. Pierce, Guillermo J. Tearney, and Brett E. Bouma. 2003. “Improved Signal-to-Noise Ratio in Spectral-Domain Compared with Time-Domain Optical Coherence Tomography.” *Optics Letters* 28 (21): 2067.

Boland, M. V., P. Gupta, F. Ko, D. Zhao, E. Guallar, and D. S. Friedman. 2016. “Evaluation of Frequency-Doubling Technology Perimetry as a Means of Screening for Glaucoma and Other Eye Diseases Using the National Health and Nutrition Examination Survey.” *JAMA Ophthalmology* 134 (1). https://doi.org/10.1001/jamaophthalmol.2015.4459.

Bonomi, L., G. Marchini, M. Marraffa, P. Bernardi, I. De Franco, S. Perfetti, A. Varotto, and V. Tenna. 1998. “Prevalence of Glaucoma and Intraocular Pressure Distribution in a Defined Population. The Egna-Neumarkt Study.” *Ophthalmology* 105 (2). https://doi.org/10.1016/s0161-6420(98)92665-3.

Boote, Craig, Ian A. Sigal, Rafael Grytz, Yi Hua, Thao D. Nguyen, and Michael J. A. Girard. 2020. “Scleral Structure and Biomechanics.” *Progress in Retinal and Eye Research*. https://doi.org/10.1016/j.preteyeres.2019.100773.

Bourne, Rupert R. A., Hugh R. Taylor, Seth R. Flaxman, Jill Keeffe, Janet Leasher, Kovin Naidoo, Konrad Pesudovs, et al. 2016. “Number of People Blind or Visually Impaired by Glaucoma Worldwide and in World Regions 1990 – 2010: A Meta-Analysis.” *PloS One* 11 (10): e0162229.

Boyle, E. A., Y. I. Li, and J. K. Pritchard. 2017. “An Expanded View of Complex Traits: From Polygenic to Omnigenic.” *Cell* 169 (7). https://doi.org/10.1016/j.cell.2017.05.038.

Bradley, J. M., A. M. Anderssohn, C. M. Colvis, D. E. Parshley, X. H. Zhu, M. S. Ruddat, J.

R. Samples, and T. S. Acott. 2000. “Mediation of Laser Trabeculoplasty-Induced Matrix Metalloproteinase Expression by IL-1beta and TNFalpha.” *Investigative Ophthalmology & Visual Science* 41 (2). https://pubmed.ncbi.nlm.nih.gov/10670472/.

Brandt, J. D. 2004. “Corneal Thickness in Glaucoma Screening, Diagnosis, and Management.” *Current Opinion in Ophthalmology* 15 (2). https://doi.org/10.1097/00055735-200404000-00004.

———. 2007. “Central Corneal Thickness, Tonometry, and Glaucoma Risk--a Guide for the Perplexed.” *Canadian Journal of Ophthalmology. Journal Canadien D’ophtalmologie* 42 (4). https://pubmed.ncbi.nlm.nih.gov/17641698/.

Breckenridge, C. B., C. Berry, E. T. Chang, R. L. Sielken, and J. S. Mandel. 2016. “Association between Parkinson’s Disease and Cigarette Smoking, Rural Living, Well-Water Consumption, Farming and Pesticide Use: Systematic Review and Meta-Analysis.” *PloS One* 11 (4). https://doi.org/10.1371/journal.pone.0151841.

Browning, S. R., and B. L. Browning. 2007. “Rapid and Accurate Haplotype Phasing and Missing-Data Inference for Whole-Genome Association Studies by Use of Localized Haplotype Clustering.” *American Journal of Human Genetics* 81 (5). https://doi.org/10.1086/521987.

Brubaker, Richard F. 2001. “Measurement of Uveoscleral Outflow in Humans.” *Journal of Glaucoma* 10 (5): S45.

Budu-Aggrey, Ashley, Pirro Hysi, Patrick G. Kehoe, Robert P. Igo, Janey Wiggs, Jessica Cooke Bailey, Jonathan Haines, et al. 2020. “The Relationship between Open Angle Glaucoma, Optic Disc Morphology and Alzheimer’s Disease: A Mendelian Randomization Study.” *medRxiv*.

Burdon, Kathryn P., April Crawford, Robert J. Casson, Alex W. Hewitt, John Landers, Patrick Danoy, David A. Mackey, Paul Mitchell, Paul R. Healey, and Jamie E. Craig. 2012. “Glaucoma Risk Alleles at CDKN2B-AS1 Are Associated with Lower Intraocular Pressure, Normal-Tension Glaucoma, and Advanced Glaucoma.” *Ophthalmology* 119 (8): 1539–45.

Burdon, K. P., S. Macgregor, A. W. Hewitt, S. Sharma, G. Chidlow, R. A. Mills, P. Danoy, et al. 2011. “Genome-Wide Association Study Identifies Susceptibility Loci for Open Angle Glaucoma at TMCO1 and CDKN2B-AS1.” *Nature Genetics* 43 (6). https://doi.org/10.1038/ng.824.

Burgoyne, Claude F., J. Crawford Downs, Anthony J. Bellezza, J. -K. Francis Suh, and Richard T. Hart. 2005. “The Optic Nerve Head as a Biomechanical Structure: A New Paradigm for Understanding the Role of IOP-Related Stress and Strain in the Pathophysiology of Glaucomatous Optic Nerve Head Damage.” *Progress in Retinal and Eye Research*. https://doi.org/10.1016/j.preteyeres.2004.06.001.

Burr, J. M., G. Mowatt, R. Hernández, M. A. R. Siddiqui, J. Cook, T. Lourenco, C. Ramsay, et al. 2007. “The Clinical Effectiveness and Cost-Effectiveness of Screening for Open Angle Glaucoma: A Systematic Review and Economic Evaluation.” *Health Technology Assessment* 11 (41): iii – iv, ix – x, 1–190.

Burr, J., G. Mowatt, R. Hernández, M. Siddiqui, J. Cook, T. Lourenco, C. Ramsay, et al. 2007. “The Clinical Effectiveness and Cost-Effectiveness of Screening for Open Angle Glaucoma: A Systematic Review and Economic Evaluation.” *Health Technology Assessment* 11 (41). https://doi.org/10.3310/hta11410.

Bussel, I. I., G. Wollstein, and J. S. Schuman. 2014. “OCT for Glaucoma Diagnosis, Screening and Detection of Glaucoma Progression.” *The British Journal of Ophthalmology* 98 Suppl 2 (Suppl 2). https://doi.org/10.1136/bjophthalmol-2013-304326.

Bycroft, Clare, Colin Freeman, Desislava Petkova, Gavin Band, Lloyd T. Elliott, Kevin Sharp, Allan Motyer, et al. 2018. “The UK Biobank Resource with Deep Phenotyping and Genomic Data.” *Nature* 562 (7726): 203–9.

Campbell, Robert J., Graham E. Trope, Rony Rachmiel, and Yvonne M. Buys. 2008. “Glaucoma Laser and Surgical Procedure Rates in Canada: A Long-Term Profile.” *Canadian Journal of Ophthalmology. Journal Canadien D’ophtalmologie* 43 (4): 449–53.

Camras, Carl B., Carol B. Toris, and Richard R. Tamesis. 1999. “Efficacy and Adverse Effects of Medications Used in the Treatment of Glaucoma.” *Drugs & Aging*. https://doi.org/10.2165/00002512-199915050-00005.

Caprioli, J., and A. L. Coleman. 2008. “Intraocular Pressure Fluctuation a Risk Factor for Visual Field Progression at Low Intraocular Pressures in the Advanced Glaucoma Intervention Study.” *Ophthalmology* 115 (7). https://doi.org/10.1016/j.ophtha.2007.10.031.

Caprioli, Joseph, John Mark de Leon, Parham Azarbod, Andrew Chen, Esteban Morales, Kouros Nouri-Mahdavi, Anne Coleman, Fei Yu, and Abdelmonem Afifi. 2016. “Trabeculectomy Can Improve Long-Term Visual Function in Glaucoma.” *Ophthalmology* 123 (1): 117–28.

Casey, Jillian, Riki Kawaguchi, Maria Morrissey, Hui Sun, Paul McGettigan, Jens E. Nielsen, Judith Conroy, et al. 2011. “First Implication of STRA6 Mutations in Isolated Anophthalmia, Microphthalmia, and Coloboma: A New Dimension to the STRA6 Phenotype.” *Human Mutation* 32 (12): 1417–26.

Casson, Robert J., Glyn Chidlow, John P. M. Wood, Jonathan G. Crowston, and Ivan Goldberg. 2012. “Definition of Glaucoma: Clinical and Experimental Concepts.” *Clinical & Experimental Ophthalmology* 40 (4): 341–49.

Casson, Robert J., Bruce James, Adrian Rubinstein, and Haggai Ali. 2001. “Clinical Comparison of Frequency Doubling Technology Perimetry and Humphrey Perimetry.” *The British Journal of Ophthalmology* 85 (3). https://doi.org/10.1136/bjo.85.3.360.

Cavodeassi, Florencia, Kenzo Ivanovitch, and Stephen W. Wilson. 2013. “Eph/Ephrin Signalling Maintains Eye Field Segregation from Adjacent Neural Plate Territories during Forebrain Morphogenesis.” *Development* 140 (20): 4193–4202.

Cello, Kimberly E., Jacqueline M. Nelson-Quigg, and Chris A. Johnson. 2000. “Frequency Doubling Technology Perimetry for Detection of Glaucomatous Visual Field Loss.” *American Journal of Ophthalmology* 129 (3): 314–22.

Chadha, N., J. L. Warren, J. Liu, J. C. Tsai, and C. C. Teng. 2019. “Seven- and Eight-Year Trends in Resident and Fellow Glaucoma Surgical Experience.” *Clinical Ophthalmology* 13 (February). https://doi.org/10.2147/OPTH.S185529.

Chakravarthy, U., C. Augood, G. C. Bentham, P. T. de Jong, M. Rahu, J. Seland, G. Soubrane, et al. 2007. “Cigarette Smoking and Age-Related Macular Degeneration in the EUREYE Study.” *Ophthalmology* 114 (6). https://doi.org/10.1016/j.ophtha.2006.09.022.

Chakravarthy, U., E. Biundo, R. O. Saka, C. Fasser, R. Bourne, and J. A. Little. 2017. “The Economic Impact of Blindness in Europe.” *Ophthalmic Epidemiology* 24 (4). https://doi.org/10.1080/09286586.2017.1281426.

Chang, B., R. S. Smith, M. Peters, O. V. Savinova, N. L. Hawes, A. Zabaleta, S. Nusinowitz, et al. 2001. “Haploinsufficient Bmp4 Ocular Phenotypes Include Anterior Segment Dysgenesis with Elevated Intraocular Pressure.” *BMC Genetics* 2 (November): 18.

Chan, Michelle P. Y., David C. Broadway, Anthony P. Khawaja, Jennifer L. Y. Yip, David F. Garway-Heath, Jennifer M. Burr, Robert Luben, et al. 2017. “Glaucoma and Intraocular Pressure in EPIC-Norfolk Eye Study: Cross Sectional Study.” *BMJ* 358 (September): j3889.

Chan, Michelle P. Y., Carlota M. Grossi, Anthony P. Khawaja, Jennifer L. Y. Yip, Kay-Tee Khaw, Praveen J. Patel, Peng T. Khaw, James E. Morgan, Stephen A. Vernon, and Paul J. Foster. 2016. “Associations with Intraocular Pressure in a Large Cohort.” *Ophthalmology* 123 (4): 771–82.

Chan, T. C. W., C. Bala, A. Siu, F. Wan, and A. White. 2017. “Risk Factors for Rapid Glaucoma Disease Progression.” *American Journal of Ophthalmology* 180 (August). https://doi.org/10.1016/j.ajo.2017.06.003.

Chapman, K., T. Ferreira, A. Morris, J. Asimit, and E. Zeggini. 2011. “Defining the Power Limits of Genome-Wide Association Scan Meta-Analyses.” *Genetic Epidemiology* 35 (8). https://doi.org/10.1002/gepi.20627.

Cha, Seongwon, Ji Eun Lim, Ah Yeon Park, Jun-Hyeong Do, Si Woo Lee, Chol Shin, Nam

Han Cho, et al. 2018. “Identification of Five Novel Genetic Loci Related to Facial Morphology by Genome-Wide Association Studies.” *BMC Genomics* 19 (1): 481.
Chatterjee, N., J. Shi, and M. García-Closas. 2016. “Developing and Evaluating Polygenic Risk Prediction Models for Stratified Disease Prevention.” *Nature Reviews. Genetics* 17 (7). https://doi.org/10.1038/nrg.2016.27.
Chauhan, B. C., R. Malik, L. M. Shuba, P. E. Rafuse, M. T. Nicolela, and P. H. Artes. 2014. “Rates of Glaucomatous Visual Field Change in a Large Clinical Population.” *Investigative Ophthalmology & Visual Science* 55 (7). https://doi.org/10.1167/iovs.14-14643.
Chauhan, B. C., J. R. Vianna, G. P. Sharpe, S. Demirel, C. A. Girkin, C. Y. Mardin, A. F. Scheuerle, and C. F. Burgoyne. 2020. “Differential Effects of Aging in the Macular Retinal Layers, Neuroretinal Rim, and Peripapillary Retinal Nerve Fiber Layer.” *Ophthalmology* 127 (2). https://doi.org/10.1016/j.ophtha.2019.09.013.
Cheng, Ching-Yu, Maria Schache, M. Kamran Ikram, Terri L. Young, Jeremy A. Guggenheim, Veronique Vitart, Stuart MacGregor, et al. 2013. “Nine Loci for Ocular Axial Length Identified through Genome-Wide Association Studies, Including Shared Loci with Refractive Error.” *American Journal of Human Genetics* 93 (2): 264–77.
Chen, Rui, and Michael Snyder. 2013. “Promise of Personalized Omics to Precision Medicine.” *Wiley Interdisciplinary Reviews: Systems Biology and Medicine* 5 (1): 73–82.
Chen, X., and P. F. Sullivan. 2003. “Single Nucleotide Polymorphism Genotyping: Biochemistry, Protocol, Cost and Throughput.” *The Pharmacogenomics Journal* 3 (2). https://doi.org/10.1038/sj.tpj.6500167.
Chen, Y., C. Qiu, S. Qian, J. Chen, X. Chen, L. Wang, and X. Sun. 2018. “Lack of Association of rs1192415 in TGFBR3-CDC7 With Visual Field Progression: A Cohort Study in Chinese Open Angle Glaucoma Patients.” *Frontiers in Genetics* 9 (October). https://doi.org/10.3389/fgene.2018.00488.
Chen, Yuhong, Ying Lin, Eranga N. Vithana, Liyun Jia, Xianbo Zuo, Tien Yin Wong, Li Jia Chen, et al. 2014. “Common Variants near ABCA1 and in PMM2 Are Associated with Primary Open-Angle Glaucoma.” *Nature Genetics*. https://doi.org/10.1038/ng.3078.
Chen, Z., J. Chen, R. Collins, Y. Guo, R. Peto, F. Wu, L. Li, and on behalf of the China Kadoorie Biobank (CKB) collaborative group. 2011. “China Kadoorie Biobank of 0.5 Million People: Survey Methods, Baseline Characteristics and Long-Term Follow-Up.” *International Journal of Epidemiology* 40 (6): 1652–66.
Chidlow, Glyn, John P. M. Wood, and Robert J. Casson. 2017. “Investigations into Hypoxia and Oxidative Stress at the Optic Nerve Head in a Rat Model of Glaucoma.” *Frontiers in Neuroscience*. https://doi.org/10.3389/fnins.2017.00478.
Chimusa, E. R., S. Dalvie, C. Dandara, A. Wonkam, and G. K. Mazandu. 2019. “Post Genome-Wide Association Analysis: Dissecting Computational Pathway/network-Based Approaches.” *Briefings in Bioinformatics* 20 (2). https://doi.org/10.1093/bib/bby035.
Chong, Rachel S., Miao-Li Chee, Yih-Chung Tham, Shivani Majithia, Sahil Thakur, Zhen Ling Teo, Zhi Da Soh, et al. 2020. “Association of Anti-Hypertensive Medication with Retinal Nerve Fiber Layer and Ganglion Cell-Inner Plexiform Layer Thickness.” *Ophthalmology*, July. https://doi.org/10.1016/j.ophtha.2020.07.051.
Choquet, Hélène, Seyyedhassan Paylakhi, Stephen C. Kneeland, Khanh K. Thai, Thomas J. Hoffmann, Jie Yin, Mark N. Kvale, et al. 2018. “A Multiethnic Genome-Wide Association Study of Primary Open-Angle Glaucoma Identifies Novel Risk Loci.” *Nature Communications* 9 (1): 2278.
Choquet, Hélène, Khanh K. Thai, Jie Yin, Thomas J. Hoffmann, Mark N. Kvale, Yambazi Banda, Catherine Schaefer, et al. 2017. “A Large Multi-Ethnic Genome-Wide Association Study Identifies Novel Genetic Loci for Intraocular Pressure.” *Nature Communications* 8 (1): 2108.
Chua, Sharon Yu Lin, Dhanes Thomas, Naomi Allen, Andrew Lotery, Parul Desai, Praveen Patel, Zaynah Muthy, et al. 2019. “Cohort Profile: Design and Methods in the Eye and Vision Consortium of UK Biobank.” *BMJ Open* 9 (2): e025077.
Cirrus HD OCT 5000 Manual. 2016. Dublin, CA, USA: Carl Zeiss Meditec, Inc.

Claussnitzer, M., J. H. Cho, R. Collins, N. J. Cox, E. T. Dermitzakis, M. E. Hurles, S. Kathiresan, et al. 2020. “A Brief History of Human Disease Genetics.” *Nature* 577 (7789). https://doi.org/10.1038/s41586-019-1879-7.

Clement, Colin I., Shibal Bhartiya, and Tarek Shaarawy. 2014. “New Perspectives on Target Intraocular Pressure.” *Survey of Ophthalmology* 59 (6): 615–26.

Cnaan, Avital, Nan M. Laird, and Peter Slasor. 1997. “Using the General Linear Mixed Model to Analyse Unbalanced Repeated Measures and Longitudinal Data.” *Statistics in Medicine*. https://doi.org/3.0.co;2-e">10.1002/(sici)1097-0258(19971030)16:20<2349::aid-sim667>3.0.co;2-e.

Collaborative Normal-Tension Glaucoma Study Group. 2001. “Natural History of Normal-Tension Glaucoma.” *Ophthalmology* 108 (2): 247–53.

Colomb, E., T. D. Nguyen, A. Béchetoille, J. C. Dascotte, F. Valtot, A. P. Brézin, M. Berkani, et al. 2001. “Association of a Single Nucleotide Polymorphism in the TIGR/MYOCILIN Gene Promoter with the Severity of Primary Open-Angle Glaucoma.” *Clinical Genetics* 60 (3). https://doi.org/10.1034/j.1399-0004.2001.600308.x.

Congdon, N. G., A. T. Broman, K. Bandeen-Roche, D. Grover, and H. A. Quigley. 2006. “Central Corneal Thickness and Corneal Hysteresis Associated with Glaucoma Damage.” *American Journal of Ophthalmology* 141 (5). https://doi.org/10.1016/j.ajo.2005.12.007.

Conlon, Ronan, Hady Saheb, and Iqbal Ike K. Ahmed. 2017. “Glaucoma Treatment Trends: A Review.” *Canadian Journal of Ophthalmology. Journal Canadien D’ophtalmologie* 52 (1): 114–24.

Consortium, The Haplotype Reference, and the Haplotype Reference Consortium. 2016. “A Reference Panel of 64,976 Haplotypes for Genotype Imputation.” *Nature Genetics*. https://doi.org/10.1038/ng.3643.

Consortium, The Uk10k, and The UK10K Consortium. 2015. “The UK10K Project Identifies Rare Variants in Health and Disease.” *Nature*. https://doi.org/10.1038/nature14962.

Copt, René-Pierre, Ravi Thomas, and André Mermoud. 1999. “Corneal Thickness in Ocular Hypertension, Primary Open-Angle Glaucoma, and Normal Tension Glaucoma.” *Archives of Ophthalmology* 117 (1): 14–16.

Coudrillier, Baptiste, Jing Tian, Stephen Alexander, Kristin M. Myers, Harry A. Quigley, and Thao D. Nguyen. 2012. “Biomechanics of the Human Posterior Sclera: Age- and Glaucoma-Related Changes Measured Using Inflation Testing.” *Investigative Opthalmology & Visual Science*. https://doi.org/10.1167/iovs.11-8009.

Cox, D. R., and N. Reid. 1987. “Parameter Orthogonality and Approximate Conditional Inference.” *Journal of the Royal Statistical Society. Series B, Statistical Methodology* 49 (1): 1–18.

Craig, Jamie E., Xikun Han, Ayub Qassim, Mark Hassall, Jessica N. Cooke Bailey, Tyler G. Kinzy, Anthony P. Khawaja, et al. 2020. “Multitrait Analysis of Glaucoma Identifies New Risk Loci and Enables Polygenic Prediction of Disease Susceptibility and Progression.” *Nature Genetics* 52 (2): 160–66.

Craven, Randy E., Jay L. Katz, Jeffrey M. Wells, and Jane Ellen Giamporcaro. 2012. “Cataract Surgery with Trabecular Micro-Bypass Stent Implantation in Patients with Mild-to-Moderate Open-Angle Glaucoma and Cataract: Two-Year Follow-Up.” *Journal of Cataract and Refractive Surgery* 38 (8): 1339–45.

Crowston, J. G., C. R. Hopley, P. R. Healey, A. Lee, and P. Mitchell. 2004. “The Effect of Optic Disc Diameter on Vertical Cup to Disc Ratio Percentiles in a Population Based Cohort: The Blue Mountains Eye Study.” *The British Journal of Ophthalmology* 88 (6). https://doi.org/10.1136/bjo.2003.028548.

Crow, T. J. 2011. “‘The Missing Genes: What Happened to the Heritability of Psychiatric Disorders?’” *Molecular Psychiatry* 16 (4). https://doi.org/10.1038/mp.2010.92.

Cutolo, Carlo A., Carlos G. De Moraes, Jeffrey M. Liebmann, Kaweh Mansouri, Carlo E. Traverso, and Robert Ritch. 2019. “The Effect of Therapeutic IOP-Lowering Interventions on the 24-Hour Ocular Dimensional Profile Recorded With a Sensing Contact Lens.” *Journal of Glaucoma* 28 (3): 252–57.

Das, Sayantan, Lukas Forer, Sebastian Schönherr, Carlo Sidore, Adam E. Locke, Alan Kwong, Scott I. Vrieze, et al. 2016. “Next-Generation Genotype Imputation Service and Methods.” *Nature Genetics* 48 (10): 1284–87.

Day, N., S. Oakes, R. Luben, K. T. Khaw, S. Bingham, A. Welch, and N. Wareham. 1999. “EPIC-Norfolk: Study Design and Characteristics of the Cohort. European Prospective Investigation of Cancer.” *British Journal of Cancer* 80 Suppl 1 (July): 95–103.

De Moraes, Carlos G., Shaban Demirel, Stuart K. Gardiner, Jeffrey M. Liebmann, George A. Cioffi, Robert Ritch, Mae O. Gordon, and Michael A. Kass. 2012. “Effect of Treatment on the Rate of Visual Field Change in the Ocular Hypertension Treatment Study Observation Group.” *Investigative Ophthalmology & Visual Science* 53 (4): 1704.

De Moraes, Carlos Gustavo, Kaweh Mansouri, Jeffrey M. Liebmann, Robert Ritch, and for the Triggerfish Consortium. 2018. “Association Between 24-Hour Intraocular Pressure Monitored With Contact Lens Sensor and Visual Field Progression in Older Adults With Glaucoma.” *JAMA Ophthalmology* 136 (7): 779.

De Moraes, Carlos V. Gustavo, Victoria Hill, Celso Tello, Jeffrey M. Liebmann, and Robert Ritch. 2012. “Lower Corneal Hysteresis Is Associated With More Rapid Glaucomatous Visual Field Progression.” *Journal of Glaucoma* 21 (4): 209–13.

Denis, Philippe, Antoine Lafuma, and Gilles Berdeaux. 2004. “Medical Predictive Factors of Glaucoma Treatment Costs.” *Journal of Glaucoma* 13 (4): 283.

Denniss, Jonathan, Andrew Turpin, and Allison M. McKendrick. 2019. “Relating Optical Coherence Tomography to Visual Fields in Glaucoma: Structure–function Mapping, Limitations and Future Applications.” *Clinical & Experimental Optometry: Journal of the Australian Optometrical Association* 102 (3): 291–99.

DeVience, Eva, Sona Chaudhry, and Osamah J. Saeedi. 2017. “Effect of Intraoperative Factors on IOP Reduction after Phacoemulsification.” *International Ophthalmology* 37 (1): 63–70.

Ding, Y., Y. Liu, Q. Yan, L. G. Fritsche, R. J. Cook, T. Clemons, R. Ratnapriya, et al. 2017. “Bivariate Analysis of Age-Related Macular Degeneration Progression Using Genetic Risk Scores.” *Genetics* 206 (1). https://doi.org/10.1534/genetics.116.196998.

Dirani, Mohamed, Jonathan G. Crowston, Penny S. Taylor, Peter T. Moore, Sophie Rogers, M. Lynne Pezzullo, Jill E. Keeffe, and Hugh R. Taylor. 2011. “Economic Impact of Primary Open-Angle Glaucoma in Australia.” *Clinical & Experimental Ophthalmology* 39 (7): 623–32.

Do, C. B., D. A. Hinds, U. Francke, and N. Eriksson. 2012. “Comparison of Family History and SNPs for Predicting Risk of Complex Disease.” *PLoS Genetics* 8 (10). https://doi.org/10.1371/journal.pgen.1002973.

Do, R., S. Kathiresan, and G. R. Abecasis. 2012. “Exome Sequencing and Complex Disease: Practical Aspects of Rare Variant Association Studies.” *Human Molecular Genetics* 21 (R1). https://doi.org/10.1093/hmg/dds387.

Drance, Stephen M. 1989. “Disc Hemorrhages in the Glaucomas.” *Survey of Ophthalmology* 33 (5): 331–37.

Drexler, Wolfgang, Mengyang Liu, Abhishek Kumar, Tschackad Kamali, Angelika Unterhuber, and Rainer A. Leitgeb. 2014. “Optical Coherence Tomography Today: Speed, Contrast, and Multimodality.” *Journal of Biomedical Optics* 19 (7): 071412.

Dron, J. S., and R. A. Hegele. 2019. “The Evolution of Genetic-Based Risk Scores for Lipids and Cardiovascular Disease.” *Current Opinion in Lipidology* 30 (2). https://doi.org/10.1097/MOL.0000000000000576.

Dudbridge, Frank. 2013. “Power and Predictive Accuracy of Polygenic Risk Scores.” *PLoS Genetics* 9 (3): e1003348.

Dupps, William J., Jr. 2007. “Hysteresis: New Mechanospeak for the Ophthalmologist.” *Journal of Cataract and Refractive Surgery* 33 (9): 1499–1501.

Eliasy, Ashkan, Kai-Jung Chen, Riccardo Vinciguerra, Osama Maklad, Paolo Vinciguerra, Renato Ambrósio, Cynthia J. Roberts, and Ahmed Elsheikh. 2018. “Ex-Vivo Experimental Validation of Biomechanically-Corrected Intraocular Pressure Measurements on Human Eyes Using the CorVis ST.” *Experimental Eye Research*.

https://doi.org/10.1016/j.exer.2018.06.013.
Elks, Cathy E., John R. B. Perry, Patrick Sulem, Daniel I. Chasman, Nora Franceschini, Chunyan He, Kathryn L. Lunetta, et al. 2010. “Thirty New Loci for Age at Menarche Identified by a Meta-Analysis of Genome-Wide Association Studies.” *Nature Genetics* 42 (12): 1077–85.
Enders, Philip, Jonathan Hall, Marco Bornhauser, Kaweh Mansouri, Lebriz Altay, Stefan Schrader, Thomas S. Dietlein, Bjoern O. Bachmann, Thomas Neuhann, and Claus Cursiefen. 2019. “Telemetric Intraocular Pressure Monitoring after Boston Keratoprosthesis Surgery.” *Ophthalmology* 126 (2): 322–24.
Ernest, P. J., J. S. Schouten, H. J. Beckers, F. Hendrikse, M. H. Prins, and C. A. Webers. 2013. “An Evidence-Based Review of Prognostic Factors for Glaucomatous Visual Field Progression.” *Ophthalmology* 120 (3). https://doi.org/10.1016/j.ophtha.2012.09.005.
Fadista, J., A. K. Manning, J. C. Florez, and L. Groop. 2016. “The (in)famous GWAS P-Value Threshold Revisited and Updated for Low-Frequency Variants.” *European Journal of Human Genetics: EJHG* 24 (8). https://doi.org/10.1038/ejhg.2015.269.
Fan, Bao Jian, Dan Yi Wang, Louis R. Pasquale, Jonathan L. Haines, and Janey L. Wiggs. 2011. “Genetic Variants Associated with Optic Nerve Vertical Cup-to-Disc Ratio Are Risk Factors for Primary Open Angle Glaucoma in a US Caucasian Population.” *Investigative Opthalmology & Visual Science*. https://doi.org/10.1167/iovs.10-6339.
Fan, B. J., J. C. Bailey, R. P. Igo, J. H. Kang, T. Boumenna, M. H. Brilliant, D. L. Budenz, et al. 2019. “Association of a Primary Open-Angle Glaucoma Genetic Risk Score With Earlier Age at Diagnosis.” *JAMA Ophthalmology* 137 (10). https://doi.org/10.1001/jamaophthalmol.2019.3109.
Fang, J., C. Gong, Y. Wan, Y. Xu, F. Tao, and Y. Sun. 2019. “Polygenic Risk, Adherence to a Healthy Lifestyle, and Childhood Obesity.” *Pediatric Obesity* 14 (4). https://doi.org/10.1111/ijpo.12489.
Fan, Qiao, Yik-Ying Teo, and Seang-Mei Saw. 2011. “Application of Advanced Statistics in Ophthalmology.” *Investigative Ophthalmology & Visual Science* 52 (9): 6059.
Fantus, R. J., and B. T. Helfand. 2019. “Germline Genetics of Prostate Cancer: Time to Incorporate Genetics into Early Detection Tools.” *Clinical Chemistry* 65 (1). https://doi.org/10.1373/clinchem.2018.286658.
Fan, Yuan Yao, Wei Wen Su, Chun Hsiu Liu, Henry Shen Lih Chen, Shiu Chen Wu, Shirley H. L. Chang, Kuan Jen Chen, et al. 2019. “Correlation between Structural Progression in Glaucoma and Obstructive Sleep Apnea.” *Eye* 33 (9): 1459–65.
Fea, Antonio M. 2010. “Phacoemulsification versus Phacoemulsification with Micro-Bypass Stent Implantation in Primary Open-Angle Glaucoma: Randomized Double-Masked Clinical Trial.” *Journal of Cataract and Refractive Surgery* 36 (3): 407–12.
Fea, Antonio Maria, Giulia Consolandi, Marta Zola, Giulia Pignata, Paola Cannizzo, Carlo Lavia, Teresa Rolle, and Federico Maria Grignolo. 2015. “Micro-Bypass Implantation for Primary Open-Angle Glaucoma Combined with Phacoemulsification: 4-Year Follow-Up.” *Journal of Ophthalmology* 2015: 1–4.
Feiner, Leonard, Jody R. Piltz-Seymour, and Collaborative Initial Glaucoma Treatment Study. 2003. “Collaborative Initial Glaucoma Treatment Study: A Summary of Results to Date.” *Current Opinion in Ophthalmology* 14 (2): 106–11.
Fernández-Barrientos, Yolanda, Julian García-Feijoó, Jose M. Martínez-de-la-Casa, Luis E. Pablo, Cristina Fernández-Pérez, and Julian García Sánchez. 2010. “Fluorophotometric Study of the Effect of the Glaukos Trabecular Microbypass Stent on Aqueous Humor Dynamics.” *Investigative Ophthalmology & Visual Science* 51 (7): 3327.
Ferre-Fernández, J. J., J. D. Aroca-Aguilar, C. Medina-Trillo, J. M. Bonet-Fernández, C. D. Méndez-Hernández, L. Morales-Fernández, M. Corton, et al. 2017. “Whole-Exome Sequencing of Congenital Glaucoma Patients Reveals Hypermorphic Variants in GPATCH3, a New Gene Involved in Ocular and Craniofacial Development.” *Scientific Reports* 7 (April). https://doi.org/10.1038/srep46175.
Fingert, J. H., E. Héon, J. M. Liebmann, T. Yamamoto, J. E. Craig, J. Rait, K. Kawase, et al. 1999. “Analysis of Myocilin Mutations in 1703 Glaucoma Patients from Five Different

Populations." *Human Molecular Genetics* 8 (5). https://doi.org/10.1093/hmg/8.5.899.
Fingert, J. H., A. L. Robin, J. L. Stone, B. R. Roos, L. K. Davis, T. E. Scheetz, S. R. Bennett, et al. 2011. "Copy Number Variations on Chromosome 12q14 in Patients with Normal Tension Glaucoma." *Human Molecular Genetics* 20 (12). https://doi.org/10.1093/hmg/ddr123.
Flaxman, S. R., R. R. A. Bourne, S. Resnikoff, P. Ackland, T. Braithwaite, M. V. Cicinelli, A. Das, et al. 2017. "Global Causes of Blindness and Distance Vision Impairment 1990-2020: A Systematic Review and Meta-Analysis." *The Lancet. Global Health* 5 (12). https://doi.org/10.1016/S2214-109X(17)30393-5.
Fogagnolo, Paolo, Nicola Orzalesi, Antonio Ferreras, and Luca Rossetti. 2009. "The Circadian Curve of Intraocular Pressure: Can We Estimate Its Characteristics during Office Hours?" *Invest Ophthalmol Vis Sci* 50 (5): 2209.
Foster, A., and S. Resnikoff. 2005. "The Impact of Vision 2020 on Global Blindness." *Eye* 19 (10): 1133–35.
Founti, P., C. Bunce, A. P. Khawaja, C. J. Doré, J. Mohamed-Noriega, and D. F. Garway-Heath. 2020. "Risk Factors for Visual Field Deterioration in the United Kingdom Glaucoma Treatment Study." *Ophthalmology*, June. https://doi.org/10.1016/j.ophtha.2020.06.009.
Frick, K. D., E. W. Gower, J. H. Kempen, and J. L. Wolff. 2007. "Economic Impact of Visual Impairment and Blindness in the United States." *Archives of Ophthalmology* 125 (4). https://doi.org/10.1001/archopht.125.4.544.
Fritsche, L. G., W. Igl, J. N. Bailey, F. Grassmann, S. Sengupta, J. L. Bragg-Gresham, K. P. Burdon, et al. 2016. "A Large Genome-Wide Association Study of Age-Related Macular Degeneration Highlights Contributions of Rare and Common Variants." *Nature Genetics* 48 (2). https://doi.org/10.1038/ng.3448.
Fujishiro, Takashi, Masato Matsuura, Yuri Fujino, Hiroshi Murata, Kana Tokumo, Shunsuke Nakakura, Yoshiaki Kiuchi, and Ryo Asaoka. 2020. "The Relationship Between Corvis ST Tonometry Parameters and Ocular Response Analyzer Corneal Hysteresis." *Journal of Glaucoma*. https://doi.org/10.1097/ijg.0000000000001486.
Gamazon, E. R., H. E. Wheeler, K. P. Shah, S. V. Mozaffari, K. Aquino-Michaels, R. J. Carroll, A. E. Eyler, et al. 2015. "A Gene-Based Association Method for Mapping Traits Using Reference Transcriptome Data." *Nature Genetics* 47 (9). https://doi.org/10.1038/ng.3367.
Gao, X. Raymond, Hua Huang, and Heejin Kim. 2019. "Genome-Wide Association Analyses Identify 139 Loci Associated with Macular Thickness in the UK Biobank Cohort." *Human Molecular Genetics* 28 (7): 1162–72.
Gao, X. Raymond, Hua Huang, Drew R. Nannini, Fangda Fan, and Heejin Kim. 2018. "Genome-Wide Association Analyses Identify New Loci Influencing Intraocular Pressure." *Human Molecular Genetics*, March. https://doi.org/10.1093/hmg/ddy111.
Gao, X. R., H. Huang, and H. Kim. 2019. "Polygenic Risk Score Is Associated With Intraocular Pressure and Improves Glaucoma Prediction in the UK Biobank Cohort." *Translational Vision Science & Technology* 8 (2). https://doi.org/10.1167/tvst.8.2.10.
Gardiner, S. K., D. R. Anderson, M. Fingeret, J. J. McSoley, and C. A. Johnson. 2006. "Evaluation of Decision Rules for Frequency-Doubling Technology Screening Tests." *Optometry and Vision Science: Official Publication of the American Academy of Optometry* 83 (7). https://doi.org/10.1097/01.opx.0000225912.06027.ac.
Garg, Anurag, Victoria Vickerstaff, Neil Nathwani, David Garway-Heath, Evgenia Konstantakopoulou, Gareth Ambler, Catey Bunce, Richard Wormald, Keith Barton, and Gus Gazzard. 2020. "Efficacy of Repeat Selective Laser Trabeculoplasty in Medication-Naive Open-Angle Glaucoma and Ocular Hypertension during the LiGHT Trial." *Ophthalmology* 127 (4): 467–76.
Garg, A., V. Vickerstaff, N. Nathwani, D. Garway-Heath, E. Konstantakopoulou, G. Ambler, C. Bunce, R. Wormald, K. Barton, and G. Gazzard. 2019. "Primary Selective Laser Trabeculoplasty for Open-Angle Glaucoma and Ocular Hypertension: Clinical Outcomes, Predictors of Success, and Safety from the Laser in Glaucoma and Ocular

Hypertension Trial." *Ophthalmology* 126 (9). https://doi.org/10.1016/j.ophtha.2019.04.012.
Garway-Heath, David F., Darmalingum Poinoosawmy, Frederick W. Fitzke, and Roger A. Hitchings. 2000. "Mapping the Visual Field to the Optic Disc in Normal Tension Glaucoma eyes11The Authors Have No Proprietary Interest in the Development or Marketing of Any Product or Instrument Mentioned in This Article." *Ophthalmology* 107 (10): 1809–15.
Garway-Heath, David F., Haogang Zhu, Qian Cheng, Katy Morgan, Chris Frost, David P. Crabb, Tuan-Anh Ho, and Yannis Agiomyrgiannakis. 2018. "Combining Optical Coherence Tomography with Visual Field Data to Rapidly Detect Disease Progression in Glaucoma: A Diagnostic Accuracy Study." *Health Technology Assessment* 22 (4): 1–106.
Garway-Heath, D. F., D. P. Crabb, C. Bunce, G. Lascaratos, F. Amalfitano, N. Anand, A. Azuara-Blanco, et al. 2015. "Latanoprost for Open-Angle Glaucoma (UKGTS): A Randomised, Multicentre, Placebo-Controlled Trial." *Lancet* 385 (9975). https://doi.org/10.1016/S0140-6736(14)62111-5.
Garway-Heath, D. F., G. Lascaratos, C. Bunce, D. P. Crabb, R. A. Russell, and A. Shah. 2013. "The United Kingdom Glaucoma Treatment Study: A Multicenter, Randomized, Placebo-Controlled Clinical Trial: Design and Methodology." *Ophthalmology* 120 (1). https://doi.org/10.1016/j.ophtha.2012.07.028.
Garway-Heath, D. F., A. R. Rudnicka, T. Lowe, P. J. Foster, F. W. Fitzke, and R. A. Hitchings. 1998. "Measurement of Optic Disc Size: Equivalence of Methods to Correct for Ocular Magnification." *The British Journal of Ophthalmology* 82 (6): 643–49.
Gaspar, R., L. A. Pinto, and D. C. Sousa. 2017. "Corneal Properties and Glaucoma: A Review of the Literature and Meta-Analysis." *Arquivos Brasileiros de Oftalmologia* 80 (3). https://doi.org/10.5935/0004-2749.20170050.
Gasten, A. C., W. D. Ramdas, L. Broer, L. M. van Koolwijk, M. K. Ikram, P. T. de Jong, Y. S. Aulchenko, et al. 2012. "A Genetic Epidemiologic Study of Candidate Genes Involved in the Optic Nerve Head Morphology." *Investigative Ophthalmology & Visual Science* 53 (3): 1485–91.
Gazzard, G., E. Konstantakopoulou, D. Garway-Heath, K. Barton, R. Wormald, S. Morris, R. Hunter, et al. 2018. "Laser in Glaucoma and Ocular Hypertension (LiGHT) Trial. A Multicentre, Randomised Controlled Trial: Design and Methodology." *The British Journal of Ophthalmology* 102 (5). https://doi.org/10.1136/bjophthalmol-2017-310877.
Gazzard, Gus, Evgenia Konstantakopoulou, David Garway-Heath, Anurag Garg, Victoria Vickerstaff, Rachael Hunter, Gareth Ambler, et al. 2019. "Selective Laser Trabeculoplasty versus Eye Drops for First-Line Treatment of Ocular Hypertension and Glaucoma (LiGHT): A Multicentre Randomised Controlled Trial." *The Lancet* 393 (10180): 1505–16.
Georgalas, Ilias, Dimitrios Papaconstantinou, Panagiotis Tsikripis, Chryssanthi Koutsandrea, and Michael Apostolopoulos. 2013. "The Effect of Prostaglandin Analogs on the Biomechanical Properties and Central Thickness of the Cornea of Patients with Open-Angle Glaucoma: A 3-Year Study on 108 Eyes." *Drug Design, Development and Therapy*. https://doi.org/10.2147/dddt.s50622.
Gharahkhani, P., K. P. Burdon, R. Fogarty, S. Sharma, A. W. Hewitt, S. Martin, M. H. Law, et al. 2014. "Common Variants near ABCA1, AFAP1 and GMDS Confer Risk of Primary Open-Angle Glaucoma." *Nature Genetics* 46 (10). https://doi.org/10.1038/ng.3079.
Gharahkhani, Puya, Kathryn P. Burdon, Jessica N. Cooke Bailey, Alex W. Hewitt, Matthew H. Law, Louis R. Pasquale, Jae H. Kang, et al. 2018. "Analysis Combining Correlated Glaucoma Traits Identifies Five New Risk Loci for Open-Angle Glaucoma." *Scientific Reports* 8 (1): 3124.
Gharahkhani, Puya, Kathryn P. Burdon, Alex W. Hewitt, Matthew H. Law, Emmanuelle Souzeau, Grant W. Montgomery, Graham Radford-Smith, David A. Mackey, Jamie E. Craig, and Stuart MacGregor. 2015. "Accurate Imputation-Based Screening of Gln368Ter Myocilin Variant in Primary Open-Angle Glaucoma." *Investigative*

Ophthalmology & Visual Science 56 (9): 5087–93.
Gharahkhani, Puya, Eric Jorgenson, Pirro Hysi, Anthony P. Khawaja, Sarah Pendergrass, Xikun Han, Jue Sheng Ong, et al. 2020. “A Large Cross-Ancestry Meta-Analysis of Genome-Wide Association Studies Identifies 69 Novel Risk Loci for Primary Open-Angle Glaucoma and Includes a Genetic Link with Alzheimer’s Disease.” *Genetics*. bioRxiv.
Ghorbani Mojarrad, Neema, Cathy Williams, and Jeremy A. Guggenheim. 2018. “A Genetic Risk Score and Number of Myopic Parents Independently Predict Myopia.” *Ophthalmic & Physiological Optics: The Journal of the British College of Ophthalmic Opticians* 38 (5): 492–502.
Ghorbani Mojarrad, N., D. Plotnikov, C. Williams, and J. A. Guggenheim. 2019. “Association Between Polygenic Risk Score and Risk of Myopia.” *JAMA Ophthalmology* 138 (1). https://doi.org/10.1001/jamaophthalmol.2019.4421.
Glickman, Mark E., Sowmya R. Rao, and Mark R. Schultz. 2014. “False Discovery Rate Control Is a Recommended Alternative to Bonferroni-Type Adjustments in Health Studies.” *Journal of Clinical Epidemiology* 67 (8): 850–57.
Goel, Manik, Renata G. Picciani, Richard K. Lee, and Sanjoy K. Bhattacharya. 2010. “Aqueous Humor Dynamics: A Review.” *The Open Ophthalmology Journal* 4: 52.
Gong, B., H. Zhang, L. Huang, Y. Chen, Y. Shi, P. O. Tam, X. Zhu, et al. 2019. “Mutant RAMP2 Causes Primary Open-Angle Glaucoma via the CRLR-cAMP Axis.” *Genetics in Medicine: Official Journal of the American College of Medical Genetics* 21 (10). https://doi.org/10.1038/s41436-019-0507-0.
Gordon, M. O., J. A. Beiser, J. D. Brandt, D. K. Heuer, E. J. Higginbotham, C. A. Johnson, J. L. Keltner, et al. 2002. “The Ocular Hypertension Treatment Study: Baseline Factors That Predict the Onset of Primary Open-Angle Glaucoma.” *Archives of Ophthalmology* 120 (6). https://doi.org/10.1001/archopht.120.6.714.
Gordon, M. O., and M. A. Kass. 1999. “The Ocular Hypertension Treatment Study: Design and Baseline Description of the Participants.” *Archives of Ophthalmology* 117 (5). https://doi.org/10.1001/archopht.117.5.573.
———. 2018. “What We Have Learned From the Ocular Hypertension Treatment Study.” *American Journal of Ophthalmology* 189 (May). https://doi.org/10.1016/j.ajo.2018.02.016.
Gordon, M. O., V. Torri, S. Miglior, J. A. Beiser, I. Floriani, J. P. Miller, F. Gao, et al. 2007. “Validated Prediction Model for the Development of Primary Open-Angle Glaucoma in Individuals with Ocular Hypertension.” *Ophthalmology* 114 (1). https://doi.org/10.1016/j.ophtha.2006.08.031.
Gottlieb, L. K., B. Schwartz, and S. G. Pauker. 1983. “Glaucoma Screening. A Cost-Effectiveness Analysis.” *Survey of Ophthalmology* 28 (3). https://doi.org/10.1016/0039-6257(83)90098-x.
Graham, P. A. 1972. “Epidemiology of Simple Glaucoma and Ocular Hypertension.” *The British Journal of Ophthalmology* 56 (3): 223–29.
Graham, S. L., S. M. Drance, K. Wijsman, G. R. Douglas, and F. S. Mikelberg. 1995. “Ambulatory Blood Pressure Monitoring in Glaucoma. The Nocturnal Dip.” *Ophthalmology* 102 (1). https://doi.org/10.1016/s0161-6420(95)31053-6.
Gulshan, Varun, Lily Peng, Marc Coram, Martin C. Stumpe, Derek Wu, Arunachalam Narayanaswamy, Subhashini Venugopalan, et al. 2016. “Development and Validation of a Deep Learning Algorithm for Detection of Diabetic Retinopathy in Retinal Fundus Photographs.” *JAMA: The Journal of the American Medical Association* 316 (22): 2402.
Gusev, A., A. Ko, H. Shi, G. Bhatia, W. Chung, B. W. Penninx, R. Jansen, et al. 2016. “Integrative Approaches for Large-Scale Transcriptome-Wide Association Studies.” *Nature Genetics* 48 (3). https://doi.org/10.1038/ng.3506.
Haeseleer, Françoise, and Krzysztof Palczewski. 2000. “[24] Short-Chain Dehydrogenases/reductases in Retina.” In *Methods in Enzymology*, 316:372–83. Academic Press.
Han, Xikun, Ayub Qassim, Jiyuan An, Henry Marshall, Tiger Zhou, Jue-Sheng Ong, Mark

Hassall, et al. 2019. “Genome-Wide Association Analysis of 95,549 Individuals Identifies Novel Loci and Genes Influencing Optic Disc Morphology.” *Human Molecular Genetics*, September. https://doi.org/10.1093/hmg/ddz193.
Han, X., E. Souzeau, J. S. Ong, J. An, O. M. Siggs, K. P. Burdon, S. Best, et al. 2019. “Myocilin Gene Gln368Ter Variant Penetrance and Association With Glaucoma in Population-Based and Registry-Based Studies.” *JAMA Ophthalmology* 137 (1). https://doi.org/10.1001/jamaophthalmol.2018.4477.
Harasymowycz, Paul J., Demosthenes G. Papamatheakis, Alvine Kamdeu Fansi, Jacques Gresset, and Mark R. Lesk. 2005. “Validity of Screening for Glaucomatous Optic Nerve Damage Using Confocal Scanning Laser Ophthalmoscopy (Heidelberg Retina Tomograph II) in High-Risk Populations.” *Ophthalmology* 112 (12): 2164–71.
Harper, R., B. Reeves, and G. Smith. 2000. “Observer Variability in Optic Disc Assessment: Implications for Glaucoma Shared Care.” *Ophthalmic & Physiological Optics: The Journal of the British College of Ophthalmic Opticians* 20 (4): 265–73.
Hashemi, H., A. H. Kashi, A. Fotouhi, and K. Mohammad. 2005. “Distribution of Intraocular Pressure in Healthy Iranian Individuals: The Tehran Eye Study.” *The British Journal of Ophthalmology* 89 (6): 652–57.
Hattenhauer, Matthew G., Douglas H. Johnson, Helen H. Ing, David C. Herman, David O. Hodge, Barbara P. Yawn, Linda C. Butterfield, and Darryl T. Gray. 1998. “The Probability of Blindness from Open-Angle Glaucoma.” *Ophthalmology* 105 (11): 2099–2104.
Hayashi, Ken, Hideyuki Hayashi, Fuminori Nakao, and Fumihiko Hayashi. 2001. “Effect of Cataract Surgery on Intraocular Pressure Control in Glaucoma Patients.” *Journal of Cataract and Refractive Surgery* 27 (11): 1779–86.
Healey, Paul R., Anne J. Lee, Tin Aung, Tien Y. Wong, and Paul Mitchell. 2010. “Diagnostic Accuracy of the Heidelberg Retina Tomograph for Glaucoma.” *Ophthalmology* 117 (9): 1667–73.
Healey, Paul R., and Paul Mitchell. 2015. “Presence of an Optic Disc Notch and Glaucoma.” *Journal of Glaucoma* 24 (4): 262–66.
Heijl, A., P. Buchholz, G. Norrgren, and B. Bengtsson. 2013. “Rates of Visual Field Progression in Clinical Glaucoma Care.” *Acta Ophthalmologica* 91 (5). https://doi.org/10.1111/j.1755-3768.2012.02492.x.
Heijl, Anders. 2002. *Essential Perimetry: The Field Analyzer Primer*. Carl Zeiss Meditec.
Heijl, Anders, Cristina M. Leske, Bo Bengtsson, Leslie Hyman, Boel Bengtsson, Mohamed Hussein, and Early Manifest Glaucoma Trial Group. 2002. “Reduction of Intraocular Pressure and Glaucoma Progression: Results From the Early Manifest Glaucoma Trial.” *Archives of Ophthalmology* 120 (10): 1268.
Heijl, Anders, M. Cristina Leske, Boel Bengtsson, Bo Bengtsson, Mohamed Hussein, and EMGT Group. 2003. “Measuring Visual Field Progression in the Early Manifest Glaucoma Trial.” *Acta Ophthalmologica Scandinavica* 81 (3): 286–93.
Heinze, Georg, Christine Wallisch, and Daniela Dunkler. 2018. “Variable Selection - A Review and Recommendations for the Practicing Statistician.” *Biometrical Journal. Biometrische Zeitschrift* 60 (3): 431–49.
Herndon, L. W., S. A. Choudhri, T. Cox, K. F. Damji, M. B. Shields, and R. R. Allingham. 1997. “Central Corneal Thickness in Normal, Glaucomatous, and Ocular Hypertensive Eyes.” *Archives of Ophthalmology* 115 (9). https://doi.org/10.1001/archopht.1997.01100160307007.
Hewitt, Alex W., David A. Mackey, and Jamie E. Craig. 2008. “Myocilin Allele-Specific Glaucoma Phenotype Database.” *Human Mutation* 29 (2): 207–11.
Hirabayashi, Matthew, Vikram Ponnusamy, and Jella An. 2020. “Predictive Factors for Outcomes of Selective Laser Trabeculoplasty.” *Scientific Reports* 10 (1): 1–6.
Hodapp, Elizabeth, Richard K. Parrish, and Douglas R. Anderson. 1993. *Clinical Decisions in Glaucoma*. Mosby.
Hoffmann, Esther M., Linda M. Zangwill, Jonathan G. Crowston, and Robert N. Weinreb. 2007. “Optic Disk Size and Glaucoma.” *Survey of Ophthalmology* 52 (1): 32–49.

Hollows, F. C., and P. A. Graham. 1966. “Intra-Ocular Pressure, Glaucoma, and Glaucoma Suspects in a Defined Population.” *The British Journal of Ophthalmology* 50 (10): 570–86.
Hong, Jiaxu, Jianjiang Xu, Anji Wei, Sophie X. Deng, Xinhan Cui, Xiaobo Yu, and Xinghuai Sun. 2013. “A New Tonometer—The Corvis ST Tonometer: Clinical Comparison with Noncontact and Goldmann Applanation Tonometers.” *Investigative Ophthalmology & Visual Science* 54 (1): 659.
Hood, Donald C., and Randy H. Kardon. 2007. “A Framework for Comparing Structural and Functional Measures of Glaucomatous Damage.” *Progress in Retinal and Eye Research* 26 (6): 688–710.
Hood, Donald C., Ali S. Raza, Carlos Gustavo V. de Moraes, Jeffrey M. Liebmann, and Robert Ritch. 2013. “Glaucomatous Damage of the Macula.” *Progress in Retinal and Eye Research* 32 (January): 1–21.
Hood, Donald C., Emmanouil Tsamis, Nikhil K. Bommakanti, Devon B. Joiner, Lama A. Al-Aswad, Dana M. Blumberg, George A. Cioffi, Jeffrey M. Liebmann, and Carlos G. De Moraes. 2019. “Structure-Function Agreement Is Better Than Commonly Thought in Eyes With Early Glaucoma.” *Investigative Ophthalmology & Visual Science* 60 (13): 4241.
Hou, Hei Wan, Chen Lin, and Christopher Kai-Shun Leung. 2018. “Integrating Macular Ganglion Cell Inner Plexiform Layer and Parapapillary Retinal Nerve Fiber Layer Measurements to Detect Glaucoma Progression.” *Ophthalmology* 125 (6): 822–31.
Hsu, L., J. Jeon, H. Brenner, S. B. Gruber, R. E. Schoen, S. I. Berndt, A. T. Chan, et al. 2015. “A Model to Determine Colorectal Cancer Risk Using Common Genetic Susceptibility Loci.” *Gastroenterology* 148 (7). https://doi.org/10.1053/j.gastro.2015.02.010.
Huang, Lulin, Yuhong Chen, Ying Lin, Pancy O. S. Tam, Yilian Cheng, Yi Shi, Bo Gong, et al. 2019. “Genome-Wide Analysis Identified 17 New Loci Influencing Intraocular Pressure in Chinese Population.” *Science China. Life Sciences* 62 (2): 153–64.
Hubbard, Alan E., Jennifer Ahern, Nancy L. Fleischer, Mark Van der Laan, Sheri A. Lippman, Nicholas Jewell, Tim Bruckner, and William A. Satariano. 2010. “To GEE or Not to GEE: Comparing Population Average and Mixed Models for Estimating the Associations Between Neighborhood Risk Factors and Health.” *Epidemiology* 21 (4): 467–74.
Hui, Flora, Jessica Tang, Pete A. Williams, Myra B. McGuinness, Xavier Hadoux, Robert J. Casson, Michael Coote, et al. 2020. “Improvement in Inner Retinal Function in Glaucoma with Nicotinamide (vitamin B3) Supplementation: A Crossover Randomized Clinical Trial.” *Clinical & Experimental Ophthalmology* 42 (July): 514.
Iliescu, Alexandra, Michel Gravel, Cynthia Horth, Sergio Apuzzo, and Philippe Gros. 2011. “Transmembrane Topology of Mammalian Planar Cell Polarity Protein Vangl1.” *Biochemistry* 50 (12): 2274–82.
Inouye, M., G. Abraham, C. P. Nelson, A. M. Wood, M. J. Sweeting, F. Dudbridge, F. Y. Lai, et al. 2018. “Genomic Risk Prediction of Coronary Artery Disease in 480,000 Adults: Implications for Primary Prevention.” *Journal of the American College of Cardiology* 72 (16). https://doi.org/10.1016/j.jacc.2018.07.079.
International HapMap Consortium. 2005. “A Haplotype Map of the Human Genome.” *Nature* 437 (7063). https://doi.org/10.1038/nature04226.
Issa, S. A. 2005. “A Novel Index for Predicting Intraocular Pressure Reduction Following Cataract Surgery.” *The British Journal of Ophthalmology* 89 (5): 543–46.
Ittoop, S. M., J. R. SooHoo, L. K. Seibold, K. Mansouri, and M. Y. Kahook. 2016. “Systematic Review of Current Devices for 24-H Intraocular Pressure Monitoring.” *Advances in Therapy* 33 (10). https://doi.org/10.1007/s12325-016-0388-4.
Iwase, A., A. Tomidokoro, M. Araie, S. Shirato, H. Shimizu, and Y. Kitazawa. 2007. “Performance of Frequency-Doubling Technology Perimetry in a Population-Based Prevalence Survey of Glaucoma: The Tajimi Study.” *Ophthalmology* 114 (1). https://doi.org/10.1016/j.ophtha.2006.06.041.

Iyer, Jayant Venkatramani, Michael V. Boland, Joan Jefferys, and Harry Quigley. 2020. “Defining Glaucomatous Optic Neuropathy Using Objective Criteria from Structural and Functional Testing.” *The British Journal of Ophthalmology* 38 (July): bjophthalmol – 2020–316237.

Iyer, Jayant Venkatramani, J. R. Vianna, B. C. Chauhan, and H. A. Quigley. 2020. “Toward a New Definition of Glaucomatous Optic Neuropathy for Clinical Research.” *Current Opinion in Ophthalmology* 31 (2). https://doi.org/10.1097/ICU.0000000000000644.

Jain, Mamta, Ganesh P. Bhat, K. Vijayraghavan, and Maneesha S. Inamdar. 2012. “Rudhira/BCAS3 Is a Cytoskeletal Protein That Controls Cdc42 Activation and Directional Cell Migration during Angiogenesis.” *Experimental Cell Research* 318 (6): 753–67.

Jampel, Henry D., Sandra D. Cassard, David S. Friedman, Nakul S. Shekhawat, Julia Whiteside-de Vos, Harry A. Quigley, and Emily W. Gower. 2014. “Trends Over Time and Regional Variations in the Rate of Laser Trabeculoplasty in the Medicare Population.” *JAMA Ophthalmology* 132 (6): 685.

Janz, N. K., P. A. Wren, P. R. Lichter, D. C. Musch, B. W. Gillespie, K. E. Guire, and R. P. Mills. 2001. “The Collaborative Initial Glaucoma Treatment Study: Interim Quality of Life Findings after Initial Medical or Surgical Treatment of Glaucoma.” *Ophthalmology* 108 (11). https://doi.org/10.1016/s0161-6420(01)00874-0.

Jin, Yuejiao, Xiaofei Wang, Liang Zhang, Jost B. Jonas, Tin Aung, Leopold Schmetterer, and Michaël J. A. Girard. 2018. “Modeling the Origin of the Ocular Pulse and Its Impact on the Optic Nerve Head.” *Investigative Opthalmology & Visual Science*. https://doi.org/10.1167/iovs.17-23454.

Joda, Akram Abdelazim, Mir Mohi Sefat Shervin, Daniel Kook, and Ahmed Elsheikh. 2016. “Development and Validation of a Correction Equation for Corvis Tonometry.” *Computer Methods in Biomechanics and Biomedical Engineering*. https://doi.org/10.1080/10255842.2015.1077515.

Johnson, P. B., L. J. Jatz, and D. J. Rhee. 2006. “Selective Laser Trabeculoplasty: Predictive Value of Early Intraocular Pressure Measurements for Success at 3 Months.” *The British Journal of Ophthalmology* 90 (6): 741–43.

Jonas, J. B., A. Bergua, P. Schmitz-Valckenberg, K. I. Papastathopoulos, and W. M. Budde. 2000. “Ranking of Optic Disc Variables for Detection of Glaucomatous Optic Nerve Damage.” *Investigative Ophthalmology & Visual Science* 41 (7): 1764–73.

Jonas, J. B., and L. Holbach. 2005. “Central Corneal Thickness and Thickness of the Lamina Cribrosa in Human Eyes.” *Investigative Ophthalmology & Visual Science* 46 (4). https://doi.org/10.1167/iovs.04-0851.

Jonas, J. B., A. M. Schmidt, J. A. Müller-Bergh, U. M. Schlötzer-Schrehardt, and G. O. Naumann. 1992. “Human Optic Nerve Fiber Count and Optic Disc Size.” *Investigative Ophthalmology & Visual Science* 33 (6): 2012–18.

Jonas, Jost B., Tin Aung, Rupert R. Bourne, Alain M. Bron, Robert Ritch, and Songhomitra Panda-Jonas. 2017. “Glaucoma.” *The Lancet* 390 (10108): 2183–93.

Jonas, Jost B., Wido Budde, Andrea Stroux, Isabel M. Oberacher-Velten, and Anselm Jünemann. 2005. “Single Intraocular Pressure Measurements and Diurnal Intraocular Pressure Profiles.” *American Journal of Ophthalmology*. https://doi.org/10.1016/j.ajo.2004.12.012.

Jonas, Jost B., Vinay Nangia, Arshia Matin, Ajit Sinha, Maithili Kulkarni, and Krishna Bhojwani. 2011. “Intraocular Pressure and Associated Factors: The Central India Eye and Medical Study.” *Journal of Glaucoma* 20 (7): 405–9.

Jung, Younhea, Hae-Young L. Park, Hee Jung Yang, and Chan Kee Park. 2017. “Characteristics of Corneal Biomechanical Responses Detected by a Non-Contact Scheimpflug-Based Tonometer in Eyes with Glaucoma.” *Acta Ophthalmologica* 95 (7): e556–63.

Kansal, V., J. J. Armstrong, R. Pintwala, and C. Hutnik. 2018. “Optical Coherence Tomography for Glaucoma Diagnosis: An Evidence Based Meta-Analysis.” *PloS One* 13 (1). https://doi.org/10.1371/journal.pone.0190621.

Kansal, Vinay, James J. Armstrong, Robert Pintwala, and Cindy Hutnik. 2018. “Optical Coherence Tomography for Glaucoma Diagnosis: An Evidence Based Meta-Analysis.” Edited by Patrice E. Fort. https://doi.org/10.1371/journal.pone.0190621.

Kass, M. A., D. K. Heuer, E. J. Higginbotham, C. A. Johnson, J. L. Keltner, J. P. Miller, R. K. Parrish, M. R. Wilson, and M. O. Gordon. 2002. “The Ocular Hypertension Treatment Study: A Randomized Trial Determines That Topical Ocular Hypotensive Medication Delays or Prevents the Onset of Primary Open-Angle Glaucoma.” *Archives of Ophthalmology* 120 (6). https://doi.org/10.1001/archopht.120.6.701.

Kazanskaya, Olga, Bisei Ohkawara, Melanie Heroult, Wei Wu, Nicole Maltry, Hellmut G. Augustin, and Christof Niehrs. 2008. “The Wnt Signaling Regulator R-Spondin 3 Promotes Angioblast and Vascular Development.” *Development* 135 (22): 3655–64.

Khawaja, Anthony P., Joanna H. Campbell, Nicholas Kirby, Hitesh S. Chandwani, Ian Keyzor, Mousam Parekh, Andrew I. McNaught, et al. 2020. “Real-World Outcomes of Selective Laser Trabeculoplasty in the United Kingdom.” *Ophthalmology* 127 (6): 748–57.

Khawaja, Anthony P., Michelle P. Y. Chan, Shabina Hayat, David C. Broadway, Robert Luben, David F. Garway-Heath, Justin C. Sherwin, et al. 2013. “The EPIC-Norfolk Eye Study: Rationale, Methods and a Cross-Sectional Analysis of Visual Impairment in a Population-Based Cohort.” *BMJ Open*. https://doi.org/10.1136/bmjopen-2013-002684.

Khawaja, Anthony P., David P. Crabb, and Nomdo M. Jansonius. 2013. “The Role of Ocular Perfusion Pressure in Glaucoma Cannot Be Studied With Multivariable Regression Analysis Applied to Surrogates.” *Investigative Ophthalmology & Visual Science* 54 (7): 4619–20.

Khawaja, A. P., Cooke Bailey Jn, N. J. Wareham, R. A. Scott, M. Simcoe, R. P. Igo, Y. E. Song, et al. 2018. “Genome-Wide Analyses Identify 68 New Loci Associated with Intraocular Pressure and Improve Risk Prediction for Primary Open-Angle Glaucoma.” *Nature Genetics* 50 (6). https://doi.org/10.1038/s41588-018-0126-8.

Khawaja, A. P., and A. C. Viswanathan. 2018. “Are We Ready for Genetic Testing for Primary Open-Angle Glaucoma?” *Eye* 32 (5). https://doi.org/10.1038/s41433-017-0011-1.

Khera, A. V., M. Chaffin, K. G. Aragam, M. E. Haas, C. Roselli, S. H. Choi, P. Natarajan, et al. 2018. “Genome-Wide Polygenic Scores for Common Diseases Identify Individuals with Risk Equivalent to Monogenic Mutations.” *Nature Genetics* 50 (9). https://doi.org/10.1038/s41588-018-0183-z.

Khera, A. V., C. A. Emdin, I. Drake, P. Natarajan, A. G. Bick, N. R. Cook, D. I. Chasman, et al. 2016. “Genetic Risk, Adherence to a Healthy Lifestyle, and Coronary Disease.” *The New England Journal of Medicine* 375 (24). https://doi.org/10.1056/NEJMoa1605086.

Khor, C. C., W. D. Ramdas, E. N. Vithana, B. K. Cornes, X. Sim, W. T. Tay, S. M. Saw, et al. 2011. “Genome-Wide Association Studies in Asians Confirm the Involvement of ATOH7 and TGFBR3, and Further Identify CARD10 as a Novel Locus Influencing Optic Disc Area.” *Human Molecular Genetics* 20 (9). https://doi.org/10.1093/hmg/ddr060.

Khorrami-Nejad, M., A. Sarabandi, M. R. Akbari, and F. Askarizadeh. 2016. “The Impact of Visual Impairment on Quality of Life.” *Medical Hypothesis, Discovery & Innovation Ophthalmology Journal* 5 (3). https://pubmed.ncbi.nlm.nih.gov/28293655/.

Kiezun, A., K. Garimella, R. Do, N. O. Stitziel, B. M. Neale, P. J. McLaren, N. Gupta, et al. 2012. “Exome Sequencing and the Genetic Basis of Complex Traits.” *Nature Genetics* 44 (6). https://doi.org/10.1038/ng.2303.

Kim, J., D. Y. Park, H. Bae, D. Y. Park, D. Kim, C. K. Lee, S. Song, et al. 2017. “Impaired angiopoietin/Tie2 Signaling Compromises Schlemm’s Canal Integrity and Induces Glaucoma.” *The Journal of Clinical Investigation* 127 (10). https://doi.org/10.1172/JCI94668.

Kim, Ko Eun, and Ki Ho Park. 2018. “Macular Imaging by Optical Coherence Tomography in the Diagnosis and Management of Glaucoma.” https://doi.org/10.1136/bjophthalmol-2017-310869.

Kim, Yong Woo, Jin-Soo Kim, Sang Yoon Lee, Ahnul Ha, Jinho Lee, Young Joo Park, Young

Kook Kim, Jin Wook Jeoung, and Ki Ho Park. 2020. “Twenty-four–Hour Intraocular Pressure–Related Patterns from Contact Lens Sensors in Normal-Tension Glaucoma and Healthy Eyes.” *Ophthalmology*, May. https://doi.org/10.1016/j.ophtha.2020.05.010.

King, Rebecca, Felix L. Struebing, Ying Li, Jiaxing Wang, Allison Ashley Koch, Jessica N. Cooke Bailey, Puya Gharahkhani, et al. 2018. “Genomic Locus Modulating Corneal Thickness in the Mouse Identifies POU6F2 as a Potential Risk of Developing Glaucoma.” *PLoS Genetics* 14 (1): e1007145.

Kobayashi, T., K. Urabe, S. J. Orlow, K. Higashi, G. Imokawa, B. S. Kwon, B. Potterf, and V. J. Hearing. 1994. “The Pmel 17/silver Locus Protein. Characterization and Investigation of Its Melanogenic Function.” *The Journal of Biological Chemistry* 269 (46). https://pubmed.ncbi.nlm.nih.gov/7961886/.

Kohlhaas, M., A. G. Boehm, E. Spoerl, A. Pürsten, H. J. Grein, and L. E. Pillunat. 2006. “Effect of Central Corneal Thickness, Corneal Curvature, and Axial Length on Applanation Tonometry.” *Archives of Ophthalmology* 124 (4). https://doi.org/10.1001/archopht.124.4.471.

Konstantakopoulou, E., G. Gazzard, V. Vickerstaff, Y. Jiang, N. Nathwani, R. Hunter, G. Ambler, and C. Bunce. 2018. “The Laser in Glaucoma and Ocular Hypertension (LiGHT) Trial. A Multicentre Randomised Controlled Trial: Baseline Patient Characteristics.” *The British Journal of Ophthalmology* 102 (5). https://doi.org/10.1136/bjophthalmol-2017-310870.

Konstas, Anastasios G., Malik Y. Kahook, Makoto Araie, Andreas Katsanos, Luciano Quaranta, Luca Rossetti, Gábor Holló, et al. 2018. “Diurnal and 24-H Intraocular Pressures in Glaucoma: Monitoring Strategies and Impact on Prognosis and Treatment.” *Advances in Therapy* 35 (11): 1775–1804.

Kosior-Jarecka, Ewa, Dominika Wróbel-Dudzińska, Urszula Łukasik, and Tomasz Żarnowski. 2019. “Disc Haemorrhages in Polish Caucasian Patients with Normal Tension Glaucoma.” *Acta Ophthalmologica* 97 (1): 68–73.

Kotecha, Aachal, Edward White, Patricio G. Schlottmann, and David F. Garway-Heath. 2010. “Intraocular Pressure Measurement Precision with the Goldmann Applanation, Dynamic Contour, and Ocular Response Analyzer Tonometers.” *Ophthalmology* 117 (4): 730–37.

Koutsonas, A., P. Walter, G. Roessler, and N. Plange. 2015. “Implantation of a Novel Telemetric Intraocular Pressure Sensor in Patients With Glaucoma (ARGOS Study): 1-Year Results.” *Investigative Ophthalmology & Visual Science* 56 (2): 1063–69.

Krupin, Theodore, Jeffrey M. Liebmann, David S. Greenfield, Robert Ritch, and Stuart Gardiner. 2011. “A Randomized Trial of Brimonidine Versus Timolol in Preserving Visual Function: Results From the Low-Pressure Glaucoma Treatment Study.” *American Journal of Ophthalmology* 151 (4): 671–81.

Kuchenbaecker, Karoline B., Lesley McGuffog, Daniel Barrowdale, Andrew Lee, Penny Soucy, Joe Dennis, Susan M. Domchek, et al. 2017. “Evaluation of Polygenic Risk Scores for Breast and Ovarian Cancer Risk Prediction in BRCA1 and BRCA2 Mutation Carriers.” *Journal of the National Cancer Institute* 109 (7). https://doi.org/10.1093/jnci/djw302.

Kuznetsova, Alexandra, Per B. Brockhoff, and Rune H. B. Christensen. 2017. “lmerTest Package: Tests in Linear Mixed Effects Models.” *Journal of Statistical Software*. https://doi.org/10.18637/jss.v082.i13.

Lahola-Chomiak, A. A., T. Footz, K. Nguyen-Phuoc, G. J. Neil, B. Fan, K. F. Allen, D. S. Greenfield, et al. 2019. “Non-Synonymous Variants in Premelanosome Protein (PMEL) Cause Ocular Pigment Dispersion and Pigmentary Glaucoma.” *Human Molecular Genetics* 28 (8). https://doi.org/10.1093/hmg/ddy429.

Lambert, S. A., G. Abraham, and M. Inouye. 2019. “Towards Clinical Utility of Polygenic Risk Scores.” *Human Molecular Genetics* 28 (R2). https://doi.org/10.1093/hmg/ddz187.

Lambert, Samuel A., Laurent Gil, Simon Jupp, Scott C. Ritchie, Yu Xu, Annalisa Buniello, Gad Abraham, et al. 2020. “The Polygenic Score Catalog: An Open Database for Reproducibility and Systematic Evaluation.” *Genetic and Genomic Medicine*. medRxiv.

Lanzagorta-Aresti, A., M. Perez-Lopez, E. Palacios-Pozo, and J. Davo-Cabrera. 2017. “Relationship between Corneal Hysteresis and Lamina Cribrosa Displacement after Medical Reduction of Intraocular Pressure.” *The British Journal of Ophthalmology* 101 (3). https://doi.org/10.1136/bjophthalmol-2015-307428.

Lascaratos, Gerassimos, David F. Garway-Heath, Richard A. Russell, David Paul Crabb, Haogang Zhu, Cornelia Hirn, Aachal Kotecha, Katsuyoshi Suzuki, and UKGTS Investigators. 2014. “Intraocular Pressure (IOP) Measured with the Ocular Response Analyzer Is a Better Predictor of Glaucoma Progression than Goldmann IOP in the United Kingdom Glaucoma Treatment Study (UKGTS).” *Investigative Ophthalmology & Visual Science* 55 (13): 128–128.

Lascaratos, G., D. F. Garway-Heath, R. Burton, C. Bunce, W. Xing, D. P. Crabb, R. A. Russell, and A. Shah. 2013. “The United Kingdom Glaucoma Treatment Study: A Multicenter, Randomized, Double-Masked, Placebo-Controlled Trial: Baseline Characteristics.” *Ophthalmology* 120 (12). https://doi.org/10.1016/j.ophtha.2013.07.054.

Lavinsky, Fabio, Mengfei Wu, Joel S. Schuman, Katie A. Lucy, Mengling Liu, Youngseok Song, Julia Fallon, Maria de Los Angeles Ramos Cadena, Hiroshi Ishikawa, and Gadi Wollstein. 2018. “Can Macula and Optic Nerve Head Parameters Detect Glaucoma Progression in Eyes with Advanced Circumpapillary Retinal Nerve Fiber Layer Damage?” *Ophthalmology* 125 (12): 1907–12.

Lecarpentier, Julie, Valentina Silvestri, Karoline B. Kuchenbaecker, Daniel Barrowdale, Joe Dennis, Lesley McGuffog, Penny Soucy, et al. 2017. “Prediction of Breast and Prostate Cancer Risks in Male BRCA1 and BRCA2 Mutation Carriers Using Polygenic Risk Scores.” *Journal of Clinical Oncology: Official Journal of the American Society of Clinical Oncology* 35 (20): 2240–50.

Lee, K. M., T. W. Kim, E. J. Lee, M. J. A. Girard, J. M. Mari, and R. N. Weinreb. 2019. “Association of Corneal Hysteresis With Lamina Cribrosa Curvature in Primary Open Angle Glaucoma.” *Investigative Ophthalmology & Visual Science* 60 (13). https://doi.org/10.1167/iovs.19-27087.

Lee, Samantha S. Y., Nigel McArdle, Paul G. Sanfilippo, Seyhan Yazar, Peter R. Eastwood, Alex W. Hewitt, Qiang Li, and David A. Mackey. 2019. “Associations between Optic Disc Measures and Obstructive Sleep Apnea in Young Adults.” *Ophthalmology* 126 (10): 1372–84.

Leeuw, Christiaan A. de, Joris M. Mooij, Tom Heskes, and Danielle Posthuma. 2015. “MAGMA: Generalized Gene-Set Analysis of GWAS Data.” *PLoS Computational Biology* 11 (4): e1004219.

Lee, Won June, Young Kook Kim, Ki Ho Park, and Jin Wook Jeoung. 2017. “Trend-Based Analysis of Ganglion Cell–Inner Plexiform Layer Thickness Changes on Optical Coherence Tomography in Glaucoma Progression.” *Ophthalmology* 124 (9): 1383–91.

Lee, Y. A., Y. F. Shih, L. L. Lin, J. Y. Huang, and T. H. Wang. 2008. “Association between High Myopia and Progression of Visual Field Loss in Primary Open-Angle Glaucoma.” *Journal of the Formosan Medical Association = Taiwan Yi Zhi* 107 (12). https://doi.org/10.1016/S0929-6646(09)60019-X.

Leske, M. C., A. M. Connell, S. Y. Wu, L. Hyman, and A. P. Schachat. 1997. “Distribution of Intraocular Pressure. The Barbados Eye Study.” *Archives of Ophthalmology* 115 (8). https://doi.org/10.1001/archopht.1997.01100160221012.

Leske, M. C., A. Heijl, M. Hussein, B. Bengtsson, L. Hyman, and E. Komaroff. 2003. “Factors for Glaucoma Progression and the Effect of Treatment: The Early Manifest Glaucoma Trial.” *Archives of Ophthalmology* 121 (1). https://doi.org/10.1001/archopht.121.1.48.

Leske, M. C., A. Heijl, L. Hyman, and B. Bengtsson. 1999. “Early Manifest Glaucoma Trial: Design and Baseline Data.” *Ophthalmology* 106 (11). https://doi.org/10.1016/s0161-6420(99)90497-9.

Leske, M. C., A. Heijl, L. Hyman, B. Bengtsson, L. Dong, and Z. Yang. 2007. “Predictors of Long-Term Progression in the Early Manifest Glaucoma Trial.” *Ophthalmology* 114 (11). https://doi.org/10.1016/j.ophtha.2007.03.016.

Leung, Christopher Kai-Shun, Vivian Chiu, Robert N. Weinreb, Shu Liu, Cong Ye, Marco Yu,

Carol Yim-Lui Cheung, Gilda Lai, and Dennis Shun-Chiu Lam. 2011. “Evaluation of Retinal Nerve Fiber Layer Progression in Glaucoma.” *Ophthalmology* 118 (8): 1558–62.
Lichter, P. R., D. C. Musch, B. W. Gillespie, K. E. Guire, N. K. Janz, P. A. Wren, and R. P. Mills. 2001. “Interim Clinical Outcomes in the Collaborative Initial Glaucoma Treatment Study Comparing Initial Treatment Randomized to Medications or Surgery.” *Ophthalmology* 108 (11). https://doi.org/10.1016/s0161-6420(01)00873-9.
Li, Gisèle, Alvine Kamdeu Fansi, Jean-François Boivin, Lawrence Joseph, and Paul Harasymowycz. 2010. “Screening for Glaucoma in High-Risk Populations Using Optical Coherence Tomography.” *Ophthalmology* 117 (3): 453–61.
Lim, S. H., K. N. Tran-Viet, T. L. Yanovitch, S. F. Freedman, T. Klemm, W. Call, C. Powell, et al. 2013. “CYP1B1, MYOC, and LTBP2 Mutations in Primary Congenital Glaucoma Patients in the United States.” *American Journal of Ophthalmology* 155 (3). https://doi.org/10.1016/j.ajo.2012.09.012.
Lin, Chen, Heather Mak, Marco Yu, and Christopher Kai-Shun Leung. 2017. “Trend-Based Progression Analysis for Examination of the Topography of Rates of Retinal Nerve Fiber Layer Thinning in Glaucoma.” *JAMA Ophthalmology* 135 (3): 189.
Lin, Ching-Chun, Chao-Chien Hu, Jau-Der Ho, Hung-Wen Chiu, and Herng-Ching Lin. 2013. “Obstructive Sleep Apnea and Increased Risk of Glaucoma.” *Ophthalmology* 120 (8): 1559–64.
Lin, Shan C., Marisse Masis, Travis C. Porco, and Louis R. Pasquale. 2017. “Predictors of Intraocular Pressure After Phacoemulsification in Primary Open-Angle Glaucoma Eyes with Wide Versus Narrower Angles (An American Ophthalmological Society Thesis).” *Transactions of the American Ophthalmological Society* 115 (August). https://www.ncbi.nlm.nih.gov/pmc/articles/PMC5665659/.
Lisboa, Renato, Mauro Leite, Linda Zangwill, Ali Tafreshi, Robert Weinreb, and Felipe Medeiros. 2012. “Diagnosing Preperimetric Glaucoma with Spectral Domain Optical Coherence Tomography.” *Ophthalmology* 119 (11): 2261–69.
Li, T., K. Lindsley, B. Rouse, H. Hong, Q. Shi, D. S. Friedman, R. Wormald, and K. Dickersin. 2016. “Comparative Effectiveness of First-Line Medications for Primary Open-Angle Glaucoma: A Systematic Review and Network Meta-Analysis.” *Ophthalmology* 123 (1). https://doi.org/10.1016/j.ophtha.2015.09.005.
Liu, J. H., D. F. Kripke, and R. N. Weinreb. 2004. “Comparison of the Nocturnal Effects of Once-Daily Timolol and Latanoprost on Intraocular Pressure.” *American Journal of Ophthalmology* 138 (3): 389–95.
Liu, John H. K., Xiaoyan Zhang, Daniel F. Kripke, and Robert N. Weinreb. 2003. “Twenty-Four-Hour Intraocular Pressure Pattern Associated with Early Glaucomatous Changes.” *Investigative Opthalmology & Visual Science*. https://doi.org/10.1167/iovs.02-0666.
Liu, Jun, and Cynthia J. Roberts. 2005. “Influence of Corneal Biomechanical Properties on Intraocular Pressure Measurement.” *Journal of Cataract & Refractive Surgery*. https://doi.org/10.1016/j.jcrs.2004.09.031.
Liu, M. M., C. Cho, J. L. Jefferys, H. A. Quigley, and A. W. Scott. 2018. “Use of Optical Coherence Tomography by Nonexpert Personnel as a Screening Approach for Glaucoma.” *Journal of Glaucoma* 27 (1). https://doi.org/10.1097/IJG.0000000000000822.
Liu, T., D. Zeng, C. Zeng, and X. He. 2008. “Association between MYOC.mt1 Promoter Polymorphism and Risk of Primary Open-Angle Glaucoma: A Systematic Review and Meta-Analysis.” *Medical Science Monitor: International Medical Journal of Experimental and Clinical Research* 14 (7). https://pubmed.ncbi.nlm.nih.gov/18591929/.
Li, Xingyi, Wei Wang, and Xiulan Zhang. 2015. “Meta-Analysis of Selective Laser Trabeculoplasty versus Topical Medication in the Treatment of Open-Angle Glaucoma.” *BMC Ophthalmology* 15 (1): 1367.
Li, Z., R. R. Allingham, M. Nakano, L. Jia, Y. Chen, Y. Ikeda, B. Mani, et al. 2015. “A Common Variant near TGFBR3 Is Associated with Primary Open Angle Glaucoma.” *Human Molecular Genetics* 24 (13). https://doi.org/10.1093/hmg/ddv128.
Loh, Po-Ru, George Tucker, Brendan K. Bulik-Sullivan, Bjarni J. Vilhjálmsson, Hilary K.

Finucane, Rany M. Salem, Daniel I. Chasman, et al. 2015. “Efficient Bayesian Mixed-Model Analysis Increases Association Power in Large Cohorts.” *Nature Genetics* 47 (3): 284–90.

Loomis, Stephanie J., Jae H. Kang, Robert N. Weinreb, Brian L. Yaspan, Jessica N. Cooke Bailey, Douglas Gaasterland, Terry Gaasterland, et al. 2014. “Association of CAV1/CAV2 Genomic Variants with Primary Open-Angle Glaucoma Overall and by Gender and Pattern of Visual Field Loss.” *Ophthalmology* 121 (2): 508–16.

Lopes, B. T., C. J. Roberts, A. Elsheikh, R. Vinciguerra, P. Vinciguerra, S. Reisdorf, S. Berger, R. Koprowski, and R. Ambrósio. 2017. “Repeatability and Reproducibility of Intraocular Pressure and Dynamic Corneal Response Parameters Assessed by the Corvis ST.” *Journal of Ophthalmology* 2017. https://doi.org/10.1155/2017/8515742.

Lopes, Margarida C., Pirro G. Hysi, Virginie J. M. Verhoeven, Stuart Macgregor, Alex W. Hewitt, Grant W. Montgomery, Phillippa Cumberland, et al. 2013. “Identification of a Candidate Gene for Astigmatism.” *Investigative Ophthalmology & Visual Science* 54 (2): 1260–67.

Luce, D. A. 2005. “Determining in Vivo Biomechanical Properties of the Cornea with an Ocular Response Analyzer.” *Journal of Cataract and Refractive Surgery* 31 (1). https://doi.org/10.1016/j.jcrs.2004.10.044.

Ly, A., J. Phu, P. Katalinic, and M. Kalloniatis. 2019. “An Evidence-Based Approach to the Routine Use of Optical Coherence Tomography.” *Clinical & Experimental Optometry: Journal of the Australian Optometrical Association* 102 (3). https://doi.org/10.1111/cxo.12847.

Mabuchi, F., N. Mabuchi, Y. Sakurada, S. Yoneyama, K. Kashiwagi, H. Iijima, Z. Yamagata, et al. 2017. “Additive Effects of Genetic Variants Associated with Intraocular Pressure in Primary Open-Angle Glaucoma.” *PloS One* 12 (8). https://doi.org/10.1371/journal.pone.0183709.

Mabuchi, Fumihiko, Nakako Mabuchi, Yoichi Sakurada, Seigo Yoneyama, Kenji Kashiwagi, Hiroyuki Iijima, Zentaro Yamagata, et al. 2020. “Genetic Variants Associated With the Onset and Progression of Primary Open-Angle Glaucoma.” *American Journal of Ophthalmology* 215 (July): 135–40.

MacGregor, S., J. S. Ong, J. An, X. Han, T. Zhou, O. M. Siggs, M. H. Law, et al. 2018. “Genome-Wide Association Study of Intraocular Pressure Uncovers New Pathways to Glaucoma.” *Nature Genetics* 50 (8). https://doi.org/10.1038/s41588-018-0176-y.

Macgregor, Stuart, Alex W. Hewitt, Pirro G. Hysi, Jonathan B. Ruddle, Sarah E. Medland, Anjali K. Henders, Scott D. Gordon, et al. 2010. “Genome-Wide Association Identifies ATOH7 as a Major Gene Determining Human Optic Disc Size.” *Human Molecular Genetics* 19 (13): 2716–24.

Maechler, Martin, Peter Rousseeuw, Anja Struyf, Mia Hubert, and Kurt Hornik. 2019. “Cluster: Cluster Analysis Basics and Extensions.” Comprehensive R Archive Network (CRAN). https://CRAN.R-project.org/package=cluster.

Mak, T. S. H., R. M. Porsch, S. W. Choi, X. Zhou, and P. C. Sham. 2017. “Polygenic Scores via Penalized Regression on Summary Statistics.” *Genetic Epidemiology* 41 (6). https://doi.org/10.1002/gepi.22050.

Mancino, R., A. Martucci, M. Cesareo, C. Giannini, M. T. Corasaniti, G. Bagetta, and C. Nucci. 2018. “Glaucoma and Alzheimer Disease: One Age-Related Neurodegenerative Disease of the Brain.” *Current Neuropharmacology* 16 (7). https://doi.org/10.2174/1570159X16666171206144045.

Manolio, T. A., F. S. Collins, N. J. Cox, D. B. Goldstein, L. A. Hindorff, D. J. Hunter, M. I. McCarthy, et al. 2009. “Finding the Missing Heritability of Complex Diseases.” *Nature* 461 (7265). https://doi.org/10.1038/nature08494.

Mansberger, Steven L., Mae O. Gordon, Henry Jampel, Anjali Bhorade, James D. Brandt, Brad Wilson, and Michael A. Kass. 2012. “Reduction in Intraocular Pressure after Cataract Extraction: The Ocular Hypertension Treatment Study.” *Ophthalmology* 119 (9): 1826–31.

Mansouri, Kaweh, Felipe A. Medeiros, and Robert N. Weinreb. 2015. “Effect of Glaucoma

Medications on 24-Hour Intraocular Pressure-Related Patterns Using a Contact Lens Sensor: 24-H Effects of Glaucoma Drops." *Clinical & Experimental Ophthalmology* 43 (9): 787–95.
Mansouri, Kaweh, and Robert N. Weinreb. 2015. "Ambulatory 24-H Intraocular Pressure Monitoring in the Management of Glaucoma." *Current Opinion in Ophthalmology*. https://doi.org/10.1097/icu.0000000000000144.
Mansouri, K., F. A. Medeiros, A. Tafreshi, and R. N. Weinreb. 2012. "Continuous 24-Hour Monitoring of Intraocular Pressure Patterns with a Contact Lens Sensor: Safety, Tolerability, and Reproducibility in Patients with Glaucoma." *Archives of Ophthalmology* 130 (12). https://doi.org/10.1001/archophthalmol.2012.2280.
Mansouri, K., and T. Shaarawy. 2011. "Continuous Intraocular Pressure Monitoring with a Wireless Ocular Telemetry Sensor: Initial Clinical Experience in Patients with Open Angle Glaucoma." *The British Journal of Ophthalmology* 95 (5): 627–29.
Mansouri, K., A. P. Tanna, C. G. De Moraes, A. S. Camp, and R. N. Weinreb. 2020. "Review of the Measurement and Management of 24-Hour Intraocular Pressure in Patients with Glaucoma." *Survey of Ophthalmology* 65 (2). https://doi.org/10.1016/j.survophthal.2019.09.004.
Marchini, Jonathan, Bryan Howie, Simon Myers, Gil McVean, and Peter Donnelly. 2007. "A New Multipoint Method for Genome-Wide Association Studies by Imputation of Genotypes." *Nature Genetics* 39 (7): 906–13.
Margeta, M. A., S. M. Letcher, R. P. Igo, Cooke Bailey Jn, L. R. Pasquale, J. L. Haines, O. Butovsky, and J. L. Wiggs. 2020. "Association of APOE With Primary Open-Angle Glaucoma Suggests a Protective Effect for APOE ε4." *Investigative Ophthalmology & Visual Science* 61 (8). https://doi.org/10.1167/iovs.61.8.3.
Marin-Franch, I., and W. H. Swanson. 2013. "The visualFields Package: A Tool for Analysis and Visualization of Visual Fields." *Journal of Vision* 13 (4): 10–10.
Marshall, Henry, Sean Mullany, Ayub Qassim, Mark Hassall, Owen Siggs, Bronwyn Ridge, Thi Nguyen, et al. 2020. "Cardiovascular Disease Predicts Structural and Functional Progression in Early Glaucoma." *Ophthalmology*, July. https://doi.org/10.1016/j.ophtha.2020.06.067.
Marshall, Henry N., Nicholas H. Andrew, Mark Hassall, Ayub Qassim, Emmanuelle Souzeau, Bronwyn Ridge, Thi Nguyen, et al. 2019. "Macular Ganglion Cell–Inner Plexiform Layer Loss Precedes Peripapillary Retinal Nerve Fiber Layer Loss in Glaucoma with Lower Intraocular Pressure." *Ophthalmology* 126 (8): 1119–30.
Martin, A. R., M. Kanai, Y. Kamatani, Y. Okada, B. M. Neale, and M. J. Daly. 2019. "Clinical Use of Current Polygenic Risk Scores May Exacerbate Health Disparities." *Nature Genetics* 51 (4). https://doi.org/10.1038/s41588-019-0379-x.
Masis, Marisse, Patrick J. Mineault, Eileen Phan, and Shan C. Lin. 2018. "The Role of Phacoemulsification in Glaucoma Therapy: A Systematic Review and Meta-Analysis." *Survey of Ophthalmology* 63 (5): 700–710.
Maslin, J. S., K. Mansouri, and S. K. Dorairaj. 2015. "HRT for the Diagnosis and Detection of Glaucoma Progression." *The Open Ophthalmology Journal* 9 (May). https://doi.org/10.2174/1874364101509010058.
Mavaddat, N., K. Michailidou, J. Dennis, M. Lush, L. Fachal, A. Lee, J. P. Tyrer, et al. 2019. "Polygenic Risk Scores for Prediction of Breast Cancer and Breast Cancer Subtypes." *American Journal of Human Genetics* 104 (1). https://doi.org/10.1016/j.ajhg.2018.11.002.
McCarthy, Davis J., Yunshun Chen, and Gordon K. Smyth. 2012. "Differential Expression Analysis of Multifactor RNA-Seq Experiments with Respect to Biological Variation." *Nucleic Acids Research* 40 (10): 4288–97.
McCarthy, S., S. Das, W. Kretzschmar, O. Delaneau, A. R. Wood, A. Teumer, H. M. Kang, et al. 2016. "A Reference Panel of 64,976 Haplotypes for Genotype Imputation." *Nature Genetics* 48 (10). https://doi.org/10.1038/ng.3643.
McCarty, Cathy A., B. N. Mukesh, Cara L. Fu, and Hugh R. Taylor. 1999. "The Epidemiology of Cataract in Australia." *American Journal of Ophthalmology* 128 (4): 446–65.

McClellan, J., and M. C. King. 2010. “Genetic Heterogeneity in Human Disease.” *Cell* 141 (2). https://doi.org/10.1016/j.cell.2010.03.032.
Medeiros, F. A., and R. N. Weinreb. 2006. “Evaluation of the Influence of Corneal Biomechanical Properties on Intraocular Pressure Measurements Using the Ocular Response Analyzer.” *Journal of Glaucoma* 15 (5). https://doi.org/10.1097/01.ijg.0000212268.42606.97.
Medeiros, F. A., R. N. Weinreb, P. A. Sample, C. F. Gomi, C. Bowd, J. G. Crowston, and L. M. Zangwill. 2005. “Validation of a Predictive Model to Estimate the Risk of Conversion from Ocular Hypertension to Glaucoma.” *Archives of Ophthalmology* 123 (10). https://doi.org/10.1001/archopht.123.10.1351.
Medeiros, Felipe A., Renato Lisboa, Robert N. Weinreb, Christopher A. Girkin, Jeffrey M. Liebmann, and Linda M. Zangwill. 2012. “A Combined Index of Structure and Function for Staging Glaucomatous Damage.” *Archives of Ophthalmology* 130 (9). https://doi.org/10.1001/archophthalmol.2012.827.
Medeiros, Felipe A., Daniel Meira-Freitas, Renato Lisboa, Tung-Mei Kuang, Linda M. Zangwill, and Robert N. Weinreb. 2013. “Corneal Hysteresis as a Risk Factor for Glaucoma Progression: A Prospective Longitudinal Study.” *Ophthalmology* 120 (8): 1533–40.
Medeiros, Felipe A., Pamela A. Sample, and Robert N. Weinreb. 2004. “Frequency Doubling Technology Perimetry Abnormalities as Predictors of Glaucomatous Visual Field Loss.” *American Journal of Ophthalmology* 137 (5): 863–71.
Medeiros, Felipe A., and Robert N. Weinreb. 2012. “Is Corneal Thickness an Independent Risk Factor for Glaucoma?” *Ophthalmology* 119 (3): 435–36.
Mega, J. L., N. O. Stitziel, J. G. Smith, D. I. Chasman, M. Caulfield, J. J. Devlin, F. Nordio, et al. 2015. “Genetic Risk, Coronary Heart Disease Events, and the Clinical Benefit of Statin Therapy: An Analysis of Primary and Secondary Prevention Trials.” *Lancet* 385 (9984). https://doi.org/10.1016/S0140-6736(14)61730-X.
Megevand, Gordana Sunaric, and Alain M. Bron. 2020. “Personalising Surgical Treatments for Glaucoma Patients.” *Progress in Retinal and Eye Research*, June. https://doi.org/10.1016/j.preteyeres.2020.100879.
Melancia, Diana, Luis Abegão Pinto, and Carlos Marques-Neves. 2015. “Cataract Surgery and Intraocular Pressure.” *Ophthalmic Research* 53 (3): 141–48.
Melki, S., A. Todani, and G. Cherfan. 2014. “An Implantable Intraocular Pressure Transducer: Initial Safety Outcomes.” *JAMA Ophthalmology* 132 (10). https://doi.org/10.1001/jamaophthalmol.2014.1739.
Memarzadeh, Farnaz, Mei Ying-Lai, Stanley P. Azen, and Rohit Varma. 2008. “Associations with Intraocular Pressure in Latinos: The Los Angeles Latino Eye Study.” *American Journal of Ophthalmology* 146 (1): 69–76.
Meyer, David, Evgenia Dimitriadou, Kurt Hornik, Andreas Weingessel, and Friedrich Leisch. 2019. “e1071: Misc Functions of the Department of Statistics, Probability Theory Group (Formerly: E1071), TU Wien.” Comprehensive R Archive Network (CRAN). https://CRAN.R-project.org/package=e1071.
Micheal, S., S. N. Siddiqui, S. N. Zafar, A. Iqbal, M. I. Khan, and A. I. den Hollander. 2016. “Identification of Novel Variants in LTBP2 and PXDN Using Whole-Exome Sequencing in Developmental and Congenital Glaucoma.” *PloS One* 11 (7). https://doi.org/10.1371/journal.pone.0159259.
Mikelberg, F. S., C. M. Parfitt, N. V. Swindale, S. L. Graham, S. M. Drance, and R. Gosine. 1995. “Ability of the Heidelberg Retina Tomograph to Detect Early Glaucomatous Visual Field Loss.” *Journal of Glaucoma* 4 (4). https://pubmed.ncbi.nlm.nih.gov/19920681/.
Miki, Atsuya, Yuichi Yasukura, Robert N. Weinreb, Tomomi Yamada, Shizuka Koh, Tomoko Asai, Yasushi Ikuno, Naoyuki Maeda, and Kohji Nishida. 2019. “Dynamic Scheimpflug Ocular Biomechanical Parameters in Healthy and Medically Controlled Glaucoma Eyes.” *Journal of Glaucoma*. https://doi.org/10.1097/ijg.0000000000001268.
Mistry, S., J. R. Harrison, D. J. Smith, V. Escott-Price, and S. Zammit. 2018. “The Use of Polygenic Risk Scores to Identify Phenotypes Associated with Genetic Risk of

Schizophrenia: Systematic Review." *Schizophrenia Research* 197 (July). https://doi.org/10.1016/j.schres.2017.10.037.
Mitchell, Paul, Elena Rochtchina, Anne J. Lee, and Jie Jin Wang. 2002. "Bias in Self-Reported Family History and Relationship to Glaucoma: The Blue Mountains Eye Study." *Ophthalmic Epidemiology* 9 (5): 333–45.
Mitchell, Paul, Wayne Smith, Karin Attebo, and Paul R. Healey. 1996. "Prevalence of Open-Angle Glaucoma in Australia." *Ophthalmology* 103 (10): 1661–69.
Mitchell, P., W. Smith, K. Attebo, and P. R. Healey. 1996. "Prevalence of Open-Angle Glaucoma in Australia. The Blue Mountains Eye Study." *Ophthalmology* 103 (10): 1661–69.
Mitchell, P., W. Smith, K. Attebo, and J. J. Wang. 1995. "Prevalence of Age-Related Maculopathy in Australia. The Blue Mountains Eye Study." *Ophthalmology* 102 (10): 1450–60.
Mollan, S. P., J. S. Wolffsohn, M. Nessim, M. Laiquzzaman, S. Sivakumar, S. Hartley, and S. Shah. 2008. "Accuracy of Goldmann, Ocular Response Analyser, Pascal and TonoPen XL Tonometry in Keratoconic and Normal Eyes." *The British Journal of Ophthalmology* 92 (12). https://doi.org/10.1136/bjo.2007.136473.
Montana, Cynthia L., and Anjali M. Bhorade. 2018. "Glaucoma and Quality of Life: Fall and Driving Risk." *Current Opinion in Ophthalmology* 29 (2): 135–40.
Moraes, Carlos Gustavo De, Carlos Gustavo De Moraes, Kaweh Mansouri, Jeffrey M. Liebmann, Robert Ritch, and for the Triggerfish Consortium. 2018. "Association Between 24-Hour Intraocular Pressure Monitored With Contact Lens Sensor and Visual Field Progression in Older Adults With Glaucoma." *JAMA Ophthalmology*. https://doi.org/10.1001/jamaophthalmol.2018.1746.
Morales, Joannella, Danielle Welter, Emily H. Bowler, Maria Cerezo, Laura W. Harris, Aoife C. McMahon, Peggy Hall, et al. 2018. "A Standardized Framework for Representation of Ancestry Data in Genomics Studies, with Application to the NHGRI-EBI GWAS Catalog." *Genome Biology* 19 (1): 21.
Morgan, J. E., N. J. L. Sheen, R. V. North, Y. Choong, and E. Ansari. 2005. "Digital Imaging of the Optic Nerve Head: Monoscopic and Stereoscopic Analysis." *The British Journal of Ophthalmology* 89 (7): 879–84.
Moroi, Sayoko E., David M. Reed, David S. Sanders, Ahmed Almazroa, Lawrence Kagemann, Neil Shah, Nakul Shekhawat, and Julia E. Richards. 2019. "Precision Medicine to Prevent Glaucoma-Related Blindness." *Current Opinion in Ophthalmology* 30 (3): 187–98.
Mosaed, Sameh, John H. K. Liu, and Robert N. Weinreb. 2005. "Correlation between Office and Peak Nocturnal Intraocular Pressures in Healthy Subjects and Glaucoma Patients." *American Journal of Ophthalmology*. https://doi.org/10.1016/j.ajo.2004.09.062.
Mottet, Benjamin, Florent Aptel, Jean-Paul Romanet, Ralitsa Hubanova, Jean-Louis Pépin, and Christophe Chiquet. 2013. "24 - Hour Intraocular Pressure Rhythm in Young Healthy Subjects Evaluated With Continuous Monitoring Using a Contact Lens Sensor." *JAMA Ophthalmology* 131 (12): 1507.
Musch, D. C., B. W. Gillespie, P. R. Lichter, L. M. Niziol, and N. K. Janz. 2009. "Visual Field Progression in the Collaborative Initial Glaucoma Treatment Study the Impact of Treatment and Other Baseline Factors." *Ophthalmology* 116 (2). https://doi.org/10.1016/j.ophtha.2008.08.051.
Nagai, T., J. Aruga, S. Takada, T. Günther, R. Spörle, K. Schughart, and K. Mikoshiba. 1997. "The Expression of the Mouse Zic1, Zic2, and Zic3 Gene Suggests an Essential Role for Zic Genes in Body Pattern Formation." *Developmental Biology* 182 (2): 299–313.
Na, Jung Hwa, Kyung Rim Sung, Seunghee Baek, Yoon Jeon Kim, Mary K. Durbin, Hye Jin Lee, Hwang Ki Kim, and Yong Ho Sohn. 2012. "Detection of Glaucoma Progression by Assessment of Segmented Macular Thickness Data Obtained Using Spectral Domain Optical Coherence Tomography." *Investigative Ophthalmology & Visual Science* 53 (7): 3817–26.

Nakagawa, Shinichi, Paul C. D. Johnson, and Holger Schielzeth. 2017. “The Coefficient of Determination R 2 and Intra-Class Correlation Coefficient from Generalized Linear Mixed-Effects Models Revisited and Expanded.” *Journal of the Royal Society, Interface / the Royal Society* 14 (134): 20170213.
Nakano, T., M. Tatemichi, Y. Miura, M. Sugita, and K. Kitahara. 2005. “Long-Term Physiologic Changes of Intraocular PressureA 10-Year Longitudinal Analysis in Young and Middle-Aged Japanese Men.” *Ophthalmology* 112 (4): 609–16.
Nannini, D. R., H. Kim, F. Fan, and X. Gao. 2018. “Genetic Risk Score Is Associated with Vertical Cup-to-Disc Ratio and Improves Prediction of Primary Open-Angle Glaucoma in Latinos.” *Ophthalmology* 125 (6). https://doi.org/10.1016/j.ophtha.2017.12.014.
N’Diaye, Amidou, Gary K. Chen, Cameron D. Palmer, Bing Ge, Bamidele Tayo, Rasika A. Mathias, Jingzhong Ding, et al. 2011. “Identification, Replication, and Fine-Mapping of Loci Associated with Adult Height in Individuals of African Ancestry.” *PLoS Genetics* 7 (10): e1002298.
Newman, Alexander R., and Nicholas H. Andrew. 2018. “Changes in Australian Practice Patterns for Glaucoma Management.” *Clinical & Experimental Ophthalmology*, December. https://doi.org/10.1111/ceo.13456.
Nguyen, B. Audrey, B. Audrey Nguyen, Matthew A. Reilly, and Cynthia J. Roberts. 2020. “Biomechanical Contribution of the Sclera to Dynamic Corneal Response in Air-Puff Induced Deformation in Human Donor Eyes.” *Experimental Eye Research*. https://doi.org/10.1016/j.exer.2019.107904.
Nguyen, Q. D., J. S. Heier, D. V. Do, A. C. Mirando, N. B. Pandey, H. Sheng, and T. Heah. 2020. “The Tie2 Signaling Pathway in Retinal Vascular Diseases: A Novel Therapeutic Target in the Eye.” *International Journal of Retina and Vitreous* 6 (October). https://doi.org/10.1186/s40942-020-00250-z.
NHMRC. 2010. “Guidelines for the Screening, Prognosis, Diagnosis, Management and Prevention of Glaucoma.” CP113. NHMRC. https://www.nhmrc.gov.au/about-us/publications/guidelines-screening-prognosis-diagnosis-management-and-prevention-glaucoma.
Nouri-Mahdavi, K., D. Hoffman, A. L. Coleman, G. Liu, G. Li, D. Gaasterland, and J. Caprioli. 2004. “Predictive Factors for Glaucomatous Visual Field Progression in the Advanced Glaucoma Intervention Study.” *Ophthalmology* 111 (9). https://doi.org/10.1016/j.ophtha.2004.02.017.
Nouri-Mahdavi, Kouros. 2005. “Pointwise Linear Regression for Evaluation of Visual Field Outcomes and Comparison With the Advanced Glaucoma Intervention Study Methods.” *Archives of Ophthalmology* 123 (2): 193.
O’Leary, Neil, Balwantray C. Chauhan, and Paul H. Artes. 2012. “Visual Field Progression in Glaucoma: Estimating the Overall Significance of Deterioration with Permutation Analyses of Pointwise Linear Regression (PoPLR).” *Investigative Ophthalmology & Visual Science* 53 (11): 6776.
Olsen, Catherine M., Adèle C. Green, Rachel E. Neale, Penelope M. Webb, Rebekah A. Cicero, Lea M. Jackman, Suzanne M. O’Brien, et al. 2012. “Cohort Profile: The QSkin Sun and Health Study.” *International Journal of Epidemiology* 41 (4): 929–929i.
Pajic, Bojan, Brigitte Pajic-Eggspuchler, and Ivan Haefliger. 2011. “Continuous IOP Fluctuation Recording in Normal Tension Glaucoma Patients.” *Current Eye Research* 36 (12): 1129–38.
Panagiotou, O. A., and J. P. Ioannidis. 2012. “What Should the Genome-Wide Significance Threshold Be? Empirical Replication of Borderline Genetic Associations.” *International Journal of Epidemiology* 41 (1). https://doi.org/10.1093/ije/dyr178.
Park, J. H., S. Wacholder, M. H. Gail, U. Peters, K. B. Jacobs, S. J. Chanock, and N. Chatterjee. 2010. “Estimation of Effect Size Distribution from Genome-Wide Association Studies and Implications for Future Discoveries.” *Nature Genetics* 42 (7). https://doi.org/10.1038/ng.610.
Parrish, R. K., S. J. Gedde, I. U. Scott, W. J. Feuer, J. C. Schiffman, C. M. Mangione, and A. Montenegro-Piniella. 1997. “Visual Function and Quality of Life among Patients with

Glaucoma." *Archives of Ophthalmology* 115 (11). https://doi.org/10.1001/archopht.1997.01100160617016.
Pasquale, L. R., and J. H. Kang. 2009. "Lifestyle, Nutrition, and Glaucoma." *Journal of Glaucoma* 18 (6). https://doi.org/10.1097/IJG.0b013e31818d3899.
Pasutto, Francesca, Heinrich Sticht, Gerhard Hammersen, Gabriele Gillessen-Kaesbach, David R. Fitzpatrick, Gudrun Nürnberg, Frank Brasch, et al. 2007. "Mutations in STRA6 Cause a Broad Spectrum of Malformations Including Anophthalmia, Congenital Heart Defects, Diaphragmatic Hernia, Alveolar Capillary Dysplasia, Lung Hypoplasia, and Mental Retardation." *American Journal of Human Genetics* 80 (3): 550–60.
Pepe, M. S., and H. E. Janes. 2008. "Gauging the Performance of SNPs, Biomarkers, and Clinical Factors for Predicting Risk of Breast Cancer." *Journal of the National Cancer Institute* 100 (14). https://doi.org/10.1093/jnci/djn215.
Pezzullo, L., J. Streatfeild, P. Simkiss, and D. Shickle. 2018. "The Economic Impact of Sight Loss and Blindness in the UK Adult Population." *BMC Health Services Research* 18 (1). https://doi.org/10.1186/s12913-018-2836-0.
Pfeiffer, Norbert, Julian Garcia-Feijoo, Jose M. Martinez-de-la-Casa, Jose M. Larrosa, Antonio Fea, Hans Lemij, Stefano Gandolfi, Oliver Schwenn, Katrin Lorenz, and Thomas W. Samuelson. 2015. "A Randomized Trial of a Schlemm's Canal Microstent with Phacoemulsification for Reducing Intraocular Pressure in Open-Angle Glaucoma." *Ophthalmology* 122 (7): 1283–93.
Pickrell, J. K., T. Berisa, J. Z. Liu, L. Ségurel, J. Y. Tung, and D. A. Hinds. 2016. "Detection and Interpretation of Shared Genetic Influences on 42 Human Traits." *Nature Genetics* 48 (7). https://doi.org/10.1038/ng.3570.
Pohjalainen, Tuula, Eija Vesti, Risto J. Uusitalo, and Leila Laatikainen. 2001. "Intraocular Pressure after Phacoemulsification and Intraocular Lens Implantation in Nonglaucomatous Eyes with and without Exfoliation." *Journal of Cataract and Refractive Surgery* 27 (3): 426–31.
Poinoosawmy, D., L. Fontana, J. X. Wu, C. V. Bunce, and R. A. Hitchings. 1998. "Frequency of Asymmetric Visual Field Defects in Normal-Tension and High-Tension Glaucoma." *Ophthalmology* 105 (6): 988–91.
Poitras, V., C. Wells, C. Hutnik, S. Klarenback, H. So, B. Tsoi, A. Smith, et al. 2019. "Optimal Use of Minimally Invasive Glaucoma Surgery: A Health Technology Assessment [Internet]," January. https://pubmed.ncbi.nlm.nih.gov/31305970/.
Polansky, J. R., R. P. Juster, and G. L. Spaeth. 2003. "Association of the Myocilin mt.1 Promoter Variant with the Worsening of Glaucomatous Disease over Time." *Clinical Genetics* 64 (1). https://doi.org/10.1034/j.1399-0004.2003.00099.x.
Poley, Brooks J., Richard L. Lindstrom, Thomas W. Samuelson, and Richard Schulze Jr. 2009. "Intraocular Pressure Reduction after Phacoemulsification with Intraocular Lens Implantation in Glaucomatous and Nonglaucomatous Eyes: Evaluation of a Causal Relationship between the Natural Lens and Open-Angle Glaucoma." *Journal of Cataract and Refractive Surgery* 35 (11): 1946–55.
Prendergast, Lisa, Chelly van Vuuren, Agnieszka Kaczmarczyk, Volker Doering, Daniela Hellwig, Nadine Quinn, Christian Hoischen, Stephan Diekmann, and Kevin F. Sullivan. 2011. "Premitotic Assembly of Human CENPs -T and -W Switches Centromeric Chromatin to a Mitotic State." *PLoS Biology* 9 (6): e1001082.
Purcell, Shaun, Benjamin Neale, Kathe Todd-Brown, Lori Thomas, Manuel A. R. Ferreira, David Bender, Julian Maller, et al. 2007. "PLINK: A Tool Set for Whole-Genome Association and Population-Based Linkage Analyses." *American Journal of Human Genetics* 81 (3): 559–75.
Qassim, A., E. Souzeau, O. M. Siggs, M. M. Hassall, X. Han, H. L. Griffiths, N. A. Frost, et al. 2020. "An Intraocular Pressure Polygenic Risk Score Stratifies Multiple Primary Open-Angle Glaucoma Parameters Including Treatment Intensity." *Ophthalmology* 127 (7). https://doi.org/10.1016/j.ophtha.2019.12.025.
Qassim, Ayub, Mona S. Awadalla, Sean Mullany, Mark Hassall, Owen Siggs, Emmanuelle Souzeau, Thi Nguyen, et al. 2020. "A Polygenic Risk Score Predicts Intraocular

Pressure Fluctuation and Readings Outside Office Hours as Measured by Home Tonometry." *Investigative Ophthalmology & Visual Science* 61 (7): 3491–3491.
Qassim, Ayub, Sean Mullany, Farshad Abedi, Henry Marshall, Mark M. Hassall, Antonia Kolovos, Lachlan S. W. Knight, et al. 2020. "Corneal Stiffness Parameters Are Predictive of Structural and Functional Progression in Glaucoma Suspects." *Ophthalmology*, November. https://doi.org/10.1016/j.ophtha.2020.11.021.
Qassim, Ayub, Mark J. Walland, John Landers, Mona Awadalla, Thi Nguyen, Jason Loh, Angela M. Schulz, et al. 2020. "Effect of Phacoemulsification Cataract Surgery on Intraocular Pressure in Early Glaucoma: A Prospective Multi-site Study." *Clinical & Experimental Ophthalmology* 48 (4): 442–49.
Qiu, Mary, Michael V. Boland, and Pradeep Y. Ramulu. 2017. "Cup-to-Disc Ratio Asymmetry in U.S. Adults." *Ophthalmology* 124 (8): 1229–36.
Quigley, H. A. 1999. "Neuronal Death in Glaucoma." *Progress in Retinal and Eye Research* 18 (1). https://doi.org/10.1016/s1350-9462(98)00014-7.
———. 2019. "21st Century Glaucoma Care." *Eye* 33 (2). https://doi.org/10.1038/s41433-018-0227-8.
Quigley, H. A., A. Brown, and M. E. Dorman-Pease. 1991. "Alterations in Elastin of the Optic Nerve Head in Human and Experimental Glaucoma." *The British Journal of Ophthalmology* 75 (9): 552–57.
Quigley, H. A., A. E. Brown, J. D. Morrison, and S. M. Drance. 1990. "The Size and Shape of the Optic Disc in Normal Human Eyes." *Archives of Ophthalmology* 108 (1): 51–57.
Quigley, Harry A. 1981. "Optic Nerve Damage in Human Glaucoma: II. The Site of Injury and Susceptibility to Damage." *Archives of Ophthalmology* 99 (4): 635.
———. 1998. "Identification of Glaucoma-Related Visual Field Abnormality with the Screening Protocol of Frequency Doubling technology11Welch-Allyn, Inc, Skaneateles, New York, Provided an Instrument on Loan and an Unrestricted Donation." *American Journal of Ophthalmology* 125 (6): 819–29.
Rabiolo, Alessandro, Esteban Morales, Lilian Mohamed, Vicente Capistrano, Ji Hyun Kim, Abdelmonem Afifi, Fei Yu, Anne L. Coleman, Kouros Nouri-Mahdavi, and Joseph Caprioli. 2019. "Comparison of Methods to Detect and Measure Glaucomatous Visual Field Progression." *Translational Vision Science & Technology* 8 (5): 2.
Raina, P. S., C. Wolfson, S. A. Kirkland, L. E. Griffith, M. Oremus, C. Patterson, H. Tuokko, et al. 2009. "The Canadian Longitudinal Study on Aging (CLSA)." *Canadian Journal on Aging = La Revue Canadienne Du Vieillissement* 28 (3). https://doi.org/10.1017/S0714980809990055.
Rajkomar, Alvin, Jeffrey Dean, and Isaac Kohane. 2019. "Machine Learning in Medicine." *The New England Journal of Medicine* 380 (14): 1347–58.
Ramdas, Wishal D., Leonieke M. E. van Koolwijk, M. Kamran Ikram, Nomdo M. Jansonius, Paulus T. V. M. de Jong, Arthur A. B. Bergen, Aaron Isaacs, et al. 2010. "A Genome-Wide Association Study of Optic Disc Parameters." *PLoS Genetics* 6 (6): e1000978.
Ramjaun, A. R., S. Tomlinson, A. Eddaoudi, and J. Downward. 2007. "Upregulation of Two BH3-Only Proteins, Bmf and Bim, during TGF Beta-Induced Apoptosis." *Oncogene* 26 (7): 970–81.
Reis, L. M., R. C. Tyler, E. Weh, K. E. Hendee, K. F. Schilter, J. A. Phillips, S. Sequeira, A. Schinzel, and E. V. Semina. 2016. "Whole Exome Sequencing Identifies Multiple Diagnoses in Congenital Glaucoma with Systemic Anomalies." *Clinical Genetics* 90 (4). https://doi.org/10.1111/cge.12816.
Resnikoff, S., D. Pascolini, D. Etya'ale, I. Kocur, R. Pararajasegaram, G. P. Pokharel, and S. P. Mariotti. 2004. "Global Data on Visual Impairment in the Year 2002." *Bulletin of the World Health Organization* 82 (11). https://pubmed.ncbi.nlm.nih.gov/15640920/.
Rezaie, T., A. Child, R. Hitchings, G. Brice, L. Miller, M. Coca-Prados, E. Héon, et al. 2002. "Adult-Onset Primary Open-Angle Glaucoma Caused by Mutations in Optineurin." *Science* 295 (5557). https://doi.org/10.1126/science.1066901.
Reznicek, Lukas, Daniel Muth, Anselm Kampik, Aljoscha S. Neubauer, and Christoph Hirneiss. 2013. "Evaluation of a Novel Scheimpflug-Based Non-Contact Tonometer in

Healthy Subjects and Patients with Ocular Hypertension and Glaucoma." *The British Journal of Ophthalmology* 97 (11): 1410–14.
Riboli, E., and R. Kaaks. 1997. "The EPIC Project: Rationale and Study Design. European Prospective Investigation into Cancer and Nutrition." *International Journal of Epidemiology* 26 Suppl 1: S6–14.
Roberts, Cynthia J., Ashraf M. Mahmoud, Jeffrey P. Bons, Arif Hossain, Ahmed Elsheikh, Riccardo Vinciguerra, Paolo Vinciguerra, and Renato Ambrósio. 2017. "Introduction of Two Novel Stiffness Parameters and Interpretation of Air Puff–Induced Biomechanical Deformation Parameters With a Dynamic Scheimpflug Analyzer." *Journal of Refractive Surgery*. https://doi.org/10.3928/1081597x-20161221-03.
Robinson, Mark D., Davis J. McCarthy, and Gordon K. Smyth. 2010. "edgeR: A Bioconductor Package for Differential Expression Analysis of Digital Gene Expression Data." *Bioinformatics* 26 (1): 139–40.
Robinson, Mark D., and Alicia Oshlack. 2010. "A Scaling Normalization Method for Differential Expression Analysis of RNA-Seq Data." *Genome Biology* 11 (3): R25.
Rutten-Jacobs, L. C., S. C. Larsson, R. Malik, K. Rannikmäe, C. L. Sudlow, M. Dichgans, H. S. Markus, and M. Traylor. 2018. "Genetic Risk, Incident Stroke, and the Benefits of Adhering to a Healthy Lifestyle: Cohort Study of 306 473 UK Biobank Participants." *BMJ* 363 (October). https://doi.org/10.1136/bmj.k4168.
Saeedi, Osamah J., Tobias Elze, Loris D'Acunto, Ramya Swamy, Vikram Hegde, Surabhi Gupta, Amin Venjara, et al. 2019. "Agreement and Predictors of Discordance of 6 Visual Field Progression Algorithms." *Ophthalmology* 126 (6): 822–28.
Saika, Shizuya. 2006. "TGFbeta Pathobiology in the Eye." *Laboratory Investigation; a Journal of Technical Methods and Pathology* 86 (2): 106–15.
Saks, Danit, Angela Schulz, Jamie Craig, Stuart Graham, and the PROGRESSA Study Group. 2020. "Determination of Retinal Nerve Fibre Layer and Ganglion Cell/inner Plexiform Layers Progression Rates Using Two Optical Coherence Tomography Systems: The PROGRESSA Study." *Clinical & Experimental Ophthalmology* 9 (August): 31.
Sanfilippo, Paul G., Alex W. Hewitt, Chris J. Hammond, and David A. Mackey. 2010. "The Heritability of Ocular Traits." *Survey of Ophthalmology* 55 (6): 561–83.
Saunders, L. J., R. A. Russell, J. F. Kirwan, A. I. McNaught, and D. P. Crabb. 2014. "Examining Visual Field Loss in Patients in Glaucoma Clinics during Their Predicted Remaining Lifetime." *Investigative Ophthalmology & Visual Science* 55 (1). https://doi.org/10.1167/iovs.13-13006.
Scheetz, Todd E., Ben Faga, Lizette Ortega, Ben R. Roos, Mae O. Gordon, Michael A. Kass, Kai Wang, and John H. Fingert. 2016. "Glaucoma Risk Alleles in the Ocular Hypertension Treatment Study." *Ophthalmology* 123 (12): 2527–36.
Seddon, J. M., and B. Rosner. 2019. "Validated Prediction Models for Macular Degeneration Progression and Predictors of Visual Acuity Loss Identify High-Risk Individuals." *American Journal of Ophthalmology* 198 (February). https://doi.org/10.1016/j.ajo.2018.10.022.
Sharma, S., K. P. Burdon, G. Chidlow, S. Klebe, A. Crawford, D. P. Dimasi, A. Dave, et al. 2012. "Association of Genetic Variants in the TMCO1 Gene with Clinical Parameters Related to Glaucoma and Characterization of the Protein in the Eye." *Investigative Ophthalmology & Visual Science* 53 (8). https://doi.org/10.1167/iovs.11-9047.
Shen, W., B. Huang, and J. Yang. 2019. "Ocular Surface Changes in Prostaglandin Analogue-Treated Patients." *Journal of Ophthalmology* 2019 (December). https://doi.org/10.1155/2019/9798272.
Sheu, Ching-Fan. 2000. "Regression Analysis of Correlated Binary Outcomes." *Behavior Research Methods, Instruments, & Computers*. https://doi.org/10.3758/bf03207794.
Shingleton, Bradford J., James J. Pasternack, James W. Hung, and Mark W. O??Donoghue. 2006. "Three and Five Year Changes in Intraocular Pressures After Clear Corneal Phacoemulsification in Open Angle Glaucoma Patients, Glaucoma Suspects, and Normal Patients." *Journal of Glaucoma* 15 (6): 494–98.

Shin, Joong Won, Kyung Rim Sung, Gary C. Lee, Mary K. Durbin, and Daniel Cheng. 2017. “Ganglion Cell–Inner Plexiform Layer Change Detected by Optical Coherence Tomography Indicates Progression in Advanced Glaucoma.” *Ophthalmology* 124 (10): 1466–74.
Shi, Yuhua, Panpan Liu, Jian Guan, Yan Lu, and Kaiming Su. 2015. “Association between Glaucoma and Obstructive Sleep Apnea Syndrome: A Meta-Analysis and Systematic Review.” Edited by Shahrad Taheri. https://doi.org/10.1371/journal.pone.0115625.
Shungin, Dmitry, Thomas W. Winkler, Damien C. Croteau-Chonka, Teresa Ferreira, Adam E. Locke, Reedik Mägi, Rona J. Strawbridge, et al. 2015. “New Genetic Loci Link Adipose and Insulin Biology to Body Fat Distribution.” *Nature* 518 (7538): 187–96.
Sigal, Ian A., John G. Flanagan, and C. Ross Ethier. 2005. “Factors Influencing Optic Nerve Head Biomechanics.” *Investigative Opthalmology & Visual Science*. https://doi.org/10.1167/iovs.05-0541.
Siggs, O. M., E. Souzeau, J. Breen, A. Qassim, T. Zhou, A. Dubowsky, J. B. Ruddle, and J. E. Craig. 2019. “Autosomal Dominant Nanophthalmos and High Hyperopia Associated with a C-Terminal Frameshift Variant in MYRF.” *Molecular Vision* 25 (September). https://pubmed.ncbi.nlm.nih.gov/31700225/.
Siggs, O. M., E. Souzeau, D. A. Taranath, A. Dubowsky, A. Chappell, T. Zhou, S. Javadiyan, et al. 2020. “Biallelic CPAMD8 Variants Are a Frequent Cause of Childhood and Juvenile Open-Angle Glaucoma.” *Ophthalmology* 127 (6). https://doi.org/10.1016/j.ophtha.2019.12.024.
Simcoe, M. J., A. P. Khwaja, U. K. B. Eye, Consortium V, P. G. Hysi, and C. J. Hammond. 2020. “Genome-Wide Association Study of Corneal Biomechanical Properties Identifies over 200 Loci Providing Insight into the Genetic Aetiology of Ocular Diseases.” *Human Molecular Genetics*, July. https://doi.org/10.1093/hmg/ddaa155.
Siva, Nayanah. 2008. “1000 Genomes Project.” *Nature Biotechnology* 26 (3): 256–256.
Skene, L., and R. Smallwood. 2002. “Informed Consent: Lessons from Australia.” *BMJ* 324 (7328). https://doi.org/10.1136/bmj.324.7328.39.
Sng, C. C., M. Ang, and K. Barton. 2017. “Central Corneal Thickness in Glaucoma.” *Current Opinion in Ophthalmology* 28 (2). https://doi.org/10.1097/ICU.0000000000000335.
Song, Ge, Kengyeh K. Chu, Sanghoon Kim, Michael Crose, Brian Cox, Evan T. Jelly, J. Niklas Ulrich, and Adam Wax. 2019. “First Clinical Application of Low-Cost OCT.” *Translational Vision Science & Technology* 8 (3): 61–61.
Souma, T., S. W. Tompson, B. R. Thomson, O. M. Siggs, K. Kizhatil, S. Yamaguchi, L. Feng, et al. 2016. “Angiopoietin Receptor TEK Mutations Underlie Primary Congenital Glaucoma with Variable Expressivity.” *The Journal of Clinical Investigation* 126 (7). https://doi.org/10.1172/JCI85830.
Souzeau, E., K. P. Burdon, A. Dubowsky, S. Grist, B. Usher, J. T. Fitzgerald, A. Crawford, et al. 2013. “Higher Prevalence of Myocilin Mutations in Advanced Glaucoma in Comparison with Less Advanced Disease in an Australasian Disease Registry.” *Ophthalmology* 120 (6). https://doi.org/10.1016/j.ophtha.2012.11.029.
Souzeau, Emmanuelle, Ivan Goldberg, Paul R. Healey, Richard A. D. Mills, John Landers, Stuart L. Graham, John R. B. Grigg, et al. 2012. “Australian and New Zealand Registry of Advanced Glaucoma: Methodology and Recruitment: Australasian Advanced Glaucoma Registry.” *Clinical & Experimental Ophthalmology* 40 (6): 569–75.
Souzeau, E., K. H. Tram, M. Witney, J. B. Ruddle, S. L. Graham, P. R. Healey, I. Goldberg, et al. 2017. “Myocilin Predictive Genetic Testing for Primary Open-Angle Glaucoma Leads to Early Identification of At-Risk Individuals.” *Ophthalmology* 124 (3). https://doi.org/10.1016/j.ophtha.2016.11.011.
Springelkamp, Henriët, René Höhn, Aniket Mishra, Pirro G. Hysi, Chiea-Chuen Khor, Stephanie J. Loomis, Jessica N. Cooke Bailey, et al. 2014. “Meta-Analysis of Genome-Wide Association Studies Identifies Novel Loci That Influence Cupping and the Glaucomatous Process.” *Nature Communications* 5 (September): 4883.
Springelkamp, Henriët, Aniket Mishra, Pirro G. Hysi, Puya Gharahkhani, René Höhn, Chiea-Chuen Khor, Jessica N. Cooke Bailey, et al. 2015. “Meta-Analysis of Genome-Wide

Association Studies Identifies Novel Loci Associated With Optic Disc Morphology." *Genetic Epidemiology* 39 (3): 207–16.
Springelkamp, H., A. I. Iglesias, G. Cuellar-Partida, N. Amin, K. P. Burdon, E. M. van Leeuwen, P. Gharahkhani, et al. 2015. "ARHGEF12 Influences the Risk of Glaucoma by Increasing Intraocular Pressure." *Human Molecular Genetics*. https://doi.org/10.1093/hmg/ddv027.
Springelkamp, H., A. I. Iglesias, A. Mishra, R. Höhn, R. Wojciechowski, A. P. Khawaja, A. Nag, et al. 2017. "New Insights into the Genetics of Primary Open-Angle Glaucoma Based on Meta-Analyses of Intraocular Pressure and Optic Disc Characteristics." *Human Molecular Genetics* 26 (2). https://doi.org/10.1093/hmg/ddw399.
Stone, E. M., J. H. Fingert, W. L. Alward, T. D. Nguyen, J. R. Polansky, S. L. Sunden, D. Nishimura, et al. 1997. "Identification of a Gene That Causes Primary Open Angle Glaucoma." *Science* 275 (5300). https://doi.org/10.1126/science.275.5300.668.
Suda, Kenji, Tadamichi Akagi, Hideo Nakanishi, Hisashi Noma, Hanako Ohashi Ikeda, Takanori Kameda, Tomoko Hasegawa, and Akitaka Tsujikawa. 2018. "Evaluation of Structure-Function Relationships in Longitudinal Changes of Glaucoma Using the Spectralis OCT Follow-Up Mode." *Scientific Reports* 8 (1): 1711.
Sudlow, Cathie, John Gallacher, Naomi Allen, Valerie Beral, Paul Burton, John Danesh, Paul Downey, et al. 2015. "UK Biobank: An Open Access Resource for Identifying the Causes of a Wide Range of Complex Diseases of Middle and Old Age." *PLOS Medicine*. https://doi.org/10.1371/journal.pmed.1001779.
Sudlow, C., J. Gallacher, N. Allen, V. Beral, P. Burton, J. Danesh, P. Downey, et al. 2015. "UK Biobank: An Open Access Resource for Identifying the Causes of a Wide Range of Complex Diseases of Middle and Old Age." *PLoS Medicine* 12 (3). https://doi.org/10.1371/journal.pmed.1001779.
Suh, Min Hee, Ki Ho Park, Hyunjoong Kim, Tae-Woo Kim, Seok Hwan Kim, Sun-Young Kim, and Dong Myung Kim. 2012. "Glaucoma Progression After the First-Detected Optic Disc Hemorrhage by Optical Coherence Tomography." *Journal of Glaucoma* 21 (6): 358.
Sultan, Marla B., Steven L. Mansberger, and Paul P. Lee. 2009. "Understanding the Importance of IOP Variables in Glaucoma: A Systematic Review." *Survey of Ophthalmology*. https://doi.org/10.1016/j.survophthal.2009.05.001.
Susanna, Bianca N., Nara G. Ogata, Fábio B. Daga, Carolina N. Susanna, Alberto Diniz-Filho, and Felipe A. Medeiros. 2019. "Association between Rates of Visual Field Progression and Intraocular Pressure Measurements Obtained by Different Tonometers." *Ophthalmology* 126 (1): 49–54.
Susanna, Bianca N., Nara G. Ogata, Alessandro A. Jammal, Carolina N. Susanna, Samuel I. Berchuck, and Felipe A. Medeiros. 2019. "Corneal Biomechanics and Visual Field Progression in Eyes with Seemingly Well-Controlled Intraocular Pressure." *Ophthalmology* 126 (12): 1640–46.
Susanna, Carolina N., Alberto Diniz-Filho, Fábio B. Daga, Bianca N. Susanna, Feilin Zhu, Nara G. Ogata, and Felipe A. Medeiros. 2018. "A Prospective Longitudinal Study to Investigate Corneal Hysteresis as a Risk Factor for Predicting Development of Glaucoma." *American Journal of Ophthalmology* 187 (March): 148–52.
Swaminathan, Swarup S., Amitabha S. Bhakta, Wei Shi, William J. Feuer, Alexandre R. Abreu, Alejandro D. Chediak, and David S. Greenfield. 2018. "Is Obstructive Sleep Apnea Associated With Progressive Glaucomatous Optic Neuropathy?" *Journal of Glaucoma* 27 (1): 1–6.
Szigiato, Andrei-Alexandru, Graham E. Trope, Yaping Jin, and Yvonne M. Buys. 2015. "Trends in Glaucoma Surgical Procedures in Ontario: 1992–2012." *Canadian Journal of Ophthalmology. Journal Canadien D'ophtalmologie* 50 (5): 338–44.
Takagi, Daisuke, Akira Sawada, and Tetsuya Yamamoto. 2017. "Evaluation of a New Rebound Self-Tonometer, Icare HOME: Comparison With Goldmann Applanation Tonometer." *Journal of Glaucoma* 26 (7): 613–18.
Tanigawa, Y., M. Wainberg, J. Karjalainen, T. Kiiskinen, G. Venkataraman, S. Lemmelä, J. A. Turunen, et al. 2020. "Rare Protein-Altering Variants in ANGPTL7 Lower Intraocular

Pressure and Protect against Glaucoma." *PLoS Genetics* 16 (5). https://doi.org/10.1371/journal.pgen.1008682.
Tan, Nicholas Y. Q., David S. Friedman, Ingeborg Stalmans, Iqbal Ike K. Ahmed, and Chelvin C. A. Sng. 2020. "Glaucoma Screening: Where Are We and Where Do We Need to Go?" *Current Opinion in Ophthalmology* 31 (2): 91–100.
Taylor, Hugh R., Jill E. Keeffe, Hien T. V. Vu, Jie Jin Wang, Elena Rochtchina, Paul Mitchell, and M. Lynne Pezzullo. 2005. "Vision Loss in Australia." *The Medical Journal of Australia* 182 (11): 565–68.
Tedja, M. S., R. Wojciechowski, P. G. Hysi, N. Eriksson, N. A. Furlotte, V. J. M. Verhoeven, A. I. Iglesias, et al. 2018. "Genome-Wide Association Meta-Analysis Highlights Light-Induced Signaling as a Driver for Refractive Error." *Nature Genetics* 50 (6). https://doi.org/10.1038/s41588-018-0127-7.
Teng, C. C., C. G. De Moraes, T. S. Prata, C. Tello, R. Ritch, and J. M. Liebmann. 2010. "Beta-Zone Parapapillary Atrophy and the Velocity of Glaucoma Progression." *Ophthalmology* 117 (5). https://doi.org/10.1016/j.ophtha.2009.10.016.
Termühlen, Julia, Natasa Mihailovic, Maged Alnawaiseh, Thomas S. Dietlein, and André Rosentreter. 2016. "Accuracy of Measurements With the iCare HOME Rebound Tonometer." *Journal of Glaucoma* 25 (6): 533–38.
Tham, Y. C., J. Liao, E. N. Vithana, C. C. Khor, Y. Y. Teo, E. S. Tai, T. Y. Wong, T. Aung, and C. Y. Cheng. 2015. "Aggregate Effects of Intraocular Pressure and Cup-to-Disc Ratio Genetic Variants on Glaucoma in a Multiethnic Asian Population." *Ophthalmology* 122 (6). https://doi.org/10.1016/j.ophtha.2015.01.024.
Tham, Yih-Chung, Xiang Li, Tien Y. Wong, Harry A. Quigley, Tin Aung, and Ching-Yu Cheng. 2014. "Global Prevalence of Glaucoma and Projections of Glaucoma Burden through 2040." *Ophthalmology* 121 (11): 2081–90.
The All of Us Research Program Investigators. 2019. "The 'All of Us' Research Program." *The New England Journal of Medicine* 381 (7): 668–76.
Therneau, Terry, and Thomas Lumley. 2009. "Survival: Survival Analysis, Including Penalised Likelihood. R Package Version 2.35-7." *R Foundation for Statistical Computing2011*.
Therneau, Terry M., Patricia M. Grambsch, and V. Shane Pankratz. 2003. "Penalized Survival Models and Frailty." *Journal of Computational and Graphical Statistics*. https://doi.org/10.1198/1061860031365.
Thomas, Sera-Melisa, Maya Jeyaraman, William G. Hodge, Cindy Hutnik, John Costella, and Monali S. Malvankar-Mehta. 2014. "The Effectiveness of Teleglaucoma versus In-Patient Examination for Glaucoma Screening: A Systematic Review and Meta-Analysis." *PloS One* 9 (12): e113779.
Thomson, Benjamin R., Marta Grannonico, Feng Liu, Mingna Liu, Parrykumar Mendapara, Ying Xu, Xiaorong Liu, and Susan E. Quaggin. 2020. "Angiopoietin-1 Knockout Mice as a Genetic Model of Open-Angle Glaucoma." *Translational Vision Science & Technology* 9 (4): 16.
Thomson, B. R., S. Heinen, M. Jeansson, A. K. Ghosh, A. Fatima, H. K. Sung, T. Onay, et al. 2014. "A Lymphatic Defect Causes Ocular Hypertension and Glaucoma in Mice." *The Journal of Clinical Investigation* 124 (10). https://doi.org/10.1172/JCI77162.
Thomson, B. R., T. Souma, S. W. Tompson, T. Onay, K. Kizhatil, O. M. Siggs, L. Feng, et al. 2017. "Angiopoietin-1 Is Required for Schlemm's Canal Development in Mice and Humans." *The Journal of Clinical Investigation* 127 (12). https://doi.org/10.1172/JCI95545.
Thorleifsson, G., K. P. Magnusson, P. Sulem, G. B. Walters, D. F. Gudbjartsson, H. Stefansson, T. Jonsson, et al. 2007. "Common Sequence Variants in the LOXL1 Gene Confer Susceptibility to Exfoliation Glaucoma." *Science* 317 (5843). https://doi.org/10.1126/science.1146554.
Thorleifsson, G., G. B. Walters, A. W. Hewitt, G. Masson, A. Helgason, A. DeWan, A. Sigurdsson, et al. 2010. "Common Variants near CAV1 and CAV2 Are Associated with Primary Open-Angle Glaucoma." *Nature Genetics* 42 (10).

https://doi.org/10.1038/ng.661.
Tian, Lei, Dajiang Wang, Ying Wu, Xiaoli Meng, Bing Chen, Mei Ge, and Yifei Huang. 2016. “Corneal Biomechanical Characteristics Measured by the CorVis Scheimpflug Technology in Eyes with Primary Open-Angle Glaucoma and Normal Eyes.” *Acta Ophthalmologica* 94 (5): e317–24.
Tielsch, James M., Joanne Katz, Kuldev Singh, Harry A. Quigley, John D. Gottsch, Jonathan Javitt, and Alfred Sommer. 1991. “A Population-Based Evaluation of Glaucoma Screening: The Baltimore Eye Survey.” *American Journal of Epidemiology* 134 (10): 1102–10.
Tielsch, J. M., J. Katz, A. Sommer, H. A. Quigley, and J. C. Javitt. 1994. “Family History and Risk of Primary Open Angle Glaucoma. The Baltimore Eye Survey.” *Archives of Ophthalmology* 112 (1). https://doi.org/10.1001/archopht.1994.01090130079022.
Timpson, N. J., C. M. T. Greenwood, N. Soranzo, D. J. Lawson, and J. B. Richards. 2018. “Genetic Architecture: The Shape of the Genetic Contribution to Human Traits and Disease.” *Nature Reviews. Genetics* 19 (2). https://doi.org/10.1038/nrg.2017.101.
Tojo, Naoki, Atsushi Hayashi, and Mitsuya Otsuka. 2020. “Correlation between 24-H Continuous Intraocular Pressure Measurement with a Contact Lens Sensor and Visual Field Progression.” *Graefe's Archive for Clinical and Experimental Ophthalmology = Albrecht von Graefes Archiv Fur Klinische Und Experimentelle Ophthalmologie* 258 (1): 175–82.
Tojo, Naoki, Miyako Oka, Akio Miyakoshi, Hironori Ozaki, and Atsushi Hayashi. 2014. “Comparison of Fluctuations of Intraocular Pressure Before and After Selective Laser Trabeculoplasty in Normal-Tension Glaucoma Patients.” *Journal of Glaucoma* 23 (8): e138–43.
Tojo, Naoki, Mitsuya Otsuka, Akio Miyakoshi, Kazuya Fujita, and Atsushi Hayashi. 2014. “Improvement of Fluctuations of Intraocular Pressure after Cataract Surgery in Primary Angle Closure Glaucoma Patients.” *Graefe's Archive for Clinical and Experimental Ophthalmology = Albrecht von Graefes Archiv Fur Klinische Und Experimentelle Ophthalmologie* 252 (9): 1463–68.
Torkamani, Ali, Nathan E. Wineinger, and Eric J. Topol. 2018. “The Personal and Clinical Utility of Polygenic Risk Scores.” *Nature Reviews. Genetics* 19 (9): 581–90.
Trikha, S., E. Saffari, M. Nongpiur, M. Baskaran, H. Ho, Z. Li, P. Y. Tan, et al. 2015. “A Genetic Variant in TGFBR3-CDC7 Is Associated with Visual Field Progression in Primary Open-Angle Glaucoma Patients from Singapore.” *Ophthalmology* 122 (12). https://doi.org/10.1016/j.ophtha.2015.08.016.
Turley, Patrick, Raymond K. Walters, Omeed Maghzian, Aysu Okbay, James J. Lee, Mark Alan Fontana, Tuan Anh Nguyen-Viet, et al. 2018. “Multi-Trait Analysis of Genome-Wide Association Summary Statistics Using MTAG.” *Nature Genetics* 50 (2): 229–37.
Verhoeven, Virginie J. M., Pirro G. Hysi, Robert Wojciechowski, Qiao Fan, Jeremy A. Guggenheim, René Höhn, Stuart MacGregor, et al. 2013. “Genome-Wide Meta-Analyses of Multiancestry Cohorts Identify Multiple New Susceptibility Loci for Refractive Error and Myopia.” *Nature Genetics* 45 (3): 314–18.
Verhoeven, V. J., K. T. Wong, G. H. Buitendijk, A. Hofman, J. R. Vingerling, and C. C. Klaver. 2015. “Visual Consequences of Refractive Errors in the General Population.” *Ophthalmology* 122 (1). https://doi.org/10.1016/j.ophtha.2014.07.030.
Vessani, Roberto M., Rodrigo Moritz, Lúcia Batis, Roberta Benetti Zagui, Silvia Bernardoni, and Remo Susanna. 2009. “Comparison of Quantitative Imaging Devices and Subjective Optic Nerve Head Assessment by General Ophthalmologists to Differentiate Normal From Glaucomatous Eyes.” *Journal of Glaucoma* 18 (3): 253–61.
Vickers, J. C., J. E. Craig, J. Stankovich, G. H. McCormack, A. K. West, J. L. Dickinson, P. J. McCartney, M. A. Coote, D. L. Healey, and D. A. Mackey. 2002. “The Apolipoprotein epsilon4 Gene Is Associated with Elevated Risk of Normal Tension Glaucoma.” *Molecular Vision* 8 (October). https://pubmed.ncbi.nlm.nih.gov/12379839/.
Vilhjálmsson, B. J., J. Yang, H. K. Finucane, A. Gusev, S. Lindström, S. Ripke, G. Genovese, et al. 2015. “Modeling Linkage Disequilibrium Increases Accuracy of

Polygenic Risk Scores." *American Journal of Human Genetics* 97 (4). https://doi.org/10.1016/j.ajhg.2015.09.001.
Vinciguerra, Riccardo, Ahmed Elsheikh, Cynthia J. Roberts, Renato Ambrósio, David Sung Yong Kang, Bernardo T. Lopes, Emanuela Morenghi, Claudio Azzolini, and Paolo Vinciguerra. 2016. "Influence of Pachymetry and Intraocular Pressure on Dynamic Corneal Response Parameters in Healthy Patients." *Journal of Refractive Surgery*. https://doi.org/10.3928/1081597x-20160524-01.
Vinciguerra, Riccardo, Salwah Rehman, Neeru A. Vallabh, Mark Batterbury, Gabriela Czanner, Anshoo Choudhary, Robert Cheeseman, Ahmed Elsheikh, and Colin E. Willoughby. 2020. "Corneal Biomechanics and Biomechanically Corrected Intraocular Pressure in Primary Open-Angle Glaucoma, Ocular Hypertension and Controls." *British Journal of Ophthalmology*. https://doi.org/10.1136/bjophthalmol-2018-313493.
Vingerling, J. R., A. Hofman, D. E. Grobbee, and P. T. de Jong. 1996. "Age-Related Macular Degeneration and Smoking. The Rotterdam Study." *Archives of Ophthalmology* 114 (10). https://doi.org/10.1001/archopht.1996.01100140393005.
Visscher, P. M., M. A. Brown, M. I. McCarthy, and J. Yang. 2012. "Five Years of GWAS Discovery." *American Journal of Human Genetics* 90 (1). https://doi.org/10.1016/j.ajhg.2011.11.029.
Visscher, P. M., N. R. Wray, Q. Zhang, P. Sklar, M. I. McCarthy, M. A. Brown, and J. Yang. 2017. "10 Years of GWAS Discovery: Biology, Function, and Translation." *American Journal of Human Genetics* 101 (1). https://doi.org/10.1016/j.ajhg.2017.06.005.
Vold, Steven, Iqbal Ike K. Ahmed, E. Randy Craven, Cynthia Mattox, Robert Stamper, Mark Packer, Reay H. Brown, and Tsontcho Ianchulev. 2016. "Two-Year COMPASS Trial Results: Supraciliary Microstenting with Phacoemulsification in Patients with Open-Angle Glaucoma and Cataracts." *Ophthalmology* 123 (10): 2103–12.
Wainberg, M., N. Sinnott-Armstrong, N. Mancuso, A. N. Barbeira, D. A. Knowles, D. Golan, R. Ermel, et al. 2019. "Opportunities and Challenges for Transcriptome-Wide Association Studies." *Nature Genetics* 51 (4). https://doi.org/10.1038/s41588-019-0385-z.
Wang, J. S., H. T. Xie, Y. Jia, and M. C. Zhang. 2016. "Retinal Nerve Fiber Layer Thickness Changes in Obstructive Sleep Apnea Syndrome: A Systematic Review and Meta-Analysis." *International Journal of Ophthalmology* 9 (11). https://doi.org/10.18240/ijo.2016.11.19.
Wang, Kai, Mingyao Li, and Hakon Hakonarson. 2010. "ANNOVAR: Functional Annotation of Genetic Variants from High-Throughput Sequencing Data." *Nucleic Acids Research* 38 (16): e164.
Wang, K., H. Gaitsch, H. Poon, N. J. Cox, and A. Rzhetsky. 2017. "Classification of Common Human Diseases Derived from Shared Genetic and Environmental Determinants." *Nature Genetics* 49 (9). https://doi.org/10.1038/ng.3931.
Wang, Nan, Shravan K. Chintala, M. Elizabeth Fini, and Joel S. Schuman. 2003. "Ultrasound Activates the TM ELAM-1/IL-1/NF-κB Response: A Potential Mechanism for Intraocular Pressure Reduction after Phacoemulsification." *Investigative Ophthalmology & Visual Science* 44 (5): 1977.
Wang, Peiyu, Jian Shen, Ryuna Chang, Maemae Moloney, Mina Torres, Bruce Burkemper, Xuejuan Jiang, Damien Rodger, Rohit Varma, and Grace M. Richter. 2019. "Machine Learning Models for Diagnosing Glaucoma from Retinal Nerve Fiber Layer Thickness Maps." *Ophthalmology Glaucoma* 2 (6): 422–28.
Wang, T., Y. Heianza, D. Sun, T. Huang, W. Ma, E. B. Rimm, J. E. Manson, F. B. Hu, W. C. Willett, and L. Qi. 2018. "Improving Adherence to Healthy Dietary Patterns, Genetic Risk, and Long Term Weight Gain: Gene-Diet Interaction Analysis in Two Prospective Cohort Studies." *BMJ* 360 (January). https://doi.org/10.1136/bmj.j5644.
Wang, Wei, Shaolin Du, and Xiulan Zhang. 2015. "Corneal Deformation Response in Patients With Primary Open-Angle Glaucoma and in Healthy Subjects Analyzed by Corvis ST." *Investigative Ophthalmology & Visual Science* 56 (9): 5557.
Wang, Y. X., L. Xu, R. X. Zhang, and J. B. Jonas. 2007. "Frequency-Doubling Threshold

Perimetry in Predicting Glaucoma in a Population-Based Study: The Beijing Eye Study." *Archives of Ophthalmology* 125 (10). https://doi.org/10.1001/archopht.125.10.1402.
Watanabe, Kyoko, Erdogan Taskesen, Arjen van Bochoven, and Danielle Posthuma. 2017. "Functional Mapping and Annotation of Genetic Associations with FUMA." *Nature Communications* 8 (1): 1826.
Weigl, K., J. Chang-Claude, P. Knebel, L. Hsu, M. Hoffmeister, and H. Brenner. 2018. "Strongly Enhanced Colorectal Cancer Risk Stratification by Combining Family History and Genetic Risk Score." *Clinical Epidemiology* 10 (January). https://doi.org/10.2147/CLEP.S145636.
Weinreb, R. N., J. D. Brandt, D. Garway-Heath, and F. Medeiros. 2007. *Intraocular Pressure*. Kugler Publications.
Weinreb, R. N., D. S. Friedman, R. D. Fechtner, G. A. Cioffi, A. L. Coleman, C. A. Girkin, J. M. Liebmann, et al. 2004. "Risk Assessment in the Management of Patients with Ocular Hypertension." *American Journal of Ophthalmology* 138 (3). https://doi.org/10.1016/j.ajo.2004.04.054.
Weinreb, Robert N., Tin Aung, and Felipe A. Medeiros. 2014. "The Pathophysiology and Treatment of Glaucoma: A Review." *JAMA: The Journal of the American Medical Association* 311 (18): 1901.
Weinreb, Robert N., and Peng Tee Khaw. 2004. "Primary Open-Angle Glaucoma." *The Lancet* 363 (9422): 1711–20.
Weinreb, Robert N., Jeffrey M. Liebmann, George A. Cioffi, Ivan Goldberg, James D. Brandt, Chris A. Johnson, Linda M. Zangwill, Susan Schneider, Hanh Badger, and Marina Bejanian. 2018. "Oral Memantine for the Treatment of Glaucoma." *Ophthalmology* 125 (12): 1874–85.
Wey, S., S. Amanullah, G. L. Spaeth, M. Ustaoglu, K. Rahmatnejad, and L. J. Katz. 2019. "Is Primary Open-Angle Glaucoma an Ocular Manifestation of Systemic Disease?" *Graefe's Archive for Clinical and Experimental Ophthalmology = Albrecht von Graefes Archiv Fur Klinische Und Experimentelle Ophthalmologie* 257 (4). https://doi.org/10.1007/s00417-019-04239-9.
Wickham, Hadley. 2014. "Tidy Data." *Journal of Statistical Software* 59 (10). https://doi.org/10.18637/jss.v059.i10.
Wiggs, Janey L., Michael A. Hauser, Wael Abdrabou, Robert Rand Allingham, Donald L. Budenz, Elizabeth Delbono, David S. Friedman, et al. 2013. "The NEIGHBOR Consortium Primary Open-Angle Glaucoma Genome-Wide Association Study: Rationale, Study Design, and Clinical Variables." *Journal of Glaucoma* 22 (7): 517–25.
Wiggs, Janey L., and Louis R. Pasquale. 2017. "Genetics of Glaucoma." *Human Molecular Genetics* 26 (R1): R21.
Wiggs, J. L., R. R. Allingham, D. Vollrath, K. H. Jones, De La Paz M, J. Kern, K. Patterson, et al. 1998. "Prevalence of Mutations in TIGR/Myocilin in Patients with Adult and Juvenile Primary Open-Angle Glaucoma." *American Journal of Human Genetics* 63 (5). https://doi.org/10.1086/302098.
Wiggs, J. L., and L. R. Pasquale. 2014. "Expression and Regulation of LOXL1 and Elastin-Related Genes in Eyes with Exfoliation Syndrome." *Journal of Glaucoma* 23 (8 Suppl 1). https://doi.org/10.1097/IJG.0000000000000124.
Wiggs, J. L., B. L. Yaspan, M. A. Hauser, J. H. Kang, R. R. Allingham, L. M. Olson, W. Abdrabou, et al. 2012. "Common Variants at 9p21 and 8q22 Are Associated with Increased Susceptibility to Optic Nerve Degeneration in Glaucoma." *PLoS Genetics* 8 (4). https://doi.org/10.1371/journal.pgen.1002654.
Willer, Cristen J., Yun Li, and Gonçalo R. Abecasis. 2010. "METAL: Fast and Efficient Meta-Analysis of Genomewide Association Scans." *Bioinformatics* 26 (17): 2190–91.
Williams, S. E., B. T. Whigham, Y. Liu, T. R. Carmichael, X. Qin, S. Schmidt, M. Ramsay, M. A. Hauser, and R. R. Allingham. 2010. "Major LOXL1 Risk Allele Is Reversed in Exfoliation Glaucoma in a Black South African Population." *Molecular Vision* 16 (April). https://pubmed.ncbi.nlm.nih.gov/20431720/.
Wishart, P. K., G. L. Spaeth, and E. M. Poryzees. 1985. "Anterior Chamber Angle in the

Exfoliation Syndrome." *The British Journal of Ophthalmology* 69 (2): 103–7.
Witte, J. S., P. M. Visscher, and N. R. Wray. 2014. "The Contribution of Genetic Variants to Disease Depends on the Ruler." *Nature Reviews. Genetics* 15 (11). https://doi.org/10.1038/nrg3786.
Wolff, T., and G. M. Rubin. 1998. "Strabismus, a Novel Gene That Regulates Tissue Polarity and Cell Fate Decisions in Drosophila." *Development* 125 (6): 1149–59.
Wolfs, R. C., C. C. Klaver, R. S. Ramrattan, C. M. van Duijn, A. Hofman, and P. T. de Jong. 1998. "Genetic Risk of Primary Open-Angle Glaucoma. Population-Based Familial Aggregation Study." *Archives of Ophthalmology* 116 (12). https://doi.org/10.1001/archopht.116.12.1640.
Wolfs, R. C., C. C. Klaver, J. R. Vingerling, D. E. Grobbee, A. Hofman, and P. T. de Jong. 1997. "Distribution of Central Corneal Thickness and Its Association with Intraocular Pressure: The Rotterdam Study." *American Journal of Ophthalmology* 123 (6). https://doi.org/10.1016/s0002-9394(14)71125-0.
Wolfs, R. C., R. S. Ramrattan, A. Hofman, and P. T. de Jong. 1999. "Cup-to-Disc Ratio: Ophthalmoscopy versus Automated Measurement in a General Population: The Rotterdam Study." *Ophthalmology* 106 (8): 1597–1601.
Wong, M. O., J. W. Lee, B. N. Choy, J. C. Chan, and J. S. Lai. 2015. "Systematic Review and Meta-Analysis on the Efficacy of Selective Laser Trabeculoplasty in Open-Angle Glaucoma." *Survey of Ophthalmology* 60 (1). https://doi.org/10.1016/j.survophthal.2014.06.006.
Won, H., L. de la Torre-Ubieta, J. L. Stein, N. N. Parikshak, J. Huang, C. K. Opland, M. J. Gandal, et al. 2016. "Chromosome Conformation Elucidates Regulatory Relationships in Developing Human Brain." *Nature* 538 (7626). https://doi.org/10.1038/nature19847.
Wray, N. R. 2005. "Allele Frequencies and the r2 Measure of Linkage Disequilibrium: Impact on Design and Interpretation of Association Studies." *Twin Research and Human Genetics: The Official Journal of the International Society for Twin Studies* 8 (2). https://doi.org/10.1375/1832427053738827.
Wright, David M., Evgenia Konstantakopoulou, Giovanni Montesano, Neil Nathwani, Anurag Garg, David Garway-Heath, David P. Crabb, and Gus Gazzard. 2020. "Visual Field Outcomes from the Multicenter, Randomized Controlled Laser in Glaucoma and Ocular Hypertension Trial." *Ophthalmology*, April. https://doi.org/10.1016/j.ophtha.2020.03.029.
Wu, Yang, Zhili Zheng, Peter M. Visscher, and Jian Yang. 2017. "Quantifying the Mapping Precision of Genome-Wide Association Studies Using Whole-Genome Sequencing Data." *Genome Biology* 18 (1): 86.
Wu, Zhichao, David P. Crabb, Balwantray C. Chauhan, Jonathan G. Crowston, and Felipe A. Medeiros. 2019. "Improving the Feasibility of Glaucoma Clinical Trials Using Trend-Based Visual Field Progression End Points." *Ophthalmology Glaucoma* 2 (2): 72–77.
Yaggi, H. K., J. Concato, W. N. Kernan, J. H. Lichtman, L. M. Brass, and V. Mohsenin. 2005. "Obstructive Sleep Apnea as a Risk Factor for Stroke and Death." *The New England Journal of Medicine* 353 (19). https://doi.org/10.1056/NEJMoa043104.
Yamada, Erika, Noriko Himori, Hiroshi Kunikata, Kazuko Omodaka, Hiromasa Ogawa, Masakazu Ichinose, and Toru Nakazawa. 2018. "The Relationship between Increased Oxidative Stress and Visual Field Defect Progression in Glaucoma Patients with Sleep Apnoea Syndrome." *Acta Ophthalmologica* 96 (4): e479–84.
Yang, J., B. Benyamin, B. P. McEvoy, S. Gordon, A. K. Henders, D. R. Nyholt, P. A. Madden, et al. 2010. "Common SNPs Explain a Large Proportion of the Heritability for Human Height." *Nature Genetics* 42 (7). https://doi.org/10.1038/ng.608.
Yang, Jian, Teresa Ferreira, Andrew P. Morris, Sarah E. Medland, Genetic Investigation of ANthropometric Traits (GIANT) Consortium, DIAbetes Genetics Replication And Meta-analysis (DIAGRAM) Consortium, Pamela A. F. Madden, et al. 2012. "Conditional and Joint Multiple-SNP Analysis of GWAS Summary Statistics Identifies Additional Variants Influencing Complex Traits." *Nature Genetics* 44 (4): 369–75, S1–3.
Yoshikawa, T., K. Obayashi, K. Miyata, K. Saeki, and N. Ogata. 2019. "Increased Nighttime Blood Pressure in Patients with Glaucoma: Cross-Sectional Analysis of the LIGHT

Study." *Ophthalmology* 126 (10). https://doi.org/10.1016/j.ophtha.2019.05.019.
Yu, Marco, Chen Lin, Robert N. Weinreb, Gilda Lai, Vivian Chiu, and Christopher Kai-Shun Leung. 2016. "Risk of Visual Field Progression in Glaucoma Patients with Progressive Retinal Nerve Fiber Layer Thinning." *Ophthalmology* 123 (6): 1201–10.
Zanon-Moreno, V., C. Ortega-Azorin, E. M. Asensio-Marquez, J. J. Garcia-Medina, Pinazo-Duran, O. Coltell, J. M. Ordovas, and D. Corella. 2017. "A Multi-Locus Genetic Risk Score for Primary Open-Angle Glaucoma (POAG) Variants Is Associated with POAG Risk in a Mediterranean Population: Inverse Correlations with Plasma Vitamin C and E Concentrations." *International Journal of Molecular Sciences* 18 (11). https://doi.org/10.3390/ijms18112302.
Zhang, Bing, Yusrah Shweikh, Anthony P. Khawaja, John Gallacher, Sarah Bauermeister, Paul J. Foster, and UK Biobank Eye and Vision Consortium. 2019. "Associations with Corneal Hysteresis in a Population Cohort: Results from 96 010 UK Biobank Participants." *Ophthalmology* 126 (11): 1500–1510.
Zhang, Y., G. Qi, J. H. Park, and N. Chatterjee. 2018. "Estimation of Complex Effect-Size Distributions Using Summary-Level Statistics from Genome-Wide Association Studies across 32 Complex Traits." *Nature Genetics* 50 (9). https://doi.org/10.1038/s41588-018-0193-x.
Zheng, Jie, A. Mesut Erzurumluoglu, Benjamin L. Elsworth, John P. Kemp, Laurence Howe, Philip C. Haycock, Gibran Hemani, et al. 2017. "LD Hub: A Centralized Database and Web Interface to Perform LD Score Regression That Maximizes the Potential of Summary Level GWAS Data for SNP Heritability and Genetic Correlation Analysis." *Bioinformatics* 33 (2): 272–79.
Zheng, Yingfeng, Tien Y. Wong, Ecosse Lamoureux, Paul Mitchell, Seng-Chee Loon, Seang Mei Saw, and Tin Aung. 2010. "Diagnostic Ability of Heidelberg Retina Tomography in Detecting Glaucoma in a Population Setting." *Ophthalmology* 117 (2): 290–97.
Zhou, Alysia W., Jason Giroux, Alexander J. Mao, and Cindy M. L. Hutnik. 2010. "Can Preoperative Anterior Chamber Angle Width Predict Magnitude of Intraocular Pressure Change after Cataract Surgery?" *Canadian Journal of Ophthalmology. Journal Canadien D'ophtalmologie* 45 (2): 149–53.
Zhou, Tiger, Emmanuelle Souzeau, Shiwani Sharma, John Landers, Richard Mills, Ivan Goldberg, Paul R. Healey, et al. 2017. "Whole Exome Sequencing Implicates Eye Development, the Unfolded Protein Response and Plasma Membrane Homeostasis in Primary Open-Angle Glaucoma." Edited by James Fielding Hejtmancik. https://doi.org/10.1371/journal.pone.0172427.
Zhou, Tiger, Emmanuelle Souzeau, Shiwani Sharma, Owen M. Siggs, Ivan Goldberg, Paul R. Healey, Stuart Graham, et al. 2016. "Rare Variants in Optic Disc Area Gene CARD10 Enriched in Primary Open-Angle Glaucoma." *Molecular Genetics & Genomic Medicine* 4 (6): 624–33.
Zhu, Z., F. Zhang, H. Hu, A. Bakshi, M. R. Robinson, J. E. Powell, G. W. Montgomery, et al. 2016. "Integration of Summary Data from GWAS and eQTL Studies Predicts Complex Trait Gene Targets." *Nature Genetics* 48 (5). https://doi.org/10.1038/ng.3538.
Zimprich, L., J. Diedrich, A. Bleeker, and J. A. Schweitzer. 2020. "Corneal Hysteresis as a Biomarker of Glaucoma: Current Insights." *Clinical Ophthalmology* 14 (August). https://doi.org/10.2147/OPTH.S236114.
Zode, Gulab S., Abbot F. Clark, and Robert J. Wordinger. 2009. "Bone Morphogenetic Protein 4 Inhibits TGF-beta2 Stimulation of Extracellular Matrix Proteins in Optic Nerve Head Cells: Role of Gremlin in ECM Modulation." *Glia* 57 (7): 755–66.